AD_____

CONTRACT NO: DAMD17-93-C-3098

TITLE: USE OF COMBINATION THERMAL THERAPY AND RADIATION IN BREAST CONSERVING TREATMENT OF EXTENSIVE INTRADUCTAL BREAST CANCER

PRINCIPAL INVESTIGATOR: Goran K. Svensson, Ph.D.

CONTRACTING ORGANIZATION: New England Deaconess Hospital
185 Pilgrim Road
Boston, Massachusetts 02215-5399

REPORT DATE: April 28, 1995

TYPE OF REPORT: Annual Report

PREPARED FOR: U.S. Army Medical Research and Materiel Command
Fort Detrick
Frederick, Maryland 21702-5012

DISTRIBUTION STATEMENT: Approved for public release;
distribution unlimited

DISCLAIMER NOTICE

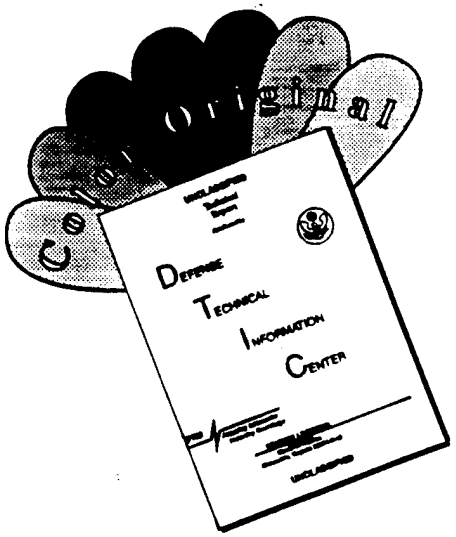

THIS DOCUMENT IS BEST QUALITY AVAILABLE. THE COPY FURNISHED TO DTIC CONTAINED A SIGNIFICANT NUMBER OF COLOR PAGES WHICH DO NOT REPRODUCE LEGIBLY ON BLACK AND WHITE MICROFICHE.

REPORT DOCUMENTATION PAGE

Form Approved
OMB No. 0704-0188

1. AGENCY USE ONLY *(Leave blank)*	2. REPORT DATE	3. REPORT TYPE AND DATES COVERED
	4/28/95	Annual Report (3/29/94-3/28/95)

4. TITLE AND SUBTITLE
"Use of Combination Thermal Therapy and Radiation in Breast Conserving Treatment of Extensive Intraductal Breast Cancer"

5. FUNDING NUMBERS
Contract No.
DAMD17-93-C-3098

6. AUTHOR(S)
Goran K. Svensson, Ph.D.
Everette C. Burdette, Ph.D.

7. PERFORMING ORGANIZATION NAME(S) AND ADDRESS(ES)
New England Deaconess Hospital
185 Pilgrim Road
Boston, Massachusetts 02215-5399

8. PERFORMING ORGANIZATION REPORT NUMBER

9. SPONSORING/MONITORING AGENCY NAME(S) AND ADDRESS(ES)
U.S. Army Medical Research, Development, Acquisition and Logistics Command (Provisional),
Fort Detrick
Frederick, Maryland 21702-5012

10. SPONSORING/MONITORING AGENCY REPORT NUMBER

11. SUPPLEMENTARY NOTES Prepared with contributions from: B.A. Bornstein, M.D., J.R. Harris, M.D., Xing-Qi Lu, Ph.D. Subcontract work: Dornier Medical Systems, Inc. 206 North Randolph Street, Champaign, IL 61820

12a. DISTRIBUTION/AVAILABILITY STATEMENT
Approved for public release; distribution unlimited

12b. DISTRIBUTION CODE

13. ABSTRACT *(Maximum 200 words)*

Year 02 of this contract continues to support the development of a thermal therapy system for the treatment of breast carcinoma. The complex system instrumentation has been designed and during year 02 the fabrication and the testing of all system modules was completed. Experiments in breast phantoms and non-perfused muscle tissue demonstrate that the applicator performs according to specifications. The agreement between experiments and computer simulations is excellent, and simulations will be used for planning of individual treatments. Final systems tests will be done in June 1995 and then the system will be shipped to its clinical site. A Phase I device evaluation protocol has been developed and received IRB approval. The program has been reviewed by an external review group. Recommended revisions by this group and scientific and technical considerations have delayed the progress by approximately six months. The revisions have significantly improved the spatial resolution to allow treatment of smaller targets in the breast and by redesigning the electronics, we have improved the capability for non-invasive treatment monitoring. To compensate for this delay, we have requested a six-months no-cost extension. Several new scientific challenges have been identified and are presented in the Conclusion as areas for future research.

14. SUBJECT TERMS	15. NUMBER OF PAGES
Thermal Therapy, Breast Cancer, Extensive Intraductal Component, Ductal Carcinoma in Situ, Device evaluation Protocol, Ultrasound Transducers, Thermometry, Non-Invasive Monitoring	91 (Excl. Append.)
	16. PRICE CODE

17. SECURITY CLASSIFICATION OF REPORT	18. SECURITY CLASSIFICATION OF THIS PAGE	19. SECURITY CLASSIFICATION OF ABSTRACT	20. LIMITATION OF ABSTRACT
Unclassified	Unclassified	Unclassified	Unlimited

GENERAL INSTRUCTIONS FOR COMPLETING SF 298

The Report Documentation Page (RDP) is used in announcing and cataloging reports. It is important that this information be consistent with the rest of the report, particularly the cover and title page. Instructions for filling in each block of the form follow. It is important to ***stay within the lines*** to meet ***optical scanning requirements***.

Block 1. Agency Use Only *(Leave blank)*.

Block 2. Report Date. Full publication date including day, month, and year, if available (e.g. 1 Jan 88). Must cite at least the year.

Block 3. Type of Report and Dates Covered. State whether report is interim, final, etc. If applicable, enter inclusive report dates (e.g. 10 Jun 87 - 30 Jun 88).

Block 4. Title and Subtitle. A title is taken from the part of the report that provides the most meaningful and complete information. When a report is prepared in more than one volume, repeat the primary title, add volume number, and include subtitle for the specific volume. On classified documents enter the title classification in parentheses.

Block 5. Funding Numbers. To include contract and grant numbers; may include program element number(s), project number(s), task number(s), and work unit number(s). Use the following labels:

C	- Contract	**PR**	- Project
G	- Grant	**TA**	- Task
PE	- Program Element	**WU**	- Work Unit Accession No.

Block 6. Author(s). Name(s) of person(s) responsible for writing the report, performing the research, or credited with the content of the report. If editor or compiler, this should follow the name(s).

Block 7. Performing Organization Name(s) and Address(es). Self-explanatory.

Block 8. Performing Organization Report Number. Enter the unique alphanumeric report number(s) assigned by the organization performing the report.

Block 9. Sponsoring/Monitoring Agency Name(s) and Address(es). Self-explanatory.

Block 10. Sponsoring/Monitoring Agency Report Number. *(If known)*

Block 11. Supplementary Notes. Enter information not included elsewhere such as: Prepared in cooperation with...; Trans. of...; To be published in.... When a report is revised, include a statement whether the new report supersedes or supplements the older report.

Block 12a. Distribution/Availability Statement. Denotes public availability or limitations. Cite any availability to the public. Enter additional limitations or special markings in all capitals (e.g. NOFORN, REL, ITAR).

- **DOD** - See DoDD 5230.24, "Distribution Statements on Technical Documents."
- **DOE** - See authorities.
- **NASA** - See Handbook NHB 2200.2.
- **NTIS** - Leave blank.

Block 12b. Distribution Code.

- **DOD** - Leave blank.
- **DOE** - Enter DOE distribution categories from the Standard Distribution for Unclassified Scientific and Technical Reports.
- **NASA** - Leave blank.
- **NTIS** - Leave blank.

Block 13. Abstract. Include a brief *(Maximum 200 words)* factual summary of the most significant information contained in the report.

Block 14. Subject Terms. Keywords or phrases identifying major subjects in the report.

Block 15. Number of Pages. Enter the total number of pages.

Block 16. Price Code. Enter appropriate price code *(NTIS only)*.

Blocks 17. - 19. Security Classifications. Self-explanatory. Enter U.S. Security Classification in accordance with U.S. Security Regulations (i.e., UNCLASSIFIED). If form contains classified information, stamp classification on the top and bottom of the page.

Block 20. Limitation of Abstract. This block must be completed to assign a limitation to the abstract. Enter either UL (unlimited) or SAR (same as report). An entry in this block is necessary if the abstract is to be limited. If blank, the abstract is assumed to be unlimited.

★U.S.GPO:1991-0-299-935

FOREWORD

Opinions, interpretations, conclusions and recommendations are those of the author and are not necessarily endorsed by the US Army.

____ Where copyrighted material is quoted, permission has been obtained to use such material.

____ Where material from documents designated for limited distribution is quoted, permission has been obtained to use the material.

____ Citations of commercial organizations and trade names in this report do not constitute an official Department of Army endorsement or approval of the products or services of these organizations.

____ In conducting research using animals, the investigator(s) adhered to the "Guide for the Care and Use of Laboratory Animals," prepared by the Committee on Care and Use of Laboratory Animals of the Institute of Laboratory Resources, National Research Council (NIH Publication No. 86-23, Revised 1985).

____ For the protection of human subjects, the investigator(s) adhered to policies of applicable Federal Law 45 CFR 46.

____ In conducting research utilizing recombinant DNA technology, the investigator(s) adhered to current guidelines promulgated by the National Institutes of Health.

____ In the conduct of research utilizing recombinant DNA, the investigator(s) adhered to the NIH Guidelines for Research Involving Recombinant DNA Molecules.

____ In the conduct of research involving hazardous organisms, the investigator(s) adhered to the CDC-NIH Guide for Biosafety in Microbiological and Biomedical Laboratories.

Accession For	
NTIS GRA&I	☑
DTIC TAB	☐
Unannounced	☐
Justification	
By	
Distribution/	
Availability Codes	
Dist	Avail and/or Special
A-1	

Graham Souder 4/25/95

PI - Signature Date

III. TABLE OF CONTENTS.

Page number.

IV. INTRODUCTION.

1. NATURE OF THE CLINICAL PROBLEM, BACKGROUND AND HYPOTHESIS.

Contract DAMD17-93-C-3098 supports the development of a technique for adjuvant treatment of breast cancer using thermal therapy (hyperthermia). The contract will also support a clinical study of the safety and efficacy of using thermal therapy in combination with radiation for treatment of breast cancer patients with an extensive intraductal component of their infiltrating tumor or patients with pure intraductal carcinoma (Ductal Carcinoma *in situ*). Breast cancer patients with these histologies have a higher risk of local recurrence than patients without these histologies (Solin et al. 1991).

Intraductal carcinoma is characterized by cancer cells spreading within the lactiferous ducts (Schnitt et al. 1988, Bornstein et al. 1991). It is suggested that intraductal carcinoma is associated with tumor necrosis within the ducts and that the necrotic tumor cells are related to the absence of blood supply with resulting hypoxia (Mayr et al. 1991). It is well known that thermal therapy, in contrast to radiation, is more effective in killing hypoxic cells as compared to well oxygenated cells (Hahn, 1982).

The clinical rationale and hypothesis for this work is that patients with infiltrating breast cancer containing an extensive intraductal component or patients with pure intraductal carcinoma will have a reduced risk for local recurrence from a combined and non-disfiguring treatment approach using thermal therapy and irradiation. This will extend the indications for breast conserving therapy and eliminate the need for mastectomy for many patients. We also postulate that the thermal therapy is most effectively and controllably delivered to the breast tissue using a breast site specific ultrasound applicator.

The technical rationale and criteria for the design of the ultrasound therapy system and applicator are derived from the tissue characteristics and features of the breast:

a. The breast is an external, convex shaped organ. When submerged into a temperature controlled water bath, the temperature boundaries are well defined and the skin temperature can be well controlled.

b. Ultrasound heating is suitable for the breast, because there is no intervening gas or bone in the breast tissue. With the patient in the prone position and the breast submerged into a water bath, the breast tissue can be surrounded with an array of ultrasound transducers and achieve tangential incidence of the ultrasound beam relative to the chest wall. Tangential incidence is desired to avoid interaction between the ribcage and the ultrasound pressure wave.

c. There are no major blood vessels that carry away heat from the breast tissue, which can reduce the ability to deliver therapeutic heat.

d. The target volume can be the whole breast, a quadrant of the breast, or even a smaller specific tumor mass. Energy deposition which may heat sensitive regions, such

as a lumpectomy scar, must be avoided or minimized. It is therefore essential that the energy deposition be controlled and focused on specific sites within the breast tissue. Ultrasound permits this level of control.

e. Although our initial pilot study will aim for a target temperature of $T_{90} \geq 40.5^{o}C$ and $T_{max} < 45^{o}C$, the device must be able to heat the breast tissue within an even more narrow temperature range ($42^{o}C$ - $44^{o}C$) over a reasonable range of tissue perfusion (i.e. 30 to 200 ml, kg^{-1}, min^{-1}).

2. RESEARCH OBJECTIVES.

The first research objective is to build a cylindrical, multi-transducer, dual frequency, intensity controlled ultrasound therapy applicator and instrumentation system for treatment of breast cancer. The system must be capable of delivering controllable energy for the purpose of heating the whole breast or a small volume of breast tissue as defined by the clinical situation and the criteria in Section IV.1. The intensity control of the applicator must permit heating within a narrow temperature range, i.e. $42^{o}C \leq T_{tissue} \leq 44^{o}C$ (Svensson et al., 1994, Lu et al., 1994). Many scientific and technical problems associated with the individual subsystems have now been solved and the sophisticated system is assembled in the laboratories at Dornier Medical Systems, Inc., Champaign, Illinois, where final integration and overall systems tests are underway.

A second objective is to develop an effective pre-treatment planning and real-time treatment control system (Hansen et al., 1994). One aspect of this effort is to perform the thermal therapy using dense thermometry (Bowman et al., 1991). It is essential for the assessment of outcome that temperatures are measured during thermal therapy in a large number of points throughout the breast tissue volume. The objective is to accomplish this through new technologies using minimally invasive or non-invasive thermometry. The minimally invasive temperature measurements will be achieved by using small multi-sensor thermistor probes (dense thermometry), developed at the Massachusetts Institute of Technology (MIT) under the direction of Dr. F. Bowman, who is a consultant to our contract. Thermal dose concepts (Sapareto et al., 1984) will be used to assess the treatment success. To augment the dense thermometry mapping, we will continue to investigate a tomographic non-invasive technique for measurement of through-transmission power deposition and for imaging of temperature sensitive tissue parameters as a means of non-invasive monitoring. The non-invasive monitoring was initially proposed as a separate development during year 02 and 03. However, it became obvious that a problem of this complexity needed to be included as an integral part of the system instrumentation design in order to avoid major redesign efforts and expense at a later date. It turns out that the receiving system associated with non-invasive monitoring and breast contour imaging became the predominant limiting and controlling factor for the electronics design, and is in part responsible for the delays we have encountered.

A third objective is to develop ultrasound thermal therapy protocols. The first is a Phase I protocol for device evaluation (Appendix G). It intends to evaluate the user interaction of the breast treatment system under clinical conditions. This protocol was not in the original proposal, but it was recommended by our External Review Group (Dewhirst et al., 1993) during their review visit in April 1994, due to the fact that this is a

totally new treatment device. This protocol has now been reviewed and approved by the IRB at the Dana Farber Cancer Institute and is under review by the IRB of the New England Deaconess Hospital. It has also been submitted for review by the Army. Fifteen patients will be treated under this protocol. The second protocol will be a Phase I/II treatment protocol for evaluating toxicity and dose-response, which was anticipated in the original proposal. Contingent upon its success, a Phase III protocol for randomized trials will be developed.

V. BODY OF ANNUAL REPORT

1. RESEARCH METHODOLOGY

1.A. Program Organization.

The contract is sponsored by the New England Deaconess Hospital (NEDH); a Harvard Medical School (HMS) affiliated hospital in Boston, Massachusetts. The program director, Goran K. Svensson, Ph.D. is an Associate Professor at HMS and he is responsible for the progress of the scientific, technical and clinical developments. Dr. Svensson is also the Director of Physics at the Joint Center for Radiation Therapy (JCRT). The JCRT provide radiation therapy and thermal therapy services to New England Deaconess Hospital (NEDH), Dana Farber Cancer Institute (DFCI), Beth Israel Hospital (BIH), Brigham and Women's Hospital (BWH) and Children's Hospital (CH). This network of hospitals are all affiliated with Harvard Medical School.

Development of treatment protocols and all clinical work will be done at the NEDH. Clinical research protocols used by the JCRT member hospital network require IRB approval from the participating hospitals. The Dana Farber Cancer Institute has a large Breast Evaluation Center (BEC), which is an important referral base for breast cancer patients. We have therefore chosen to seek IRB approval for thermal therapy, using this device, from DFCI and from the sponsoring hospital NEDH.

Theoretical simulations and treatment planning require large computational resources. This work will take place at the NEDH.

The electronic design and the fabrication of the ultrasound treatment system and breast applicator is subcontracted to Dornier Medical Systems Inc. (DMSI) with headquarters in Atlanta, Georgia. The actual work is performed at the DMSI R&D Laboratory in Champaign, Illinois under the direction of Everette C. Burdette, Ph.D. Dr. Burdette directs advanced technology research for DMSI.

1.B. Summary of Second Year Progress.

1.B.1. Overall Progress.

The clinical objectives are to deliver effective hyperthermia to the breast or sub-volume of the breast for cancer patients with an extensive intraductal component of their infiltrating tumor or patients with pure intraductal carcinoma. To reach that clinical goal several new and important clinical considerations were introduced into our program. They were necessitated by the advise from our External Review Committee, consisting of Daniel Kapp, M.D., Ph.D., Professor of Radiation Oncology at Stanford University

Medical Center and Mark Dewhirst, DVM, Ph.D., Professor of Radiation Oncology at Duke University Medical Center. In addition to program revisions suggested by our external review committee, we have experienced difficult technical and scientific challenges requiring complex solutions before the system could be completed. Logistical delays, related to the hospital IRB approval process, have also been encountered. This is due to recent changes in the process of acquiring a hospital IRB approval of the clinical protocols.

Toxicities associated with thermal therapy are well documented (Kapp et al., 1992, Bornstein et al., 1992). A major concern, expressed by our Review Committee, is that women that have undergone lumpectomy or surgical biopsy are left with a scar cavity within the breast. The scar tissue has in general much lower perfusion than surrounding normal tissue. The clinical experience is that the poorly perfused scar tissue easily over-heats during thermal therapy leaving burns and blisters as undesired toxicity. The treatment system must have very accurate temporal and spatial power control to reduce the temperature in and around the scar tissue. The requirement for this level of accuracy was not appreciated in our original application and has resulted in several design improvements. To achieve this level of control, we have increased both the number of therapy transducers and the emphasis on real time non-invasive monitoring during therapy. This significantly increases the complexity of the instrumentation which must be developed. In fact, in the original application, we proposed to add non-invasive radiometric temperature sensing to the system during year 02 and 03. Instead, we have addressed the need for noninvasive monitoring throughout the design process and designed the best possible electronics and computer system to meet that goal. This has caused delays and changes in the originally proposed schedule, but in the long term it will result in both time and cost savings and a clinically much better optimized system.

During year 01 and 02, the breast treatment applicator and the associated complex instrumentation system has been designed, fabricated and in part tested. During year 02 we have completed the fabrication and testing of all submodules. They have been assembled and the complex computer systems are fully integrated to one system. This work has been done at the DMSI Laboratory in Champaign Illinois. As the subsystems have been completed, the results and performance have been reviewed by the clinical and technical personnel at the NEDH. The system is now undergoing final assembly and testing before shipment to its clinical site at NEDH.

In the interest of high quality patient care, we are completely committed to resolve all clinical, scientific and technical considerations that we have encountered during this research program. As a result, there has been an approximately six months delay in the progress. To complete this contract and to compensate for the delays, we have requested, in a separate communication to the Director for the Breast Cancer Research Program, a six months no-cost extension of this program. However, in spite of a delay in progress, the quality of the treatment system is excellent and the hypothesis and goals of this research program remain unchanged.

1.B.2. Specific Progress and Program Revisions during Year 02.

The second year progress is summarized below. Detailed description of the experimental methods and results are presented in Section V.2.C.

- A Phase I, device evaluation protocol, has been completed and received IRB approval by the DFCI Human Subjects Committee. It has been submitted for approval by the NEDH Human Subjects Committee and by the US Army Human Use Review and Regulatory Affairs Division.

- Both DFCI and NEDH require an approved IDE application to the FDA prior to the start of the clinical protocol. The IDE application to the FDA is near completion. We had anticipated an early submission for an IDE. However, due to delays caused by technical and scientific considerations, we have not yet collected enough data from the integrated system to satisfy the FDA requirements for the IDE application. This is one reason for the proposed no cost extension.

- All theoretical simulations leading to the systems design have been completed. This work has lead to the publications attached as Appendices A and B.

- The cylindrical transducer array subsystem is completed and tested. Each of the 384 transducers has been individually characterized and selected. An unexpectedly high rejection rate required significantly more transducers to be built than originally anticipated. Delays and considerable expense were experienced in contracting the fabrication of more transducers.

- The electronics subsystems have been completed and tested. The need for real-time monitoring of transmitted and reflected power required a new and refined design paying special attention to fast Transmit/Receive switching, board layouts and signal to noise considerations. The changes have improved the quality and functionality significantly but caused some delays.

- The computer subsystems have been completed and the necessary messaging and communication paths have been established. Each software module is written, functioning, and tested.

- The sophisticated breast ultrasound treatment system allows monitoring of transmitted and reflected power. We have begun to develop a three-dimensional reconstruction algorithm for display of these data. Also, DMSI has provided for future addition of a Digital Signal Processor (DSP) in the receive subsystem. This work is beyond the scope of the present contract and will require additional future research and funding. This work is further discussed in section VI.B.

2. BREAST THERAPY SYSTEM DESCRIPTION, METHODOLOGY, & TESTS

The final system consists of the hardware components illustrated in Figure 1. A breast site-specific cylindrical array applicator of ultrasound transducers is used for thermal therapy induction and for multiple monitoring functions. The "heart" of the hardware consists of the cylindrical array of transducers which both deposit power into the breast tissue for therapy and monitor the dynamic course of the treatment. The ultrasound array is described in more detail below. The ultrasound transducers are geometrically arranged and operated to provide several monitoring functions. The monitoring functions are comprised of: diagnostic pulse-echo monitoring to determine breast contour and location within the treatment cylinder; through transmission monitoring of power during therapy for determination of absorbed power distribution (SAR) in the breast tissue being monitored; measurement of "time-of-flight" throughout regions of the target breast tissue referenced to a limited number of invasive temperature measurements for non-invasive mapping of temperatures throughout the treatment volume.

The system consists of an Instrument Computer which provides all direct control and data interaction with the TMR Subsystem, circuits, Receiver circuits, /Transmit/Receive/Multiplexing Modules, Thermistor Thermometry Subsystem, and Cooling Subsystem. The system electronics, Instrument Computer, and Cylindrical Transducer Array/Treatment Cavity are integrated into a Patient Table Assembly/Subsystem, which provides a comfortable treatment support for the patient, accurate positioning of the breast within the treatment cavity, and a convenient means for consolidating system components and functions.

2.A. Ultrasound Breast Applicator

The Transducer Array Subsystem is illustrated graphically in Figure 2. And a photo of the cylindrical array is shown in Figure 3. The array consists of eight (8) individual rings which are stacked with water-tight seals between rings. Each ring accommodates up to 48 transducers. Based on analyses performed, it is not necessary to fill all available ring locations with transducers, in order to achieve adequate therapy, but populating all positions is important to noninrasive monitoring. Each transducer is square having dimensions of 1.5cm x 1.5cm. Spacing between transducers along the vertical dimension of the cylinder is 2.4mm. and a bottom clearance of 1cm is added. Therefore, 8 rings accommodates breast lengths of 14cm or less. Table 1 states the number of rings, transducers per ring, and the frequencies of the transducers in each ring. Table 2 indicates expected ring activation for examples of large and small breasts.

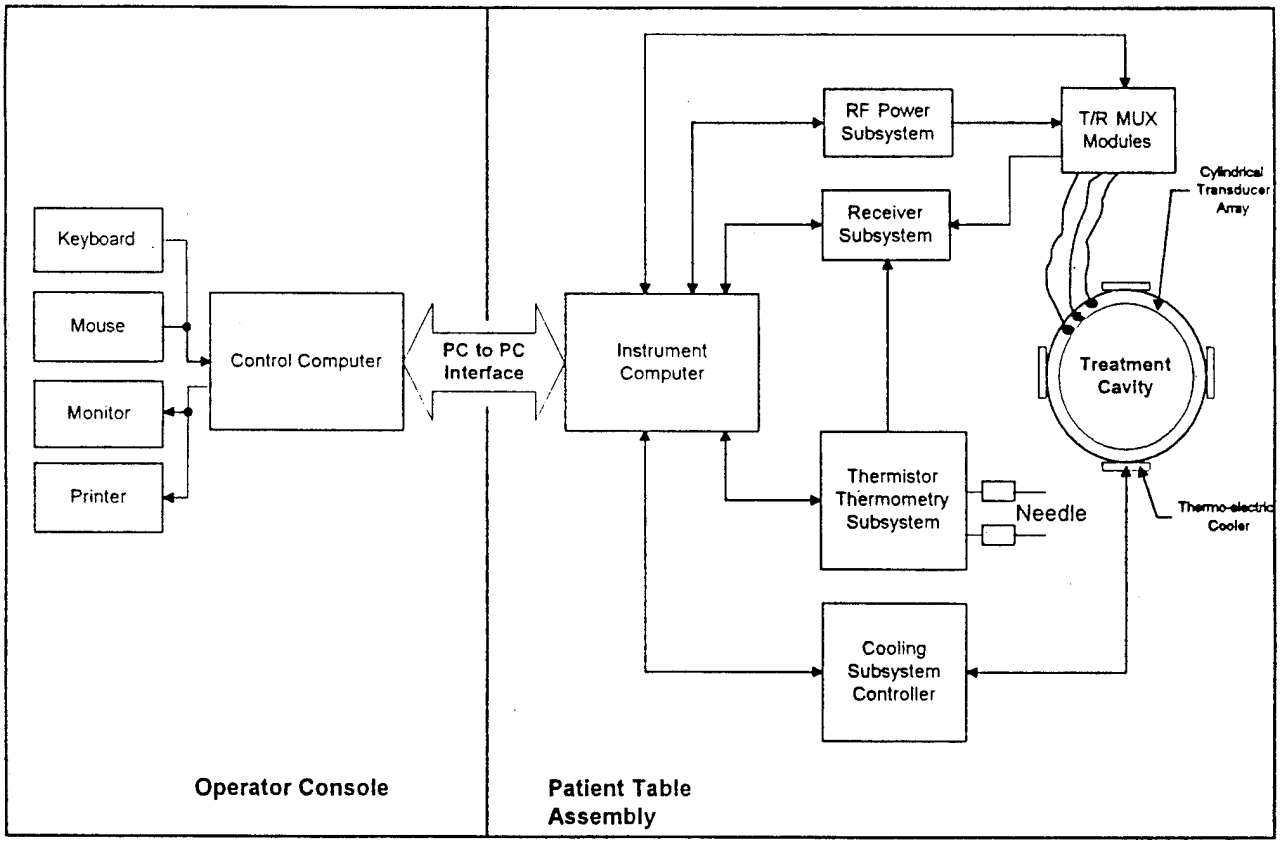

System Hardware Block Diagram

Figure 1.

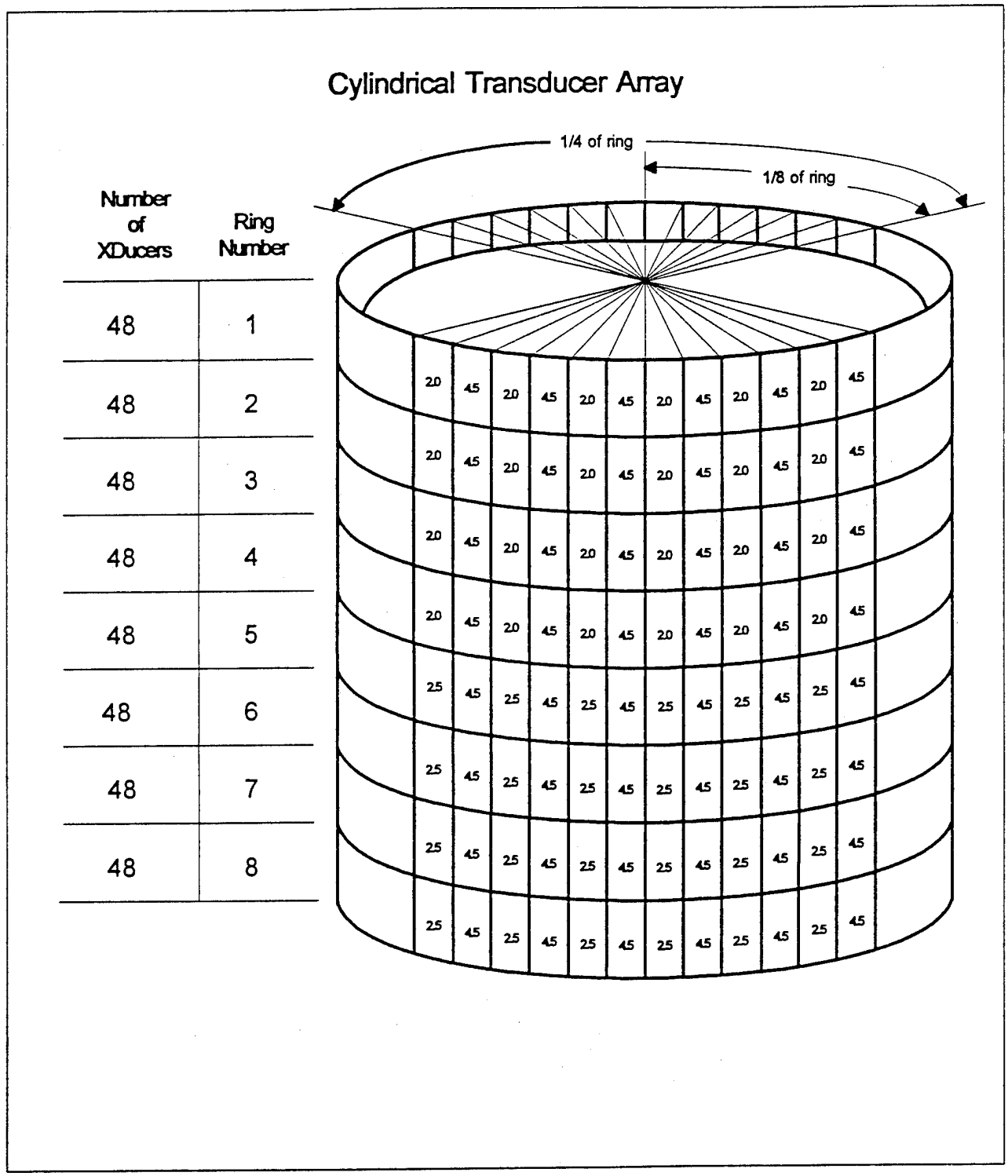

Figure 2. Transducer array configuration arranged in rings of cylinder.

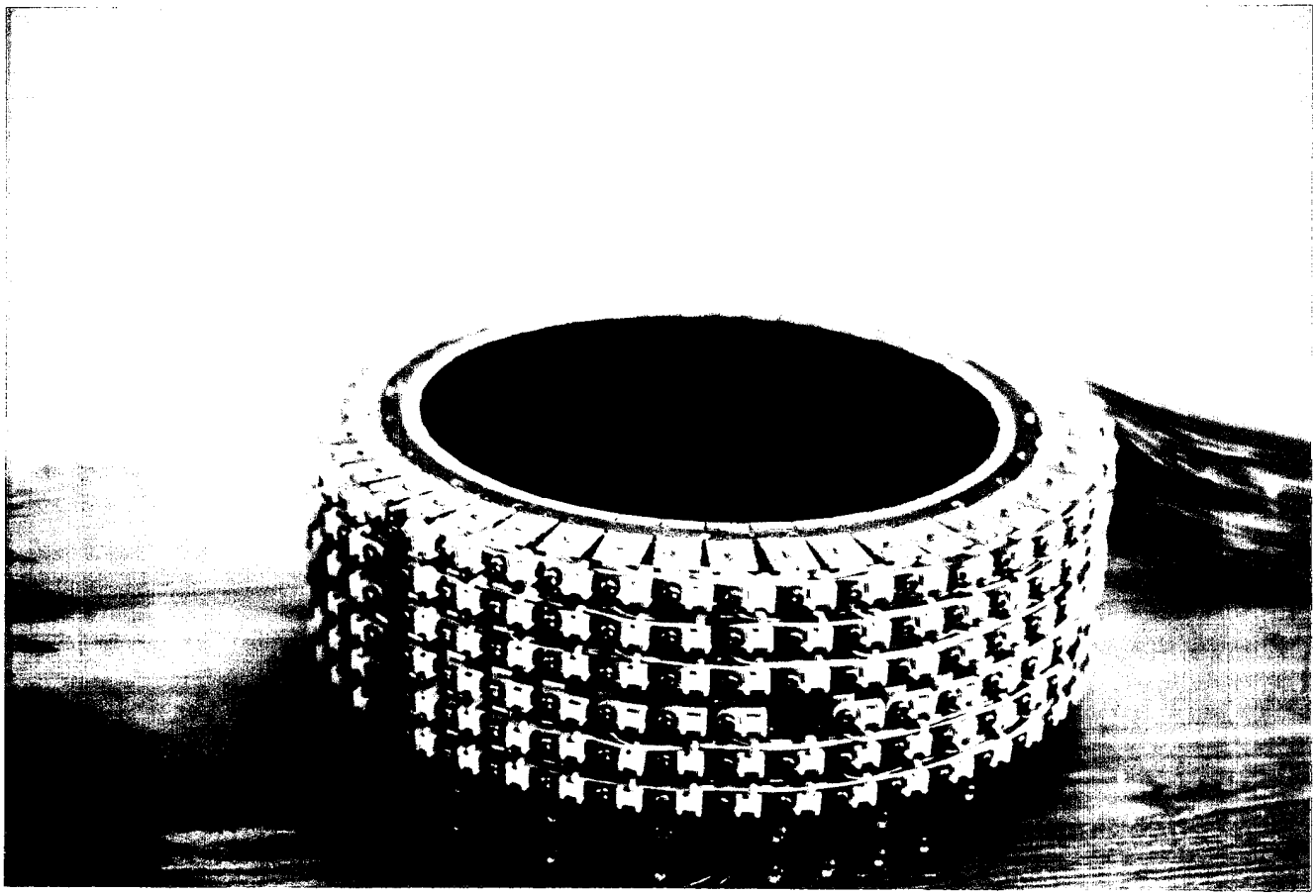

Figure 3. Photo of cylindrical array of transducers consisting of eight stacked circular rings each containing 48 transducers.

Table 1. Numbers and distribution of transducers per ring.

CYLINDRICAL ARRAY APPLICATOR DESIGN			
Total Cylinder I.D. = 25 cm Transducers: 15 mm x 15 mm Rings of Transducers: 10 (numbered from top down) Each 1/8 ring vertical section driven by RF Amplifiers whose outputs are multiplexed to step around ring			
Ring No.	FQ 1 (MHz)/No. XDCRS	FQ 2 (MHz)/No. XDCRS	TOTAL XDCRS
1	4.5/24	2.0/24	48
2	4.5/24	2.0/24	48
3	4.5/24	2.0/24	48
4	4.5/24	2.0/24	48
5	4.5/24	2.5/24	48
6	4.5/24	2.5/24	48
7	4.5/24	2.5/24	48
8	4.5/24	2.5/24	48
		TOTAL	384

Table 2 . The table illustrates how many rings and transducer elements in a ring that will be activated when treating a large breast and a small breast respectively.

CYLINDRICAL ARRAY APPLICATOR DESIGN				
Total Cylinder I.D. = 25 cm Transducers: 15 mm x 15 mm Rings of Transducers: 8 (numbered from top down) Each 1/8 ring vertical section driven by RF amplifiers whose outputs are multiplexed to "step around" ring				
Ring No.	No. Transducers	Breast Size (cm) Large	Small	No Transducers in 1/8 of ring
1	48	15	8	6
2	48	14	7	6
3	48	12	6	6
4	48	10	5	6
5	48	8	4	6
6	48	7	3	6
7	48	6	0	6
8	48	4	0	6

The transducers used in the cylindrical array subsystem were fabricated with the crystal (2.0, 2.5, or 4.5 MHz) mounted in a machined transducer housing, sealed with a watertight seal and faced with a matching layer. Each transducer was individually performance-tested to determine its operating acoustic efficiency, center frequency and bandwidth. Tables containing the efficiency data for each transducer in the cylindrical array are presented in Appendix C. Frequency bandwidth and efficiency data for three selected transducers at each frequency are shown in Figures 4 through 12.

Each transducer in each ring of the cylinder is "mapped" into both the cylindrical array and to the multiplexer-T/R-RF generator port and card. A diagram of the T/R MUX applicator transducer interconnections map is shown in Appendix D .

Close up views of the cylindrical array of transducers are shown in Figures 13 and 14. Angular beam plots for 2.0 and 4.5 Mhz transducers are shown in Appendix E.

2.B. Patient Table Subsystem

The patient table subsystem in shown in the two perspective photos in Figures 15 and 16 (indicating front side and rear views, respectively). A close up of the shroud covering the cylindrical array is shown in Figure 17. The patient table is designed to maximize utilization of symmetry of the breast by positioning the patient in a prone position with the breast suspended through an opening in the table top. Its specifications are described in Table 3. The table top consists of sheet steel with a tubular steel outer frame fabricated to provide for insertion of a 1.5" foam padding insert. The foam is sealed and the entire table top covered with a naugahyde covering which is stretched tight and snapped into place, and is easily removed for cleaning. The foam insert (and naugahyde) taper near the hole through which the breast is suspended in order to ensure that the entire breast can be extended beneath the table top for treatment if indicated. The patient table top was completed in year 01 and delivered to NEDH for evaluation, and returned for integration into the system in year 02.

The central column, or "pedestal", beneath the table houses all of the system electronics, water cooling and circulation, power supplies, and cylindrical array of transducers. The Instrument Computer is also located within the pedestal behind a side cover panel. Drawings of the internal layout are shown in Figures 18 and 19. Note the positions of the key electronic system components. The 25 TMR subsystems and microcontrollers are located in the two card cage racks above the fan trays. The transducer coaxial cable connections are routed from the rear of the card cages to panel connectors on a subpanel behind the dress panel at the front of the system (just behind the cylindrical array).

Transducer Number		4-241A				% Efficiency	
Freq. MHz	DC mA	DC Volts	US Watts	DC Watts	RF Watts	DC to US	RF to US
4.42	130.30	26.08	0.82	3.40	2.01	24.13%	40.78%
4.52	144.90	26.03	1.14	3.77	2.23	30.22%	51.08%
4.62	178.60	25.93	1.60	4.63	2.74	34.55%	58.39%
4.72	221.40	25.81	2.02	5.71	3.38	35.35%	59.74%
4.82	246.00	25.74	2.06	6.33	3.75	32.53%	54.98%
4.92	260.10	25.71	2.02	6.69	3.96	30.21%	51.05%
5.02	254.50	25.72	1.72	6.55	3.87	26.28%	44.41%

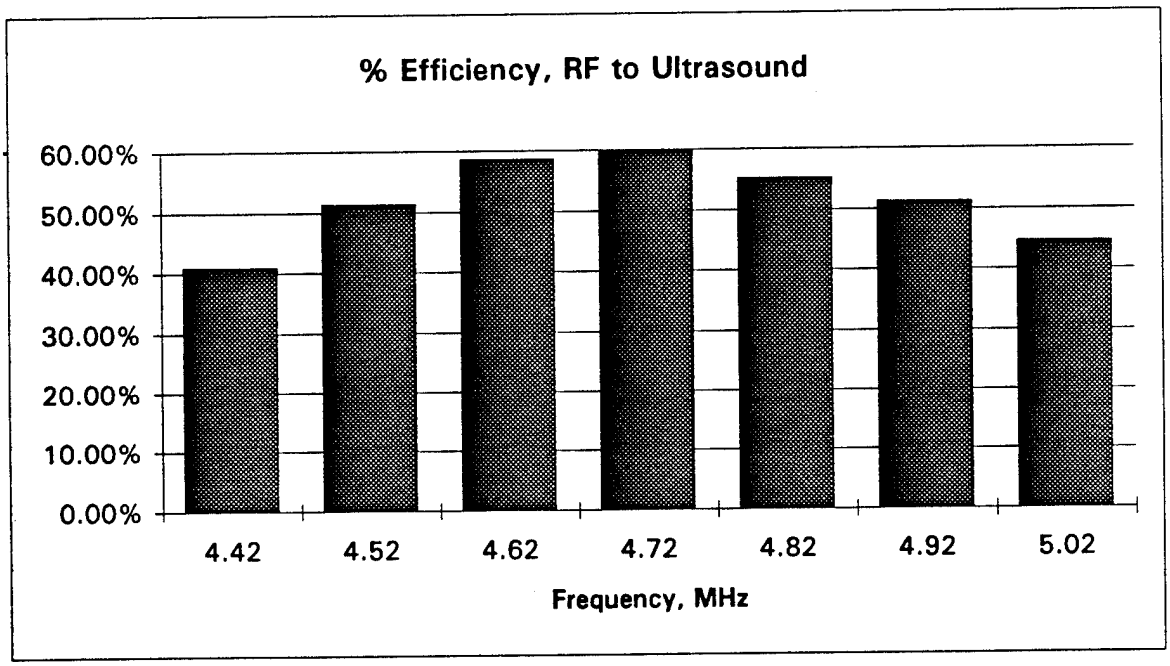

Figure 4. Acoustic efficiency as a function of frequency for a typical 4.5 MHz transducer used in the cylindrical array. Similar data exsist for each of the 384 transducers.

Transducer Number		4-227				% Efficiency	
Freq. MHz	DC mA	DC Volts	US Watts	DC Watts	RF Watts	DC to US	RF to US
4.38	148.50	26.03	0.98	3.87	2.29	25.35%	42.85%
4.48	171.20	25.96	1.30	4.44	2.63	29.25%	49.43%
4.58	203.90	25.86	1.52	5.27	3.12	28.83%	48.72%
4.68	229.40	25.79	1.42	5.92	3.50	24.00%	40.56%
4.78	234.30	25.78	1.06	6.04	3.57	17.55%	29.66%
4.88	223.00	25.81	0.92	5.76	3.41	15.98%	27.01%
4.98	215.60	25.83	0.85	5.57	3.30	15.26%	25.79%

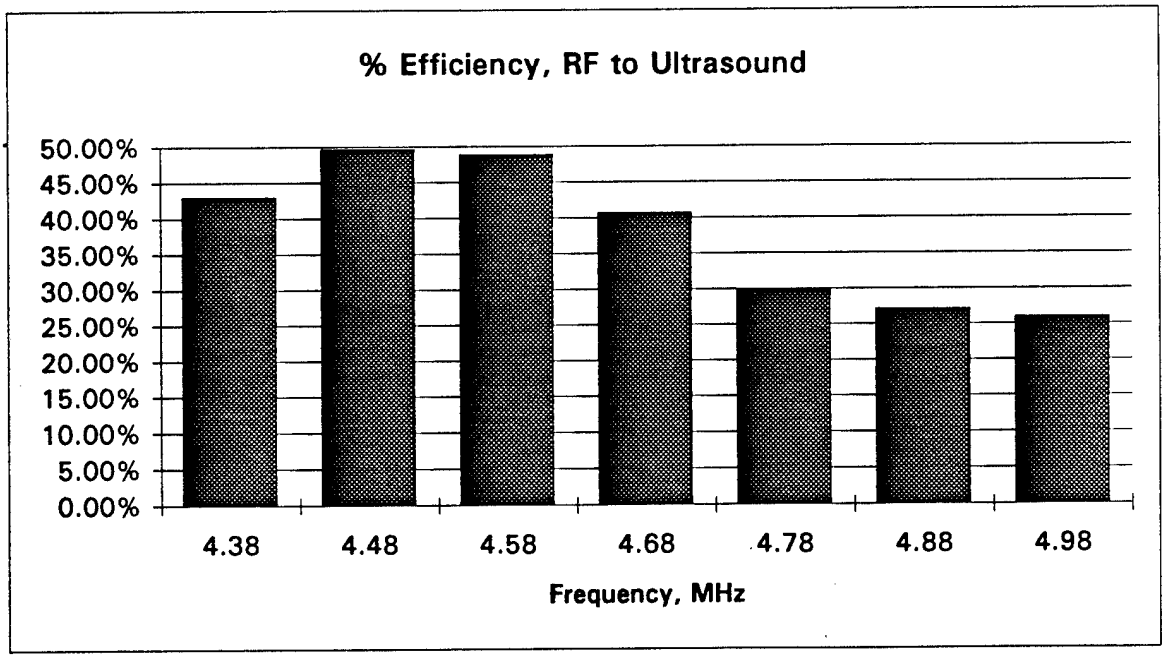

Figure 5. Acoustic efficiency as a function of frequency for a typical 4.5 MHz transducer used in the cylindrical array. Similar data exsists for each of the 384 transducers.

Transducer Number		4-239				% Efficiency	
Freq. MHz	DC mA	DC Volts	US Watts	DC Watts	RF Watts	DC to US	RF to US
4.48	139.80	26.05	0.78	3.64	2.15	21.42%	36.20%
4.58	176.00	25.94	1.36	4.57	2.70	29.79%	50.34%
4.68	208.80	25.84	1.58	5.40	3.19	29.28%	49.49%
4.78	236.80	25.77	1.52	6.10	3.61	24.91%	42.10%
4.88	238.40	25.77	1.30	6.14	3.64	21.16%	35.76%
4.98	233.30	25.78	1.18	6.01	3.56	19.62%	33.16%
5.08	223.20	25.81	1.20	5.76	3.41	20.83%	35.20%

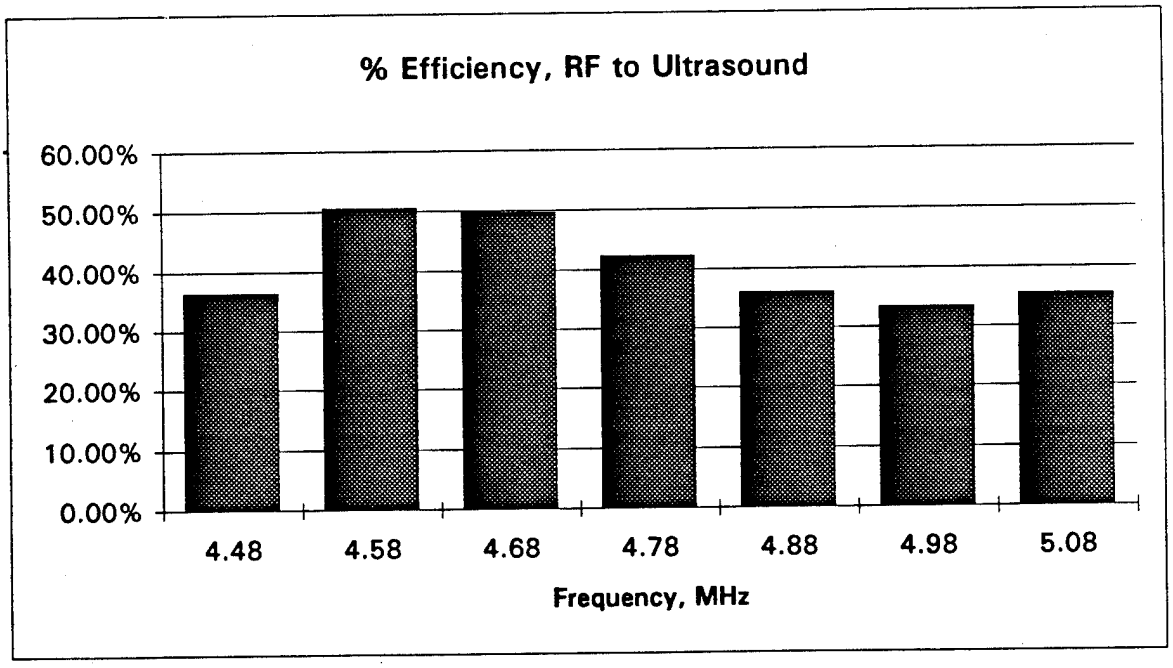

Figure 6. Acoustic efficiency as a function of frequency for a typical 4.5 MHz transducer used in the cylindrical array. Similar data exsists for each of the 384 transducers.

Transducer Number		2.5-113				% Efficiency	
Freq. MHz	DC mA	DC Volts	US Watts	DC Watts	RF Watts	DC to US	RF to US
2.47	188.90	24.85	1.90	4.69	2.83	40.48%	62.01%
2.48	184.40	24.89	1.86	4.59	2.76	40.53%	62.08%
2.49	180.40	24.93	1.88	4.50	2.71	41.80%	64.04%
2.50	180.70	24.92	1.96	4.50	2.71	43.53%	66.68%
2.51	183.00	24.9	2.00	4.56	2.75	43.89%	67.24%
2.52	182.30	24.91	1.98	4.54	2.74	43.60%	66.80%
2.53	180.40	24.93	1.98	4.50	2.71	44.03%	67.45%
2.54	180.50	24.93	1.98	4.50	2.71	44.00%	67.41%
2.55	182.00	24.91	2.02	4.53	2.73	44.56%	68.26%
2.56	181.20	24.92	2.00	4.52	2.72	44.29%	67.86%
2.57	177.80	24.95	1.98	4.44	2.67	44.63%	68.38%
2.58	178.50	24.94	2.02	4.45	2.68	45.38%	69.51%
2.59	182.90	24.9	2.08	4.55	2.74	45.67%	69.97%
2.60	186.30	24.88	2.12	4.64	2.79	45.74%	70.07%
2.61	188.00	24.86	2.12	4.67	2.82	45.36%	69.49%
2.62	191.30	24.83	2.20	4.75	2.86	46.32%	70.96%
2.63	198.70	24.77	2.28	4.92	2.96	46.32%	70.97%
2.64	203.80	24.73	2.30	5.04	3.04	45.64%	69.91%
2.65	203.40	24.73	2.30	5.03	3.03	45.72%	70.05%
2.66	203.40	24.73	2.30	5.03	3.03	45.72%	70.05%
2.67	210.50	24.67	2.34	5.19	3.13	45.06%	69.03%

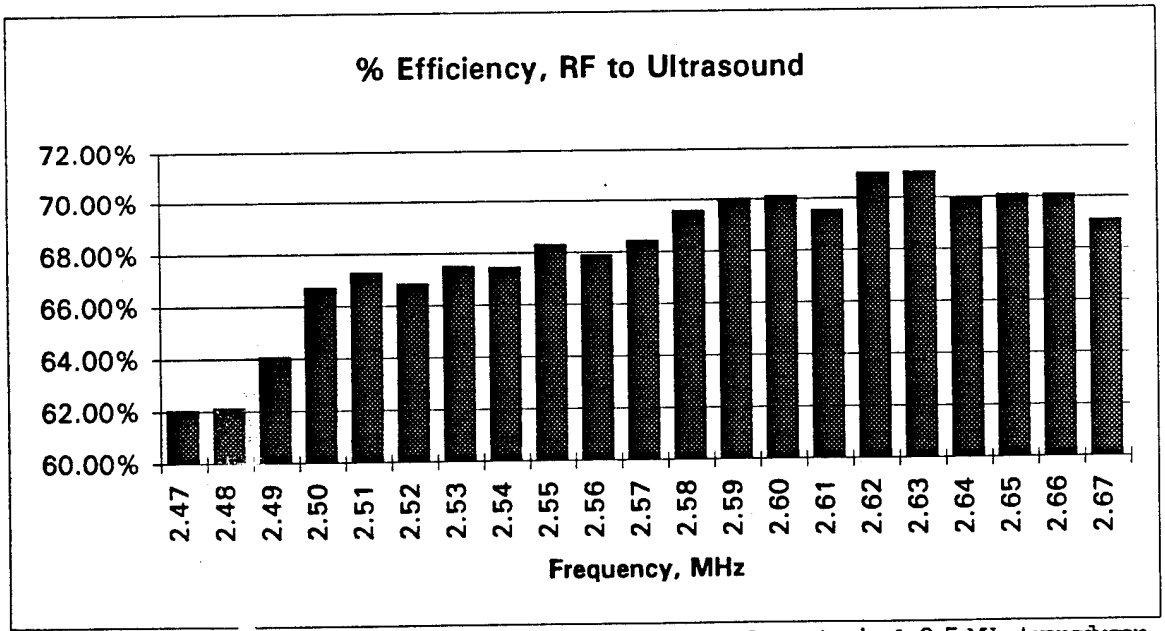

Figure 7. Acoustic effiency as a function of frequency for a typical 2.5 MHz transducer used in the cylindrical array. Similar data exsists for each of the 384 transducers.

Transducer Number		2.5-124				% Efficiency	
Freq. MHz	DC mA	DC Volts	US Watts	DC Watts	RF Watts	DC to US	RF to US
2.42	199.6	24.76	2.00	4.94	3.23	40.47%	62.00%
2.43	196.2	24.79	2.00	4.86	3.17	41.12%	63.00%
2.44	192.1	24.83	2.00	4.77	3.11	41.93%	64.24%
2.45	190.6	24.84	2.02	4.73	3.09	42.67%	65.37%
2.46	188.4	24.86	2.02	4.68	3.06	43.13%	66.08%
2.47	184.5	24.89	2.00	4.59	3.00	43.55%	66.73%
2.48	183.1	24.9	2.04	4.56	2.98	44.74%	68.56%
2.49	185.5	24.88	2.08	4.62	3.01	45.07%	69.05%
2.50	186.8	24.87	2.10	4.65	3.03	45.20%	69.26%
2.51	184.2	24.89	2.08	4.58	2.99	45.37%	69.51%
2.52	181.1	24.92	2.08	4.51	2.95	46.09%	70.62%
2.53	182.5	24.91	2.12	4.55	2.97	46.63%	71.45%
2.54	183.6	24.9	2.14	4.57	2.98	46.81%	71.72%
2.55	182.4	24.91	2.12	4.54	2.97	46.66%	71.49%
2.56	181.9	24.91	2.14	4.53	2.96	47.23%	72.36%
2.57	186.8	24.87	2.20	4.65	3.03	47.36%	72.56%
2.58	193.8	24.81	2.26	4.81	3.14	47.00%	72.02%
2.59	196.0	24.79	2.26	4.86	3.17	46.51%	71.27%
2.60	196.0	24.79	2.26	4.86	3.17	46.51%	71.27%
2.61	198.9	24.77	2.28	4.93	3.22	46.28%	70.91%
2.62	203.6	24.73	2.34	5.04	3.29	46.47%	71.21%

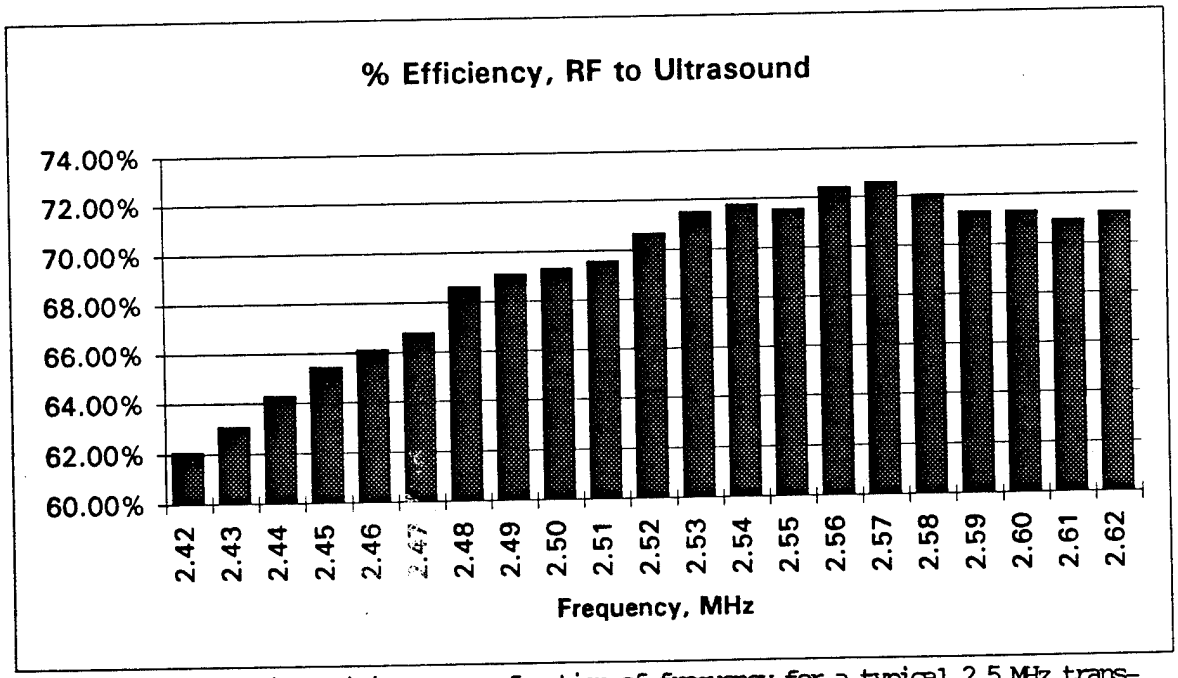

Figure 8. Acoustic efficiency as a function of frequency for a typical 2.5 MHz transducer used in the cylindrical array. Similar data exsists for each of 384 transducers.

Transducer Number		2-123				% Efficiency	
Freq. MHz	DC mA	DC Volts	US Watts	DC Watts	RF Watts	DC to US	RF to US
2.06	228.40	25.85	2.92	5.90	3.56	49.46%	82.10%
2.07	220.90	25.87	2.86	5.71	3.44	50.05%	83.08%
2.08	218.00	25.88	2.86	5.64	3.40	50.69%	84.15%
2.09	219.90	25.87	2.88	5.69	3.43	50.63%	84.04%
2.10	218.20	25.88	2.84	5.65	3.40	50.29%	83.48%
2.11	214.50	25.89	2.80	5.55	3.35	50.42%	83.70%
2.12	211.00	25.90	2.74	5.46	3.29	50.14%	83.23%
2.13	211.90	25.90	2.74	5.49	3.31	49.93%	82.88%
2.14	212.90	25.89	2.72	5.51	3.32	49.35%	81.92%
2.15	208.60	25.90	2.64	5.40	3.25	48.86%	81.11%
2.16	201.70	25.91	2.50	5.23	3.15	47.84%	79.41%
2.17	203.30	25.91	2.46	5.27	3.17	46.70%	77.52%
2.18	207.90	25.90	2.48	5.38	3.24	46.06%	76.45%
2.19	210.10	25.89	2.50	5.44	3.28	45.96%	76.29%
2.20	210.20	25.90	2.46	5.44	3.28	45.19%	75.01%

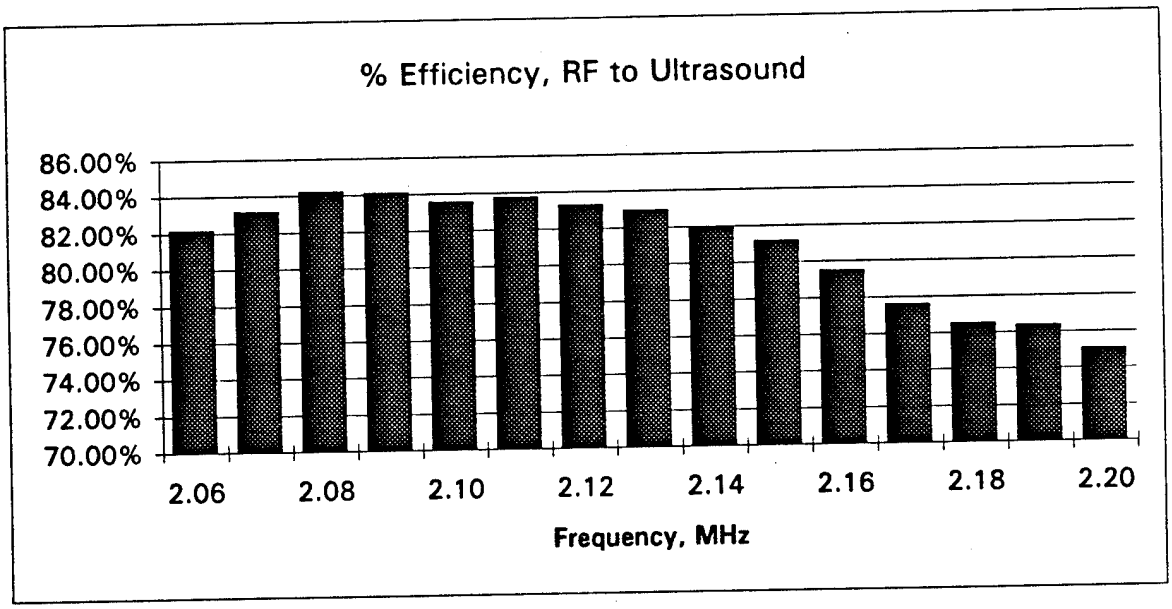

Efficiency from DC to RF is 60% as measured with Bird meter at 2 to 3 watts ultrasound.
DC to RF efficiency increases to around 75% at 10 watts ultrasound power
DC to RF efficiency increases to around 90% at 20 watts ultrasound power

Figure 9. Acoustic efficiency as a function for a typical 2.0 MHz transducer used in the cylindrical array. Similar data exsists for each of the 384 transducers.

Transducer Number		2-120				% Efficiency	
Freq. MHz	DC mA	DC Volts	US Watts	DC Watts	RF Watts	DC to US	RF to US
2.07	218.50	25.88	2.80	5.65	3.41	49.52%	82.20%
2.08	210.30	25.90	2.72	5.45	3.28	49.94%	82.90%
2.09	206.00	25.91	2.68	5.34	3.22	50.21%	83.35%
2.10	203.80	25.92	2.68	5.28	3.18	50.73%	84.22%
2.11	201.40	25.92	2.64	5.22	3.14	50.57%	83.95%
2.12	197.00	25.94	2.58	5.11	3.08	50.49%	83.81%
2.13	195.40	25.94	2.56	5.07	3.05	50.51%	83.84%
2.14	196.20	25.94	2.54	5.09	3.07	49.91%	82.85%
2.15	194.40	25.95	2.50	5.04	3.04	49.56%	82.26%
2.16	190.80	25.95	2.42	4.95	2.98	48.88%	81.13%
2.17	189.70	25.94	2.38	4.92	2.96	48.37%	80.29%
2.18	193.00	25.94	2.36	5.01	3.02	47.14%	78.25%
2.19	196.10	25.93	2.38	5.08	3.06	46.81%	77.70%
2.20	196.30	25.93	2.36	5.09	3.07	46.36%	76.97%
2.21	199.30	25.92	2.30	5.17	3.11	44.52%	73.91%

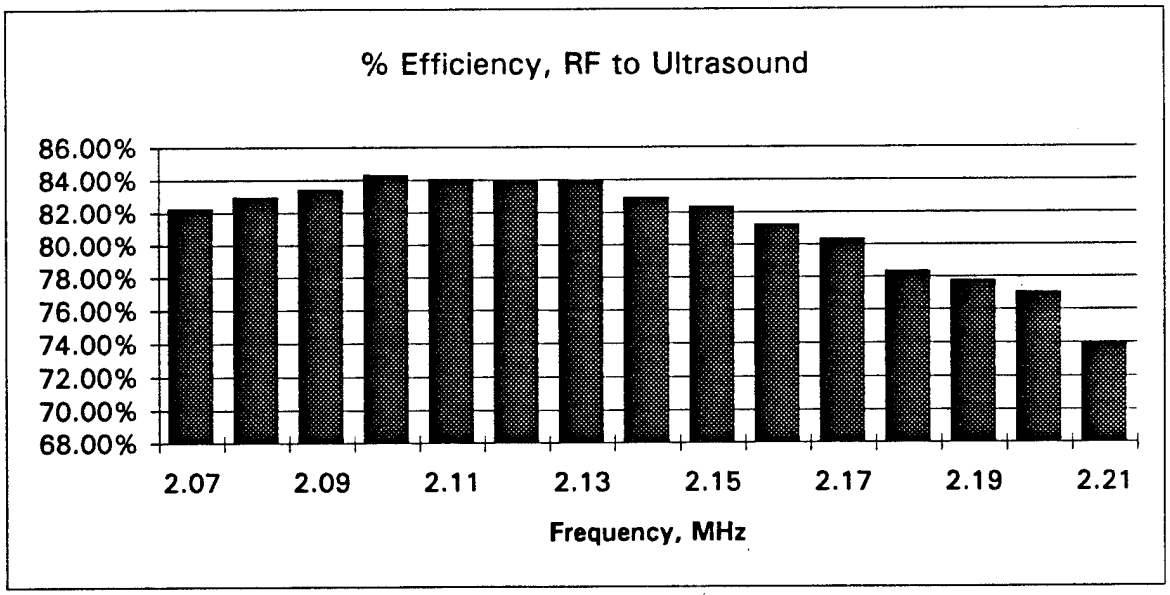

Efficiency from DC to RF is 60% as measured with Bird meter at 2 to 3 watts ultrasound.
DC to RF efficiency increases to around 75% at 10 watts ultrasound power
DC to RF efficiency increases to around 90% at 20 watts ultrasound power

Figure 10. Acoustic effiency as a function of frequency for a typical 2.0 MHz transducer used in the cylindrical array. Similar data exsists for each of the 384 transducers.

11-Apr-95 2:16 PM

Transducer Number		S-5C009				% Efficiency	
Freq. MHz	DC mA	DC Volts	US Watts	DC Watts	RF Watts	DC to US	RF to US
2.13	192.10	26.17	2.44	5.03	3.30	48.54%	74.02%
2.14	189.00	26.19	2.42	4.95	3.25	48.89%	74.56%
2.15	186.30	26.20	2.40	4.88	3.20	49.17%	74.98%
2.16	183.70	26.21	2.38	4.81	3.16	49.43%	75.38%
2.17	180.50	26.23	2.36	4.73	3.10	49.85%	76.02%
2.18	177.00	26.24	2.30	4.64	3.05	49.52%	75.52%
2.19	174.80	26.25	2.26	4.59	3.01	49.25%	75.11%
2.20	174.10	26.25	2.24	4.57	3.00	49.01%	74.75%
2.21	174.30	26.25	2.22	4.58	3.00	48.52%	73.99%
2.22	174.40	26.25	2.22	4.58	3.00	48.49%	73.95%
2.23	174.20	26.25	2.18	4.57	3.00	47.67%	72.70%
2.24	174.50	26.25	2.16	4.58	3.00	47.16%	71.91%
2.25	175.40	26.25	2.12	4.60	3.02	46.04%	70.22%
2.26	176.90	26.24	2.08	4.64	3.04	44.81%	68.33%
2.27	180.30	26.23	2.06	4.73	3.10	43.56%	66.43%

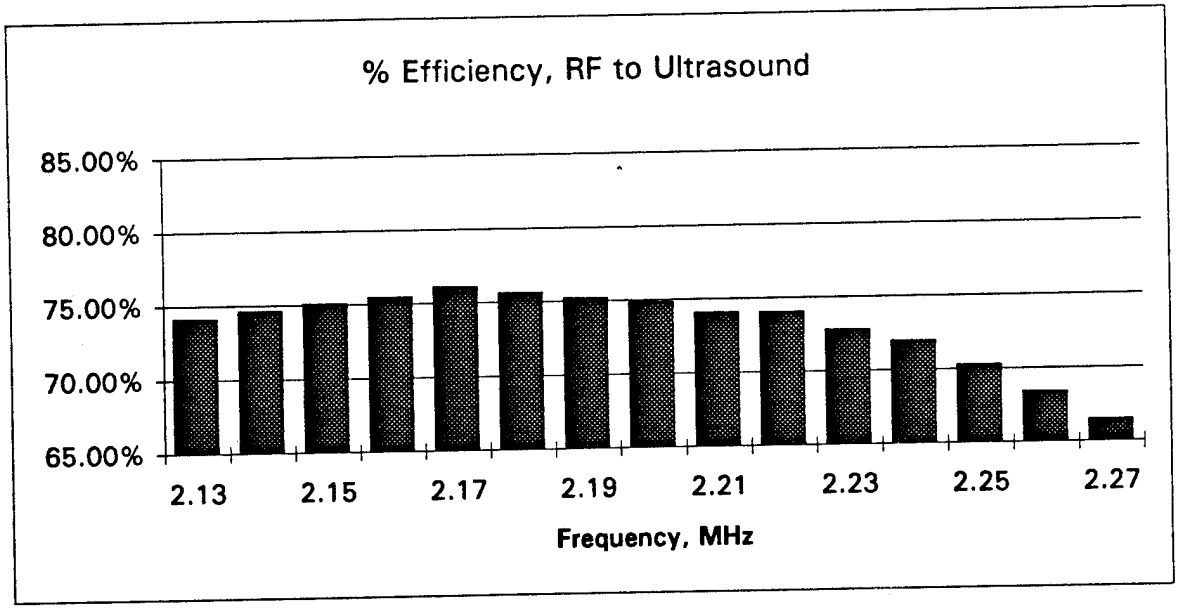

Efficiency from DC to RF is 60% as measured with Bird meter at 2 to 3 watts ultrasound.
DC to RF efficiency increases to around 75% at 10 watts ultrasound power
DC to RF efficiency increases to around 90% at 20 watts ultrasound power

Figure 11. Acoustic effiency as a function of frequency for a typical 2.0 MHz tranducer used in the cylindrical array. Similar data exsists for each of the 384 transducers.

11-Apr-95 2:18 PM

Transducer Number		S-5C005				% Efficiency	
Freq. MHz	DC mA	DC Volts	US Watts	DC Watts	RF Watts	DC to US	RF to US
2.10	191.90	26.18	2.40	5.02	3.29	47.77%	72.85%
2.11	188.40	26.19	2.36	4.93	3.24	47.83%	72.94%
2.12	185.00	26.21	2.32	4.85	3.18	47.85%	72.97%
2.13	182.90	26.22	2.32	4.80	3.14	48.38%	73.78%
2.14	181.20	26.23	2.30	4.75	3.12	48.39%	73.80%
2.15	180.10	26.23	2.30	4.72	3.10	48.69%	74.25%
2.16	178.20	26.24	2.28	4.68	3.07	48.76%	74.36%
2.17	176.00	26.25	2.24	4.62	3.03	48.48%	73.94%
2.18	173.70	26.26	2.20	4.56	2.99	48.23%	73.55%
2.19	172.40	26.26	2.18	4.53	2.97	48.15%	73.43%
2.20	171.60	26.27	2.16	4.51	2.96	47.92%	73.07%
2.21	172.00	26.27	2.12	4.52	2.96	46.92%	71.55%
2.22	173.00	26.26	2.12	4.54	2.98	46.67%	71.16%
2.23	174.60	26.26	2.08	4.58	3.01	45.37%	69.18%
2.24	176.90	26.24	2.08	4.64	3.04	44.81%	68.33%

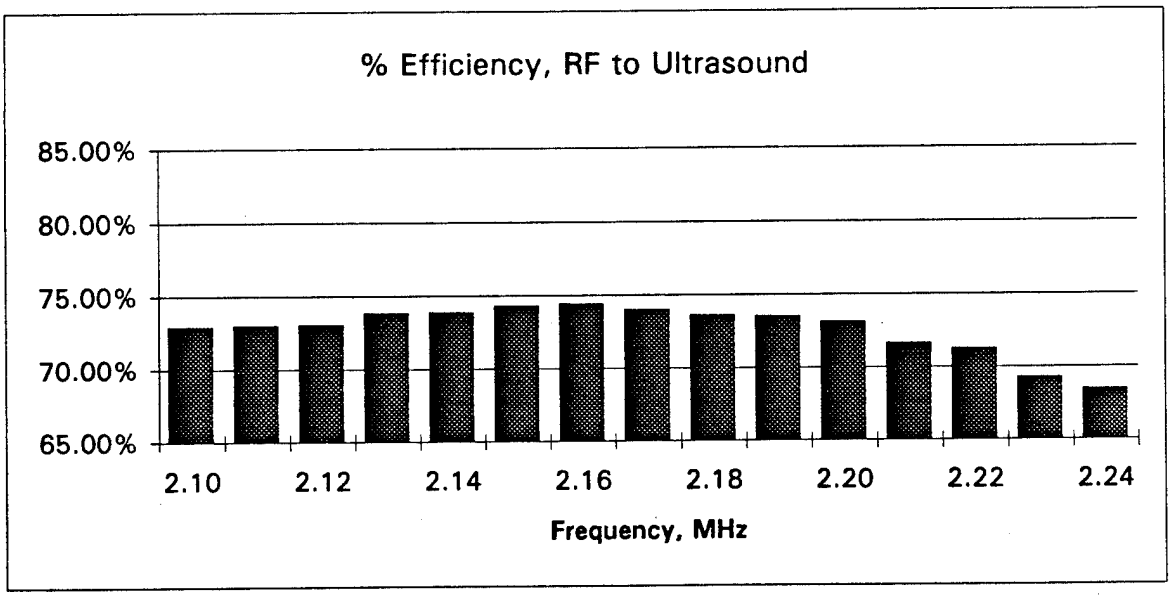

Efficiency from DC to RF is 60% as measured with Bird meter at 2 to 3 watts ultrasound.
DC to RF efficiency increases to around 75% at 10 watts ultrasound power
DC to RF efficiency increases to around 90% at 20 watts ultrasound power

Figure 12. Acoustic effiency as a function of frequency for a typical 2.0 MHz transducer used in the cylindrical array. Similar data exsists for each of the 384 transducers.

Note: This figure is the same as figure 3 on page 13.

Figure 13. Side view of rings comprising cylinder of 384 transducers.

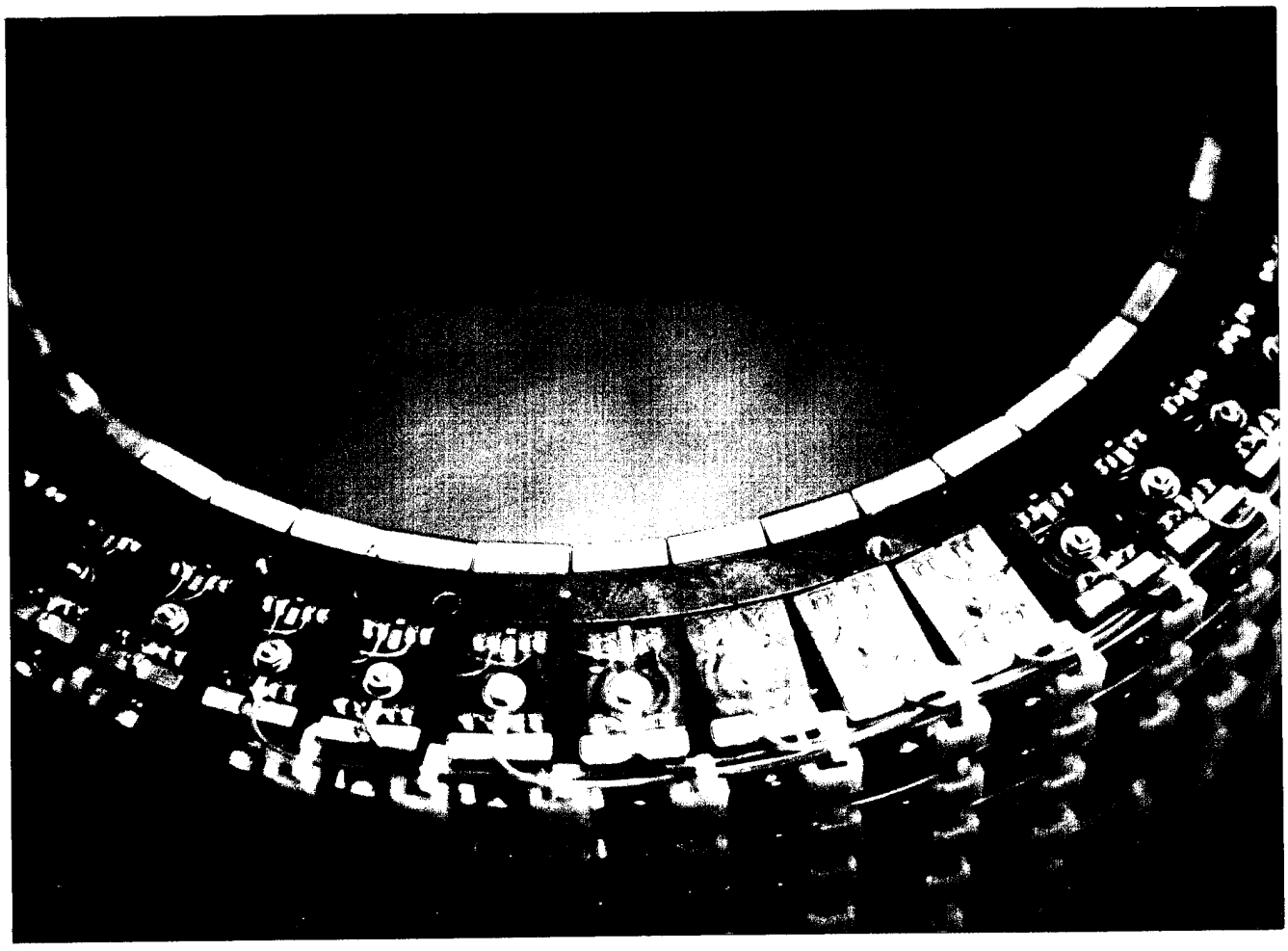

Figure 14. Close up view of a section of the cylindrical array.

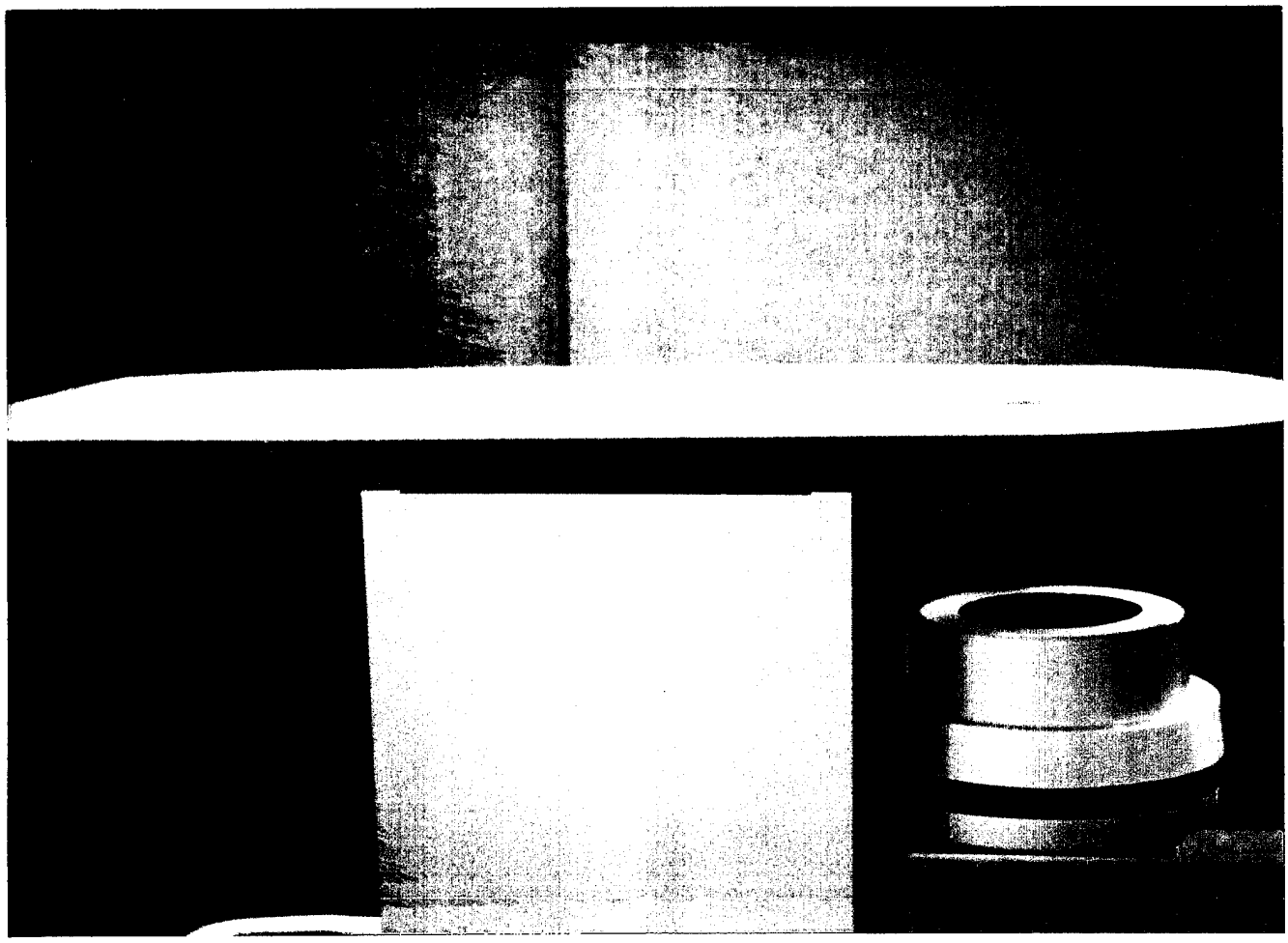

Figure 15. Side view of the patient table subsystem. All system electronics are housed within the enclosed central support structure. The cylindrical array is located beneath the aperture in the table top (right side of photo).

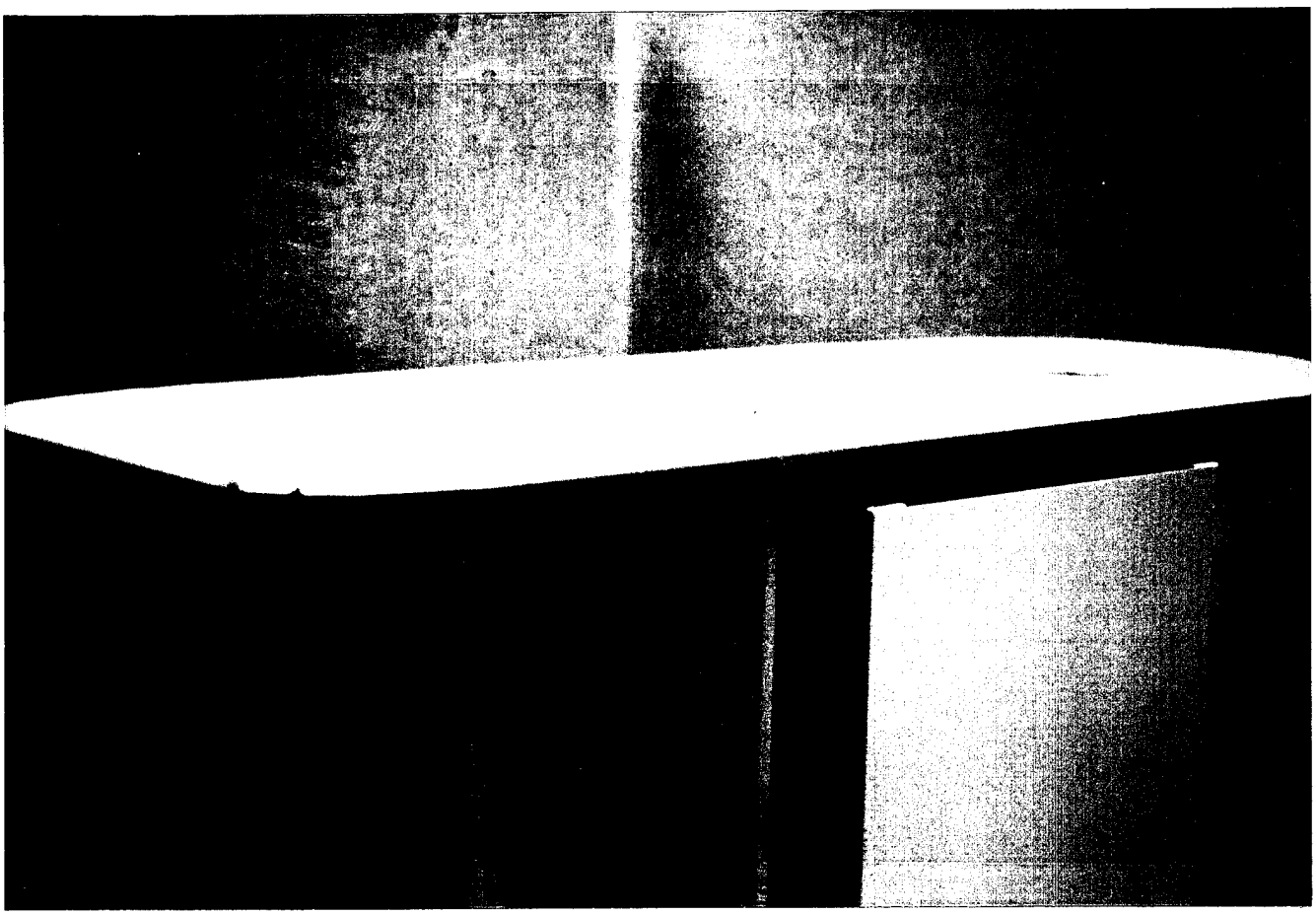

Figure 16. Rear view of patient table subsystem. Curved panel at rear is a hinged access door to most system electronics. The instrument computer and thermometry subsystem are housed behind the dress panel covering both sides of the central enclosure.

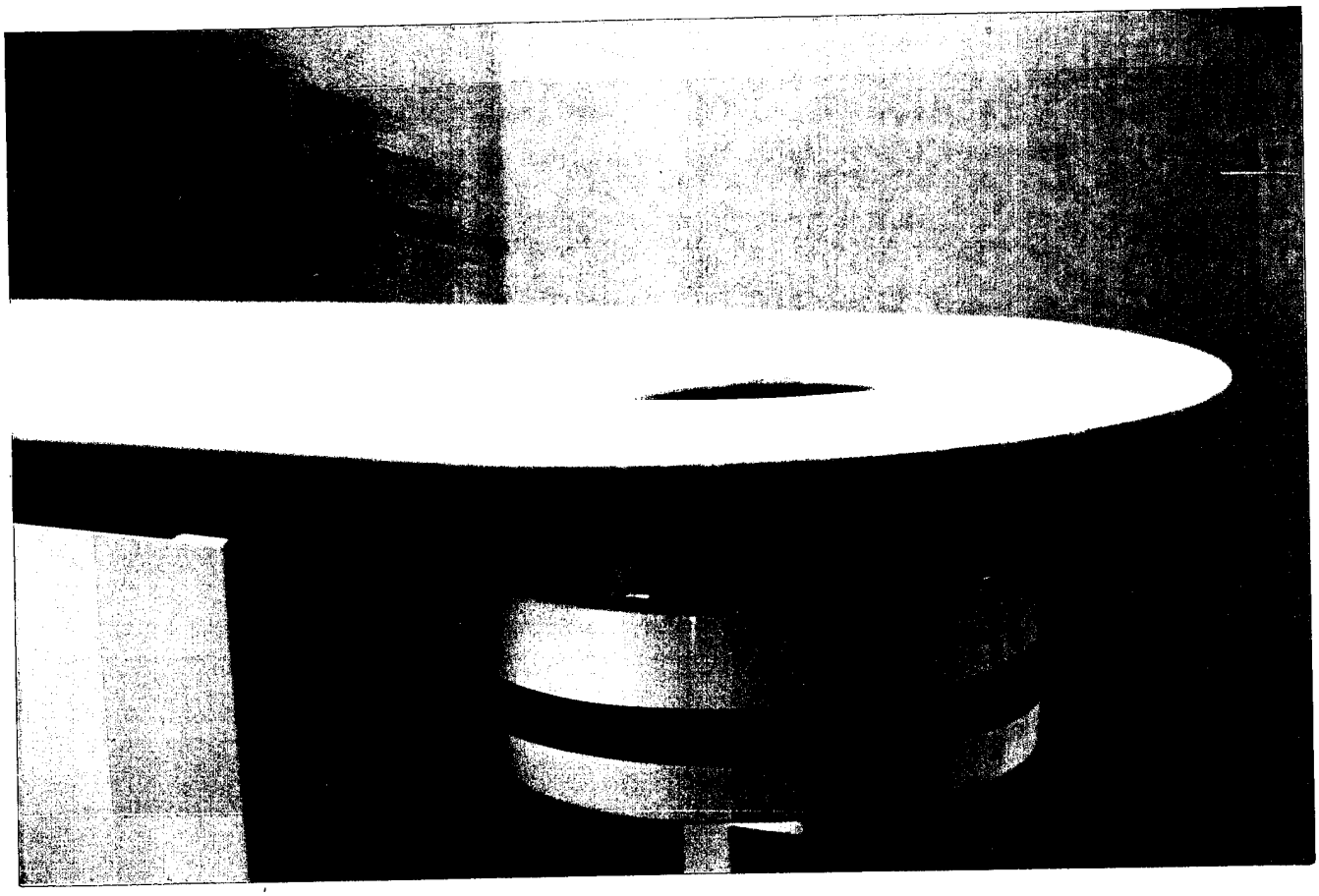

Figure 17. Close up view of the patient table front and shroud enclosing the cylindrical array of transducers.

PATIENT TABLE SYSTEM SPECIFICATIONS	
Table Top Overall Length:	78"
Table Top Height (to floor):	37"
X-Y Table: Positioning	± 2.5" X-Y Vernier Drive ± 6" Vertical Motion Motor Drive 180° Rotation Capability - Motor Drive
Structural Materials:	Stainless steel
Paint:	Non-toxic textured (Color chip supplied by Dornier)
Construction Restrictions:	No sharp edges
Aesthetics:	Per design drawings
Load Capacity:	300 lbs.
Table Top Hole Size:	10" diameter
Table Top Cover:	Naugahyde cover (with snaps or velcro) over 1 1/4" foam pad
Other Requirements:	Make sure areas that could get patient fluids on them can be easily cleaned. There should be no areas where spilled fluids could be trapped.

TABLE 3

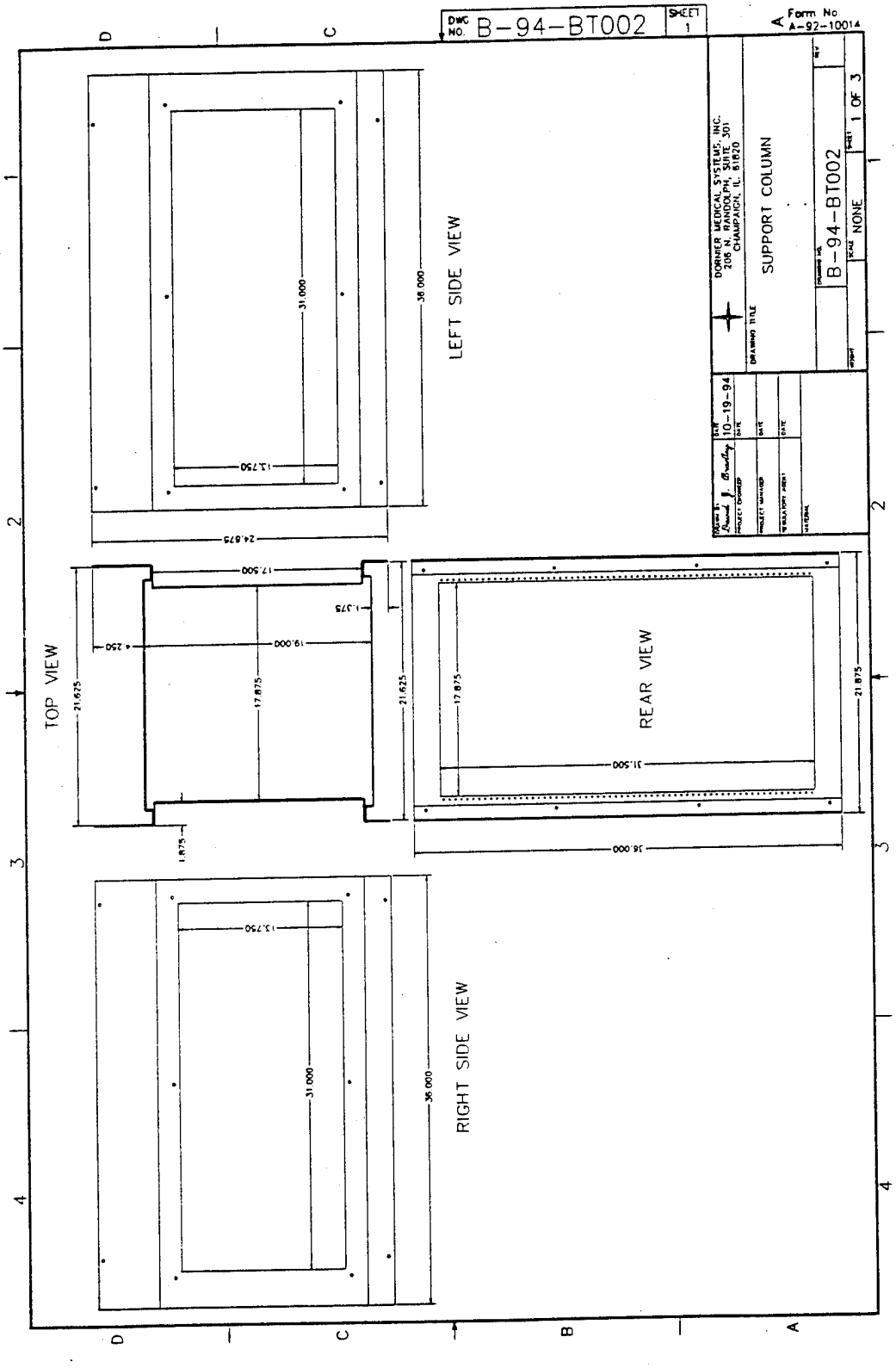

Figure 18. View of support column.

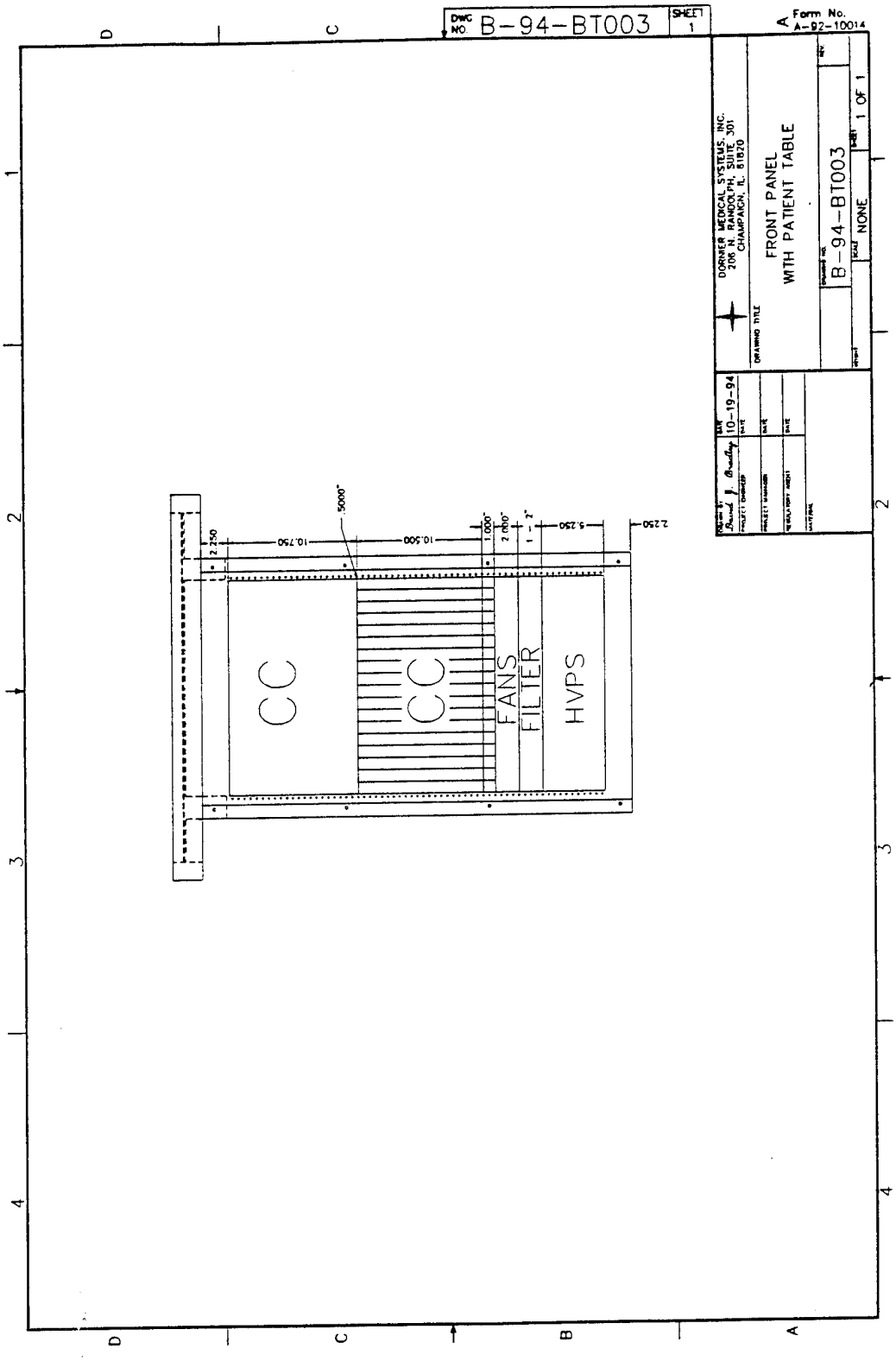

Figure 19. Drawing of internal layout of the key electronic system components inside the table central column

2.C. System Control Design

When power is turned on to the system, the treatment software initializes automatically so that no interaction is required by the user to start the software. All available options are displayed to the user in a graphical format. Options that will be available at the startup screen include access to the treatment planning software, file handling utilities, diagnostic mode selections, treatment record printing, and treatment initiation. The user makes requests of the system via the computer keyboard, computer mouse, or a mechanical pause switch during all phases of the treatment. A hardware Pause switch is provided that guarantees no power output will occur in case of emergency.

Prior to beginning a treatment, the user will be required to complete a treatment plan. The treatment planning software is in graphical form to simplify data entry, such as target volume locations, the number and location of temperature sensors, target temperatures for each sensor, scar tissue locations, and patient information.

The computer system can perform the treatment in both automated and manual modes. When performing a treatment in the automated mode, very little user interaction will be required during the treatment; however, the user will still be capable of interrupting the computer and/or provide advice to the computer concerning the treatment. When in manual mode, the user will be allowed to select different target tissue regions on the computer screen and set a new target temperature value for each region. The computer system will then determine which ultrasound transducer's output power needs to be adjusted to accommodate the user's request.

Treatment progress and status information is available to the user via a graphical user interface that provides treatment information such as temperature distribution, power absorption distribution, thermal dose distribution, target contour information, and treatment time information. The operator is not required to determine power levels for the individual transducers since temperature distribution information is continually available on a graphics screen. The operator has the capability to make suggestions about the target temperatures for locations where implanted sensors are placed as well as other locations in the target volume. Further, the operator may manually select and adjust the power on any active transducers (e.g. reduce power deposition directly over a scar). Selection of active transducers, control of receive and transmit mode and gated on-off periods are under control of the Instrument Computer.

Once a treatment has been completed, the user will be returned to the startup screen so that printing of the treatment information may be performed, and duplication of the treatment files may be accomplished.

2.D. TMR Subsystem

The TMR (Transmit-Multiplex-Receive) subsystem is the "heart" of the system's electronics. It resides on a custom 10in. x 16in. four layer circuit board, with sockets for two daughter boards - a microcontroller board(MCB) and a digital signal processor

(DSP). The TMR subsystem includes the RF power generators and VCO's, transmit-receive (T/R) circuits, receiver circuits, transducer multiplexer circuits, an on-board microcontroller, daughter card and provision for addition of a DSP. The breast therapy system contains 25 TMR subsystem boards, 24 being for system therapy and noninvasive interrogation operation and one for temperature probe location. Each TMR subsystem contains four independent RF generators with separate VCO's, receiver circuits, T/R switches, and multiplexers for driving 16 transducers. All functions on the TMR are controlled via the daughter board microcontroller (a custom-designed six-layer surface-mount board). The microcontroller interfaces to the system's Instrument Computer.

The evolution of this design has taken 1 1/2 years. The initial system concept provided for a curvilinear array of 32 to 64 transducers, with separate RF power generation circuits. The modeling and simulations performed in Year 01 defined the need for greater control of power deposition than could be achieved with a 32-64 transducer array. Since microwave radiometry originally was planned for making noninvasive temperature measurements, there were no receiver circuits, T/R switches, or multiplexers in the design. However, performance analysis of the microwave radiometry resulted in its abandonment due to several reasons: 1) opportunity for better spatial resolution and use of ultrasound therapy array (cylindrical) to "map" breast cross-sections real-time and provide better noninvasive feedback; 2) poor spatial resolution of target by microwave radiometry; 3) poor penetration depth of microwave radiometry; and 4) difficulties in implementing both microwave and ultrasound arrays simultaneously covering the same target. Thus, the need for a separate ultrasound measurement receiver system was determined, which would function integrally with the system's cylindrical array of ultrasound transducers. This opened the requirement to provide low-noise, low-loss, high power handling capacity signal multiplexing and T/R switching. The computer modeling and breast simulations performed in year 01 defined the need for many more ultrasound transducers than anticipated in the original proposed design (close to and 400 transducers instead of 64 total). This requirement determined that many RF generators would be required (1 for every 4 transducers). The new design results in far more system capability and flexibility, both for therapy and noninvasive monitoring.

Each circuit in the TMR subsystem was designed and breadbroarded in Year 01. During Year 02, many changes related to improved performance or adding subsequent functionality were made in the design. Again, each modified/improved circuits was breadboarded and tested. Late in Year 02 the custom board layouts were developed. A block diagram and root schematic of the TMR subsystem is shown in Figures 20 and 21, respectively.

This comprehensive design, including T/R switches and receivers plus DSP provisions, required nearly three-quarters of a year to develop and breadboard test. It is important to realize, however, that proceeding with the therapeutic section of the system without completing the integration designs, breadboards, and testing of the pulse receiver and T/Rs would have meant major redesigns and retrofits at a

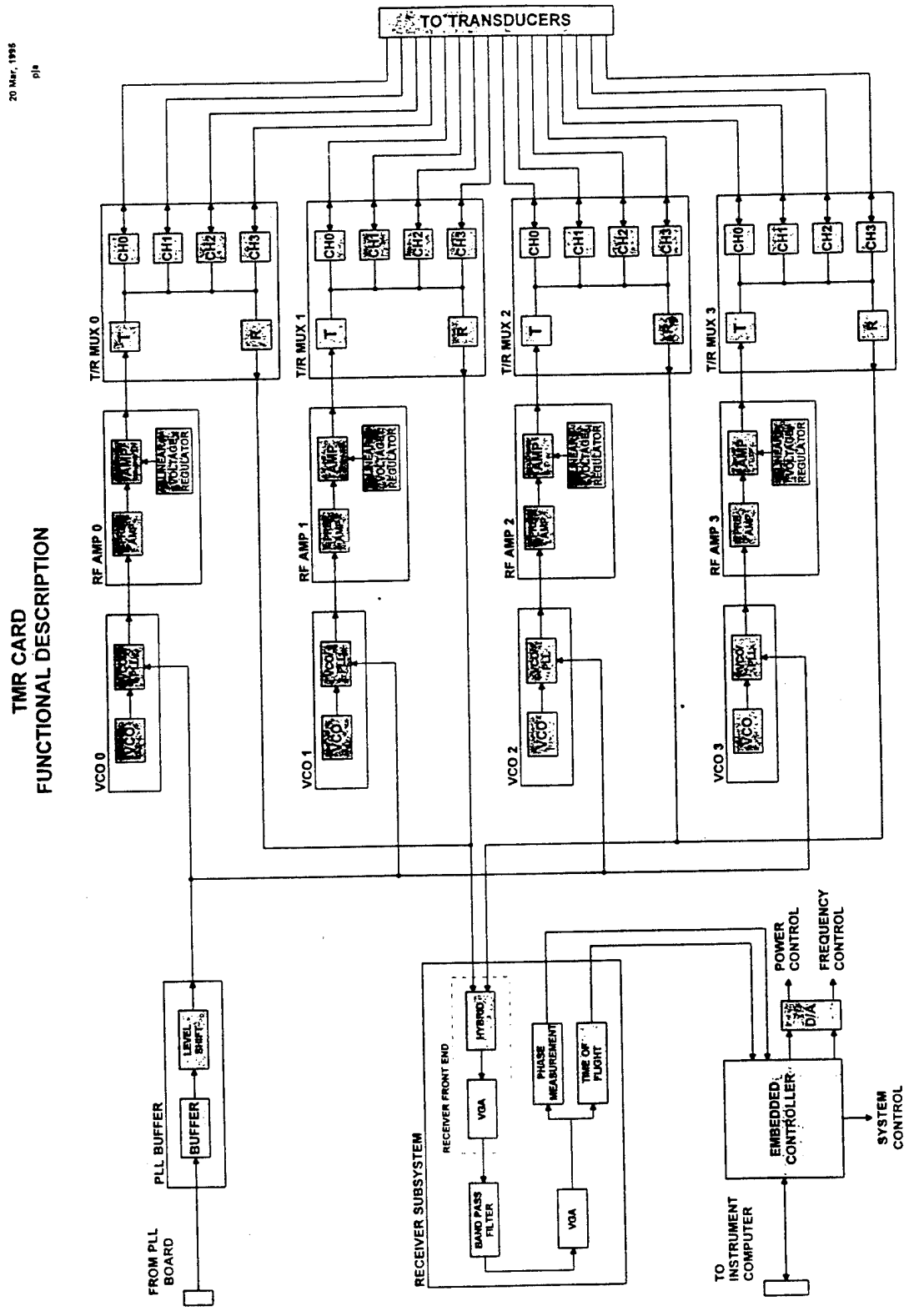

Figure 20. Functional block diagram of TMR subsystem.

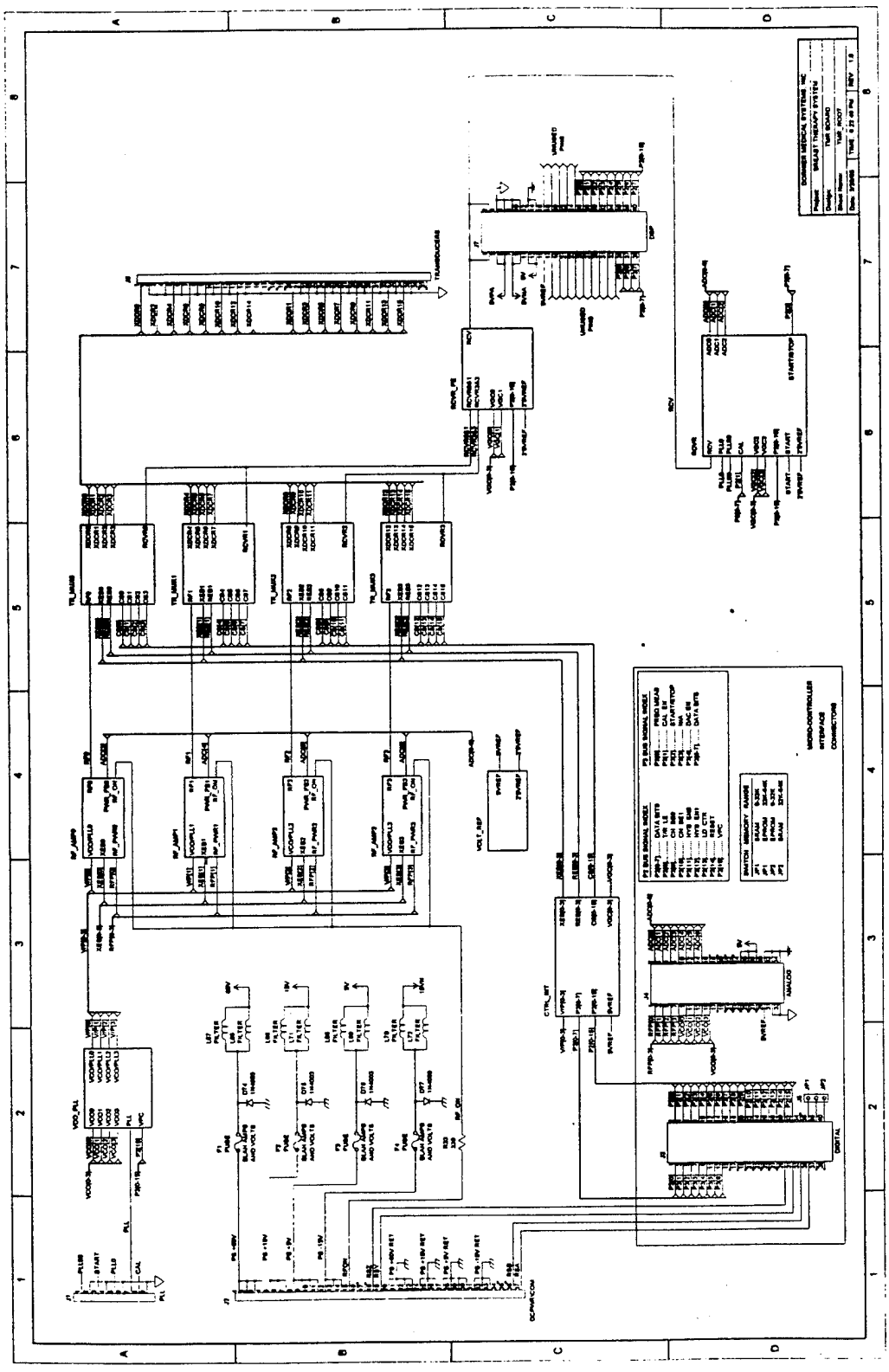

Figure 21. TMR subsystem schematic denoting the various modules/sections contained within each TMR board.

subsequent time. All of the system circuit boards would have necessarily been replaced at significant time loss. Thus, it was more efficient to "design in" the added functionality.

Each section of the TMR subsystem is described in detail as follows.

2.D.1. RF Section

The RF Power Section consists of 96 independent RF amplifiers driven by 96 separate oscillator sources. Each oscillator consists of a computer-controlled VCO operating over the frequency range of 1 - 5 MHz and is used to drive one RF amplifier. Each oscillator is preset to operate at one of the three operating frequencies (2.0, 2.5, 4.5MHz). The individual VCOs frequency may controlled by the microcontrollers under direction of the Instrument Computer. Each of the 96 independent RF amplifiers incorporates its own voltage control/regulator circuit which provides independent computer control of amplitude (output power level) for each amplifier channel. A block diagram of the RF Amplifier Subsystem is shown in Figure 22. Each RF amplifier output is connected to a T/R MUX input circuit.

2.D.2. Receiver Section

The Receiver Section consists of 25 independent receiver with 24 dedicated to noninvasive monitoring and one for temperature probe location. Inputs can be received from any of the 384 transducers in the array, dependent upon multiplexer selection. Each of 24 receiver circuits receives inputs from up to 16 transducers and multiplexes those transducer signals to two receiver hybrids per card. There are 24 identical circuits comprising the Receiver Section plus two cards with sampling, phase comparator, and PLL circuits. Specifications for the receiver hybrids are listed in Table 4. Each hybrid consists of an analog multiplexer and a 15dB low noise amplifier as illustrated in Figure 23. The hybrid output is processed through two high gain VGA stages as shown in Figure 22. Receiver outputs are digitized and sent to the Instrument Computer for processing. The complete Receiver Section block diagram is illustrated in Figures 24 and 25.

2.D.3. T/R Mux Section

The Transmit-Receive Multiplexer blocks connect each of the transducers in the array to the RF amplifiers and the receivers. The fundamental block has 6 ports, 4 of these are for individual transducers, 1 is for transmit RF, and 1 is for receive. The design consists of 6 single pole RF diode switches all connected to one common pole. Certain switch combinations are not desired such as transmitting at high power levels into the receiver so control logic prevents this and other undesired combinations. Performance of the design was evaluated at 4.5 MHz and is slightly better at 2.5 and 2.0 MHz. Transmit loss was around 0.1 dB, receiver loss was 1.0 dB, transmit receive isolation was 58 dB, and cross channel isolation was 35 dB. Each TMR card has 4 of the basic T/R Mux blocks, the system has 24 fully used TMR cards so 96 of the T/R

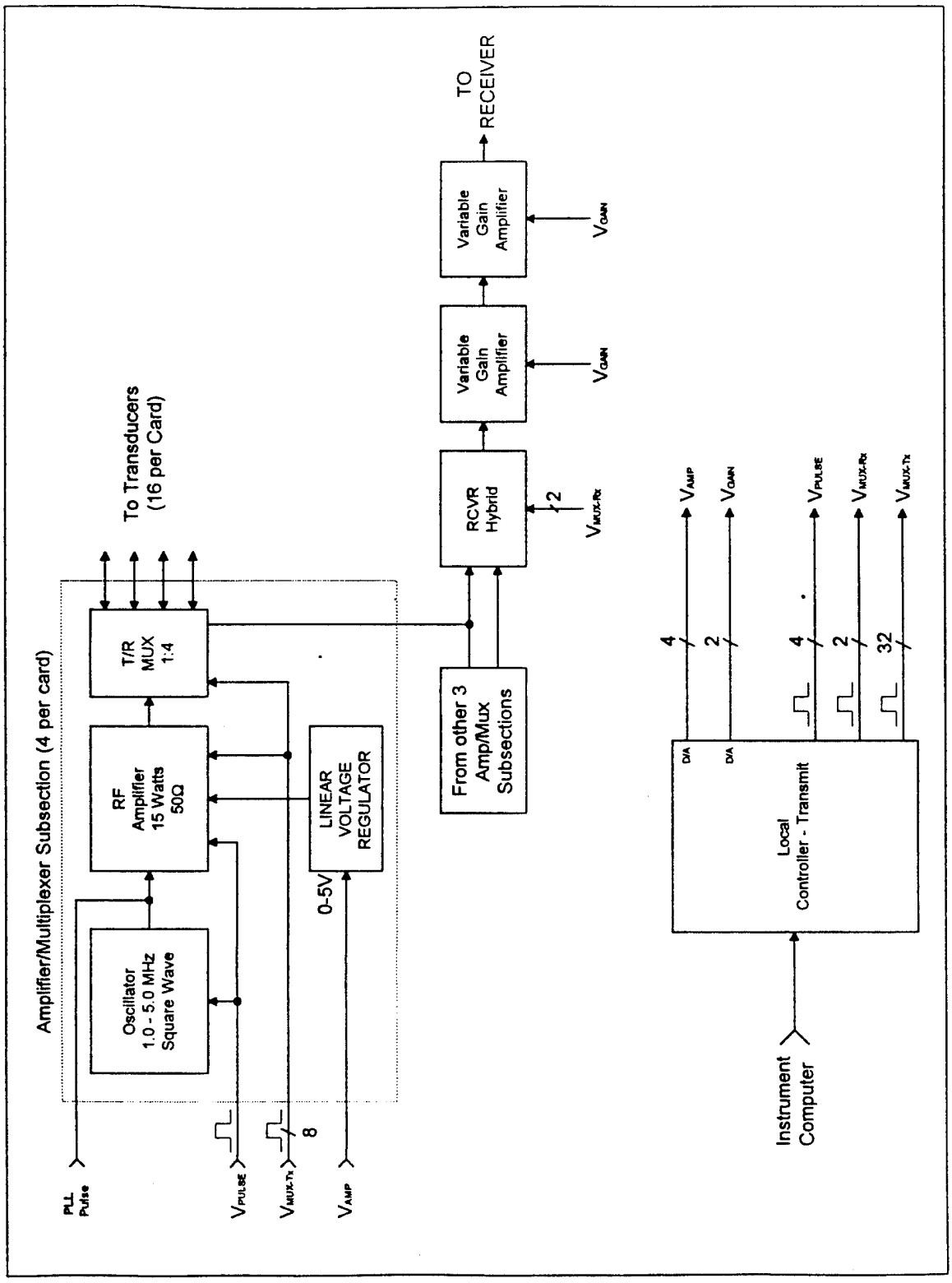

Figure 22. Transmitter/Multiplexer/Receiver (TMR) Section (1 of 2)

RECEIVER HYBRID PERFORMANCE & INTERFACE SPECIFICATIONS	
Output Impedance:	50 ± 10Ω at 5.0MHz
Output Level:	1.0Vpp, non-distorting 5.5Vpp, Max.
Gain:	15 ± 1.0dB
Gain Flatness:	≤ 0.5dB, from 2 to 20 MHz
Equivalent Input Noise:	2nV/_Hz with Rs = 100Ω
Frequency Response, -3dB	50kHz - 42MHz, typical, 200kHz - 40MHz, worst case.
Isolation:	35dB @ 10MHz, adjacent channels
Input Impedance:	RF: 620Ω 92pF
DC Input Bias:	-2.55 V ± 0.07 V (selected), +1.57 V ± 0.1 V (not selected). 5 mA typ from a DC short.
Input Overvoltage: pulsed clamp	POSITIVE: +60V (1A max. current), +20V continuous. NEGATIVE: -140V. max.
Receiver Recovery Time:	1μS typ. after pulser fire.
Receiver Enable/Disable Time:	≤ 10 μS from control signal.
Differential Group Delay:	≤ 2 nS, 2MHz to 20MHz.
Control Signals (ENX, ENY) Selected: Unselected:	 +5.25Vmax, +3.90min. +3.00Vmax, -1.00min.
Control Signal Current:	≤ 1μA @ +5.0V, 1mA @ 0.0V, 5mA max transition.
Power Consumption:	+5V @ 5.0 ± 0.5mA +12V @ 20 ± 2mA -12V @ 26 ± 2mA

TABLE 4

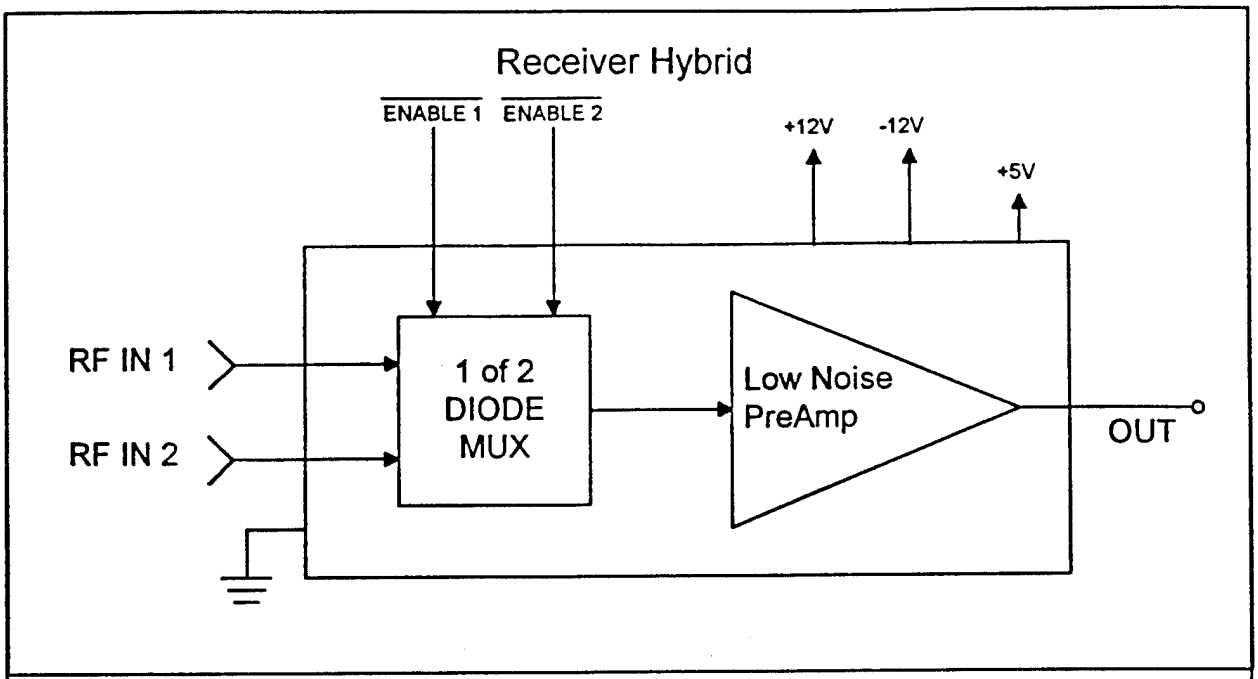

Figure 23. Receiver Hybrid

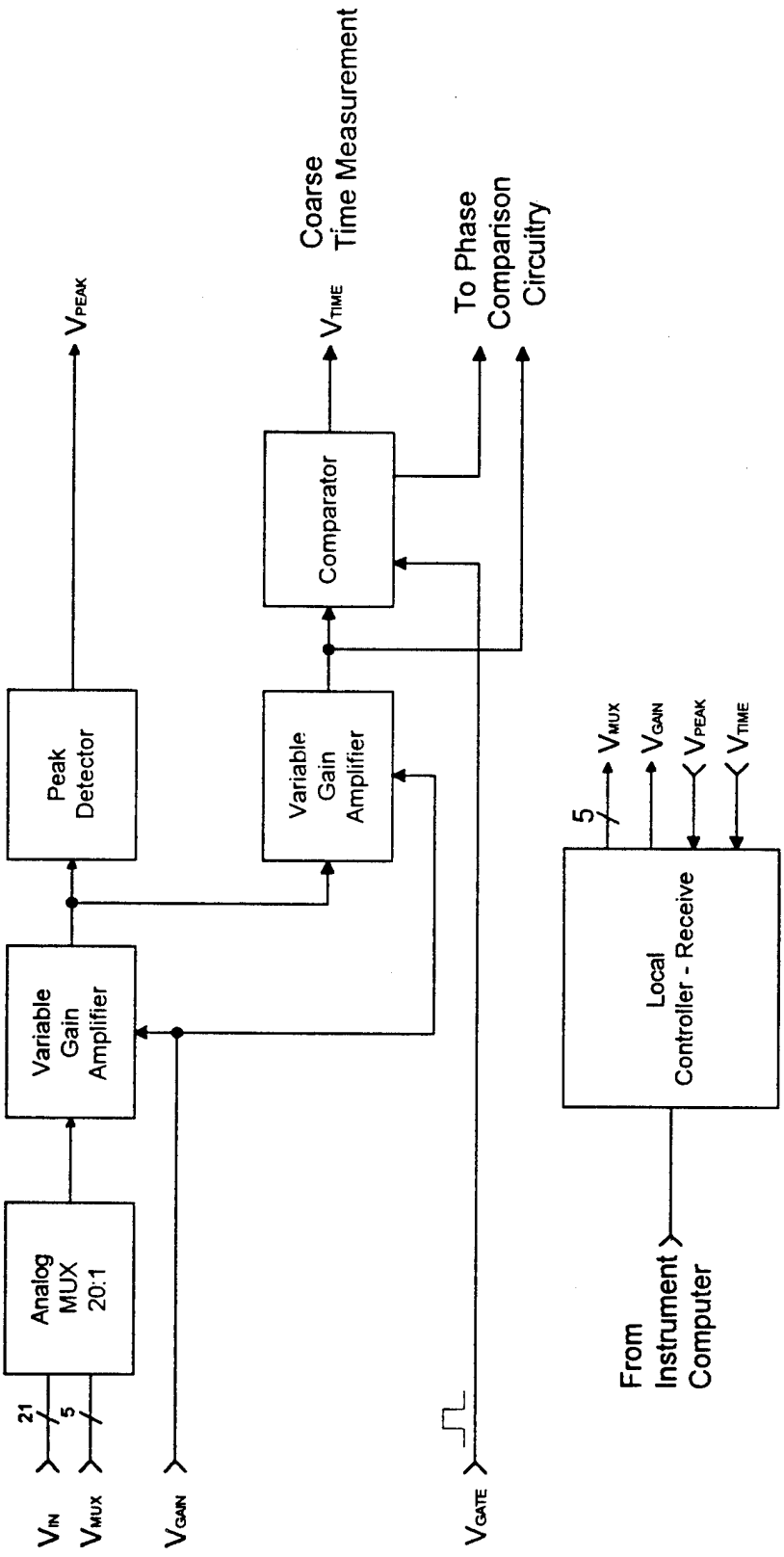

Figure 24. RF receiver amplitude and coarse TOF measurement.

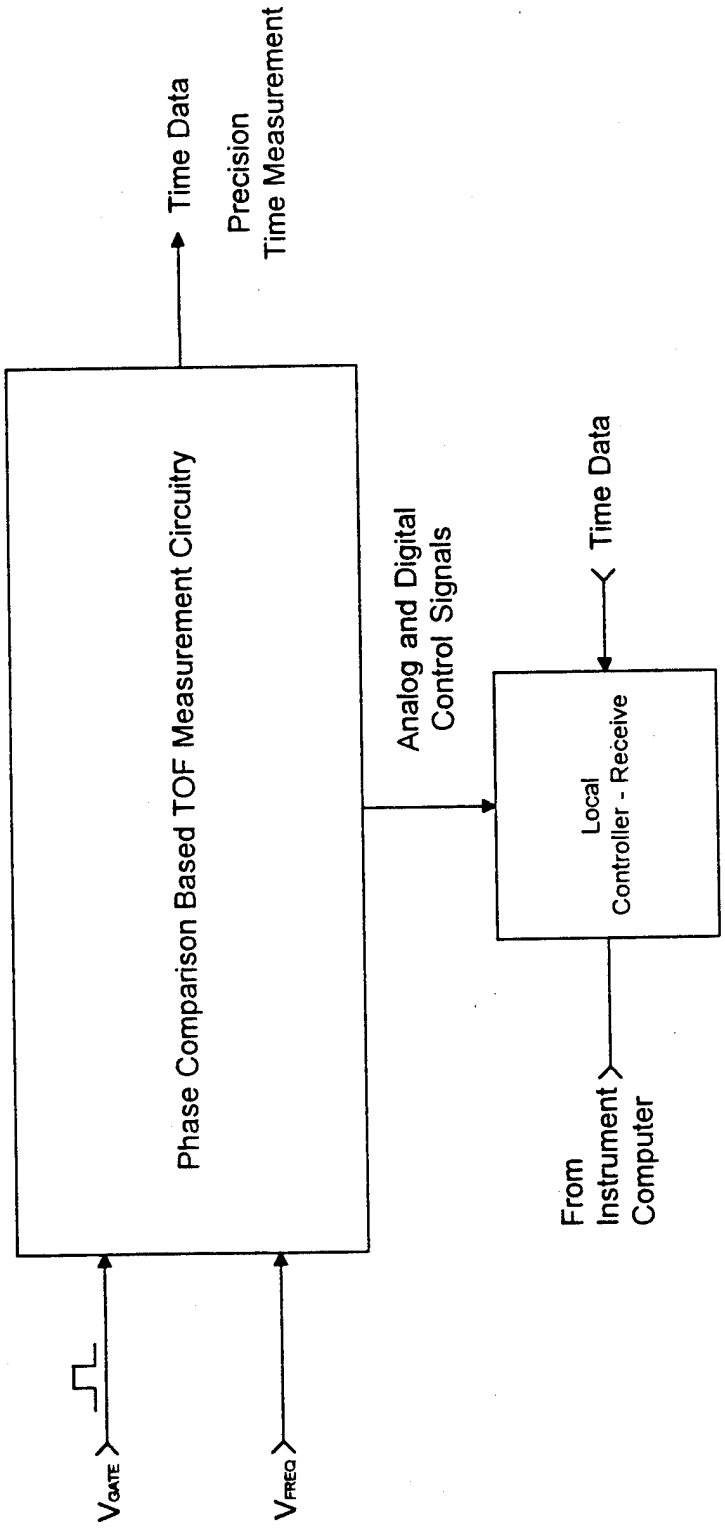

Figure 25. Phase comparison based TOF measurement circuitry.

Mux circuits allow for 96 RF amps to drive 384 transducers and 96 receiver ports are further multiplexed down to 24 receivers.

2.D.4. Microcontroller Section

A separate surface-mount microcontroller daughter card is mounted onto (and plugged into) the TMR subsystem board. The microcontroller was designed and fabricated during year 02. The original design did not include a microcontroller for each group of 4 amplifiers(16 transducer channels); instead, all control and monitoring functions were handled directly by the Instrument Computer. While this approach was probably workable, it severely limited the overall functionality of the system. Changes to the applicator array or to the receivers would be very difficult to accommodate without the on-board local controllers. Further, without the microcontrollers, implementation of on-board digital signal processing of the noninvasive monitoring data would be close to impossible.

The schematic of the microcontroller daughter card is shown in Figure 26. The processor contains on-board memory and 64 Bytes of SRAM. Each mocrocontroller board also contains 16 digital control lines and 8 each A/D and D/A lines. The requirements of this therapy system were unique enough that it would have been very difficult to implement an "off the shelf" controller board. Also, physical space constraints in this system are severe. As a result, we designed and layed out our own circuit card a 6-layer surface mount 3"x 5" package. The microcontroller card layout is shown in Figure 27. Much of the receiver peak-detect and A/D functionality have been shifted to the microcontroller, whose programmable functions can be optimized.

2.D.5. VCO/PLL Input Section

The TMR subsystem board contains a section which permits injection of a phase-locked oscillator source into the RF generator/amplifier circuits on a selected channel basis. The PLL input is buffered through phase-matched buffer arrays to maintain equal phases to all amplifier inputs. This permits use of the same generator/amplifiers for both therapy and pulsed signal interrogation. During the therapy mode, the VCO on each generator section drives the RF amplifier. The VCO frequency is computer-controlled by the microcontroller under direction of the Instrument Computer. Since each RF generator/amplifier section of the TMR subsystem has its own VCO, the outputs of each amplifier are incoherent. This permits avoidance of any undesired phase addition or cancellation in the emitted ultrasound energy used for thermal therapy. During the interrogation mode of system operation, it is imperative that the pulse signal be phase-locked to a single source in order to permit accurate measurement of pulse-echo and through-transmission times. This in turn permits accurate representation of the breast contour on the operator's treatment screen. Also, it is essential for noninvasive monitoring and reconstruction. This section of the TMR subsystem functions to switch the generators/amplifiers between these two modes and to provide buffered, phase-matched signals to the drivers. It is shown on the upper right corner of the TMR layout in Figure 28.

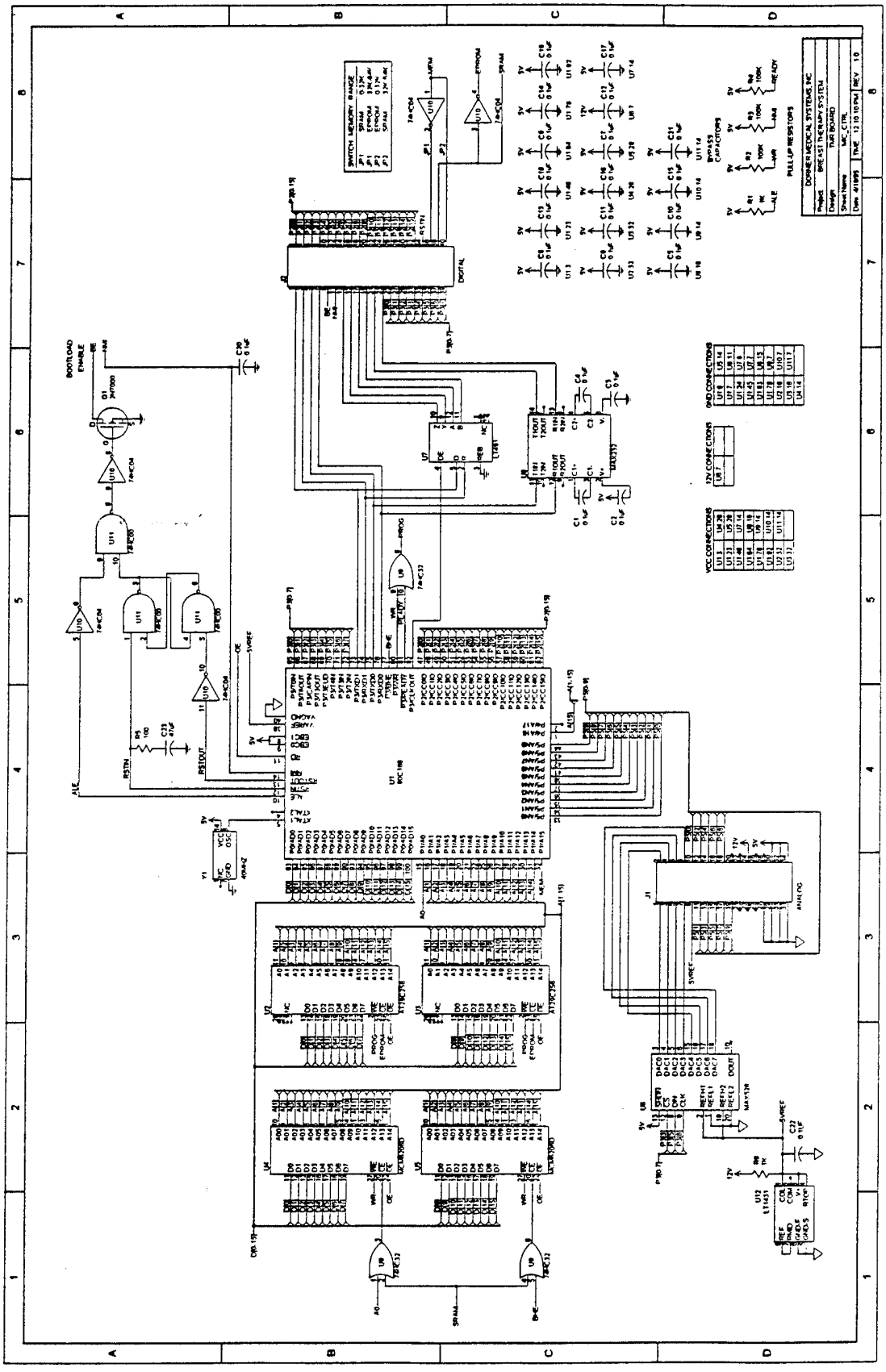

Figure 26. Schematic of the TMR microcontroller used for all local control and data acquisition functions.

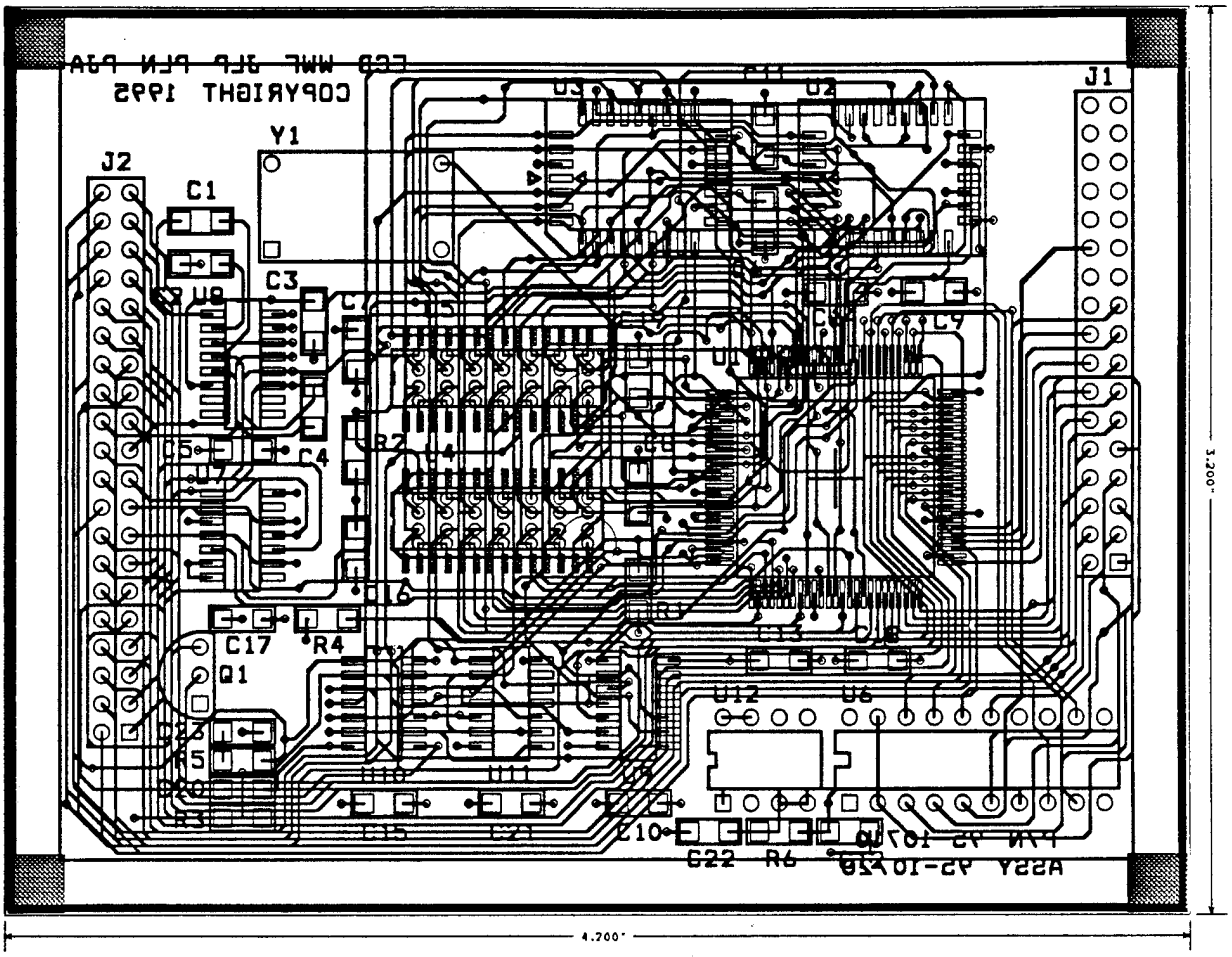

HOLE LEGEND				
SYM	DIAM	TOL	QTY	NOTE
×	0.020	+/- 0.005	282	(IN)
+	0.022	+/- 0.005	56	(IN)
◇	0.034	+/- 0.005	35	(IN)
⊠	0.040	+/- 0.005	74	(IN)
TOTAL			447	

Figure 27. Microcontroller card layout.

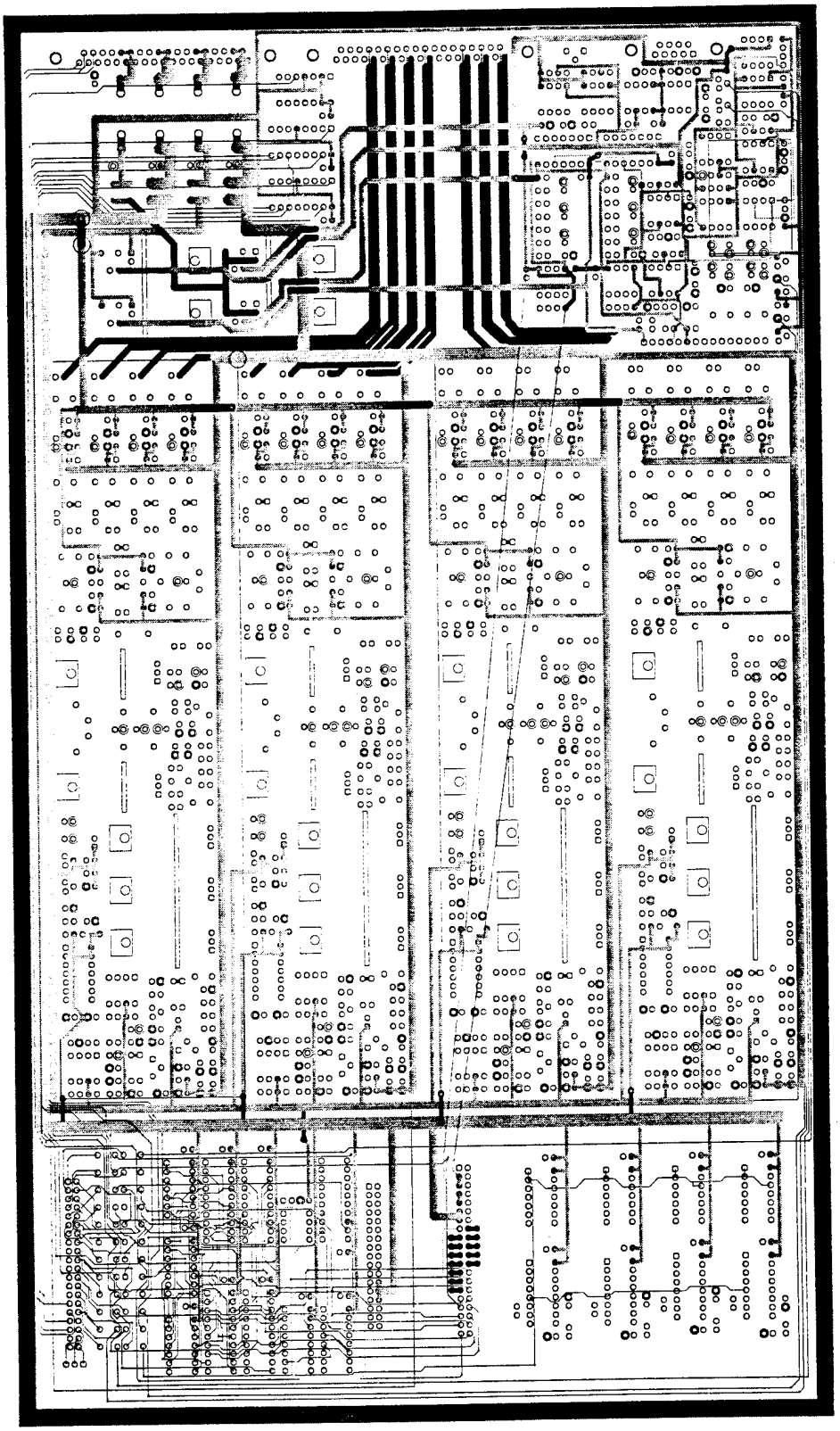

Figure 28. Transmitter/Multiplexer/Receiver (TMR) card layout.

2.D.6. DSP Add-On Provision

This section of the TMR subsystem represents one of the important "looking ahead" features which has been incorporated into the breast ultrasound therapy system. The TMR circuit board contains sockets for plug-in addition of a digital signal processor (DSP) to be developed at a future date (Figure 28). DSPs are widely used today in many applications and in this case, will provide the only reliable method to obtain "clean" received signals for the through-transmission data to be used for both noninvasive temperature monitoring and real-time breast image reconstruction within the treatment system. This work is beyond the scope of the present contract. It is a very important provision, however, and is the only method whereby these capabilities may be readily retrofitted to the overall system without complete rework of the TMR subsystem at considerable cost and time consumption.

2.E. Non-Invasive Monitoring Subsystem

The noninvasive monitoring subsystem resides on the TMR subsystem circuit cards and on three separate circuit cards contained within the system enclosure.

The receiver section of the TMR subsystem, in conjunction with the T/R Mux circuits and VCO/PLL control circuits comprise the heart of the noninvasive monitoring subsystem. This portion of the system changes the functional state of the transducers from therapy to target interrogation and receives both reflected and transmitted signals from and through the breast, respectively. Functional descriptions of each of these TMR subsystem sections are given previously in Section 2.D. of this report.

One of the three additional circuit cards contains the phase-locked oscillators for each of the three transducer interrogation-mode operating frequencies (2.0, 2.5, 4.5 Mhz), filters for eliminating noise from the high-resolution time measurement signals, and the time-of-flight (TOF) measurement circuitry. A microcontroller also resides on this card for the purpose of communicating with the Instrument Computer which directs the TOF measurements. The other two cards contain large phase-matched buffer arrays for distributing the phase-locked oscillator outputs to each of the 96 RF generator/amplifier channels. These systems are now complete and functionally tested.

The functionality of the receiver and noninvasive measurement circuits were tested through a series of laboratory measurements. A single 48-transducer ring from the cylindrical applicator was set up in the laboratory and excited using the phase-locked pulsed RF generator circuits. A tissue-equivalent breast phantom was inserted into the applicator ring for these measurements. Each transducer in the ring was individually excited and both reflection and through-transmission measurement data recorded. Baseline data were first recorded without a target and then with the breast phantom in place. A summary of the pulse-echo results is presented in Table 5. These data include both and time and amplitude information for both cases. Data were taken for both the 2.0 MHz and 4.5 MHz transducers and the distance to the far wall of the

Table 5. Ping-Echo results.

	With Breast Target					Without Breast Target					
Transducer Number	Actual Input Voltage	Actual Received Voltage	Normalized Received Voltage	Echo Time (2-way)	Distance to Target	Actual Input Voltage	Actual Received Voltage	Normalized Received Voltage	Echo Time (2-way)	Distance to Far Wall	Frequency
1	15	0.48	2.720E-03	92	6.81	0.103	6.10	5.034E+00	340	25.16	2.143
2	63	5.60	7.556E-03	92	6.81	0.25	5.20	1.768E+00	340	25.16	4.471
3	15	2.50	1.417E-02	98	7.25	0.103	6.40	5.282E+00	340	25.16	2.16
4	63	1.75	2.361E-03	96	7.10	0.25	2.35	7.990E-01	340	25.16	4.562
5	15	1.00	5.667E-03	96	7.10	0.103	6.00	4.951E+00	340	25.16	2.041
6	63	3.00	4.048E-03	94	6.96	0.25	5.80	1.972E+00	340	25.16	4.532
7	15	2.90	1.643E-02	99	7.33	0.103	5.60	4.621E+00	340	25.16	2.03
8	63	4.90	6.611E-03	98	7.25	0.25	4.00	1.360E+00	340	25.16	4.481
9	15	3.50	1.983E-02	101	7.47	0.103	6.70	5.529E+00	335	24.79	2.153
10	63	2.00	2.698E-03	98	7.25	0.25	2.90	9.860E-01	340	25.16	4.349
11	15	1.50	8.500E-03	100	7.40	0.103	6.80	5.612E+00	335	24.79	2.135
12	63	3.60	4.857E-03	94	6.96	0.25	2.60	8.840E-01	340	25.16	4.456
13	15	1.15	6.517E-03	92	6.81	0.103	6.00	4.951E+00	335	24.79	2.071
14	63	2.70	3.643E-03	92	6.81	0.25	3.50	1.190E+00	340	25.16	4.549
15	15	2.10	1.190E-02	98	7.25	0.103	6.20	5.117E+00	335	24.79	2.077
16	63	5.90	7.960E-03	96	7.10	0.25	6.00	2.040E+00	337	24.94	4.571
17	15	1.80	1.020E-02	92	6.81	0.103	6.80	5.612E+00	335	24.79	2.052
18	63	6.10	8.230E-03	92	6.81	0.25	3.60	1.224E+00	335	24.79	4.556
19	15	1.50	8.500E-03	94	6.96	0.103	6.80	5.612E+00	335	24.79	2.195
20	63	3.40	4.587E-03	94	6.96	0.25	3.50	1.190E+00	335	24.79	4.418
21	15	4.00	2.267E-02	92	6.81	0.103	6.80	5.612E+00	335	24.79	2.022
22	63	4.80	6.476E-03	92	6.81	0.25	1.10	3.740E-01	335	24.79	4.37
23	15	2.90	1.643E-02	92	6.81	0.103	6.00	4.951E+00	335	24.79	2.048
24	63	3.00	4.048E-03	92	6.81	0.25	6.50	2.210E+00	335	24.79	4.591
Units	Volts	Volts	Volts	microsec.	cm	Volts	Volts	Volts	microsec.	cm	MHz

25cm diameter cylinder (no breast target) and to the breast target were determined. Note that the acoustically-measured diameter (distance to far wall) of the cylinder is quite accurate. The distance-to-target data are used to construct the breast contour (profile). Measurements recorded on oscilloscope traces are presented in Figures 29 and 30. In these measurements, the interrogation pulse can be identified on the left-hand of the top trace. The ring of transducers were operated in both the "collect" and the pulse-echo modes. The pulse-echo is identified as the signal near the center of the same trace, wherein the time between the two determines the distance to the breast target. The lower trace(s) in each case is the through-transmission signal measurement, with the time from the pulse to the signal near the right-hand of the trace being the TOF measurement through the breast target. This measurement is related to both the power absorption and could be correlated with temperature change. A detailed compendium of the tomographic measurements showing the attenuation through the path of each transducer and the multi-transducer measurements from a single transducer used to produce a "fan beam" reconstruction are included as Appendix F.

The data from these measurements have been further examined to ascertain if ultrasound tomographic image reconstruction from the therapy transducer array may be possible. A tomographic reconstruction algorithm was writtren which is appropriate for the density of transmitting and receiving transducers present in the system in order to test this potential. It is important to note that the development of ultrasound tomographic reconstruction techniques and imaging algorithms are clearly outside the scope of the present contract. This effort was performed only to determine the feasibility of accomplishing such an ultrasound CT image using the same arrays and system components used in the breast therapy system. The initial results are truly exciting. Both transmission data and reflection data were collected as described above. Reflection data were used to determine the external surface of the breast. This allows localization of the breast in treatment system coordinates. An iterative algebraic reconstruction technique (ART) was then used to reconstruct the interior distribution of parameters measured by transmission data. Knowledge of the external surface also provides a computational advantage. It allows us to bound the active computation area, reducing calculation time for the tomographic reconstruction. It also reduces the smearing of the final reconstruction image. We have carried out studies using simulated data to determine if it is possible to reproduce internal features based upon the transducer, receiver, and pulse-transmitter parameters of the actual breast therapy system, showing that the number of receiving transducers (which correspond to the number of therapy transducers) should be sufficient to reconstruct internal features. Reconstructions (shown in Figures 31 and 32) based on the preliminary measurements taken in the laboratory as described above (and included as Appendix F) show promise that it will be possible to implement this technique with real data.

2.F. Thermometry Subsystem

Minimally invasive thermometry is performed by a multichannel thermistor thermometry system (Profilometer) developed by Drs. Bowman and Newman at the Massachusetts Institute of Technology (Bowman, et al., 1991; Hansen, et al., 1994).

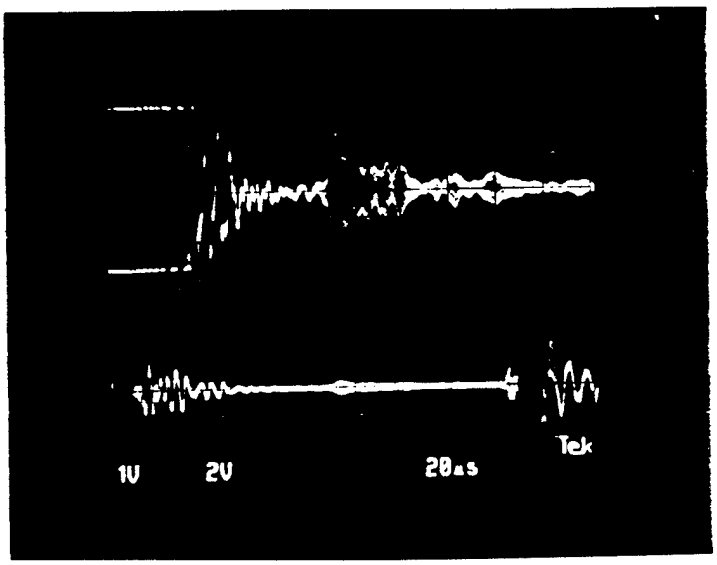

Figure 29 A. Oscilloscope recording of pulse echo/transmission results (2 MHz). The top trace shows the pulse echo. The bottom trace shows the transmission signal one way through the phantom.

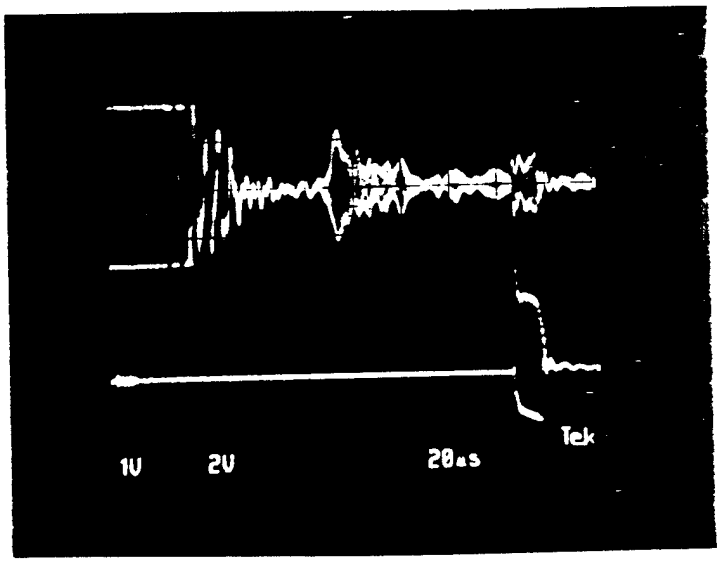

Figure 29 B. Oscilloscope recording of pulse echo/transmission results (2 MHz). The top trace shows the pulse echo. The bottom trace shows the transmission signal through the phantom the opposite way.

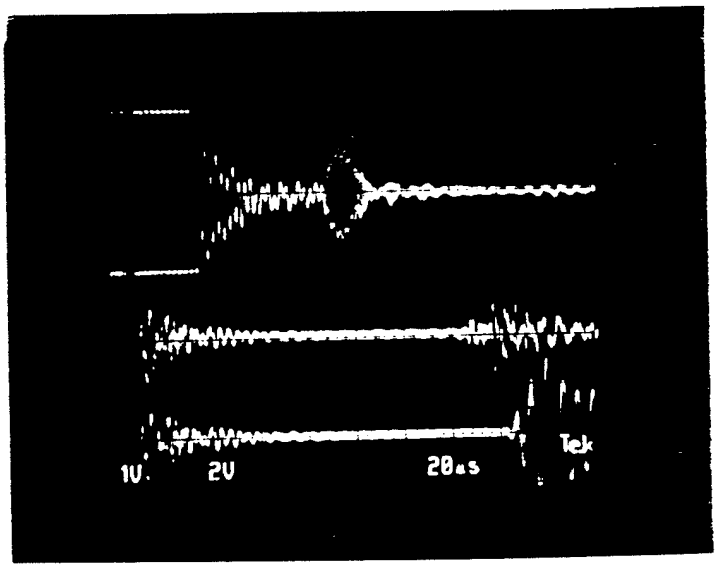

Figure 30 A. Oscilloscope recording of pulse echo/transmission results (4.5 MHz). The top trace shows the pulse echo. The bottom trace shows the transmission signal one way through the phantom.

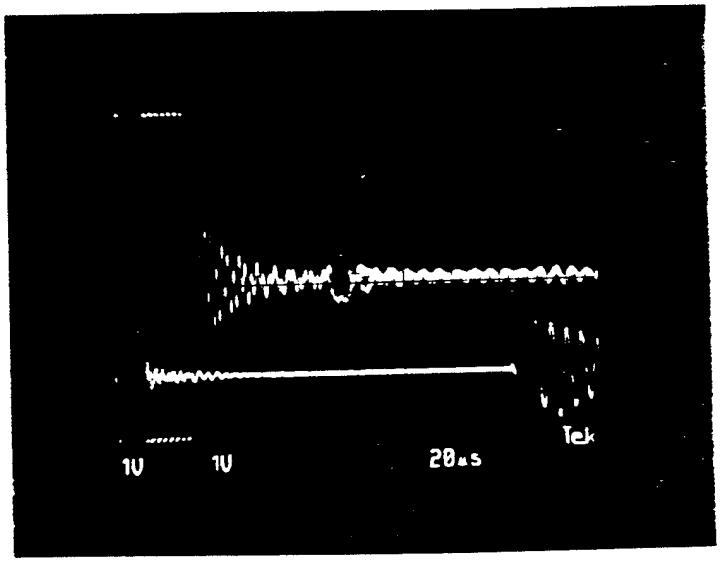

Figure 30 B. Oscilloscope recording of pulse echo/transmission results (4.5 MHz). The top trace shows the pulse echo. The bottom trace shows the transmission signal through the phantom the opposite way.

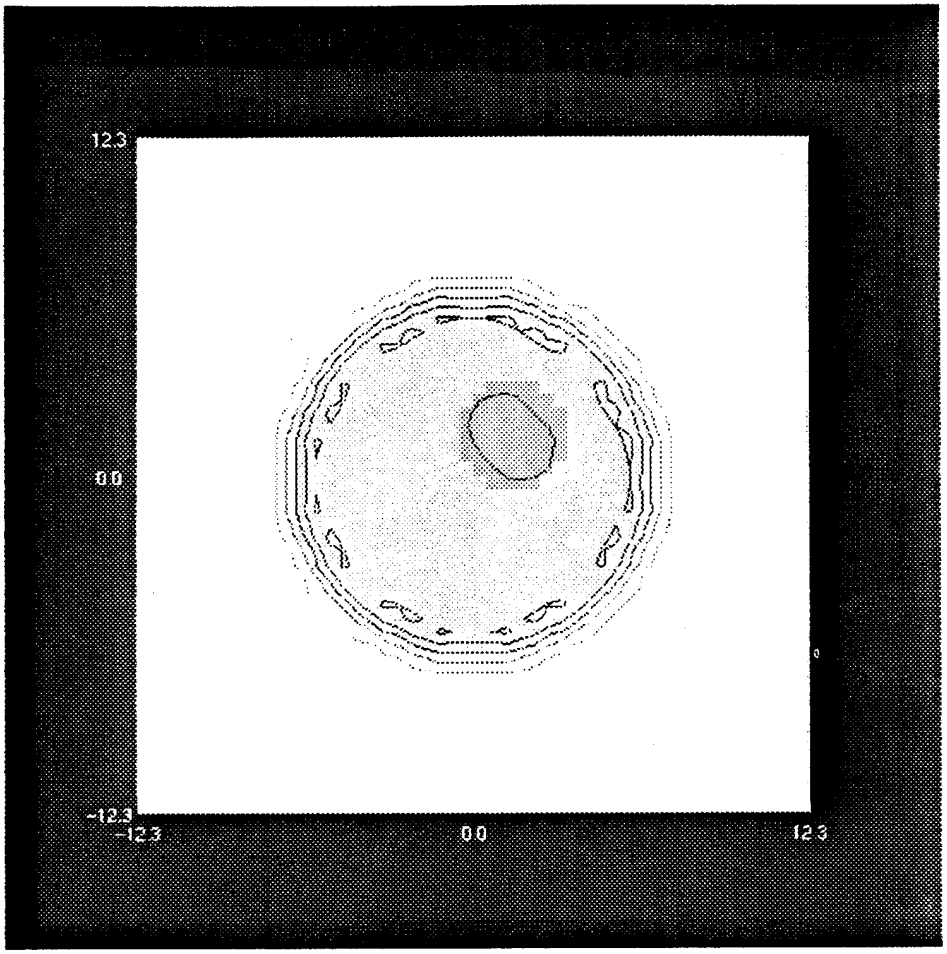

Figure 31. Comparison of reconstruction to known distribution. A 6cm radius circle is represented by light coloring, and a small region of 25% enhancement is shown as the darker region. The lines represent isolevels of the reconstructed distribution at the mean reconstructed value and 1 standard deviation above and below. The small region of enhancement is well reconstructed.

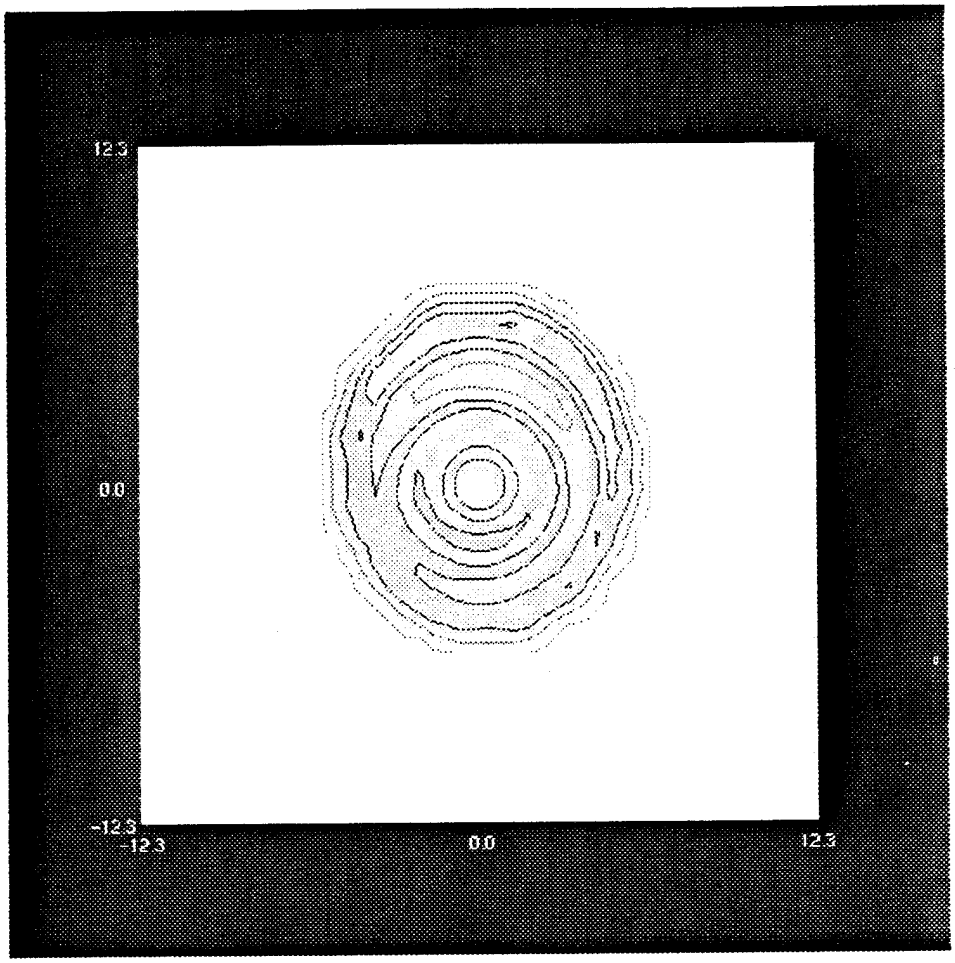

Figure 32. An example of reconstruction from measured data. This reconstruction is based on manual measurements from a few transmitters. The data is extrapolated around the ring giving the circular behavior to the reconstruction. The external contour is determined from manual measurements of the reflection time measured about a quadrant and again extrapolated about the ring. The ultrasound phantom had a uniform attenuation distribution. Lines again represent mean and 1 SD above and below mean.

The multi-channel temperature measurement instrument accomodates up to 6 multi-channel temperature probes. Each probe can measure temperature at up to 14 sites providing a total of 84 channels of information. The present instrumentation has resolution down to 10-17 millidegrees C, and temperature can be sampled at variable rates dependent on the data acquisition system being used and the amount of data averaging and signal processing. Each of the 84 channels can be sampled at 20 Hz which provides 10,080 samples of temperature data per second. Multi-site temperature data are collected and stored by the Instrument Computer. Data signal conditioning is performed by the Instrument Computer and the data then passed to the Control Computer for interaction with the control algorithm and display for the operator.

The instrument consists of two card types; the isolation cards and a digital control card. The isolation card is a medically isolated driver card external to the Instrument Computer which provides isolation for each channel and also provides multiplexing of the analog and digital signals. The digital control card provides function selection including card selection, channel selection, gain selection for a Programmable Gain Amplifier, and resetting of an Over Current Protection Latch. The controller card also handles communication to and from the Instrument Computer. Analog-digital conversion is presently handled by a commercially available system in the Instrument Computer, and all instrument control, data display, and data storage is handled by the computer.

Within the measurement instrumentation, each probe is connected to an individual, electrically isolated probe driver card. The driver cards are powered by a UL-544 approved power supply certified for medical use, and signals to and from the driver cards are passed through optical isolators and isolation amplifiers. This isolation ensures that there is no electrical connection between the patient and ground via the instrumentation.

The instrument also contains common circuitry - the controller and interface cards - for coordinating the activities of the several driver cards and for communicating with the Instrument Computer. This common circuitry is powered from a separate power supply, so that the probe driver cards are electrically isolated from the common circuitry, from the AC line, from the host computer, and from the other probes.

The probes used to measure temperature can be mounted on needles, molded into catheters, or other designs as desired. Stainless steel needle probes are planned for use with this system. These are 19 ga. needles, from 6" to 12" long, and contain 14 thermistor sensors. This range of probe configurations permits selection of a probe appropriate for the particular size breast being monitored.

The sensors used to measure temperature are thermistors. There is no electrical connection from the probe to the patient in normal operation. However, as a further safety precaution, hardware protection circuitry is provided to shut off power to a probe if an out-of-range signal is detected due to probe breakage or other mishap. Should such a condition occur, probe excitation will be shut off within 65ms. Although the isolation circuitry ensures that there is no current path from the instrument to

ground through the patient under such conditions, this additional measure of redundancy provides added assurance of patient safety.

A unique feature of this system is that various temperature displays are available in real-time on the Control Computer screen during treatment. The display modes are as follows:

- Temperature-Time Display Mode: This mode presents a graph of all sensors on a common time axis. For the breast system, use of 3 probes simultaneously is anticipated for most treatment cases, which is easily seen on the display.

- Temperature-Histogram Mode: This mode presents an instantaneous display of temperature for each sensor, with a high/low memory. Each sensor has its own histogram plot.

- Spatial Temperature Distribution Mode: This mode is displayed on the operator treatment control screen directly on the breast contour/slice map and shows spatially where each of the sensors is located within the breast profile and the temperature of each sensor.

- Thermal Dose Spatial Distribution Mode: This mode is displayed on the operator treatment control screen directly on the breast contour/slice maps and shows spatially the thermal dose distribution within the breast. Thermal dose is displayed as the instantaneous value of accumulated thermal dose, expressed as equivalent minutes at 43 deg. C.

A block diagram of the thermometry subsystem used in the breast therapy system is shown in Figure 33. Figure 34 is a photo of the Temperature-Histogram display mode output which includes historical high and low temperatures as small horizontal bars overlayed on the temperature histogram.

The profilometer system and displays are fully developed and approved by the IRB at the Dana Farber Cancer Institute. A profilometer system (operating as a stand-alone device) is currently in clinical use for other thermal therapy systems at the JCRT.

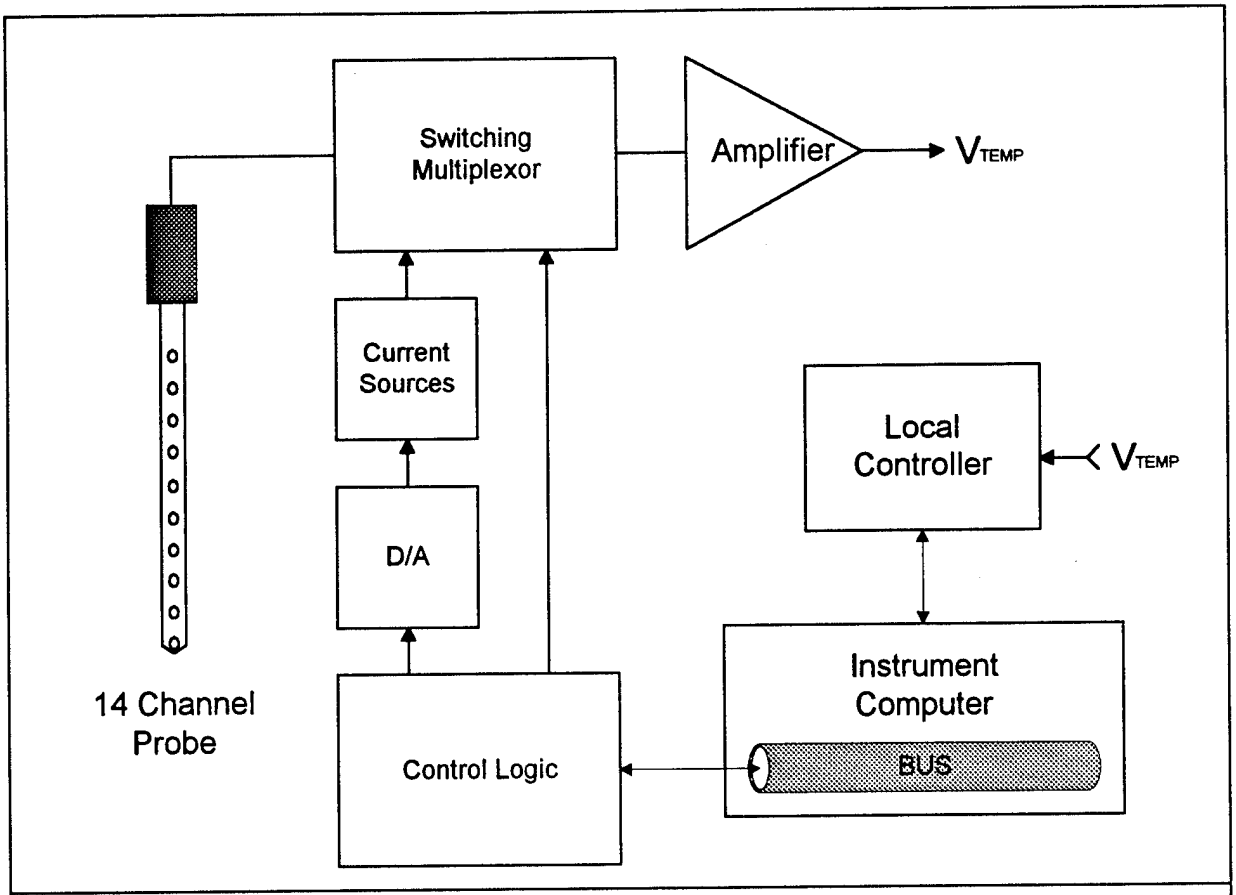

Figure 33. **Thermometry Subsystem**

2.G. Cooling/Heating and Water Circulating Subsystem

This subsystem consists of a 110 watt thermoelectric cooler/heater, water circulating system, and a temperature controller interfaced to the Instrument Computer.

The thermoelectric cooler/heater is attached to a thermal plate which includes a machined serpentine groove and cover plate for placing the tubing which carries the circulating water. Using this approach makes it possible to maintain sterility of the water which comes in contact with the patient and avoid circulating the water directly through the cooler body itself. The cooler maintains the water at a preset temperature which is under operator control via the Control and Instrument Computers. The interface communicates bi-directionally with the Instrument Computer. The temperature controller controls the setpoint temperature based upon information feedback from the thermometry monitor module and the setpoint temperature selected by the operator. A PID control algorithm is incorporated in the software. The setpoint temperature range is 25°C to 42°C.

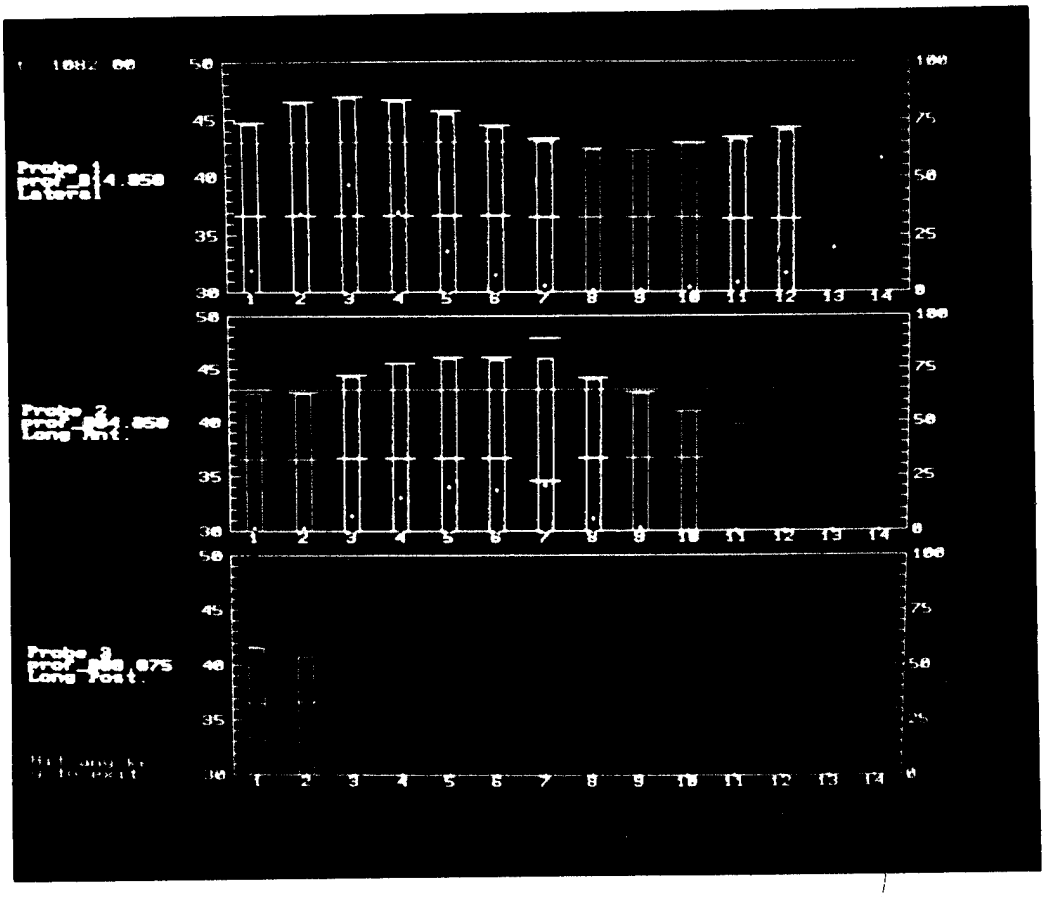

Figure 34. Temperature histogram display mode. Each histogram plot applies to an individual probe. Up to eight histograms can be displayed on the screen. Each bar refers to an individual sensor in the probe. A high-low memory is shown as a pair of horizontal lines on the histogram bar. The color coding of the sensors is chosen to reflect sensor location and temperature range. The yellow dot within each bar represent the accumulated thermal dose (Sapareto et al., 1984)

2.H. Computer Subsystem

The computational functions of the system will be divided between two computers, the Control Computer and the Instrument Computer. The control computer's primary responsibility is to control the overall treatment functions and provide an intuitive user interface via a graphics monitor, keyboard, and mouse. The Instrument Computer is primarily responsible for communicating with other hardware devices such as the Cylindrical Array Applicator, the Video system, Cooling System, Thermometry system, and the Pause switch.

2.H.1. Control Computer

The Control Computer is a standard architecture machine with no custom hardware interfacing requirements that connects to the Instrument Computer via a communications link and is also connected to a printer to allow hardcopy of the treatment information. For treatment results analysis, demo, and software development purposes the Control Computer is able to be operated without the Instrument Computer connected.

The bi-directional communications link has been implemented via a parallel port using off-the-shelf hardware. The communications software design employed is independent of the communications link technology, except for the low-level driver implementation.

Control Computer Specifications:

Processor:

- Pentium, 66 MHz
- PC/AT, MS-DOS, Windows, iRMX Compatibility
- 32 MB RAM
- 520 MB hard disk
- 3.5" 1.44 MB floppy drive
- Printer Port
- Bi-directional Communications link to Instrument Computer (Ether Express Network)

Graphics and operator entry subsystem:

- 1280 x 1024 x 256 resolution
- 21" monitor size
- PCI bus with graphics accelerator
- Standard 101-key keyboard

Microsoft Windows supported mouse

Inputs to Control Computer:

- Keyboard
- Mouse
- Ether Express Network from Instrument Computer.

Outputs from Control Computer:

Display Screen
Parallel Port to Printer
Ether Express Network to Instrument Computer.

2.H.2. Instrument Computer

The Instrument Computer implements the custom control and measurement interfaces to other hardware portions of the treatment instrument, is located within the system enclosure beneath the patient table and near the control and measurement points, and communicates with the Control Computer via a bi-directional communications link. For software design consistency and to avoid unnecessary costs, the Instrument Computer is implemented as a PC-AT compatible computer filled with interface cards.

The bi-directional communications link was implemented via a parallel port using off-the-shelf hardware. The communications software design is based on iRMX and is independent of the communications link technology, except for the low-level driver implementation.

Instrument Computer Specifications:

Processor:
- 80486 DX2/66, upgradable to Pentium
- PC/AT, MS-DOS, iRMX Compatibility
- 16 MB RAM
- 250 MB hard disk [deleted from final system]
- 3.5" 1.44 MB floppy drive [deleted from final system]
- Ether Express Network link to Treatment Control Computer

Custom designed transducer array interface hardware

TTI Temperature Profilometer System:
- Low profile card cage
- 14 Channels per board
- 6 boards
- Isolation card
- Digital control card

Coolant system interface hardware

Video system interface hardware

Inputs to Instrument Computer

Safety Controls --- Emergency Shutdown, Pause control.
T/R Switch Status
Demultiplexer Status
Receiver data
Invasive Thermometry Sensors
Coolant Temperature
Ether Express Network from Control Computer

Outputs from Instrument Computer

Safety Shutdown
Image Pulser
RF Power On/Off, Gated CW burst
RF Frequency Sweep On/Off
T/R Switch Control
Demultiplexer Switch Control
Cooling System Control
Ether Express Network to Control Computer

2.I. Video Subsystem

The breast ultrasound therapy system also incorporates a charge-coupled-device (CCD) solid-state video system for visual imaging of the breast within the treatment cylinder. This video subsystem was not anticipated in the original system design; however, several physicians within our group and our outside scientific reviewers suggested that real-time video imaging of the breast would provide useful information concerning the breast's position within the treatment cylinder and would confirm the breast contour outline provided by the noninvasive interrogation pulse-echo ultrasound. The video image from the CCD device is coupled through a video digitizer to the Instrument Computer and transferred to the Control Computer. The resultant image is displayed within a "window" on the operator treatment control screen.

2.J. Safety Subsystem

This subsystem automatically tests for any system ground faults and monitors leakage currents. It also directly monitors RF output power from the generator/amplifier subsystems independently of any computer-based monitoring of output power. It provides for system shutdown in the event of RF power malfunction, such that a "power on" failure mode is not possible. Also, a system level emergency shutdown switch is provided.

3. SYSTEM SOFTWARE

3.A. System Software Overview

The System Software Block Diagram (Figure 35) shows the system control implementation approach. System control is divided between two computers, the Control Computer and the Instrument Computer. The Control Computer provides an operator control interface, measurement interpretation, feedback control, and data recording. The Instrument Computer provides direct hardware interfacing for collecting temperature measurements, collecting measured data from receivers, setting control output levels, and controlling the timing for multiplexing the transducer array.

3.B. Operating System

The Control Computer and the Instrument Computer are each configured with a 32-bit real-time multitasking operating system (Intel's iRMX for Windows). The software for each computer is written as a collection of well-isolated tasks, with intertask communications implemented via a consistent mailbox communication approach, with each task having its own separate GDT entries for its code, data, and stack segments (except that multiple iterations of a task, if any, use a shared code segment), and with minimal use of shared memory between tasks. All tasks are written as iRMX native tasks, except in the Control Computer where the operator interface is written as a Microsoft Windows application. Any task using mutual exclusion mechanisms rigidly adheres to an access order regimen to prevent deadlock situations from occurring.

3.C. Interprocess Communication

A standard intertask communications message structure is used for most intertask communication messages. This structure contains message type, response mailbox, destination, and standard auxiliary information fields. For passing large messages, an auxiliary information field will be used to pass a pointer to a memory segment containing the passed information. To avoid conflicts, in most circumstances this segment will not be accessed again by the sending task until it is returned by the receiving task. Preallocated communications buffer queues are used where possible rather than dynamic memory allocation and deallocation to exercise explicit control over message queuing performance and to avoid memory fragmentation.

3.D. Initialization

The Initialization task has the responsibility to start up all the other primary application tasks in the system. Each iRMX task is separately bound, and loaded by the initialization task with the iRMX application loader. This approach encourages good design practices such as maintaining task isolation, automatically provides

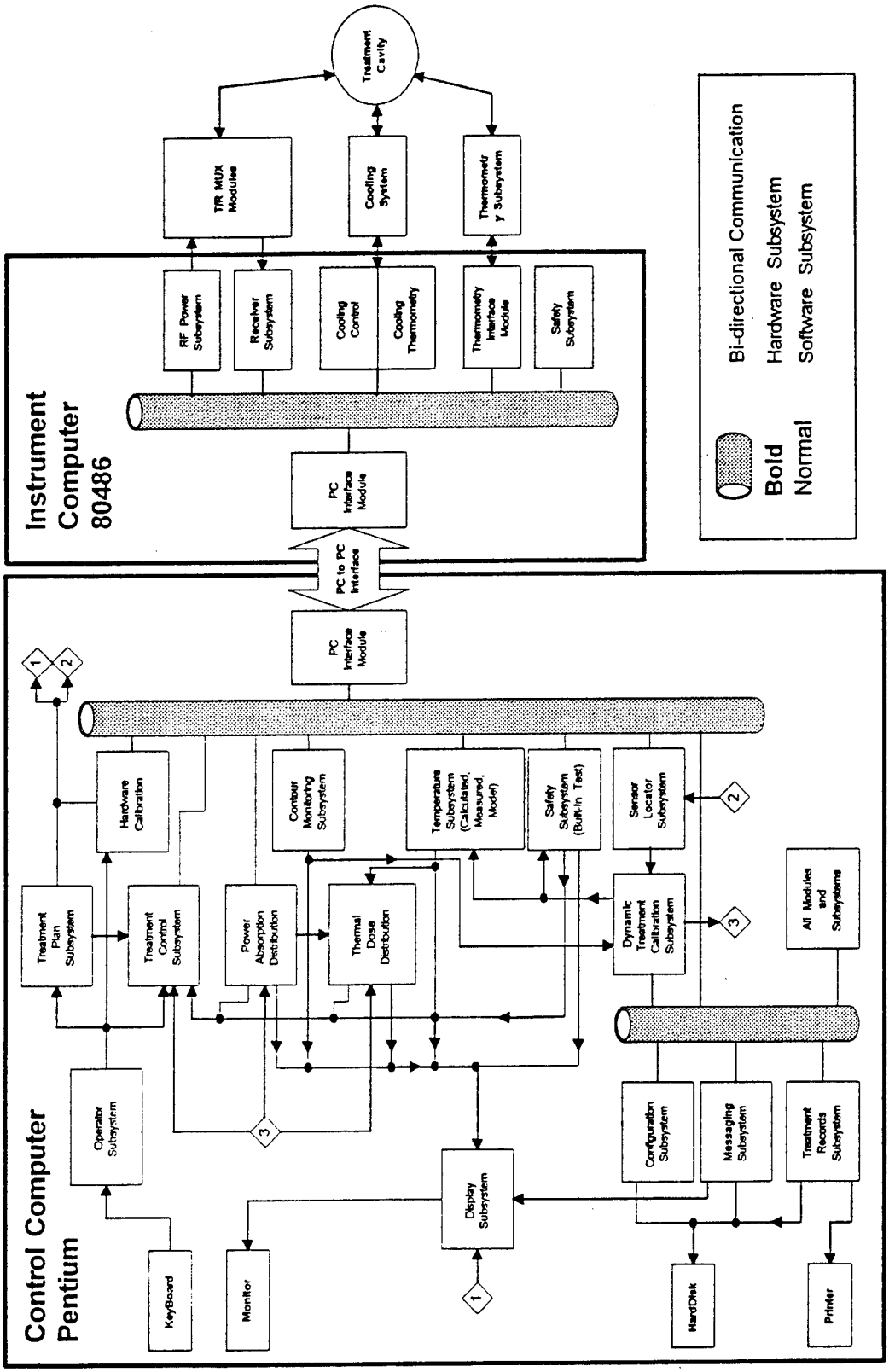

Figure 35. System software block diagram.

independent data segments for each task, and minimizes compile, build, and bind cycle time.

Each task will have a synchronous initialization phase, and may also have asynchronous initialization. During synchronous initialization, each task will establish communications mailboxes and message queues, perform any other synchronous initialization required, send the token for its main command mailbox to the initialization task, and wait for an initialization message from the initialization task. After synchronous initialization is complete, the task may also do other initializations asynchronously.

3.E. Control Computer

The Control Computer performs several interrelated functions. The operator input and display subsystem provides user control over the treatment and feedback to the user as the treatment progresses. User control over the treatment is at a high interaction level; actual control over the timing, power levels, and frequencies applied to scores of individual transducer elements is too complex and must be controlled too fast for an operator to control individual transducer parameters directly.

3.E.1. Operator Subsystem

The operator interface is one of the most important parts of the treatment system since it represents "the system" to the users. Therefore, the engineering design approach must be secondary to the user-oriented approach in this instance. Not only must the data interfaces be considered, but also the tools (keyboard, mouse, etc.) and the display organization and options. These are each discussed in the paragraphs below.

The operator interface is used to define the treatment control and reference data and to display a variety of types of treatment progress and general display information.

Treatment Definition and Control Data

Treatment definition and control data will be suggested to the operator through the presentation of a configuration file, or files, and by requests to the operator to:

1) accept the configuration file in its entirety
2) specify new data for particular fields of the file
3) specify data not included in a configuration file.

Treatment Associated Data

Treatment associated data is measured by the system from sources external to the therapy system and therefore must be provided to it. Such data includes:

1) the number of temperature probes
2) the locations of the probes
3) the number and spacing of sensors on each probe
4) the spatial locations of the temperature sensors
5) the size and location of scar tissue

6) the patient's name and any identification being used

3.E.2. Display Subsystem

The displays provided during treatment include:

1) a breast contour (every 1 to 5 seconds),
2) periodic imaging of the temperature probe(s),
3) 2D cross section breast images, each with overlays of temperature data,
4) Hot spot alerting,
5) An optional display of 2D cross sections by location,
6) continuous time and temperature monitoring displayed as a graph for each cross section.

Where temperature is to be indicated by color shading scale shown below is used. The actual temperature values that map to these colors and the colors used are defined and configurable via the Configuration Subsystem.

White - over temperature (above 44.5 °C)
Red - upper temperature threshold (44.0 °C)
Orange - 43.0 °C
Yellow - 42.0 °C
Green - 41.0 °C
Blue - below lower temperature threshold (40.5 °C)
Gray - shading

All display software are designed with the resolution-independent features available in Windows, so that the treatment software will be able to run satisfactorily on machines with lower resolution for demo and development purposes, with the acknowledgment that display detail will be lost.

3.E.3. Configuration Subsystem

System configuration information will be read from a file into a configuration information structure, then passed to each task as part of the synchronous initialization message. The configuration information will be defined as a constant structure and may be compiled into a binary file prior to system startup. The Configuration Subsystem will check for the existence of the an ASCII version of the "SYSCONFG.HC" and use it instead of the compiled file if it is present.

The system configuration information structure definition will be contained in a common file, "SYSCONFG.HC", and included by all referencing files.

The configuration subsystem reads all configurable parameters from the storage media (hard disk) and returns the appropriate data to the module that requests the

information. The types of configurable parameters that this subsystem is responsible for obtaining are power calibration table or tables and system behavioral preferences.

3.E.4. Messaging Subsystem

The messaging subsystem handles all messages that are to be displayed to the user. This subsystem uses the Display Subsystem to display pre and post treatment messages, error messages during the treatment, and informational messages that are provided for the user. This subsystem accepts messages from any of the other subsystems and displays them in the appropriate fashion. For example, if an error occurs during a treatment, this subsystem will display an error message in a pop-up window and inform the Treatment Control Subsystem to pause the treatment. If the message is an informational message, the message will be displayed in a message bar located on the display screen. All messages received are also transmitted to the Treatment Records Subsystem.

3.E.5. Treatment Records Subsystem

The function of this subsystem is the collection, organization, control, and distribution of data between subsystems, tasks, and modules, and to store all relevant treatment data for post-treatment recall and analysis. In addition, the Treatment Records Subsystem provides treatment information to the user in paper form. A printout of key treatment parameters including temperature vs. time for all of the sensors will be provided upon request.

Information that the Treatment Records Subsystem is responsible for storing and retrieving includes the system configuration, all temperature measurement results, patient information, cooling system information, treatment cell information, automated control decisions, and user keypresses and mouse events during each treatment session. This task will also allow the data to be retrieved in an off-line simulation mode, for post-mortem analysis of the treatment session, operator training, system demonstration, and software development support. Other utilities and function will also be provided to assist in hardware testing, system calibration, and printing treatment data.

3.E.6. Treatment Plan Subsystem

The Treatment Plan Subsystem is responsible for obtaining information from the user that is necessary for proper treatment operation. Information that this subsystem will require includes the number of treatment sensor probes, number of sensors per probe, spacing of the sensors on the probe, target temperature and temperature limits for individual sensors and/or subregion locations in the treatment volume, patient name and/or number identifier, and possibly suggestions about the method of heating. The treatment plan subsystem maintains this information and provides it to the other subsystems.

The Treatment Plan Subsystem will also provide a method for the user to select regions as small as an octant and select a temperature setpoint for the entire octant at once.

3.E.7. Treatment Control Subsystem

The Treatment Control Subsystem makes transducer output power and frequency decisions based on information received from the Power Absorption Distribution Subsystem, Thermal Dose Distribution Subsystem, Treatment Plan Subsystem, Dynamic Treatment Calibration Subsystem, and the Temperature Subsystem. Once output power and frequency settings have been determined the Treatment Control Subsystem sends those data to the RF Power Subsystem via the PC Interface Module so that actual power changes can be made for the Transducer Array.

The Treatment Control Subsystem operates on predefined Treatment Cell Volumes. The actual volume of each treatment cell may be determined by the configuration file. The Treatment Cell center points, volume corners, and transducers that affect a treatment cell are stored in a Treatment Cell Information File (TCIF.DAT). If the volume defined in the configuration file for a treatment cell does not match the volume used to calculate the current treatment cell information file, the Treatment Control Subsystem will generate a new treatment cell information file.

The Treatment Control Subsystem will operate in automatic mode, yet it will be capable of allowing the user to make manual adjustments of the temperature setpoints for each treatment cell volume during the treatment. The default control method will be to heat the entire breast to 42-43 °C in all treatment volume cells.

To achieve the desired temperatures for the target volume the Control Subsystem may begin the treatment by selecting the Low Frequency Setting (2.0 - 2.5 MHz) until the center treatment cells have reached their target temperatures and then switching to the High Frequency Setting (4.5 MHz) to maintain these temperatures.

Treatment Cell Volume

A Treatment Cell Volume is a volume located inside the Cylindrical Transducer array. All treatment cell volumes are the same volume (or as close to the same as possible while still cumulatively encompassing the entire volume inside the Cylindrical Transducer array). The actual value for this volume is stored in the configuration file (default = 1 cm^2). A data file containing the treatment cell center point location, volume corner points locations, and the transducers that affect each cell is accessed prior to the treatment as the Control Subsystem sets up the Treatment Cell list. The Treatment Records Subsystem will check the Treatment Cell information file to ensure that the configuration file volume selection matches the volume used to generate the treatment cell information file. If it does not match, then the Treatment Records Subsystem will call on the Control Subsystem to generate a new file prior to starting the treatment.

This subsystem calculates the center point location for each volume, the corner points for each volume, and then determines which ultrasound transducers affect this volume. Although the volume for each cell will be equal, the actual shape of each

volume will not be exactly the same. Figure 36 shows a simplified view of how the center points of each volume cell is determined for a single ring of transducers(48 in this case).

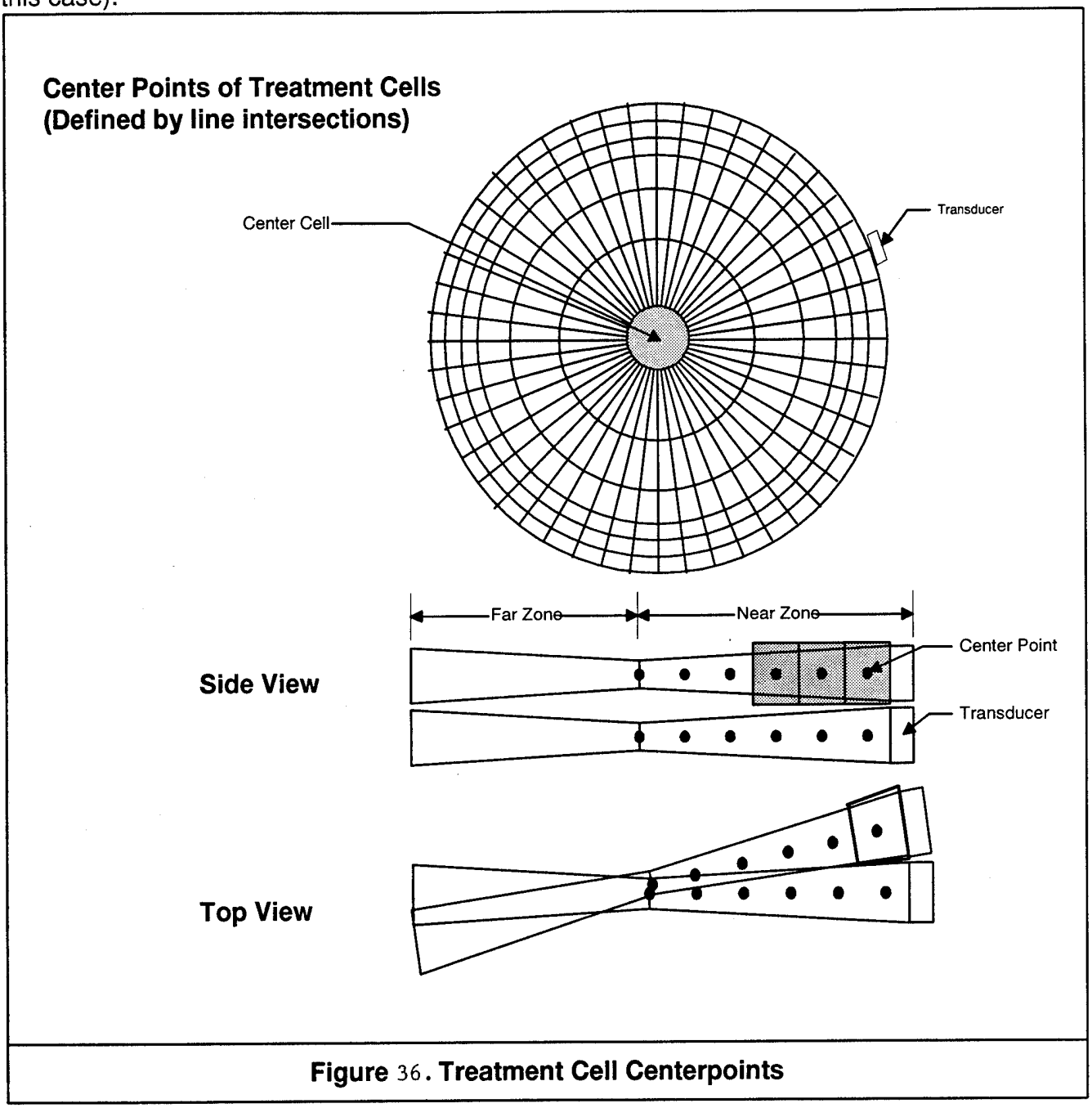

Figure 36. Treatment Cell Centerpoints

Treatment Cell Volume Centers

Each treatment cell volume's centerpoint is located on a line from the center of the face of a transducer to the centerpoint of the cylindrical array. The central treatment cell volume is actually a cylinder with a radius selected such that the volume will match the volume contained in the configuration file. The remainder of the treatment cells for a given transducer ring are in the shape of a rhombus (see Figure 37). Once the central treatment cell radius has been determined, the radius (distance from array

center) for the center point of the rest of the treatment cell volumes is calculated and the centers determined. If a volume is selected such that all cells cannot be the same size, the treatment cells located closest to the transducer face will be of different volume so that the entire cylinder volume is represented by an individual treatment cell volume (These cells could be ignored since they will never contain target tissue).

Treatment Cell Volume Corner Points

Once the center points for each treatment cell are computed, the eight corner points for the Treatment Cell Volume are calculated. Each treatment cell volume is defined by 6 planes (except for the center cells). For a given treatment cell, the top and bottom plane are horizontal planes that are centered between the ring of transducers above and below the ring that the current transducer resides (see Figures 36 and 37). The left and right planes are vertical planes that extend from between the left and right neighbors of the transducer to the center point of the Cylindrical array applicator. The front and back planes are normal to a vector originating from the center point of the cylindrical array to the center point of the transducer. The distance of the front plane is half way between the current volume center and the center of the volume closer to the origin, and the back plane is halfway to the volume center further from the origin. Once all six planes have been determined, 8 volume corner points are calculated by finding the intersection of 3 planes.

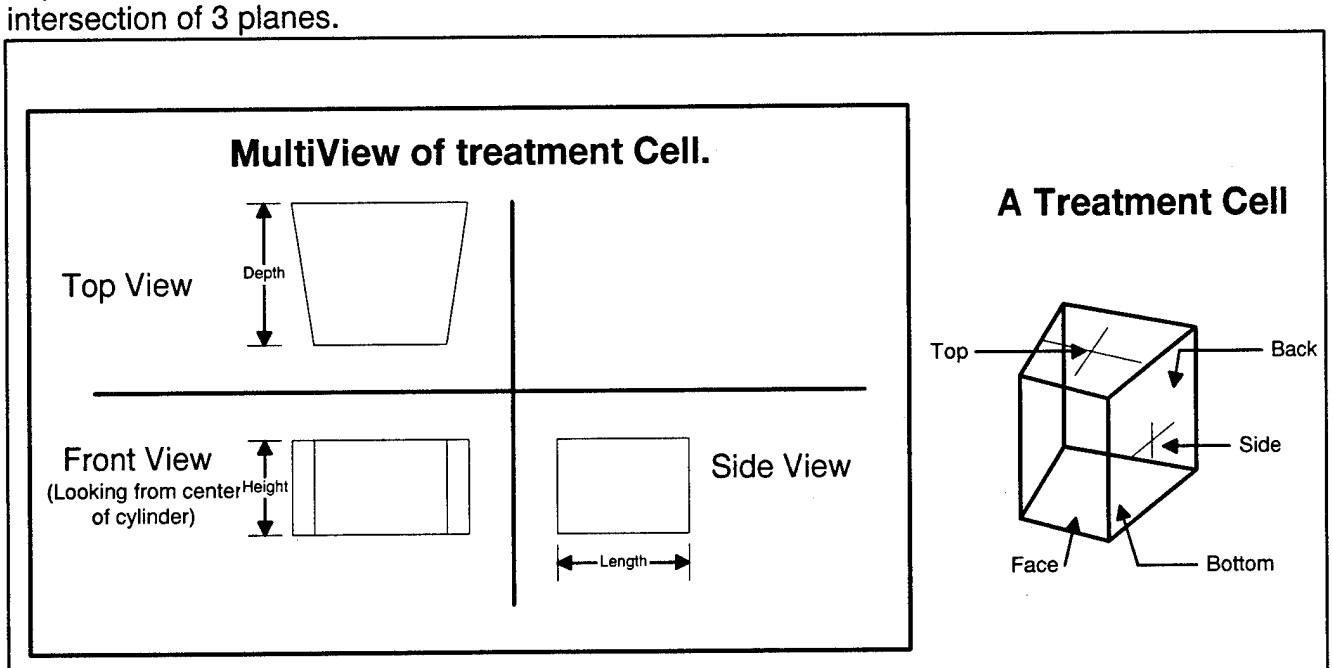

Figure 37. Treatment Cell Volume

Transducers Affecting a Particular Volume Cell

A center and 8 corner points define each volume cell. After all cell points have been calculated each of the points defining a cell are checked to see if they fall within either the Near Zone or Far Zone regions of each Transducer in the array; if so they are

said to be touching a cell. The control subsystem creates a list for each volume cell of all transducers that "touch" a volume. In addition to whether or not a transducer "touches" the volume, information about whether the ultrasound field that touches the volume is in the Near Zone or the Far Zone region is also maintained. A "strength capability value" is also given for each transducer. For example, if a given transducer touches both a corner and the center points it will be given a higher strength capability value than a transducer that only touches a corner point. The strength value will be used by the Control Subsystem during the treatment to determine what the output power configuration should be to perform the desired treatment.

Treatment Cell Structure Definition

The structure definition below describes the types of information that will be maintained for each treatment cell volume.

point	Center	Location of center of cell
point	Corners[8]	Location of 8 corners
float	Volume	Volume of this cell
float	AbsorbedPower	Current absorbed power
float	ThermalDose	Current thermal dose
float	Temperature	Current cell temperature
float	SetPoint	Temperature setpoint
float	TempLimit	Temperature limit
short	Type	Scar, NormalTissue, ContourTissue, NoTissue
sensor	*sensors	List of sensors in treatment cell
xducers	*xducers	List of transducers touching cell

3.E.8. Contour Monitoring Subsystem

Pulse-echo reflection data is collected using the cylindrical transducer array. The reflection data is collected by the Instrument Computer's Receiver Subsystem and sent to the Contour Monitoring subsystem. The Contour Monitoring Subsystem will convert this information into 3D image data that outlines the contour of the breast and prepare it for display. It will also map 3D image data into a 2D image space for the generation of 2D displays. This subsystem will also provide information to the Dynamic Treatment Calibration Subsystem to locate the breast within the treatment cylinder for detection of breast movement within extremes (boundaries) set in the Configuration file, and for updating the treatment cells in which the contour (surface of the breast) resides. Figure 38 is a simplified depiction of the pulse-echo monitoring method.

Contour Monitoring is performed by selecting a single ultrasound transducer to transmit an ultrasound pulse into the treatment cavity and then receiving the same pulse while measuring the time it takes for the pulse to return. This measurement is called a "Pulse-Echo" measurement since it measures the time it takes for a pulse to return to the transducer. The sooner a pulse returns the closer the object is to the face of the transducer. By pulsing all of the transducers one at a time a 3 dimensional contour map of the target tissue located in the applicator can be generated.

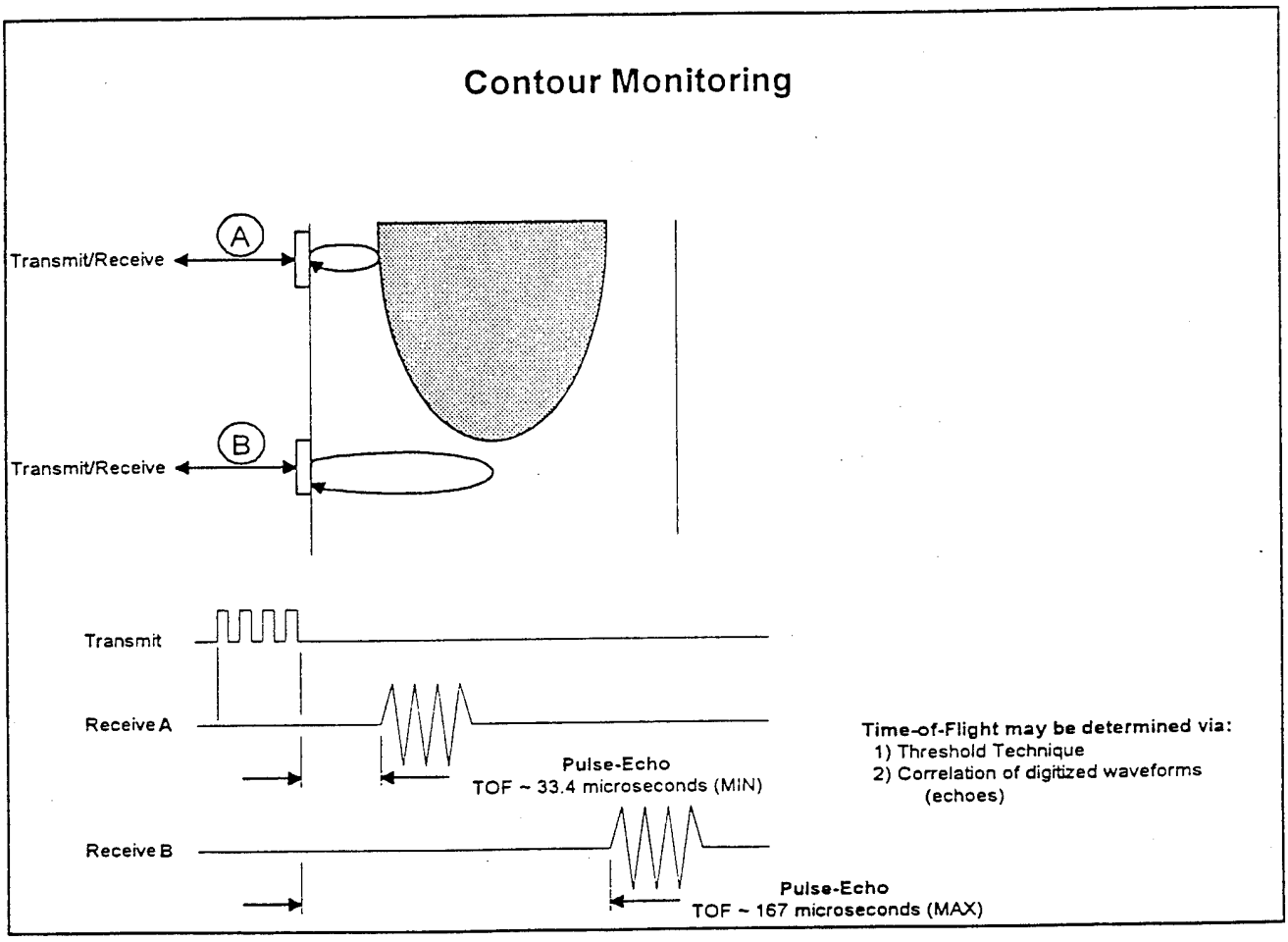

Figure 38. Contour monitoring.

3.E.9. Dynamic Treatment Calibration Subsystem

The Dynamic treatment calibration subsystem's primary responsibility is the detection of movement of the sensors, or the contour information. Once movement has been detected, this subsystem sends updated spatial target coordinate information to the subsystems that will be required to update their respective information tables.

Subsystems requiring the updated spatial information concerning target position include the Power Absorption Distribution Subsystem, the Temperature Subsystem, the Thermal Dose Distribution Subsystem, the Treatment Control Subsystem and the Safety Subsystem.

Whenever the breast moves within the treatment cylinder, new contour information is generated by the Contour Monitoring Subsystem based on pulse-echo measurements which are made every 4 seconds. This new breast contour information is passed to the Dynamic Treatment Calibration Subsystem to update the breast/target 3-dimensional spatial position within the treatment cylinder volume, relative to the transducers. This information is utilized by each of the subsystems requiring the updated spatial information. The Safety Subsystem compares the new breast/target spatial location against the maximum movement threshold specified in the Configuration file in order to determine whether or not to pause treatment.

Whenever sensors move the Sensor Locator Subsystem updates its sensor location table and warns the Dynamic Treatment Calibration Subsystem. This subsystem then sends the new sensor location information to the Temperature Subsystem and/or the Safety Subsystem. If a sensor that is to be used for the treatment is not located in tissue, the Safety Subsystem must be warned so that the treatment may be paused and the sensor deselected for control purposes.

3.E.10. Power Absorption Distribution Subsystem

The Power Absorption Distribution Subsystem calculates the power deposition within the tissue based on current temperature and power information and absorption models. Figure 39 is a simplified depiction of the "Through-Transmission" power measurement.

During treatment, the actual absorption throughout the target volume for each transducer pair is measured by the Instrument Computer, and sent to this subsystem. The Power Absorption Distribution Subsystem converts this information into an array representing the computed absorption or SAR (in W/cm^3) for each treatment cell (minimum unit treatment volume). This computed absorption array is then sent to the Thermal Dose Distribution subsystem for its next simulation model cycle.

The "Through-Transmission" power is calculated by selecting a single transducer to produce an ultrasound pulse while at the same time having the transducers that are located on the other side of the cylinder (through the tissue) receive the pulse and measure the change in magnitude of the pulse (Pulse Amplitude Degradation) once it has been received. A correlation between the transmitted magnitude and the received

magnitude can then be used to determine the amount of power that was absorbed in the tissue.

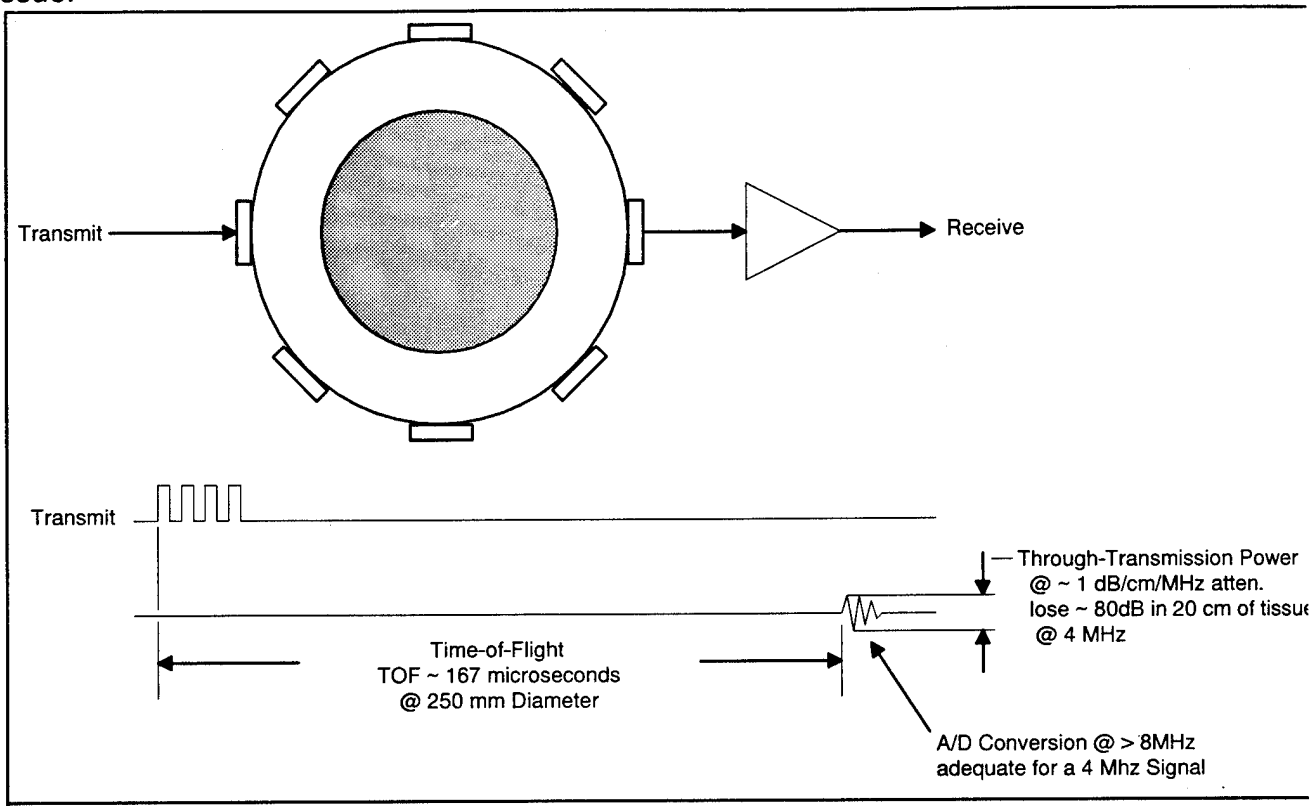

Figure 39. Power Monitoring

3.E.11. Temperature Subsystem

The Temperature Subsystem collects temperature values for all temperature sensors and "Time-of-Flight" temperature measurements from the Instrument Computer. These temperatures are then provided to the rest of the system upon request. In addition, this subsystem calculates the temperature distribution for all spatial volume cells based on the sensor, Time-of-Flight/Pulse Amplitude Degradation measurements. Invasive temperature sensor measurements and Time-of-Flight/Pulse Amplitude Degradation measurements occupying the same volume cells are set equal to the invasive sensor measured temperature and all derived temperatures in neighboring volume cells are calibrated according to the nearest invasive sensor measurement. Time-of-Flight/Pulse Amplitude Degradation measurements are depicted in Figure 40.

Actual temperature at a few points within the target volume will be directly measured with an invasive thermometry system, using two needles each carrying fourteen temperature sensors. These measurements will be collected by the Instrument Computer, and sent to the Temperature Subsystem. The Temperature Subsystem will convert the measured temperature information into an array

representing measured temperature per treatment cell, also using the needle position information provided to it by the Sensor Locator Subsystem. The measured and calculated temperature per treatment cell will be sent to the Thermal Dose Distribution and Treatment Control Subsystems.

Temperature monitoring using the ultrasound transducers is accomplished by selecting a single transducer to transmit a pulse while at the same time either one or a small set of transducers on the opposite side of the Cylindrical Array measure both the Time-of-Flight and Pulse Amplitude Degradation of the pulse that was transmitted. A correlation between the Time-of-Flight and Pulse Amplitude Degradation can then be made to the actual temperature of the treatment cells.

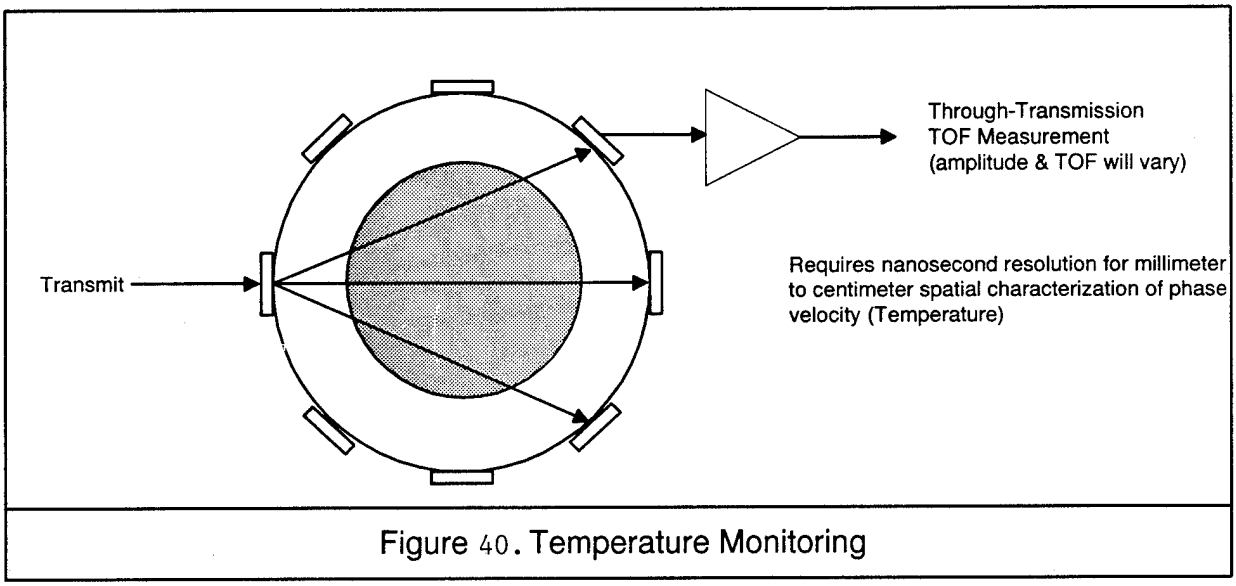

Figure 40. Temperature Monitoring

3.E.12. Thermal Dose Distribution Subsystem

The Thermal Dose Distribution Subsystem is responsible for calculating the thermal dose distribution in the tissue. This calculation is done based on the temperature for each cell over time. This information is generated by the Temperature Subsystem and consists of current measured temperature, calculated temperatures, and derived temperatures from Time of Flight/Pulse Amplitude Degradation measurements, all with 3-dimensional spatial correlation within the cylinder volume.

The Thermal Dose Distribution task will calculate cumulative thermal dose for each spatial treatment cell and update that information continually during treatment. For each treatment interval, the Thermal Dose Distribution subsystem will compute the temperature dose distribution within the breast from the measurements provided by the Power Absorption subsystem and then compare the simulation modeling results with the direct invasive temperature measurements and temperature volume-cell measurements derived from Time-of-Flight/Pulse-Amplitude-Degradation measurements in order to correct the model. The Thermal Dose Distribution subsystem will distribute modeling parameters and results to the Treatment Control

Subsystem and the Display Subsystem. This aspect of the system is still under development.

3.E.13. Hardware Calibration Subsystem

The Hardware Calibration Subsystem provides a method for calibrating the ultrasound output for each channel. The input control voltage for each channel is determined for a given ultrasound field intensity. This subsystem is executed prior to shipment of the system and may be executed again on a regular basis or when a ultrasound transducer is replaced or a portion of the circuit that feeds the transducer is changed. During the calibration procedure, a calibration table is generated. Once calibration is completed, the table is written to a file to be used for the next treatment.

3.E.14. Safety Subsystem

The Safety Subsystem checks safety relevant system hardware prior to and during the therapy session. It ensures that all safety relevant hazards are accounted for and recognized by the software.

Prior to beginning the therapy session the Safety Subsystem will test the Pause Button, Water level error latch, A/D and D/A converters, Heartbeat Error Latch, and the Power Inhibit Latch. During the therapy, this subsystem will monitor the Pause button, Water Level Signal, Water Level Latch, periodically test the A/D and D/A converters, Power Inhibit latch, and confirm that the Instrument computer is generating a Heartbeat signal appropriately. The Instrument Computer will generate a heartbeat at the same time as the Control Computer so that each computer will be watching the other.

This subsystem will also monitor and compare the breast/target positioning error threshold in the configuration file with the actual breast/target location determined by the Contour Monitoring Subsystem. The "zero reference" position will be the central axis of the treatment cylinder.

If an error condition is detected, this subsystem will be responsible for inhibiting the power supply, and/or inhibiting the Ultrasound output power.

3.E.15. Sensor Locator Subsystem

The Transducer array will be used to determine the positions of the thermometry needles. The Sensor Locator Subsystem is responsible for determining the sensor location of all sensors.

The location of each sensor is determined as follows. Each thermometry needle is a 19-gauge needle with 14 sensors. Spacing of the sensor is retrieved from the Treatment Plan Subsystem. Each needle contains two ultrasound transducer transponders which are utilized to locate the position of the implanted needle exactly within the breast and within the treatment cylinder. The known sensor spacing information is then used to determine the spatial location of each sensor within the total

treatment cylinder volume and within the breast. Within these volumes, each sensor is "assigned" by the Temperature Subsystem to a spatial volume cell.

The location of each sensor is also supplied to the Dynamic Treatment Calibration Subsystem so that movement in the sensor locations can also be recognized by the rest of the system.

3.E.16. PC Interface Subsystem

The PC Interface module initiates and maintains communications with the Instrument computer. This subsystem is capable of operating in three modes. The three modes of operation are Treatment mode, Test mode, and replay mode and are discussed below.

Treatment Mode

In the Treatment Mode, this subsystem communicates with the Instrument Computer to send and receive information about the hardware. The information received by this subsystem includes current measured forward and reflected power for each ultrasound transducer, "Time-of-Flight", Through-Transmission", and "Pulse-Echo" measurements for each ultrasound transducer, Current Cooling System Temperature and setpoint, actual temperature measurements as measured by the thermocouples, a Heartbeat signal, Video System information, and periodic safety testing information.

Simulation Mode

When operating in the Simulation Mode, this subsystem requests information from the Treatment Records Subsystem such that all requests from the other subsystems will be handled as if a Instrument Computer was present. This mode is provided primarily for testing and debug sessions when the Instrument Computer is not present.

Replay Mode

In Replay Mode this subsystem requests information from the Treatment Records Subsystem and provides this information to the other modules so that a treatment may be replayed.

3.F. Instrument Computer Functions

The Treatment Instrument Computer will receive measurement requests and control output requests via the communication link, act upon the requests as needed, and send replies to the Control Computer containing the measurement results or acknowledging the control operation. Measurement and control parameters needed are detailed below.

3.F.1. RF Power Subsystem Software

The RF Power Subsystem consists of 96 independent transmitters each driving a 4-way T/R Multiplexer which switches the RF output to the appropriate transducer.

The Instrument Computer will control the switching on/off of each of the VCO sources, the RF output power of each of the amplifier channels, the on-off status of each amplifier channel, the T/R MUX status of each channel relative to the 4 transducers which it may possibly drive, and the selection of which receivers are active at any given instant.

3.F.2. Receiver Subsystem Software

The Receiver Subsystem consists of 24 independent receiver modules which are interconnected to the T/R MUX devices as shown in Figure 20. The status of each is detected by the Instrument Computer and provided to the Contour Monitoring Subsystem, the Power Absorption Distribution Subsystem, and the Temperature Subsystem ("Time-of-Flight" data).

3.F.3. Cooling/Heating Control Software Subsystem

This subsystem is responsible for maintaining the proper coolant fluid temperature prior to and during the therapy session. This subsystem sets the cooling system temperature setpoint according to the Configuration file and continuously checks the measured cooling temperature to ensure that the cooling system has not malfunctioned. In the event that the measured temperature value is not within the tolerance (also set in the configuration file) set this subsystem will report the error to the Safety Subsystem. This subsystem is also responsible for turning on/off the cooling system as requested by the Control Subsystem.

3.F.4. Thermometry Interface Software Subsystem

The Thermometry Interface Subsystem communicates with the MIT thermometry subsystem in the appropriate manner to receive all temperature information. The temperature information is requested from the Thermometry System every 4 seconds and is then sent to the Temperature Subsystem in the Control Computer.

3.F.5. Safety Software Subsystem

The Safety Subsystem checks safety relevant system hardware prior to and during the therapy session. It ensures that all safety relevant hazards are accounted for and recognized by the software.

Prior to beginning the therapy session the Safety Subsystem will test the Pause Button, Water level error latch, A/D and D/A converters, Heartbeat Error Latch, and the Power Inhibit Latch. During the therapy, this subsystem will monitor the Pause button, Water Level Signal, Water Level Latch, periodically test the A/D and D/A converters,

Power Inhibit latch, and confirm that the Instrument computer is generating a Heartbeat signal appropriately. The Instrument Computer will generate a heartbeat at the same time as the Control Computer so that each computer will be watching the other.

This subsystem will also monitor and compare the breast/target positions within the treatment cylinder volume to the position error threshold specification in the Configuration file and pause the treatment if out of range. If an error condition is detected, this subsystem will be responsible for inhibiting the power supply, and/or inhibiting the Ultrasound output power.

4. EXPERIMENTAL STUDIES: TESTING IN PHANTOM AND NON-PERFUSED MUSCLE.

4.A. Introduction.

Sections V.2 and V.3 describe the various subsystems and test results. The purpose of the phantom and in-vitro muscle studies described below is to verify that the breast treatment system is capable of delivering adequate hyperthermia for thermal therapy of breast cancer. The complete breast treatment system was not yet integrated at the time of this report, therefore the phantom studies reported herein pertain to the use of a single ring with appropriate and previously tested electronics (See Year 01 Annual Progress Report). This is a relevant test, because the system is designed so that each of the eight rings are independent of each other and deposits energy only in the plane defined by the ring. Thus the results from a one ring experiment can be extrapolated to the full eight ring assembly. The final tests for the full assembly are scheduled to be completed in the month of June 1995.

4.B. Phantom Measurements.

4.B1. Breast Phantoms.

The phantoms consist of pharmaceutical gels containing uniform distributions of graphite and alcohol. Before being used in the experimental set-up, the physical characteristics of the materials were measured. The density of the phantom is 1.08 g, cm^{-3}, the heat capacity is 0.78 cal, g^{-1}, $(^oC)^{-1}$, the thermal conductivity is 0.0015 cal, cm^{-1}, K^{-1}, and the ultrasound attenuation coefficient is 0.75 dB, cm^{-1}, MHz^{-1}. The phantom gel is contained within a thin breast shaped rubber sheet intended to provide the structural support and prevent moisture from the phantom to escape. In spite of this, the phantom material tends to dry out after a few months with a subsequent change of material characteristics. We have therefore built several tissue-mimicking breast phantoms during the year as needed for our experiments.

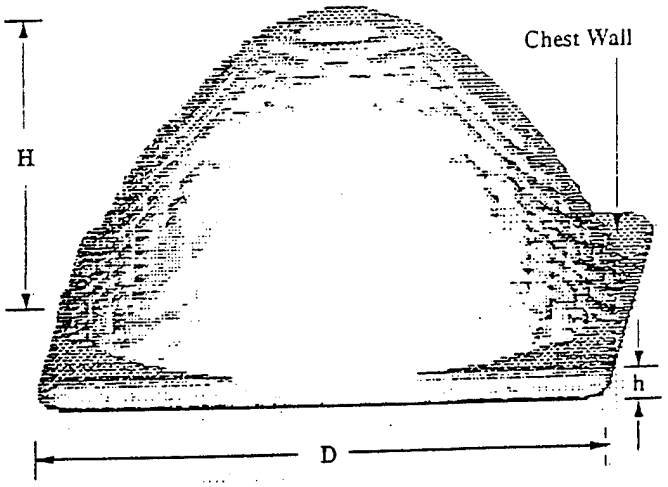

Figure 41 . Computer model of the graphite-alcohol breast phantom. The experimental phantoms were sized D=13 cm, H=8 cm, h=2 mm.

We have maintained the same dimensions of the breast phantom for all experiments and the single ring measurements have been done at different levels (H in Figure 41) representing different diameters of breast tissue. Two diameters were utilized for most of the experiments, 7 cm and 12 cm.

For testing of the completed breast treatment system, we will use a newly designed phantom that includes the chest wall with bone heterogeneities. This is a realistic ultrasound compatible phantom, which will adequately describe the three dimensional heat transfer properties and is of particular importance to study the optimal patient positioning on the table relative to the insonation portals.

4.B.2. Experimental Methods.

A single transducer ring was chosen for the experiments. The ring has 48 transducers, 24 of which operate at 2.0 MHz and the other 24 at 4.5 MHz. The two frequencies are alternated throughout the ring. The transducers have been thoroughly checked for output and bandwidth and example of such test results are presented in Section V.2.A.

Twelve amplifiers, each having its own oscillator, are used to drive the transducers. To power the 48 transducers, the output of each amplifier is connected to four transducers through a multiplexer. Consequently, there are four groups of twelve transducers (one quadrant) or eight groups of six transducers (either grouping may be selected). At any given time, six amplifiers are connected to one of the eight groups through the multiplexers. This multiplexing technique guarantees that the transducers all operate out-of-phase, thus eliminating the possibility of destructive interferences. The computer control system allows programmable adjustments of the power output to each transducer. Each transducer is sequentially powered for 55 msec. Therefore, it takes 8 X 55= 440 msec to cycle through the whole ring (or the whole ring assembly). Considering that the time constant for thermal processes are about 600 sec, this is a very fast cycling time. This rapid insonation cycle is therefore equivalent to continuos insonation at an average power, which is less than the peak power.

Multisensor thermocouple probes were used for temperature measurements. The probes were placed as shown in Figure 42.

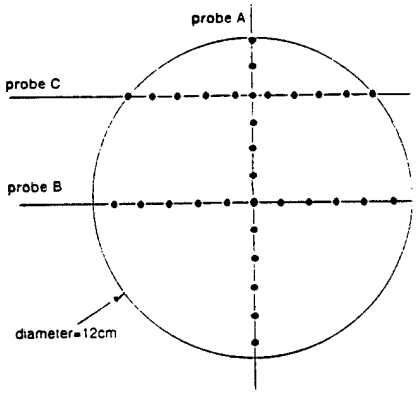

Figure 42. Probe placement

With the transducer ring submerged in degassed water, the phantom was placed and aligned within the ring. The water temperature was kept at 24°C during these experiments. SAR distributions and pseudo-steady state temperature distributions were measured for a variety of conditions. The measured data were compared to computer simulations. The simulation methods were described in detail in the Year 01 Annual Progress Report. Selected results are presented below. A more comprehensive discussion of this work is presented in Appendix A.

4.B.3. Results and discussion.

The temperature probes are labeled A, B, and C (see Figure 42).

The SAR distribution required to deliver a uniform steady state temperature is relatively small, and a direct measurement of the SAR will be difficult and inaccurate. Therefore we measured the SAR for each output power configuration at higher total power and normalized the SAR distribution to that power level. The normalized SAR (q_0) for each sensor point is calculated from the initial temperature rise and deduced from $q_0 = C_V (\Delta T/\Delta t) N^{-1}$, where ΔT is the temperature elevation at the sensor point during time interval Δt between 1 second and 11 seconds. C_V is the heat capacity and N is the total output power of the amplifiers calculated as the sum of the power for low and high frequency. The output power used in this SAR this experiment was 2.5 W and 10 W for 2 MHz and 4.5 MHz frequencies, respectively.

The cross symbols in Figure 43 show the measured steady state temperature in the phantom for probes A, B, and C. The goal was to reach a steady state temperature rise of 6°C above the water temperature, which is 24°C. The resulting 30°C was reached and maintained within 2°C, which is the design specification for the system. The experiment was simulated using a sophisticated computer algorithm (See Year 01 Annual Progress Report and Appendix A). The solid line in Figure 43 shows the simulated temperature distribution. Two sensors located at +30 mm and +50 mm disagree with the simulations by 1°C and 1.3°C respectively. Except for those discrepancies, the agreement for all probes is excellent and remains within 0.5°C-0.8°C.

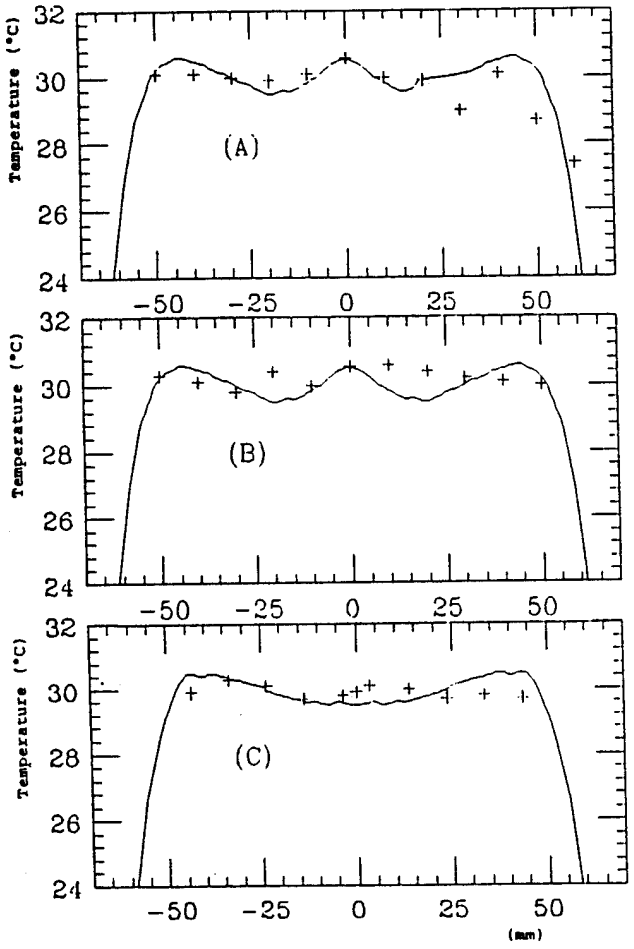

Figure 43. Temperatures in probe A, B, C.

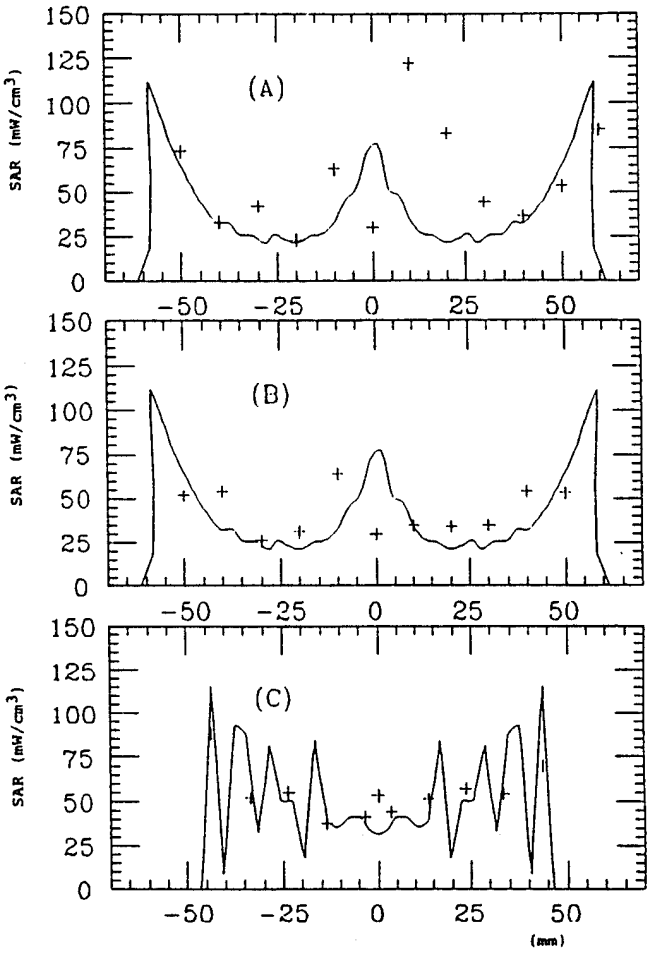

Figure 44. SAR's in probe A, B, C.

The total power required to reach the goal of a 6°C temperature rise was 1.9 W for the low frequency transducers and 15 W for the high frequency transducers. Using the formula above we can now multiply the normalized SAR (q_0) and calculate the power deposition distributions (SAR) required to reach the measured temperatures. The cross symbols in Figure 44 show the results, which are compared to the computer simulated calculations (solid line). In general the results are very good except for a few large discrepancies in probe A.

Several factors contribute to the uncertainties in the experimental temperature data, and in the measured versus calculated SAR values.

- When inserting the temperature probe, the deeper sensors may shift slightly due to bending of the probe. The location of the needle tip sensor is therefore uncertain to ≤ 1 cm. Since the SAR is very position sensitive, it is likely that the discrepancy between measured and simulated SAR distributions is due to this problem.

- In the simulation we assumed identical acoustic efficiency for all 48 transducers. In the actual applicator, transducer efficiency varied ± 6 %. Variation of a total of 12 % between individual transducers was experienced. This problem contributed to the discrepancies between the modeling and the measured results.

- We know that the phantom gel can dry out after storage, particularly after needles have penetrated the rubber sheet. Phantoms had to be re-used for a few experiments, and it is possible that some water and alcohol could have evaporated and created inhomogeneities with different ultrasound absorption characteristics in the phantom.

The excellent agreement between measured and simulated temperature distributions is a validation of the computer algorithms. We will now use simulation for patient treatment planning. One example of the use of computer simulation to plan a special patient is demonstrated in Figures 45, 46, 47, 48. Figure 45 shows a cross section through the breast of a patient. Perfusion is uniform and assumed to have a perfusion constant of 600 s at 37°C and 2000 s at 44 °C. The power deposition pattern required for a uniform steady state temperature distribution is calculated and shown in Figure 45. The resulting steady state temperature distribution is shown in Figure 46.

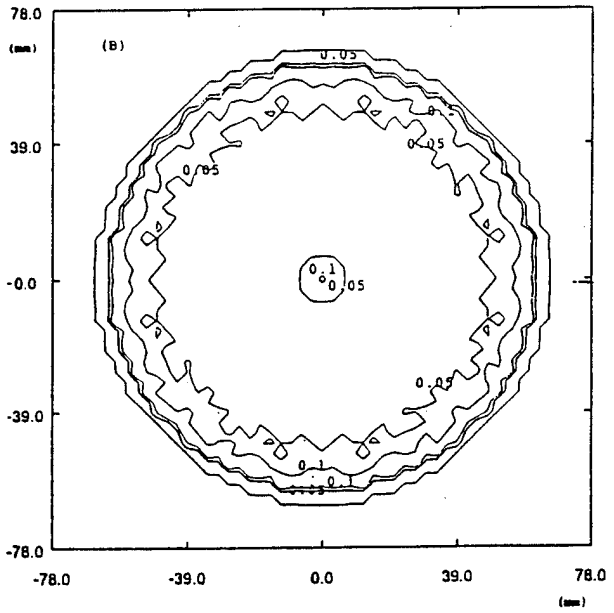

Figure 45. Power deposition pattern (SAR) for a uniform temperature distribution at equilibrium and uniform perfusion.

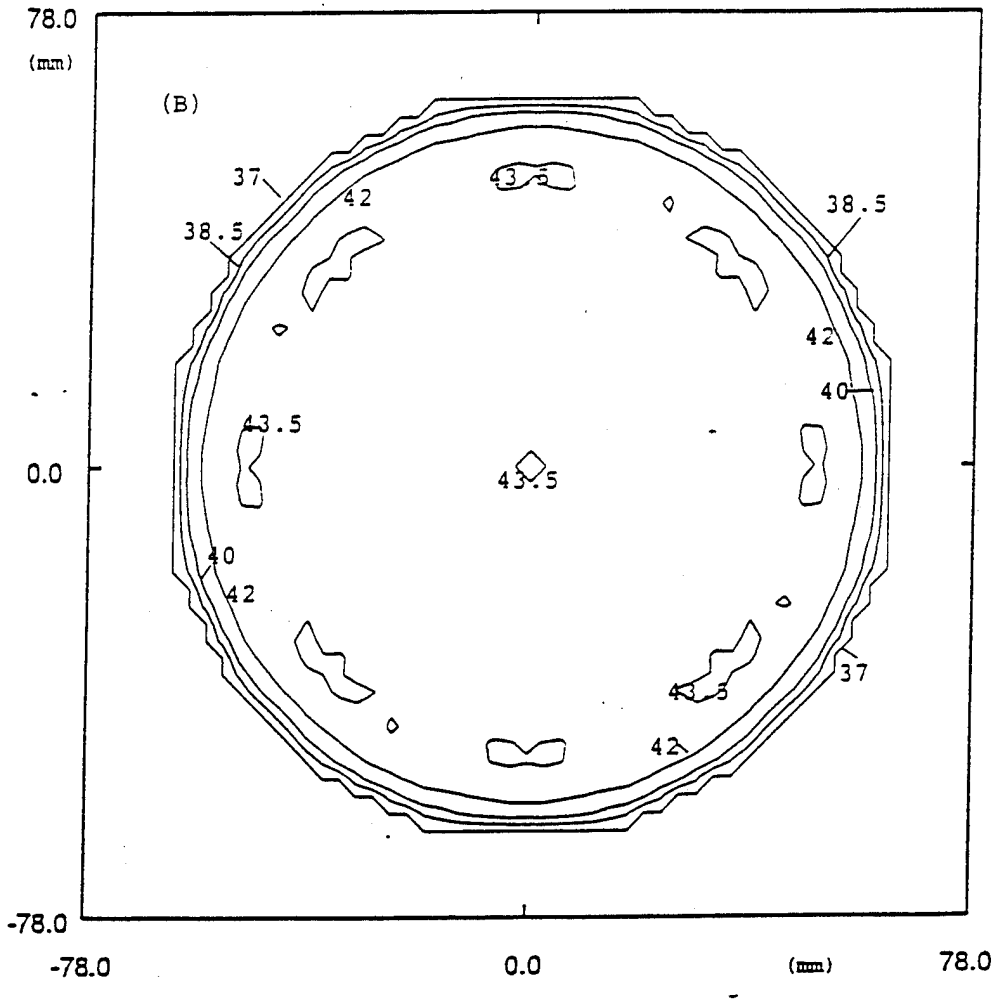

Figure 46. Equilibrium temperature distribution.

This patient had undergone a lumpectomy. A CT scan of the breast demonstrated the size and geometry of the surgical incision and the lumpectomy cavity. It is known that such scar tissue has essentially no perfusion and the uniform SAR pattern shown in Figure 45 will result in significant overheating of this region. The results of our validated simulations are shown in Figure 47 and demonstrates that the lumpectomy region is reaching a temperature of 44.5°C, which is above the temperature considered safe to avoid toxicity in our protocol ($T_{max} < 44^{o}C$). Precise spatial and power control of the system permits us to change the SAR pattern to account for the lower perfusion in this well defined region. Figure 48 shows the uniform temperature distribution resulting from the corrected energy deposition pattern in the lumpectomy region.

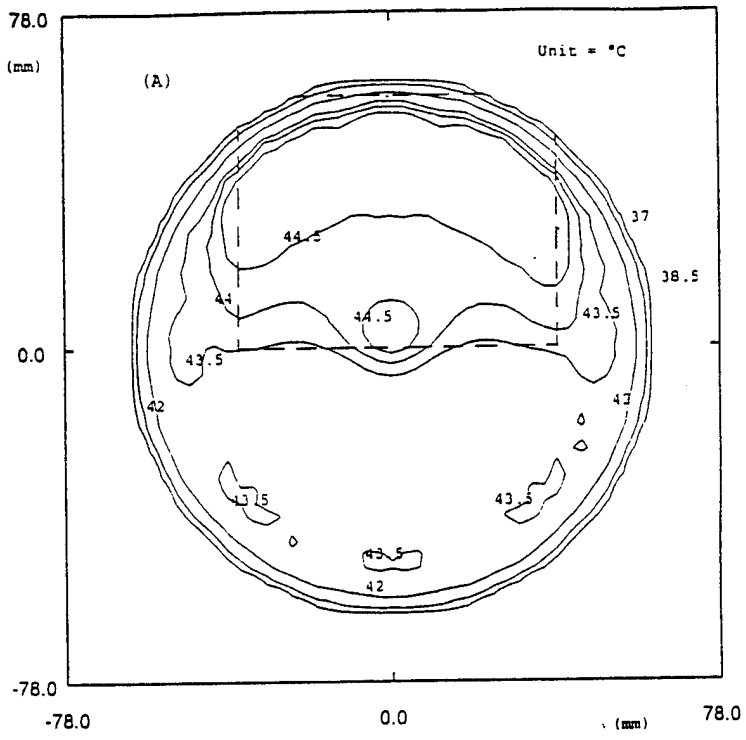

Figure 47. Increased temperature distribution in the region of the lumpectomy cavity and scar. The increased temperature is the result of low or no perfusion for a uniform SAR distribution as shown in figure 45.

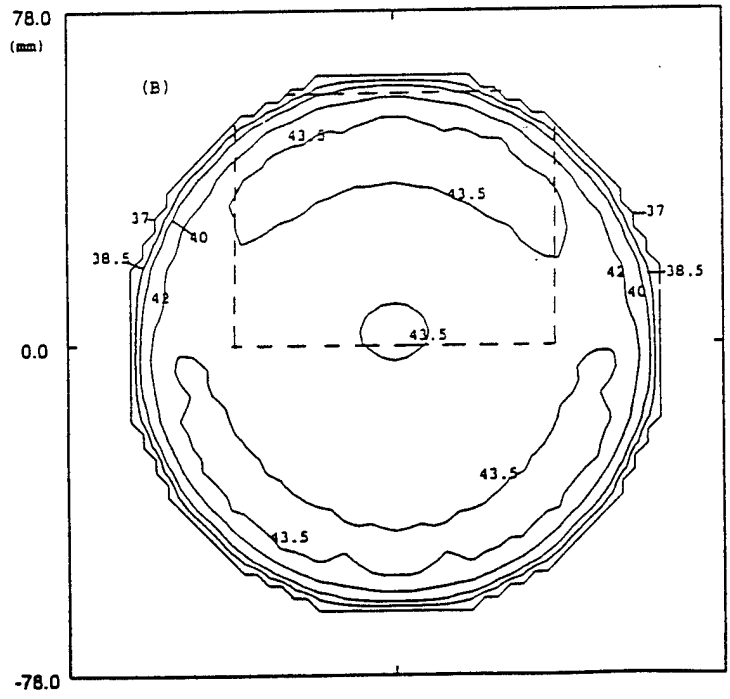

Figure 48. Shows uniform temperature distribution across the lumpectomy region after correcting the SAR distribution to account for the lower perfusion.

4.C. Experimental Tests Performed Using Non-Perfused Muscle Tissue.

4.C.1. Muscle Tissue.

This in-vitro experiment used a large piece of pig muscle with a normal content of fatty tissue.

4.C.2. Experimental Methods.

The experimental equipment and set-up is identical to that described in section V.4.B.2. The probe placement and twelve measurement points are shown in Figure 50. The water temperature during this experiment was kept at 22°C. Pseudo-steady state temperature distributions were measured with the goal of demonstrating that uniform heating of muscle tissue with fat heterogeneities can be achieved. Due to the elliptical shape of the muscle tissue, it was also possible to examine the effect of the shape factor on the resulting temperature distribution. Both 2 MHz and 4.5 MHz frequencies were used to optimize the distribution. No computer simulation of this experiment was performed because the tissue specific ultrasound parameters (i.e. attenuation, velocity etc.) needed for a calculation were not known.

4.C.3. Results and Discussion.

Figure 49 shows the temperature increase as a function of heating time for each of the twelve measurement points in the pig muscle phantom. The ultrasound power was turned on at time 33 seconds. We are interested in the temperature distribution when the temperature vs time curves have reached pseudo steady-state. Most of the measurement points seem to have reached such a state at around 1000 seconds and the temperature distribution at 1030 seconds is shown in Figure 50. A minimum of 27.4°C and a maximum of 29.6°C was reached at that point. The temperature distribution is quite uniform and 11 out of the 12 points are within the 2°C, which is the heating uniformity criteria for the system. The absence of significant hot or cold spots again confirms that there is no destructive ultrasound interference in the ultrasound field.

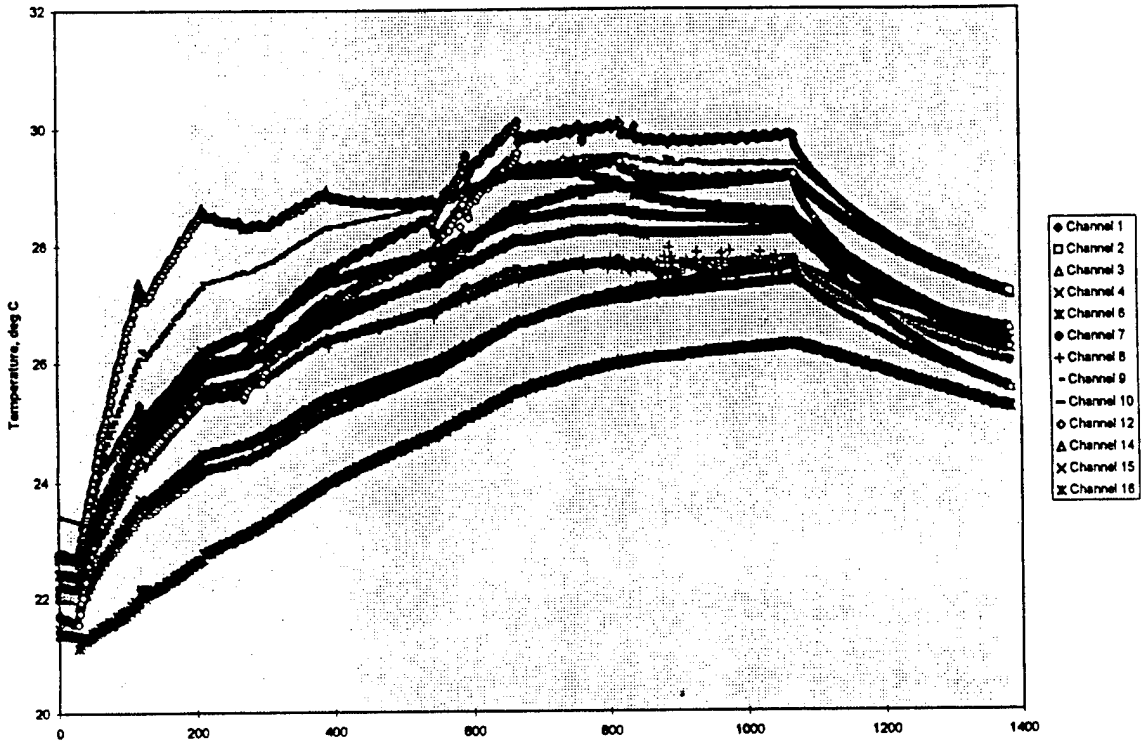

Figure 49. Temperature-time record for pig muscle heating experiment. The pig muscle contained significant amount of fatty tissue. Power was turned on at 33 seconds and pseudo steady-state condition was reached at 1030 seconds. The power was turned off at 1130 seconds.

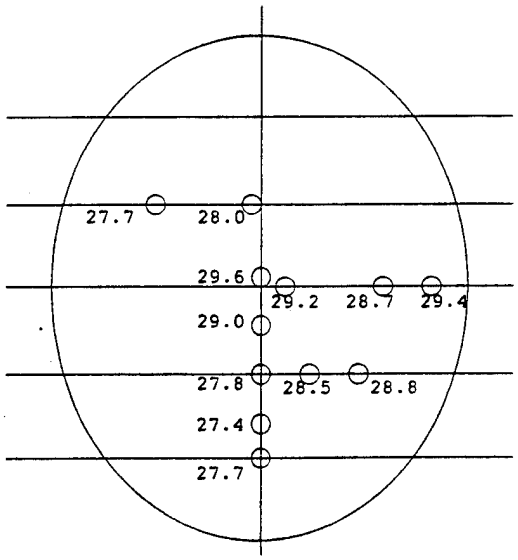

Figure 50. Cross-section of the elliptical pig muscle phantom shown with the probes and measurement points. Both low and high frequencies were used. The temperatures ranged from 27.4°C to 29.6°C.

4.E. Conclusion and Significance.

These studies have demonstrated that the breast thermal therapy applicator can deliver a power deposition capable of achieving uniform temperatures. This is achieved by using individual amplifier power control and two frequencies; 2.0 MHz and 4.5 MHz. The range of power control is large as compared to clinical needs. Consequently, it will be possible to adequately treat a wide variety of clinical situations and over a large range of breast tissue parameters, such as various perfusion and temperature boundary conditions.

These experiments did not show any unpredictable hot or cold areas (See Figure 43). This demonstrates that there are no destructive interferences between the ultrasound transducers that would create such hot or cold areas. Therefore, the electronic design and the multiplexer switching arrangements have been successfully implemented.

The excellent agreement between experimentally measured temperatures in the alcohol-Agar phantom and computer simulations has demonstrated the validity of the computer algorithm used in the simulations. It is planned to use computer simulations for planning of a variety of clinical breast treatment cases.

5. BREAST TREATMENT PROTOCOLS.

Clinical research protocols for cancer treatments using new devices are subject to increasingly rigorous scrutiny by the hospital IRB and the FDA branch that issues the Investigational Device Exemption (IDE). Recent federal regulations require the hospital to have an IDE for any new device used in therapy before the IRB approval. The branch of FDA that issues the IDE, on the other hand, require that an IRB approved protocol becomes part of the IDE application. This situation has created delays in the process of applying for and receiving both IRB approval and an IDE.

In addition, as has been mentioned in Section V.1.B., our External Review Committee recommended a Phase I device evaluation study before we continue with a Phase I/II safety-efficacy study. Thus one more protocol had to be written and conducted than originally planned.

As discussed in Program Organization (Section V.1.A.), the JCRT member hospitals network require IRB approval from all participating hospitals. It is important that our sponsoring institution (NEDH), and DFCI with its Breast Evaluation Center participate in this clinical research. Therefore, IRB approvals of our protocols is sought from both institutions as well as from the U.S. Army Human Use Review and Regulatory Affairs Division.

As it stands now, a Phase I device evaluation protocol has been IRB approved by DFCI contingent upon receiving an IDE. This protocol has been under clinical, scientific and technical scrutiny for six months. The approved protocol is attached as Appendix G to this report. It has also been submitted to the Human Subjects Committee at NEDH, where we expect a fairly rapid approval due to the fact it has already been scrutinized by another Harvard hospital. We have also submitted the protocol to the U.S. Army Human

Use Review and Regulatory Affairs Division (Ms. Catherine A. Smith, Human Use Review Specialist). Ms. Smith will begin the protocol review, pending the completion of a new federal form for "Protection of Human Subjects".

The primary purpose of this protocol is to evaluate the limitations and capabilities of the breast treatment system to deliver homogenous and controllable heat in a specified quadrant, half, or whole breast. In addition, these patients will be followed to evaluate acute and long-term toxicity and cosmetic outcome of thermal therapy combined with radiation therapy to treat early breast cancer. One important feature of this protocol is that the temperature range that the temperature range is a minimum of 40°C to a maximum of <43°C for a time of 45 minutes. This is a conservatively low temperature and thermal dose, and no toxicities or undesirable reactions are expected within this range. For this reason, the protocol is clearly focusing on device evaluation.

The next step is to develop a Phase I/II toxicity, efficacy protocol. The main clinical concern in implementing a Phase I/II protocol is that using heat treatment as an adjuvant to radiation has the potential of increasing the incidence of breast tissue fibrosis as an undesirable toxicity. The External Review Group recommends a temperature escalation study, where the maximum temperature should never exceed 44°C and the minimum temperature should start at 40.5°C to be escalated to 42°C with careful analysis of short term toxicity. If this temperature escalation is successful, the treatment objective will be to achieve a temperature range of 42°C to 44°C. Such a narrow temperature range in heterogeneous breast tissue requires highly interactive power deposition control with knowledge of the effect of perfusion on the heat transfer. These considerations will be included in the Phase I/II protocol under development within this program.

VI. CONCLUSIONS.

1. SIGNIFICANCE OF THE COMPLETED RESEARCH.

The main goal of this research program is to develop an ultrasound hyperthermia system for treatment of infiltrating carcinoma of the breast with an extensive intraductal component (EIC) or patients with ductal carcinoma in situ (DCIS) of the breast. A carefully designed Phase I device evaluation study must be completed with 15 patients accrued before the Phase I/II toxicity/efficacy study can take place.

The breast ultrasound therapy system to be used for these studies has been designed and fabricated, and its subsystems have undergone successful and rigorous testing. The results of these tests are described in this comprehensive report. The assembled subsystems are currently being interconnected and an integrated systems test is underway and will be completed during June 1995. Many important revision's in the systems designs have been made in response to our External Review Group, and as a result of research findings over the last two years. These revisions will significantly increase the safe utilization of the treatment system and improve the control of the temporal and spatial temperature distribution throughout the breast tissue. These improvements primarily consist of:

- Significantly increasing the number of transducers in the cylindrical array breast applicator (with a concomitant increase in the number of electronic channels) for

the dual purpose of much finer spatial control of therapy and improved potential for non-invasive monitoring.

- The decision to abandon the originally considered microwave radiometry in favor of utilizing the cylindrical array transducers in an interrogation mode of operation, thus permitting both real-time imaging of the breast contour/profile in the applicator and measurement of through-transmission signals. After processing, these signals provide derivative information concerning attenuation and power absorption distribution within the breast during therapy. Using the same transducers for therapy and interrogation also opens the potential for breast tomography, i.e. imaging the same "slices" that receive therapy.

- The addition of phased-locked sources for interrogation, and provision for future addition of a Digital Signal Processor (DSP) plus local microcontrollers jointly make possible future addition of on-line tomographic non-invasive imaging/mapping during therapy.

The improvements will lead to high quality clinical data from the clinical studies and improved patient safety. We believe that each of these revisions and additions to the designs are essential to the clinical success of this program. These revisions have taken extra time and significant resources and we have requested a six months no-cost extension in a separate communication to the Director for the Breast Cancer Research Program.

Recently published results from a European Phase III randomized trial (Vernon, 1994) studying the use of thermal therapy (hyperthermia) for breast cancer treatments show a significant advantage of combining thermal therapy and radiation as compared to radiation alone. This was a large cooperative study sponsored by the European Society for Hyperthermic Oncology (ESHO) accruing over 300 patients with recurrent or primary breast cancer. The results show an overall complete response rate of 60 % when using radiation plus thermal therapy as compared to 40 % for radiation alone. This is a highly significant difference and supports the use of thermal therapy for breast cancer treatment. Of special significance for this program is the fact that until now, there has been no adequate treatment device available for thermal treatment of intact breast. The system developed under this contract is the only breast-specific treatment device in existence, and is unique in its capability to treat breast safely, accurately, and precisely. This system, particularly if duplicated, will be in a unique and timely position to support additional clinical breast cancer studies that may be designed to follow up on the encouraging European results. To optimize the utilization of the breast thermal therapy system for clinical studies, future research is suggested below.

2. FUTURE WORK TO IMPROVE THE BREAST THERMAL THERAPY SYSTEM AND ITS APPLICATION.

- There is a renewed interest in applying thermal therapy to breast cancer as a result of very positive clinical trials performed in Europe (Vernon, 1994). These trials, as well as other clinical research has identified other breast cancers as being suitable for thermal therapy (Kapp et al., 1991, Oleson et al. 1993). We propose to increase our clinical efforts by designing clinical protocols for the

treatment of locally advanced breast cancer.

- Potential treatment related tissue toxicities are of extreme importance to monitor for future application of combined breast treatment modalities, including the use of thermal therapy. Analysis of cross correlated, ultrasound interaction parameters in breast tissue may provide important insight in the relative temperature distribution and associated tissue changes and their relationships to treatment course and modalities. This requires a significant research effort with additional support well beyond the scope of the current contract.

- The studies proposed can be augmented by fully developing an on-line tomographic capability. Tomographic image data will be correlated with temperature distributions and used in control of therapy. This will require further technical developments once the clinical studies proposed in the current program have commenced. The current program structure, as originally proposed, anticipates delivery of the system to JCRT for clinical trials. No effort for further development of monitoring and control software is included or supported. No provision exists for the tomographic upgrades of the DSP capability. We believe that upgrades to the system based on clinical results is a very important aspect of this research.

- The U.S. Army Medical Research and Development Command is already supporting a separate program directed to localized thermally-ablative surgery of single-focus lesions. The surgical technique uses laser energy to induce the localized heating through one or more needle insertions into the lesions. We propose to take advantage of the capabilities, features and knowledge gained from the present breast ultrasound therapy system to extend this capability and develop a non-invasive focused ultrasound thermally-ablative surgery device, incorporating real time tomographic targeting, for treatment of single-focus early stage lesions. If such an effort were to be successful this approach would be less costly and could rival the use of lesion ablation in an open MRI magnet.

VII. REFERENCES

Bornstein BA, Recht A, Connolly JL, Schnitt SJ, Cady B, Koufman C, Love S, Osteen RT, and Harris JR.: Results of treating ductal carcinoma in situ of the breast with conservative surgery and radiation therapy. Cancer Vol. 67(7-13) 1991.

Bornstein BA, Zouranjian PS, Hansen JL, Fraser SM, Gelwan LA, Teicher BA, Svensson GK. Local hyperthermia, radiation therapy, and chemotherapy in patients with local-regional recurrence of breast carcinoma. Int. J. Rad. Onc. Biol. Phys. Vol. 25 (79-85) 1992.

Bowman HF, Newman WH, Curley MG, Summit SC, Kumar S, Martin GT, Hansen J, Svensson GK. Tumor hyperthermia: dense thermometry, dosimetry, and effects of perfusion. In: Advances in Biological Heat and Mass Transfer, HTD-volume 189/BED, 18:23-31, ASME, 1991.

Dewhirst MW, Griffin TW, Smith AR, Parker RG, Hanks GE, and Brady LW. Commentary

by the Intersociety Council on Radiation Oncology Essay on the Introduction of New Medical Treatments Into Practice. J. National Cancer Inst. Vol. 85 (951-957) No 12, 1993.

Hahn GM.: Hyperthermia and cancer. p 154-163. Plenum Press, New York, 1982.

Hansen JL, Bornstein BA, Svensson GK, Newman WH, Martin GT, Sidney DA, Bowman HF: A quantitative, integrated, clinical focused ultrasound system for deep hyperthermia. Proceedings of the American Society of Mechanical Engineers' Winter Annual Meeting, November, 6 - 11, 1994 Chicago, Illinois.

Kapp DS, Barnett TA, Cox RS, Lee ER, Lohrbach A, and Fessenden P.: Hyperthermia and radiation therapy of local-regional recurrent breast cancer: prognostic factors for response and local control of diffuse or nodular tumors. Int. J. Rad. Onc. Biol. Phys. Vol. 20 (1147-1164), 1991.

Kapp, D.S., Cox , R.S., Fessenden, P., Meyer, J.L., Prionas, S.D., Lee, E.R., Bagshaw, W.A.: Parameters predictive for complications of treatment with combined hyperthermia and radiation therapy. Int. J. Rad. Onc. Biol. Phys. Vol. 22(5) 999-1008, 1992.

Kapp KS, and Kapp DS.: Hyperthermia's emerging role in cancer therapy. Contemporary Oncology. (19 - 30) June 1993.

Lu XQ, Svensson GK, Hansen JL, Bornstein BA, Harris JR, Burdette EC, Slayton M, Barthe P. Design of an ultrasound hyperthermia unit for breast cancer treatment. Abstract in Radiation Research Society - 42nd Annual Meeting, North American Hyperthermia Society - 14th Annual Meeting. Nashville, Tennessee April 29 to May 4, 1994. Page 124.

Mayr NA, Staples JJ, Robinson RA, Vanmetre JE, and Hussey DH.: Morphometric studies in intraductal breast carcinoma using computerized image analysis. Cancer, Vol. 67(2805-2812) 1991.

Oleson JR, Samulski TV, Leopold KA, Clegg ST, Dewhirst MW, Dodge RK, and George SL.: Sensitivity of hyperthermia trial outcomes to temperature and time: Implications for thermal goals of treatment. Int. J. Rad. Onc. Biol. Phys. Vol. 25 (289-297) 1993

Sapareto SA and Dewey WC.: Thermal dose determination in cancer therapy. Int. J. Rad. Onc. Biol. Phys. 10(787-800) 1984.

Schnitt SJ, Silen W, Sadowsky NL, Connolly JL, and Harris JR.: Current concepts: Ductal carcinoma in situ (intraductal carcinoma) of the breast. New Engl. J. Med. Vol. 318(898-903) 1988.

Solin LJ, Recht A, Fourquet A, Kurtz J, Kuske R, McNeese M, McCormick B, Cross MA, Schultz DJ, Bornstein BA, Spitalier JM, Vilcoq JR, Fowble BL, Harris JR, and Goodman RL.: Ten year results of breast-conserving surgery and definitive irradiation for intraductal carcinoma (ductal carcinoma in situ) of the breast. Cancer vol. 68 (2337-2344) 1991.

Svensson GK, Lu, X-Q, Hansen JL, Bornstein BA, Burdette EC. Simulation of a multi-transducer, dual frequency ultrasound applicator for hyperthermia treatment of breast cancer. Proceedings of the IEEE Int. Symposium on Electromagnetic Compatibility, Sendai, Japan May 1994. Pages 433 - 436.

Vernon CC.: Collaborative Phase III superficial hyperthermia trial (MRC/ESHO/PMH). Proceeding of Fourteenth Annual Meeting of the North American Hyperthermia Society. Nashville, TN. Page 87, 1994.

VIII. APPENDICES.

A. Manuscript: Design of an Ultrasonic Therapy System for Breast Cancer Treatment.

B. Manuscript: Ultrasound Power Deposition in a Water - Soft Tissue Medium.

C. Efficiency data for each transducer in the cylindrical array.

D. T/R MUX applicator transducer interconnections map.

E. Measured angular beam profile data for 2.0 MHz and 4.5 MHz transducers.

F. Breast phantom pulse echo and through transmission, non-invasive receiver measurements data used for tomographic reconstructions.

G. Protocol and consent form for a Phase I device evaluation study for breast ultrasound therapy system.

Appendix A

Design of an Ultrasonic Therapy System for Breast Cancer Treatment

X-Q. Lu[1], E.C. Burdette [2], B.A. Bornstein [1],
J.L. Hansen [1], G. K. Svensson [1]

Joint Center for Radiation Therapy
Department of Radiation Oncology
Harvard Medical School
Boston, MA 02115

[2]Dornier Medical Systems Inc.
Champaign, IL 61820

April 1995

Design of an Ultrasonic Therapy System for Breast Cancer Treatment

X-Q. Lu [1], E.C. Burdette [2], B. A. Bornstein [1],
J. L. Hansen [1], G. K. Svensson [1]

[1] Joint Center for Radiation Therapy
Department of Radiation Oncology
Harvard Medical School
Boston, MA 02115

[2] Dornier Medical Systems Inc.
Champaign, IL 61820

April 20, 1995

Abstract

A site-specific ultrasound hyperthermia unit has been designed to utilize the synergistic effect between thermal therapy and radiation therapy for the treatment of breast cancer The applicator is a cylinder comprised of a stack of rings. Each ring has up to 48 transducers mounted on the inside of the ring and directed towards the center. The transducers operate in one of two frequency bands (1.8-2.6 MHz for low and 4-4.7 MHz for high), and are arranged alternately in each ring. During the treatment the patient is in the prone position, and the breast will be immersed in water and surrounded by this array. This design was modeled and optimized by 3-D simulations for a variety of treatment conditions. The results demonstrate that the system has an excellent capability to achieve and maintain a temperature distribution $(41.5° - 44°C)$ in a quadrant to a whole breast. The design has been tested using a single ring of transducers that shows good agreement with simulation predictions.

Key Words: Hyperthermia, breast treatment, ultrasound field, bioheat transfer.

1 Introduction

Clinical data show that the combination of hyperthermia with radiation therapy or cytotoxic agents improve complete response rates for the treatment of many cancers (Kapp and Kapp 1993). A majority of these clinical studies pertain to hyperthermia treatment of superficial and small tumors (i.e. < 4 *cm* in diameter). Considerable problems still remain when using external hyperthermia applicators for the treatment of deep and large tumors. Ultrasound is capable of penetrating soft tissues to produce deep heating. (Lele 1983, Fessenden et al.1984, Hynynen et al. 1987, Hansen et al. 1994) To fully utilize its potential, however, tumor site specific applicators which optimize heat delivery to the tumor are needed. Only then can we expect improved efficacy and reduced complications of hyperthermia treatment.

Recent studies have shown that the use of conservative surgery and radiation in patients with an infiltrating breast cancer containing an extensive intraductal component (EIC) is associated with an increased risk of local fail-

ure (Boyages et al. 1990). Intraductal carcinoma is characterized by a proliferation of cancer cells within breast ducts typically showing central necrosis, which may correspond to hypoxic regions as indicated by a morphometric study (Mayr et al. 1991). It is know that hypoxia increases radioresistance by as much as a factor of 3 (Palcic and Skarsgard 1984) and that heat is effective at killing cells in a hypoxic environment (Dewey et al 1977). These patients, therefore, may benefit from a combined approach using hyperthermia and radiation therapy. Other potential patients who may benefit from the hyperthermia treatment include those with local recurrence after mastectomy, non-inflammatory stage III patients, and those with ipsilateral local recurrence after radiation therapy. A European phase III study randomized over 300 patients with recurrent or primary breast cancer to radiation alone or to radiation and superficial hyperthermia. The preliminary results (Vernon 1994) show an overall complete response rate of 60% for the combined treatments as compared to 40% for radiation alone.

Geometrically, the breast is a site particularly well suited for hyperthermia. This is due to its convex shape, the absence of large vessels and the relatively low perfusion. However, current applicators, using ultrasound or microwave, are still not able to deliver an optimized heating pattern for the treatment on the intact breast. For these reasons, a dedicated applicator has been designed. The goals are as follows.

- The system should be able to elevate and maintain the temperature above $41.5°\ C$ but not exceed $44°\ C$ in a treatment volume ranging from a quadrant to the whole breast. It is critical to keep the temperature within this narrow range in order to minimize potential toxicity and yet maximize effectiveness of the treatment (Kapp et al. 1992, Oleson et al. 1993).

- It should have the operational flexibility to accommodate the uncertainties in tissue characteristics, such as ultrasound attenuation and perfusion rate, and the variability in the patient geometry.

- It should be easy to use in the clinic.

These requirements present a considerable technological challenge. To meet these goals the design has to rely on general physics considerations. We consider ultrasound to be most suitable for treatment of the breast tissue

compared to other modalities. Some reasons for the choice are that the penetration and the power deposition of ultrasound can be controlled by selecting appropriate frequencies, and air cavities and bone interfaces with soft tissue are minimal in the breast. The arrangement of the transducers has to be determined by the power deposition pattern that satisfies the thermal condition for uniform temperature elevation.

The purpose of the work described here is twofold. The first is to determine the geometry and transducer characteristics to achieve adequate hyperthermia for a range of breast tissue characteristics, such as breast size, ultrasound attenuation and perfusion. The theoretical model for ultrasound power deposition calculation and the three dimensional solution to the bioheat transfer equation, which offered insights in the physical process and optimized the system, are discussed.

The second purpose is to present an experimental validation of the theoretical model. A single prototype transducer ring was used in the validation experiments. The experimental data was analyzed and compared to the theoretical models. The experiment also serves as a test of the electronics design.

2 Method

2.1 Basic design

It is desirable to achieve a uniform hyperthermic temperature region covering the tumor volume with sharp temperature gradients at the edge towards the normal tissue. Several investigators (Ocheltree and Frizzell 1987, Roemer 1991) have theoretically studied the energy deposition pattern required to achieve such temperature distribution. It was found that in the absence of large blood vessels, the ideal temperature distribution can be achieved by depositing power properly in the boundary and the interior of the treatment region. The power deposited in the boundary compensates for the conduction losses to the surrounding volume, and the power deposited interiorly in the treatment region is for overcoming the effect of blood perfusion.

An important lesson can be drawn from these studies for the design of the breast applicator. When the whole breast needs to be treated, the boundary consists of the breast surface and the chest wall. In order to elevate the tem-

perature uniformly inside the breast, independent adjustment of the power deposition in the interior of the breast and the two boundaries is necessary. We found that this capability cannot be obtained by the current ultrasound devices, in which only one frequency is applied in a treatment. It was determined that two different frequencies should be used simultaneously.

The low frequency (2 MHz for the first two ring and 2.5 MHz elsewhere) is more penetrating and deposits energy deeper into the breast tissue, thus compensating for the energy removed by blood flow in the interior of the breast. The high frequency is 4.5 MHz. With a higher attenuation rate, it deposits most of the power near the breast surface and compensates for heat loss to outside of the breast. The chest wall boundary, on the other hand, can be addressed by using both high and low frequencies. An optimized power deposition, therefore, can be obtained by an appropriate combination of these two frequencies. Furthermore, in order to spare the skin while maintaining a uniform temperature internally, a steep temperature gradient near the surface is necessary. This can be achieved by surrounding the breast tissue with a temperature controlled water bath. The water can be maintained at a constant temperature that is sufficiently cold to provide a steep temperature gradient and yet be comfortable to the patient (i.e. $\sim 30°\ C$). In addition, the surrounding water bath provides an excellent coupling for ultrasound propagation.

In some clinical situations, only a quadrant of the breast needs to be treated. The pie shaped treatment region is bounded by a quadrant of the breast tissue surface, a quadrant of the chest wall base and two planes inside the breast. The quadrant breast surface is insonated using high frequency ultrasound, and the boundaries deep into the tissue are insonated using low frequency ultrasound.

To implement this approach, a cylindrical applicator was designed which consists of a stack of 8 rings with an inner diameter of 25 cm (Figure 1). There are 48 transducers in each of the upper 4 rings, and this number decreases to 24 and 16 in the rest rings toward the apex of the breast. Low frequency (1.8-2.6 MHz) and high frequency (4.0 - 4.7 MHz) transducers are arranged alternately in each ring. The patient lies in a prone position with her breast submerged through a hole in the table into the water filled applicator. Water bath temperature is controllable from $30°C$ to $40°C$.

This arrangement takes advantage of the convex shape of the breast. One benefit of insonating the breast tangentially is that the field is parallel to the

chest wall, thus minimizing the interaction between the ribs and the ultrasound field. Furthermore, since the beams from adjacent rings are parallel to each other, their heating effects are relatively independent, which simplifies the control process.

The size of the transducers is 1.5 $cm \times 1.5$ cm. The gap between two adjacent rings is 0.24 cm. Small size transducers permits a better control for different geometry and heating patterns. This is particularly important when a surgical scar or a lumpectomy cavity is within the treatment volume. Scar tissue has poor blood supply and very low perfusion rate, therefore, tends to be overheated. The excellent spatial power control resolution inherent in the design of this system is important to minimize the risk for scar tissue overheating.

Due to the considerable uncertainties in various tissue parameters (in particular the attenuation and perfusion rate), the use of relatively broad frequency-band transducers is a necessity. This is especially true for the low frequency transducers due to the large uncertainty of the perfusion rate, and they have a 30% 3-dB bandwidth. The electronics is designed to be able to control the frequency, power and duty cycle in wide ranges for each transducer individually. This feature gives the system a great deal of flexibility to adapt to various treatment scenarios.

Intensity amplification/cancellation due to phase effects between different transducers have been exploited in focused phased array devices for the treatment of deep tumors (Ebbini and Cain, 1991). In the design of this unit, however, the phase effect is purposely avoided, since without a sophisticated spot-scanning mechanism this interference could cause unpredicted and unwanted hot spots. To make sure the phase effect is eliminated, each transducer operated at the same time must be driven by individual amplifiers with separate oscillators.

To facilitate treatment planning and control, knowledge of the breast profile is essential. This will be obtained on-line by employing pulse-echo signals using the same transducers. Two operating modes (transmit and receive) are available for each transducer and can be controlled individually. Temperature and the thermal perfusion properties will be monitored by minimally invasive multisensor probes. These probes are 22 gauge 'active needles' consisting of a series of long, thin integrated circuits (Szajda et al. 1994). Thermometric data provided by these probes will be used to control the heating patterns with the corresponding temperature fields displayed in real time.

2.2 Simulation

Due to the complexity of the acoustic wave propagation and the bio-heat transfer process, it is very difficult to predict the performance of a device without detailed calculations. It is desirable to have a comprehensive numerical model to guide the design effort. This kind of computationally intensive simulations became feasible with the availability of high-speed workstations.

The modeling efforts consist of three parts: the geometric model, the acoustic field model, and the bio-heat transfer model. The geometric model is shown in Figure 2, where a paraboloidal surface with a height H and a diameter D on the base are assumed. Clinically relevant breast sizes, when submerged in water, were estimated from direct measurements as well as CT scans on patients positioned prone with the breast hanging freely in air. The parameter h shown in Figure 2 is a depth into the chest wall, where the temperature is assumed to be maintained at 37° C. The most-likely values of these and other parameters, as well as the range being studied, are listed in Table 1.

An efficient and accurate numerical method has been reported for the acoustic field calculation in a homogeneous medium generated by a rectangular plane source (Ocheltree and Frizzell, 1989). In this method, the plane source is divided into small rectangular elements, surrounded by a rigid baffle. The method sums the contributions to the pressure at a point from all these elements. This method is recently extended to a water - soft tissue medium (Lu et al, 1995). It demonstrated that the ultrasound field in a two-layer medium can be calculated based on the same principle if the density (ρ) and the speed of sound (c) in the two layers are close so that the reflection and refraction at the interface of the two materials can be ignored. For water and breast tissue, the density and speed are 1.0 $g\ cm^{-3}$ and 1519 $m\ sec^{-1}$ (at 35° C, Kaye and Laby, 1973) for the former, $1.02 \pm 0.04\ g\ cm^{-3}$ (Duck, 1990) and $1553 \pm 35\ m\ sec^{-1}$ (Scherzinger et al. 1989) for the later. Therefore, the conditions for an appropriate approximation can be satisfied. For a uniformly excited rectangular plane source, the sound pressure amplitude P_0 at a point inside the breast then can be calculated by:

$$P_0 = \frac{j\rho c \Delta A}{\lambda} \cdot \Sigma_{n=1}^{N} [\frac{u}{R} \cdot e^{-(\alpha_w r_w + \alpha_b r_b + jkr_w + jkr_b)}.$$

$$sinc\,(\frac{kx'_n\Delta h}{2(r_w+r_b)})\cdot sinc\,(\frac{ky'_n\Delta w}{2(r_w+r_b)})], \quad (1)$$

where ρ is the density, c is the phase velocity of the sound waves, u is the velocity amplitude of the plane source, λ is the wavelength, k is the wave number, $\Delta A = \Delta h \cdot \Delta w$ is the element size, x'_n and y'_n are the coordinates of the field point with respect to the center of the element n, α_w and α_b are the attenuation coefficient in water and breast, r_w and r_b are the propagation distances within water and breast.

The size of Δw and Δh should be small enough to satisfies the conditions for the applicable far-field approximations. In this calculation, $\Delta w = \Delta h = 1\ mm$ is used. Since the breast is in the center of the applicator, the distance between the transducer and the breast is at least several centimeters, this element size has proven to be adequate (Lu et al. 1995).

The specific absorption rate (SAR), i.e. the absorbed power per unit volume in the breast, can be calculated from the acoustical pressure amplitude P_0 at the point:

$$SAR = \frac{\alpha_b P_0^2}{\rho c}, \quad (2)$$

where the attenuation coefficient α_b is used. This is valid under an assumption that the majority of the attenuated power is absorbed locally.

The SAR value is calculated at the center of each voxel inside the breast. A voxel size of $2 \times 2 \times 2\ mm^3$ is used for the smaller breast size, and $3 \times 3 \times 3\ mm^3$ for the larger breast size (refer to Table 1). To reduce the number of calculations, only the voxels within 2 cm of the plane passing through the centers of the transducers in the ring are calculated. Beyond that region the SAR value is negligible. Since this calculation is very CPU intensive, it is performed only once for each configuration. The result for each transducer is stored in a data base, in which the sum of the power absorption rates in all the voxels is normalized to 1 W. In the thermal calculation, these data can be retrieved and the actual absorption rate from each transducer can be determined once the total deposited power by the transducer is assigned. The total SAR at a field point is the arithmetic sum of the contributions by all the transducers. This simple arithmetic relation is due to the fact that there is no interference between the transducers as discussed in the previous section.

The standard bio-heat transfer equation (Pennes 1948) is used for the

thermal model. Usefulness and limitations of this model have been discussed by several authors (Chen 1980, Eberhart et al. 1980, Bowman 1982, Roemer 1988). A main concern of this model is the methodology for handling the effect of the blood flow. In contrast to the thermal conduction process, the effect of blood flow is neither well understood nor mathematically rigorously characterized. Given the complexity and variability of the blood flow patterns, it is understandable that a simple linear perfusion term in the model is a gross simplification of reality. On the other hand, this equation is still the practically operational formula, and has been successfully applied in many cases (Cravalho et al. 1980, Dickinson 1984, Roemer et al. 1984, Strohbehn and Roemer 1984). Particularly, in the absence of large vessels and when perfusion is not the dominating factor, this formula predicts well the temperature elevation produced by acoustic or electromagnetic fields. For convenience, this bio-heat transfer equation is written as follows:

$$\frac{\partial T}{\partial t} = (K/C_v)\ \nabla^2 T - (T - T_0)/\tau + q_v/c_v, \tag{3}$$

where T is the temperature, t is the time, K is the thermal conductivity, c_v is the heat capacity per unit volume, T_0 is body temperature ($37^\circ\ C$), τ is the time constant for perfusion, and q_v is the heat production rate per unit volume (i.e. the SAR calculated by the acoustic model). The heat due to metabolism is relatively small, and is ignored.

The finite difference method is used in the 3-D numerical treatment of the partial differential equation (Ames 1977, Press et al. 1985). This method provides a great deal of flexibility in dealing with different geometries, boundary, and initial conditions. Once these conditions are clearly defined and the SAR in each voxel is given, the temperature evolution for a whole treatment session, i.e. the temperature distribution in each voxel as a function of time, can be calculated. The voxels in this calculation are the same as those defined for the SAR calculation. The choice of their size is a compromise between an acceptable accuracy and a reasonable CPU time required. A time step of 3 seconds is used, which satisfies the requirement of the stability criterion (Ames 1977). In this approach, the SAR values, the boundary conditions and tissue parameters (τ etc.), all can be assigned as functions of time and position. Therefore, a realistic hyperthermia treatment can be simulated.

The breast tissue parameters listed in Table 1 are based on published data wherever available. To date there is very little perfusion data published

for breast. A recent report based on 7 hyperthermia treatments by use of a modified thermal clearance technique (Waterman and Kramer 1994) indicates that blood flow can be in a range from less than 2 $ml\ (100g)^{-1}\ min^{-1}$ in the first treatment to 8 $ml\ (100g)^{-1}\ min^{-1}$ in the later treatment. These data are consistent with the fact that there are no large blood vessels in breast, and that the breast tissue has a high content of adipose tissue, which would tend to reduce the perfusion rate. The perfusion in breast is, therefore, likely similar to or less than that of resting skeletal muscle. The perfusion time constant for anterior thigh and forearm have been measured as 2140 seconds and 1740 seconds, respectively (Sekins and Emery, 1982), which correspond to a blood flow of $3-4\ ml\ (100g)^{-1}\ min^{-1}$. Thus, the perfusion time constant for breast is assumed to be about 2000 seconds, but could be as high as 600 seconds (corresponding to a perfusion rate of $\sim 10\ ml\ (100g)^{-1}\ min^{-1}$). It was further assumed that when the temperature is elevated to $44°\ C$, the perfusion rate may increase by a factor of two. Even with this higher value, the perfusion rate is still relatively low. Consequently, the standard bio-heat transfer equation can be used and reliable results can be expected.

The initial temperature inside the breast is assumed to be $37°\ C$ uniformly. Near the surface. the actual initial temperature may be lower than this value. However, this initial uncertainty causes no concern, since it makes little difference to the temperature distribution after several minutes of heating. The water temperature is adjustable between $30° - 40°\ C$. It is assumed that the voxels in the breast adjacent to water are kept at this temperature. When the water is well circulated, this is a practical and very reasonable approximation. The uncertainty due to this assumption is in the order of a few mm. For the boundary condition below the chest wall, which is outside the ultrasound field, it is assumed that the temperature is maintained at 37° at a depth h.

The simulation is performed with the parameter values listed in Table 1. In all simulated cases the absorption rate from each transducer is adjusted interactively according to the temperature feedback until the resulting temperature elevation is satisfied. These results are presented in Section 3.

2.3 Experiment

An experiment has been carried out using one transducer ring. The purpose of this experiment is to test the ability of the system to control the tem-

perature distribution in the plane of the transducer ring and to verify the accuracy of the calculations.

This transducer ring, has 48 transducers operated alternately at low (2.0 MHz) and high (4.5 MHz) frequency. The electronic device that drives the test ring has six amplifiers, each driven by its own oscillator. The output of one amplifier is connected to eight transducers through a multiplexer. Consequently, the transducer ring is divided into eight groups, each consisting of six transducers. In any one moment the six amplifiers are connected to one of the eight transducer groups through the multiplexers (Figure 3 (A)). As a result, the beams from different transducers are always out of phase. The amplifiers and multiplexers are controlled by a computer, which permits programmable adjustment of the power outputs to each transducer.

In this experiment each transducer group is powered for a duration of 55 $msec.$ in a sequential manner. Consequently, one whole cycle is 8×55 $msec.$ $= 440$ $msec.$, which is less than the time constant relevant to thermal processes (such as τ). The insonation can therefore treated as if the transducers are turned on continuously with an averaged power.

A breast phantom made of ultrasonic tissue-mimicking material is used for the tests. The phantom consists of water-based pharmaceutical gels containing uniform distributions of graphite power and alcohol (Madsen et al. 1978). Its density, heat capacity, thermal conductivity and attenuation coefficient are determined experimentally to be 1.08 $g\ cm^{-3}$, 0.78 $cal.\ g^{-1}\ C^{\circ -1}$, 0.0015 $Cal.\ cm^{-1}K^{-1}$ and 0.75 $dB\ cm^{-1}\ MHz^{-1}$, respectively. The phantom, which has a diameter of 13 cm at the base and a height of 8 cm (D and H, respectively, in Figure 2), is immersed in water and surrounded by the transducer ring. The base is covered by a 2 mm rubber sheet. The plane in the middle of the ring is 1.35 cm below the base. Multisensor thermocouples, inserted into 20 gauge needles, were used for temperature measurement . These probes (Dickinson 1985, Hynynen and Edwards, 1989) have a fast response time (0.1 second) and minimal acoustic artifact. Three probes were inserted in the plane as shown in Figure 3 (B). The water temperature and room temperature were 24° C during the experiment. Since the geometry is symmetric, all transducers with the same frequency are supplied with equal powers.

As the first step of the experiment, the SARs, normalized to the total output power of all the amplifiers operating at the same frequency, are determined at each sensor point. SAR is calculated from the initial rate of the

temperature change from a stable state, which can be written as:

$$q_0 = q_v/N = c_v \frac{\Delta T}{\Delta t}/N, \tag{4}$$

where q_0 is denoted as the normalized SAR at each sensor point, N is the total output power by the amplifiers (2.5 W for 2 MHz and 10 W for 4.5 MHz in this experiment). ΔT is the temperature elevation at the sensor point in a small time interval Δt, which is between 1 - 11 second after the power is turned on. The measured temperature within the first second is ignored, so that the artifacts can be eliminated. This formula is deduced from Equation (3) ignoring the conductivity and perfusion terms for the small interval Δt. Normalized SARs are determined separately for the low and high frequencies.

In the second step, the output powers to the high and low frequency transducers were adjusted manually until a uniform and pseudo-steady temperature distribution in the plane ($\sim$ $6°C$ above the baseline) was reached and maintained for more than 10 minutes. The total output power by the amplifiers for this experiment was found to be 9 W for the 2.0 MHz transducers and 15 W for the 4.5 MHz transducers.

This experiment has been simulated by the methods discussed previously. The experimental results are compared to the simulations in Section 3 and discussed in Section 4.

3 Results

3.1 Simulation results

The most-likely values of ultrasound and tissue characteristics used in the simulation are listed in Table 1. They are closest to those found in the literature for the appropriate frequency and tissue type. Simulations were performed over a range of ultrasound and tissue parameters, representing extreme tissue types, breast sizes, attenuation and perfusion conditions. We have therefore can demonstrate the ability of the treatment system to control the temperature distribution over a large range of conditions.

To simulate a typical treatment the power level may be changed during the session. This is an important feature of the approach in this study. For simplicity in the presentation, however, we only show simulations in which

the powers are constant. Figure 4 shows the steady SAR distribution for the most-likely case. The total deposited power is about 42 W. Figure 4 A is the SAR in a sagital view passing through the center of the breast. In this plot, five rings with higher SAR can be seen, corresponding to the five transducer rings. Figure 4 B is the coronal view at 25.5 mm from the chest wall coincident with the second transducer ring. The contributions from each transducer is listed in Table 2. The corresponding temperature distributions after 40 minutes are shown in Figure 5 A and 5 B.

Figure 6 plots the temperature evolutions in the line passing through the center of the sagital sections and in the horizontal diameter in the coronal plane. The temperature distributions 10, 20 and 40 minutes after the power is on, and the distribution 3 minutes after the power is off are plotted. Note that after 20 minutes, the temperature distribution is approaching stable and becomes quite uniform, and that the distribution after power off becomes smooth.

The simulation parameters were changed to examine the effects of boundary conditions and perfusion rate on the computed temperature distribution. For a better understanding of the effects of these changes, only one parameter is varied at a time, and all other parameters remain as the most-likely values. In Table 2, the power contributions by each transducer for two more simulations are shown. In one case, the surrounding water temperature is kept at 30° C. In another case, the perfusion rate is increased. It is assumed that the time constant is 600 seconds (corresponding to a perfusion rate of 10 $ml\ (100g)^{-1}min^{-1}$) at 37° C and linearly changes to 300 seconds (corresponding approximately to a perfusion rate of 20 $ml\ (100g)^{-1}min^{-1}$) at 44° C. As one may expect, a higher power is needed when water temperature is lower or perfusion rate is higher. In either case, the temperature distribution remains satisfactory as shown in Figure 7. But it can be seen that a higher perfusion rate produces a less homogeneous temperature distribution.

One particular clinical concern that has been raised for recurrent breast cancer treatment is the potential of overheating scar tissue resulting from lumpectomy or other surgical interventions. Such overheating can create undesirable treatment toxicity and one goal in the design of the breast treatment system is to have adequate temperature control of the system to avoid such toxicities. To study this problem, different sizes of biopsy cavities from CT scans of breast patients were examined. These cases included a biopsy cavity of the size of $12 \times 60 \times 80\ mm^3$ which was added to the theoretical

model. It was assumed that the biopsy volume had no perfusion but that the attenuation rate and other parameters remain the same. Obviously, hot spots will occur in this area unless the heating pattern is changed accordingly. This hot area is shown in Figure 8 (A) where the the lumpectomy volume exists but the same power level as in Figure 4 is applied, and the maximum temperature reaches 45.3°. To prevent this overheating of the scar and lumpectomy volume the breast treatment applicator must have enough control capacity to reduce the power deposition locally in the biopsy scar cavity. This is shown in Figure 8 (B) where a satisfactory temperature distribution is achieved when corrected SAR is applied, and the maximum temperature is 44.0°.

To treat a quadrant of the breast, the boundaries inside the breast need to be sufficiently heated, in addition to the quadrant of the surface and the base. Figure 9 demonstrates the SAR pattern from the breast applicator needed to satisfy that requirement. The corresponding steady temperature distribution is shown in Figure 10.

3.2 Experimental results

The measured pseudo-steady temperature distribution is plotted in Figure 11 (A), (B), (C) for probes A, B, C, respectively. These figures show that in this non-perfused phantom experiment, a steady state temperature can be achieved within 2° C.

To determine the corresponding power deposition in each sensor point, the normalized SAR (q_0), deduced by Equation (4), is multiplied by the total steady power output (i.e. 1.9 W for 2.0 MHz and 15 W for 4.5 MHz). This is done separately for high and low frequencies, and their results are added together. This gives the constant SAR used in the experiment and is shown in Figure 12.

The experiment has been simulated by the 3-D acoustic models. The total absorbed powers for the low and high frequencies in the simulation were adjusted, such that the calculated SAR values in the sensor points match reasonably well with what were determined in the experiment as shown in Figure 12. Based upon this calculated SAR, the pseudo-steady state temperature distribution in the whole phantom is calculated. It is the result 20 minutes after the steady power was 'turned on' in the simulation. The computed temperature distribution in the sensor positions is superimposed by the

experiment data in Figure 11. The comparison demonstrated an excellent agreement between the model and the measurement.

The total absorbed power used in the simulation is 0.84 W for the low frequency transducers and 7.9 W for the high. These values are lower than the measured total output powers of the amplifiers (1.9 W and 15 W for low and high frequency respectively). This difference is expected due to the heat losses in the cables and transducers.

As discussed above, the heating effect of each ring is relatively independent. Therefore, this experiment is representative for the entire cylinder. Additional phantom and animal tests will be conducted for the whole applicator when completed.

4 Discussion

In this paper we have reported the models and simulations that were used to optimize the design of the ultrasound applicator for breast treatment. The theoretical work was experimentally validated.

The simulation demonstrated that a combination of low and high frequencies is capable of delivering appropriate power deposition to the boundaries and interior of the breast (Figure 4-10). This capability is enhanced by the small size of the transducer and the separate power control for each transducer. As a result, the heat losses due to conduction and perfusion can be properly compensated, and a uniform temperature distribution can be reached and maintained.

The different roles of the high and low frequency transducers for maintaining uniform temperature can be clearly seen by comparing the data in Table 2, where the power deposition per transducer with low and high frequencies are listed for three cases. When the circulating water temperature is changed from 37° to 30° C, the power of the high frequency has to be increased by more than 30% to compensate the increased heat losses to the water. Meanwhile, the low frequency power remains the same, because the perfusion rate did not change. On the other hand, when the perfusion rate is high (a perfusion constant of 600 seconds at 37° C and 300 seconds at 44° C) but the water temperature remains at 37°, the power at the low frequency has to be increased significantly to overcome the higher perfusion, while only a slight change is needed for the power at high frequency.

Since individual transducer rings are stacked together, it is found that the power deposited to a given plane is delivered predominantly from the ring that defines the plane. As a result, in the first order of approximation the temperature in a plane can be adjusted by the corresponding ring of transducers. The weak interaction between adjacent rings is a very useful feature, which makes the power control relatively easier.

The simulation is a useful tool for the design of a hyperthermia system of this complexity. However, the results are based on certain assumptions and of limited predictive value for individual patients due to uncertainties in the breast tissue characteristics. To better understand the magnitude of theses uncertainties the tissue and ultrasound paramenters have been varied over a large range of values covering both assumed extremes and published data (Table 1), The purpose of studying the effect of parameter uncertainties on the system performance is to demonstrate that the power and frequency control of the breast applicator has enough range to accommodate different clinical situations and individual breast tissue variations.

The effect of blood perfusion is a difficult parameter to simulate, because perfusion rate may vary significantly with tissue heterogeneity or changing temperature. Recently reported blood flow data measured at the same point in a human breast adenocarcinoma during hyperthermia over four weeks of hyperthermia (Waterman and Kramer 1994), indicate that the flow rate may change significantly in the same measurement point. The uncertainties in breast tissue perfusion, therefore, remains a main concern for the proper selection of transducer frequencies and operating parameters. Due to these uncertainties, we simulated the breast applicator over a wide range of constant perfusion rates and temperature dependent perfusion rates. These results demonstrate that the system can handle all levels of simulated perfusion satisfactorily (Figure 5, 7(B)) They also demonstrate the ability to deal with inhomogeneities of perfusion (Figure 8).

Measurements of the acoustic attenuation coefficient for breast tissue show variations of $\pm 40\%$ (Foster and Hunt 1979, Edmonds et al. 1991). One method of compensating for such large variations in attenuation is to vary the ultrasound frequency. The transducers in the breast applicator have a bandwidth of 30% at -3 dB of maximum. The voltage controlled oscillators (VCO) in the system can operate between 1 MHz and 5 MHz, and the desired frequency band can be selected by computer control. With these features, the system is able to compensate for the uncertainties in the assumed

attenuation coefficients.

The choice of grid size has been carefully studied. We used 2 mm for a small size model and 3 mm for a large size model. The total number of voxels used is $53 \times 53 \times 30$ in both cases. The SAR calculation is more CPU intensive than the thermal computation. When the breast is assumed to be symmetric, the CPU time needed for SAR calculation is greatly reduced. It takes about 20 minutes for five transducer rings on a dedicated work station HP 9000/735. For thermal calculation, it takes about 5 minutes for simulating a whole treatment session ($\sim$ 50 minutes). Using a smaller grid size has proven not to be beneficial because to reduce the grid size by a factor two requires CPU time increase by a factor of 2^4 in the thermal calculation and 2^3 in the SAR calculation, while the difference in the resulting temperature distribution is insignificant.

The simulation used in this work is dynamic, in which the tissue parameters can be changed over time and the the power deposited by each transducer can be adjusted based upon the feedback of the temperature distribution. It is more time consuming than steady state calculations. However, when the time to reach steady state temperature is considerable (i.e. 10 minutes or more) or when other factors such as perfusion are known to vary as a function of temperature and time, the dynamic simulation allows studying realistic temperature variations. Important parameters highly associated with the outcome of the treatment, such as the $EQ\ MIN\ T_x$ 43 (Oleson et al. 1993), can be estimated.

One important assumption in the design and simulation is that there is no phase interference between different beams. This is achieved by an electronics design that prevents any two beams from being in-phase, while keeping the number of oscillators and amplifiers moderate. The single ring experiment with associated electronics proved that the electronics design is appropriate in this respect. There were no unexpected hot spots observed. For the multi-ring applicator the circuits for any two neighboring rings are independent, which guarantees the validity of the assumption.

In this experiment a reasonable uniform temperature distribution (within approximately 2°) was indeed reached. It demonstrates that the two frequency concept is valid and works very well. Since there was no perfusion in the phantom and this was a single ring experiment, the function of the low frequency in the experiment is only to compensate the heat lost to the neighboring tissue volume. As expected, the power needed at low frequency

was small (0.84 W), compared with that at high frequency (7.9 W).

Several factors contributed to the uncertainties in the experiment. First, the sensor position is not known exactly due to some bending of the probes. The uncertainty is estimated to be ≤ 1 *cm* at the tip of the probes. Since SAR is very sensitive to position, this may explain the substantial discrepancies at some points between the SAR measurement and the simulation (Figure 12). The second source of uncertainty resulted from non-uniformity in transducer efficiency. Due to differences in individual acoustic efficiencies, total output power of the transducers varied as much as 12% for equal RF excitation power. Also, inhomogeneities can occur in the phantom material due to evaporation of water and alcohol. In the simulation, however, it was assumed that all transducers were identical and the phantom was homogeneous. Given these uncertainties, the agreement between the experimental data and the simulation (shown in Figure 11, 12) is remarkable.

The use of the minimally invasive sensors, currently being developed (Szajda et al. 1994), will be more tolerable to patients due to its small size (22 Gauge). Still, the number of probes will be limited to, perhaps, three in a patient. The arrangement of these probes needs to be studied and optimized. Treatment planing and on-line control will require further development. Several authors have been working on the method and algorithm for on-line control in the hyperthermia treatment (Hartov et al. 1993, VanBaren and Ebbini, 1995). These approaches will be examined for on-line control of this system.

5 Conclusions

A therapeutic ultrasound system dedicated for breast cancer treatment has been developed. It consists of an array of dual frequency, multilayer transducer rings and associated electronics, coupled with the thermometry and closed-loop control. Its performance has been modeled and optimized using a comprehensive 3-D simulation, which offers insights in the physical process and the design criteria. An experiment using a single ring has been performed, which is in excellent agreement with the theoretical prediction. The simulations and experimental results demonstrate the system's capability to deliver a power deposition capable of achieving uniform hyperthermia ($41.5° - 44°$ *C*) under various perfusion and boundary conditions.

6 Acknowledgement

This work is supported by the US Army Medical Research and Development Command, under contract #DAMD 17-93-C-3098. The views, opinions and/or findings contained in this paper are those of the authors and should not be construed as an official department of the Army position, policy or decision unless so designated by other documentation. The authors would like to thank H.F. Bowman, W.H. Newman of MIT, R.X. Huang of Woods Hole Oceanographic Institution, and P. Barthe, M.H. Slayton of Dornier-AI for many helpful discussions, and Jamie Pellegati for his technical support.

References

- Ames, W. F. 1977, Numerical Methods for Partial Differential Equations. New York Academic Press.
- Bowman, H. F., 1981, Heat Transfer and Thermal Dosimetry, Journal of Microwave Power, **16(2)**, 121-133.
- Bowman, H. F., 1982, Thermodynamics of Tissue Heating: Modeling and Measurements for Temperature Distributions, in Physics Aspect of Hyperthermia, edited by G.H. Nussbaum, American Institute of Physics, New York, 511-548.
- Boyages, J., Recht., A, Connolly, J., Schnitt, S.J., Gelman, R., Kooy, H., Love, S., Osteen, R.T., Cady, B., Silver, B., and Harris, J.R., Early breast cancer: predictors of breast recurrence for patients treated with conservative surgery and radiation therapy. Radiother. Oncol. **19**, 29-41, 1990.
- Chen, M. M., 1980, Microvascular Contributions in Tissue Heat Transfer, Annals of New York Academy of Sciences, **335**, 137-150.
- Cravalho, E. G. , Fox, L. R., and Kan, J. C., 1980, The application of the bio-heat equation to the design of thermal protocols for local hyperthermia. Annals of the New York Academy of Sciences, **335**, 86-97.
- Dewey, W.C., Hopwood, L.E., Sapareto, S.A., Gerweck, L.E., 1977, Cellular response to combinations of hyperthermia and radiation, Radiology, **123**, 463-474.
- Dickinson, R. J., 1984, An Ultrasonic system for local hyperthermia using scanned focused transducers, IEEE Transactions Biomedical Engineering, **31**, 120-125.
- Dickinson, R. J., 1985, Thermal Conduction Errors of Manganin-Constanian Thermocouple Arrays, Phys. Med. Biol. **30**, 445-453.
- Duck, F. A., 1990, Physical Properties of Tissue - A Comprehensive Reference Book, Academic Press Inc., 138.

- Ebbini, E. S., Cain, C. A., 1991, A Spherical-Section Ultrasound Phased Array Applicator for Deep Localized Hyperthermia, IEEE Transactions on Biomedical Engineering. **38**, 634-644.

- Eberhart, R. C., Shitzer, A. and Hernandez, E. J., 1980, Thermal dilution methods[2 ; Estimation of tissue blood flow and metabolism", Annals N.Y. Acad. Sci. **335**, 107-132.

- Edmonds, P. D., Mortensen, C. L., Hill, J. R., Holland, S. K., Jensen, J. F., Schattner, P, Valders, A. D., Lee, R. H., Marzoni, F. A., 1991, Ultrasound Tissue Characterization of Breast Biopsy Specimens, Ultrasonic Imaging **13**, 162-185.

- Fessenden, P., Lee, E.R., Andeson, T.L., Strohbehn, J.W., Meyer, J.L., Samulski, T.V. and Marmor,, J.B., Experience with a multitransducer ultrasound system for localized hyperthermia of deep tissues. IEEE Trans. of Biomedical Engineering, **31(1)**, 126-134.

- Foster, F. S. and Hunt, J. W., 1979, Transmission of ultrasound beams through human tissue - focusing and attenuation studies, Ultrasound in Med & Biol., **5**, 257-268.

- Hartov, A, Colacchio, T.A., Strohbehn, J.W., 1993, Performance of an adaptive MIMO controller for a multiple-element ultrasound hyperthermia system, Int. J. Hyperthermia, **9(4)**, 563-579.

- Hansen, J.L., Bornstein, B.A., Svensson, G.K., Newman, W.H., Martin, G.T., Sidney, D.A., Frederick, B., A quantitative, integrated, clinical focused ultrasound system for deep hyperthermia, 1994, Presented at the 1994 ASME International Mechanical Engineering Congress & Exhibition,

- Hynynen, K,, Roemer, R., Anhalt, D., Johnson, C., Xu, Z.X., Swindell, W. and Cetas, T., 1987, A scanned, focused, multiple transducer ultrasonic system for localized hyperthermia treatments, Int. J. Hyperthermia, **3(1)**, 21-35.

- Hynynen, K. and Edwards, D.K. 1989, Temperature Measurement During Ultrasound Hyperthermia, Med. Phys. **16(4)**, 618-626.

- Kapp, D.S, Cos, R. S., Fessenden P., Meyer, J. L., Prionas, S. D., Lee, E. R., Bargshaw, M. A., 1992, Parameters predictive for complications of treatment with combined hyperthermia and radiation therapy. International Journal of radiation Oncology, Biology, Physics, **22(5)**, 999-1008.

- Kapp, K. S.; D. S. Kapp, 1993, Hyperthermia's emerging rule in cancer therapy, Contemporary Oncology, 21-30.

- Kaye, G.W.C. and Laby, T. H., 1973, Tables of Physical and Chemical Constants, Longman, London.

- Lele, P.P., 1983, Physical aspects and clinical studies with ultrasound hyperthermia. Hyperthermia in Cancer Therapy, edited by F.C. Storm (Boston: Hall Medical Publishers), 333-367.

- Lu, X-Q., Burdette, E.C., Svensson, G.K., 1995, Ultrasound Power Deposition In a Water-Soft Tissue Medium, Submitted to Int. J. Hyperthermia.

- Madsen, E.L., Zagzebski, J.A., Banjavie, R.A. and Jutila, R.E, 1978, Tissue mimicking materials for ultrasound phantoms Med. Phys. **5(5)**, 391-394.

- Mayr, N. A., Staples, J. J., Robinson, R. A., Vanmetre, J. E., Hussey, D. H., 1991, Morphometric Studies in Intraductal Breast Carcinoma Using Computerized Image Analysis. Cancer 1991, **67**, 2805-2812.

- Ocheltree, K. B. and Frizzell, L. A., 1987, Determination of Power deposition patterns for localized hyperthermia, a steady-state analysis., Int. J. Hyperthermia, **3(3)**, 269-279.

- Ocheltree, K. B. and Frizzell, L. A., Sound Field Calculation for Rectangular Sources, 1989, IEEE Transactions on Ultrasonic, Ferroelectrics, and Frequency Control. **36(2)**, 242-247.

- Oleson, J.R., Samulski, T.V., Leopold, K.A., Clegg, S.T., Dewhirst, M.W., Dodge, R.K., George, S. L., 1993, Sensitivity of hyperthermia trial outcomes to temperature and time: implications for thermal goals

of treatment. International Journal of Radiation Oncology, Biology, Physics, **25(2)**, 289-97.

- Palcic, B., Skarsgard, L.D., Reduced oxygen enhancement ratio at low doses of ionizing radiation. Radiat. Res. **100**:328-339.

- Pennes, H. H., 1948, Analysis of tissue and arterial blood temperatures in the resting human forearm, J. Appl Physiology. **1**, 93-122.

- Press, W. H., Flannery, B. P., Teukolsky, S. A., Vetterling, W. T., 1985, Numerical Recipes, The Art of Scientific Computing. Cambridge University Press.

- Roemer, R. B., 1991, Optimal power deposition in hyperthermia. I. The treatment goal: the ideal temperature distribution: the role of large blood vessel. International Journal of Hyperthermia, **7 (2)**, 317-341.

- Roemer, R. B., Swindell, W., Clegg, S. T. and Kress, R. L., 1984, Simulation of focused scanned ultrasonic heating of deep-seated tumors: the effect of blood perfusion. IEEE transactions Sonics and Ultrasonics, **31**, 457-466.

- Roemer, R. B, 1988, Heat transfer in hyperthermia treatment: Basic principles and applications. American Association of Physicists in Medicine, Medical Physics Monograph No. 16, 210-242.

- Schesinger A.L.,Belgam, R.A., Carson, P.L., et al. 1989, Assessment of Ultrasonic Computed Tomography in Symptomatic Breast Patients by Discriminant Analysis, Ultrasound in Med & Biol, **15**, 21-28.

- Sekins and Emery, 1982, Thermal science for physical medicine, Chapter 3, in Therapeutic Heat and Cold, Lehmann, J. F., Ed, Williams and Wilkins, Baltimore, Maryland.

- Strohbehn, J. W., Roemer, R. B., 1984, A survey of computer simulations of hyperthermia treatments. IEEE Transactions Biomedical Engineering, **31**, 136-149.

- Szajda, K. S., Sodini, C. G., Bowman, H.F., The active needle for in-vivo temperature measurement, Program & Abstracts of Fourteenth Annual Meeting of the North American Hyperthermia Society, 111.

- VanBaren, P. and Ebbini, E.S., 1995, Multi-Point temperature control during hyperthermia treatments: theory and simulation, IEEE Transactions on Biomedical Engineering, accepted for publication.

- Vernon, C. C., 1994, Collaborative phase III superficial hyperthermia Trial (MRC/ESHO/PMH), Program & Abstracts of Fourteenth Annual Meeting of the North American Hyperthermia Society, 87.

- Waterman, F.M., Kramer, D.B., 1994, Changes in Human Tumor Blood Flow During Four Weeks of Hyperthermia, Program & Abstracts of Fourteenth Annual Meeting of the North American Hyperthermia Society, 125.

Figure Captions

Figure 1. The dual frequency, cylindrical transducer array mounted on a hyperthermia treatment table. Circulating water inside the array is maintained at a constant, adjustable temperature ($30° - 40° C$).

Figure 2. The geometric model for the breast used in the simulation. The surface is assumed to be a paraboloid. H is the height, D is the diameter at the base, h is the depth beneath the chest wall (where the temperature is assumed constant at $37° C$).

Figure 3. (A). The schematic diagram of the electronics used in the single ring experiment. Six RF generators, each consists of a voltage controlled oscillator (VCO) and an amplifiers, are connected to one of the octant of the 48 transducers for a duration of 55 *msec.*. The eight octants are powered alternately by the six generators. As a result, the ultrasound beams from different transducers are always out of phase. It also shows that the system can work on transmit or receive mode. All these operations are under the control of a PC. (B). Cross section coincident with the centers of transducers in the single ring experiment. The lines represent the positions of the probes. The dots represent the positions of the sensors.

Figure 4. Simulated SAR distribution applied in the simulation. The most-likely parameter values in Table 1 are used. (a). Sagital section passing through the center of the breast. (b). Coronal section at 25.5 mm from the chest wall, corresponding to the second transducer ring.

Figure 5. Simulated temperature distribution 40 minutes after the steady SAR shown in Figure 4 is applied. Maximum temperature is $44.0° C$. (a). Sagital section passing through the center of the breast. (b). Coronal section at 25.5 mm from the chest wall, corresponding to the second transducer ring.

Figure 6. Simulated temperature distribution 10, 20, 40 minutes after the corresponding SAR shown in Figure 6 is applied and the the distribution 3 minutes after the power is off. (a). The distribution in a perpendicular line

passing through the center of the sagital section. (b). The distribution in a perpendicular line passing through the center of the coronal section.

Figure 7. Sagital section passing through the center of the breast for simulated temperature distribution 40 min. after steady SAR described in Table 2 is applied (A) Water temperature is changed to 30° C. Other parameters remain as the most-likely values in Table 1. (B). A high perfusion rate is used (600 second at 37° C and 300 second at 44° C). Other parameters remain as the most-likely values in Table 1.

Figure 8. Sagital section of simulated temperature distribution 40 minutes after power is "on". It is assumed that there is no perfusion in a volume indicated by the dash lines ($12 \times 60 \times$ 80 mm^3). (A). The steady SAR. shown in Figure 4, is applied. The maximum temperature is 45.3°. (B). Corrected SAR is applied. The maximum temperature is 44.0°.

Figure 9. Steady SAR distribution to treat a quadrant of the breast. The most-likely parameter values in the Table 1 are used. (a). Sagital section passing through the center of the breast. (b). Coronal section at 25.5 mm from the chest wall, corresponding to the second transducer ring.

Figure 10. Temperature distribution 40 minutes after the steady SAR, shown in Figure 9, is applied. (a). Sagital section passing through the center of the breast. (b). Coronal section at 25.5 mm from the chest wall, corresponding to the second transducer ring.

Figure 11. Measured temperature distribution (shown as +) by the probes in the single ring experiment, compared with the simulation results shown by solid lines. (A), (B), (C) correspond to the probe A, B, C, respectively. The water and room temperature was maintained at 24° during the experiment.

Figure 12. Measured SAR (shown as +) by the probes in the single ring experiment. The simulated results are shown by solid lines. The total power deposited in the simulation was adjusted to match the measured data. (A), (B), (C) correspond to the probes A, B, C, respectively.

Table 1

Parameter	Most-likely Value	Range Studied
Attenuation in breast	0.086 ($f^{1.5} np\ cm^{-1}$) (Foster et al. 1979)	0.052 - 0.12
Attenuation in water	0.0002 ($f^2 np\ cm^{-1}$) (Kaye 1973)	
Conductivity in breast	0.5 ($W\ m^{-1}\ K^{-1}$) (Bowman 1981)	0.3 - 0.8
Heat Capacity for unit volume	3. ($J\ g^{-1}\ K^{-1}$)	3. - 3.5
Perfusion Time Constant in breast	2000 * (at 37°) 600 ** (at 44°) ($second$)	600-2000 300-600
T_{water}	37° c	30° – 40°
D	15.3 (cm)	10.2, 15.3
H	7.8 (cm)	5.2, 7.8
h	7.5 mm	0-12

Parameters used in the model. * Corresponds to a perfusion rate of $\sim$ $3\ ml\,(100g)^{-1} min^{-1}$. ** Corresponds to a perfusion rate of $\sim$ $10\ ml\,(100g)^{-1} min^{-1}$. Paramenters D, H, h are indicated in Figure 2. The most-likely tissue parameters are closest to those found in the literatures. A large breast size is used as the most-likely value.

Table 2

Ring	Frequency (MHz)	Number of Transducers	Power Deposition (W) / Transducer		
			M.L. Values	$T_{water} = 30°$	High Perfusion
1	2	24	0.42	0.41	0.62
	4.5	24	0.28	0.38	0.32
2	2	24	0.15	0.15	0.31
	4.5	24	0.26	0.45	0.3
3	2.5	24	0.16	0.15	0.31
	4.5	24	0.20	0.3	0.22
4	2.5	24	0.04	0.04	0.07
	4.5	24	0.18	0.33	0.26
5	2.5	12	0.08	0.04	0.04
	4.5	12	0.08	0.10	0.04
Total			41.5	54.8	58.8

The power deposited in the breast by each transducer required to maintain the steady state temperature distribution. Three cases are shown. 'M.L. Value' means the most-likely parameter values listed in Table 1. The power distribution for this case is also shown in Figure 5. '$T_{water} = 30°$' indicates the circulating water temperature is changed to 30°. 'High Perfusion' indicates the perfusion time constant is changed from 600 sec at 37° C to 300 sec at 44° C. All other parameters remain as the most-likely values.

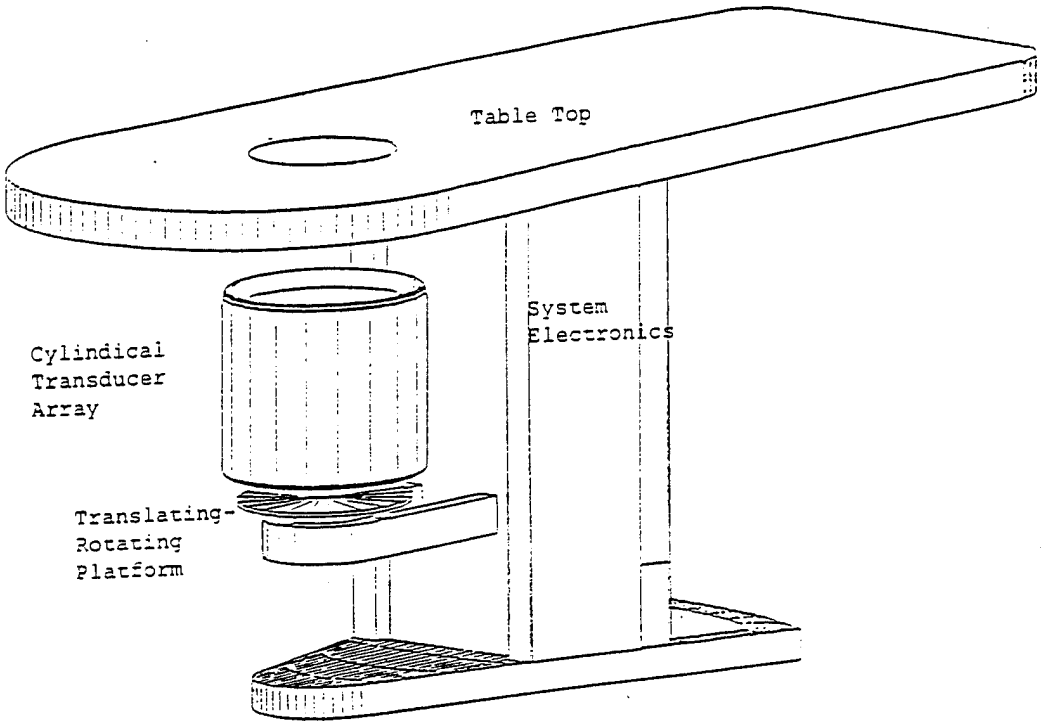

FIGURE 1

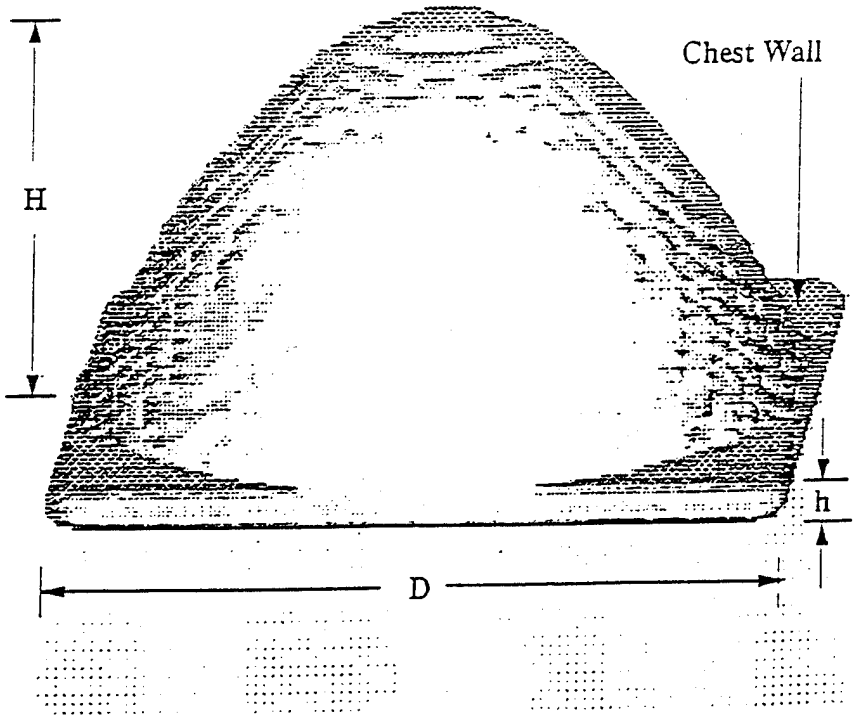

FIGURE 2

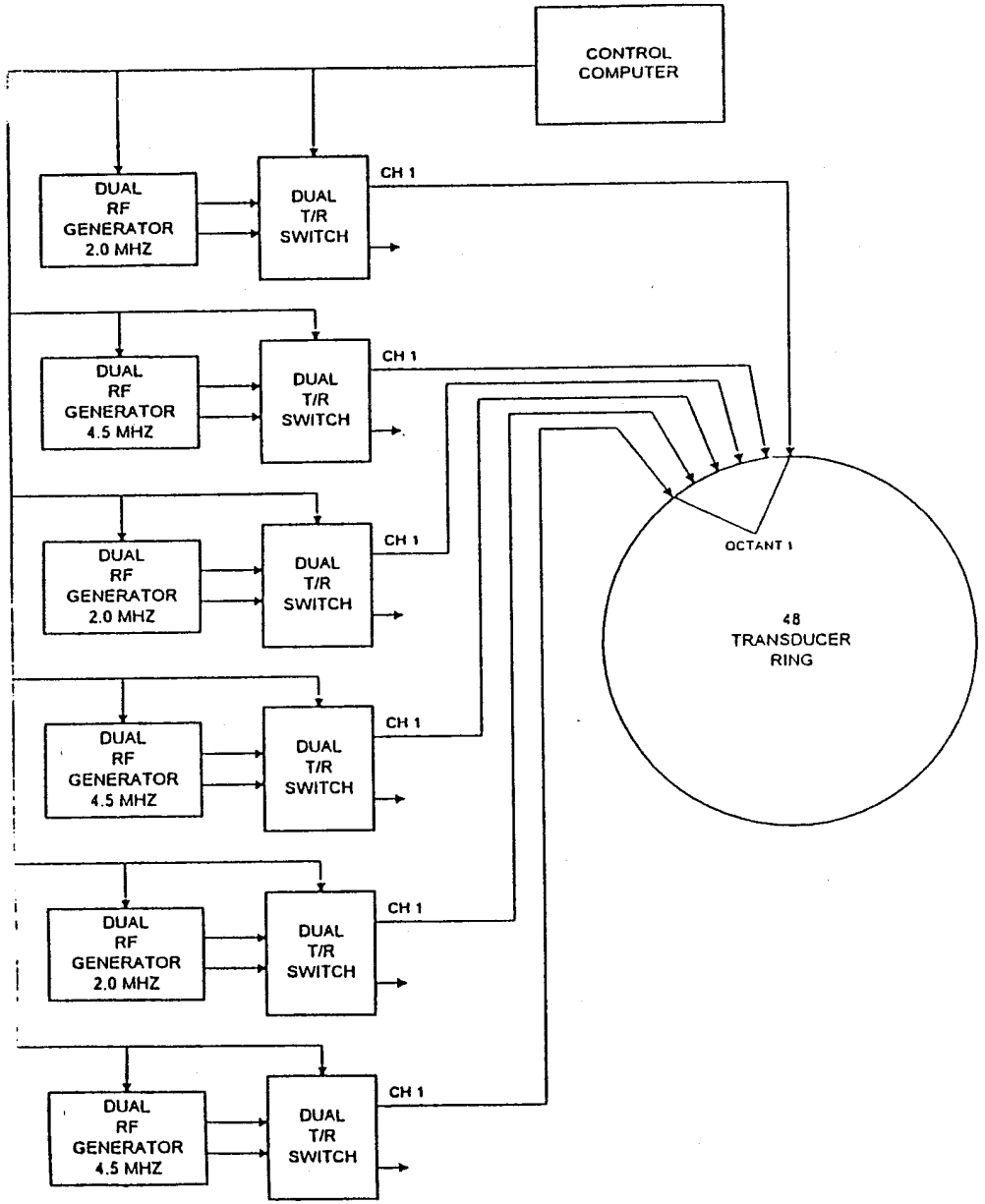

FIGURE 3 (A)

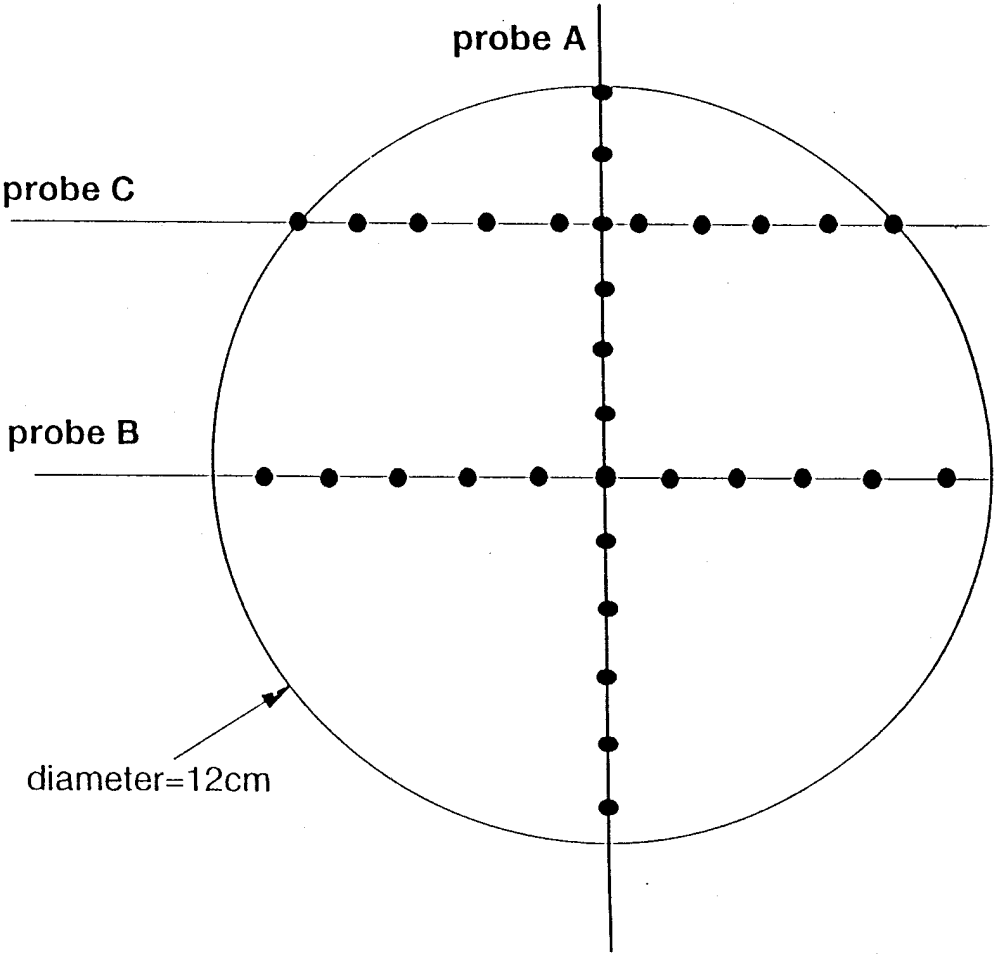

FIGURE 3 (B)

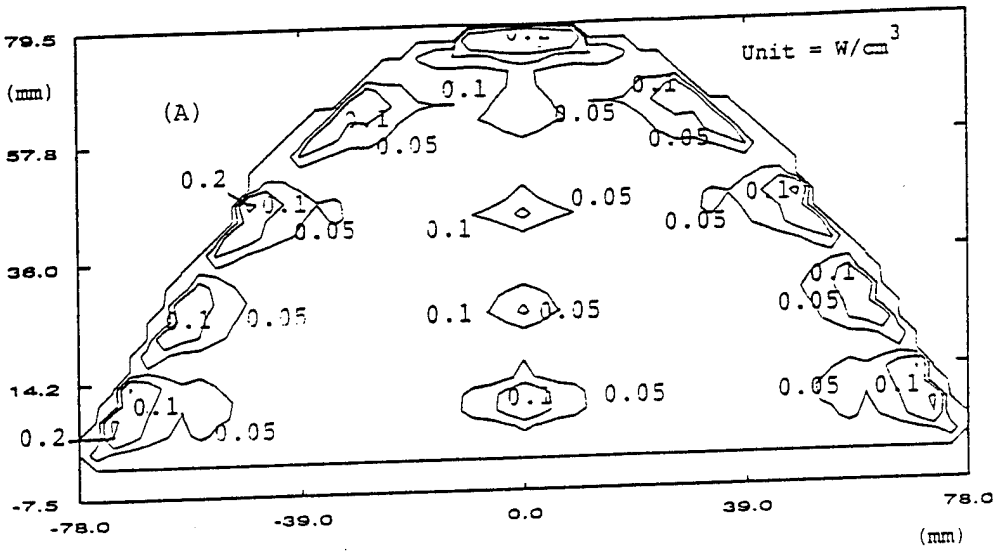
(A)
Unit = W/cm3
79.5
(mm)
57.8
36.0
14.2
-7.5
-78.0
-39.0
0.0
39.0
78.0
(mm)
0.2
0.1
0.05

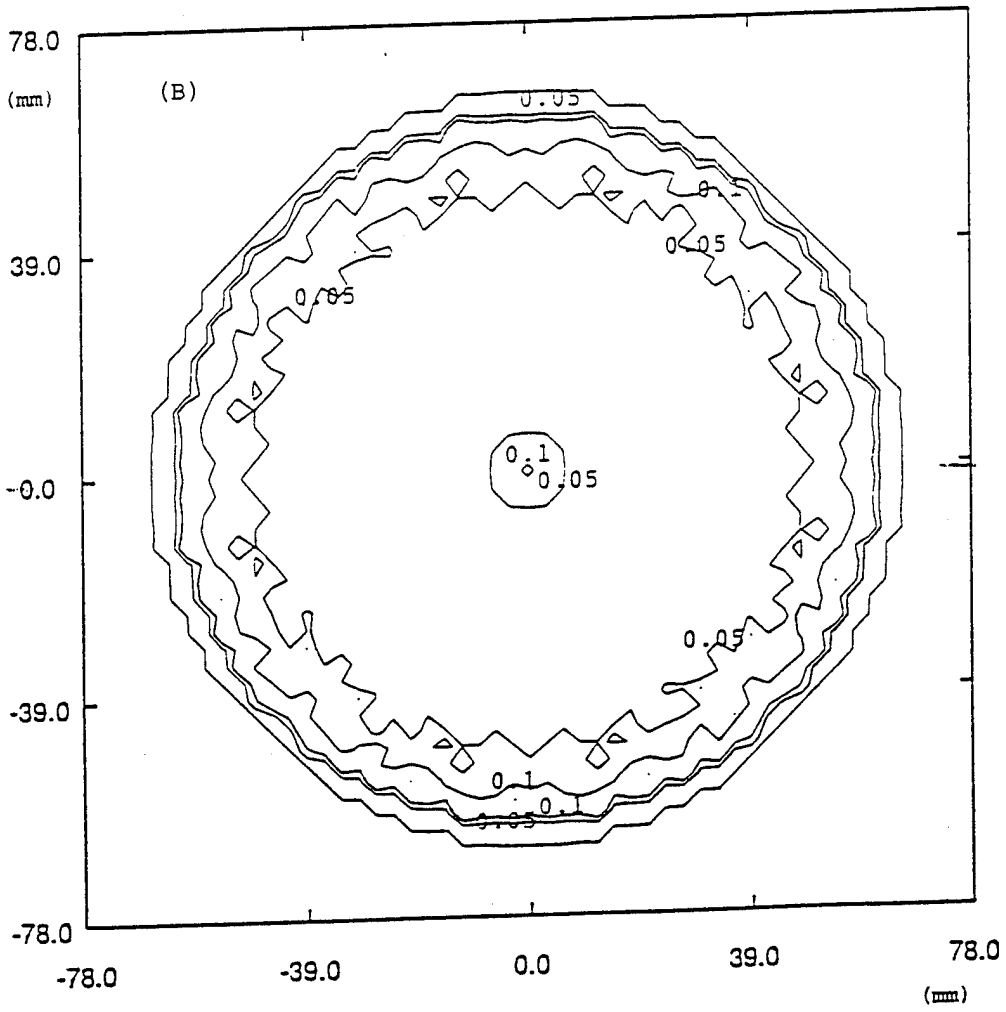
(B)
78.0
(mm)
39.0
-0.0
-39.0
-78.0
-78.0
-39.0
0.0
39.0
78.0
(mm)
0.1
0.05

FIGURE 4

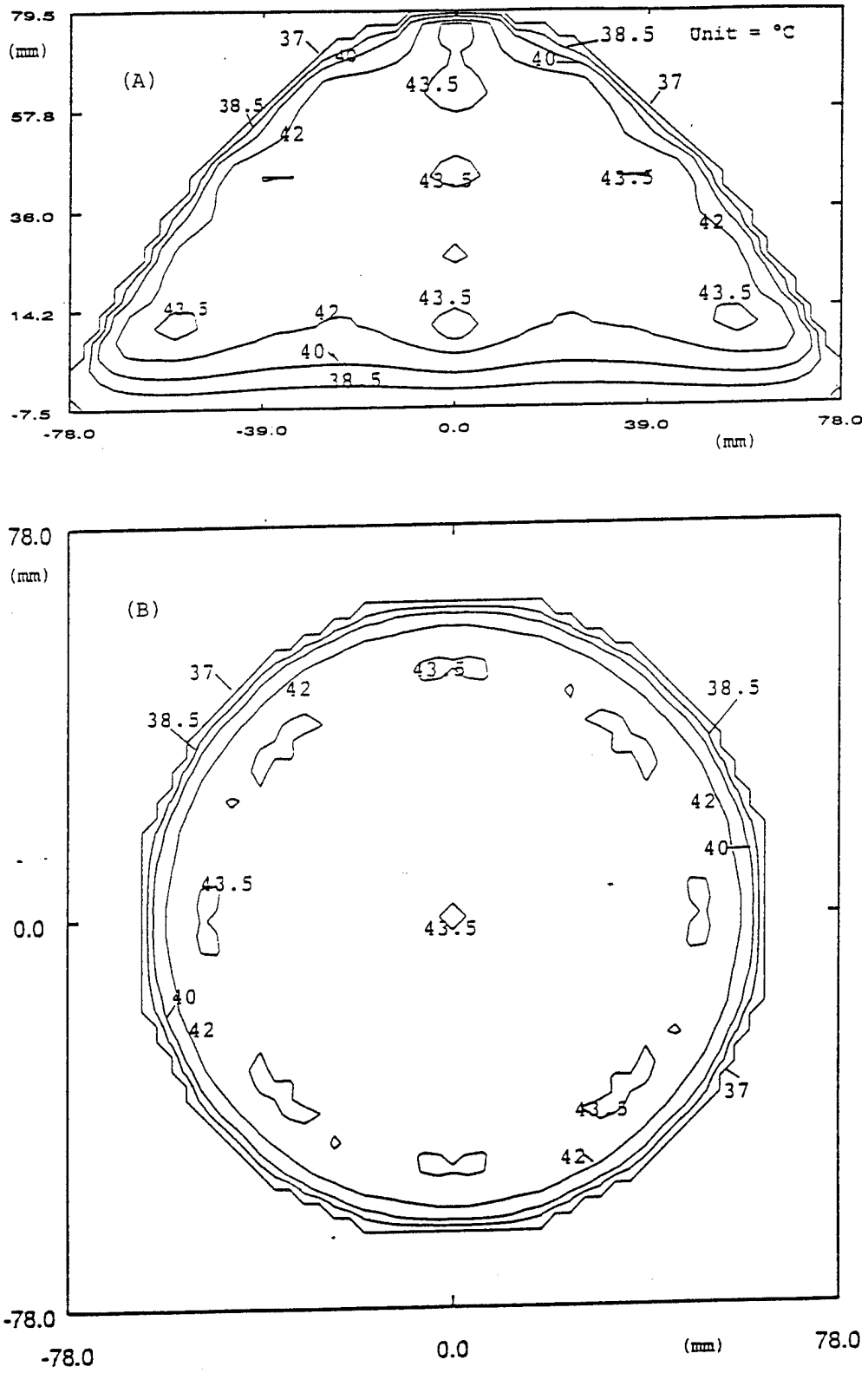
79.5
(mm)
(A)
57.8
36.0
14.2
-7.5
-78.0
-39.0
0.0
39.0
78.0
(mm)
Unit = °C
37
38.5
40
43.5
42
78.0
(mm)
(B)
0.0
-78.0
-78.0
0.0
(mm)
78.0

FIGURE 5

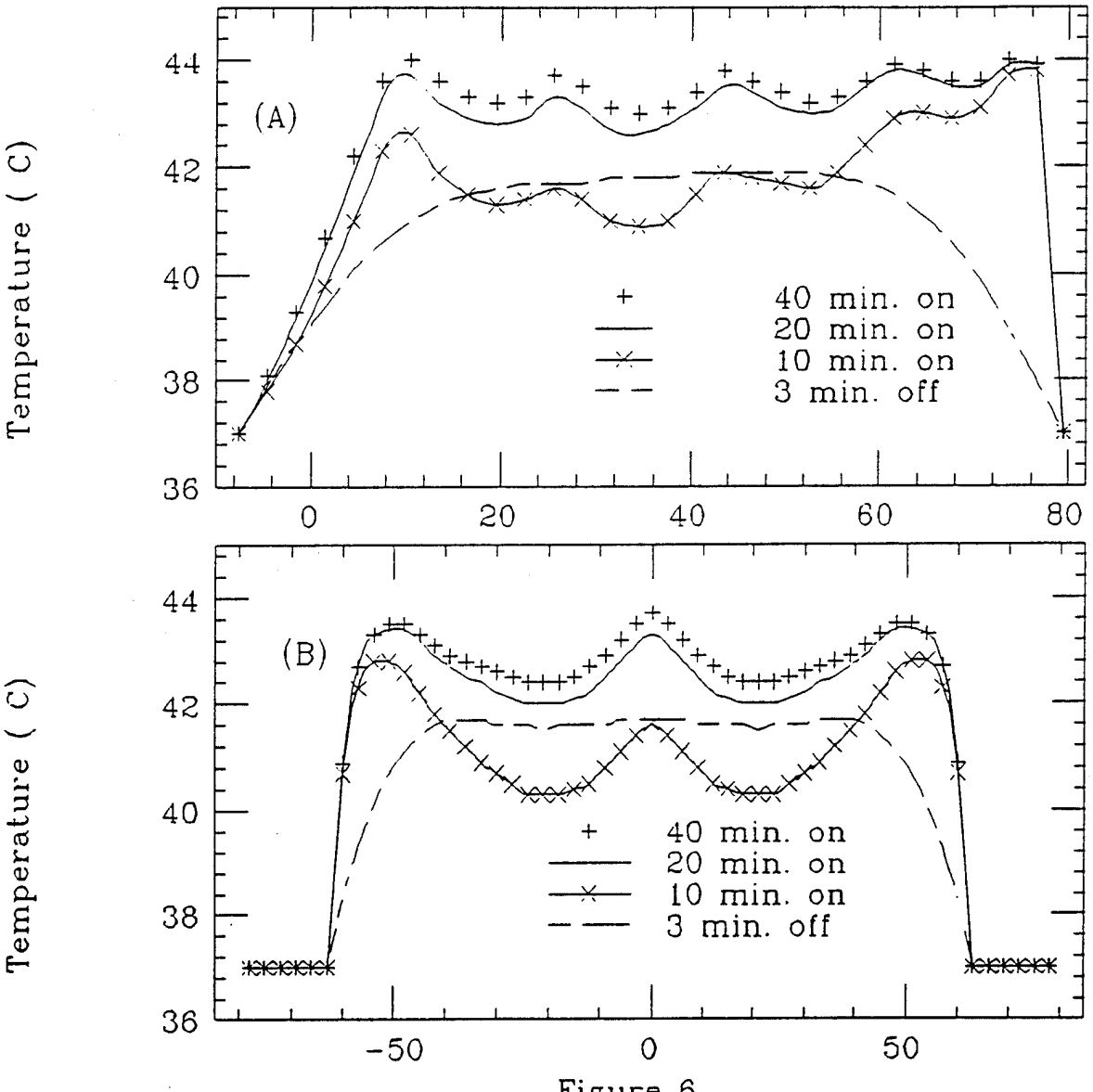
Temperature (C)
(A)
44
42
40
38
36
0
20
40
60
80
40 min. on
20 min. on
10 min. on
3 min. off
Temperature (C)
(B)
44
42
40
38
36
-50
0
50
40 min. on
20 min. on
10 min. on
3 min. off

Figure 6

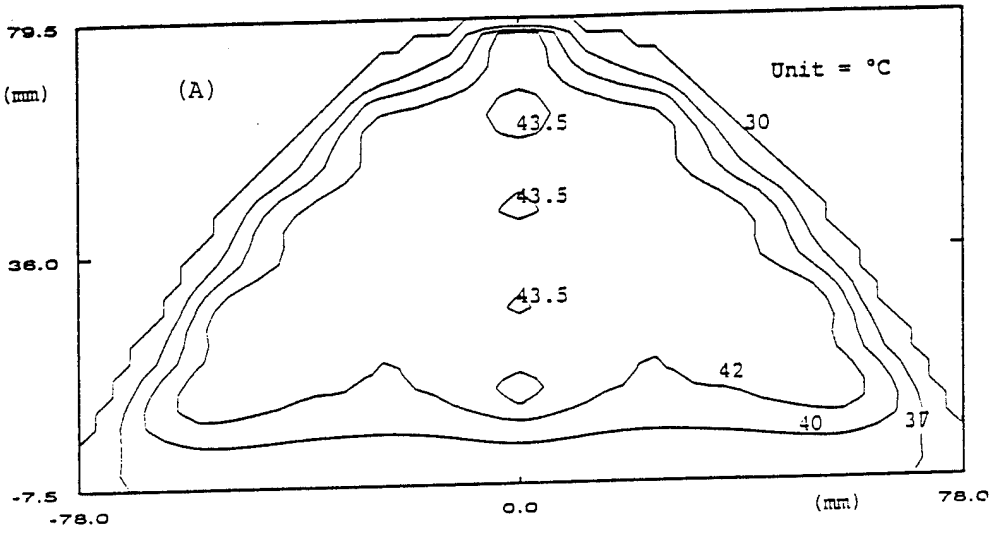
79.5
(mm)
(A)
Unit = °C
43.5
30
43.5
36.0
43.5
42
40
37
-7.5
-78.0
0.0
(mm)
78.0

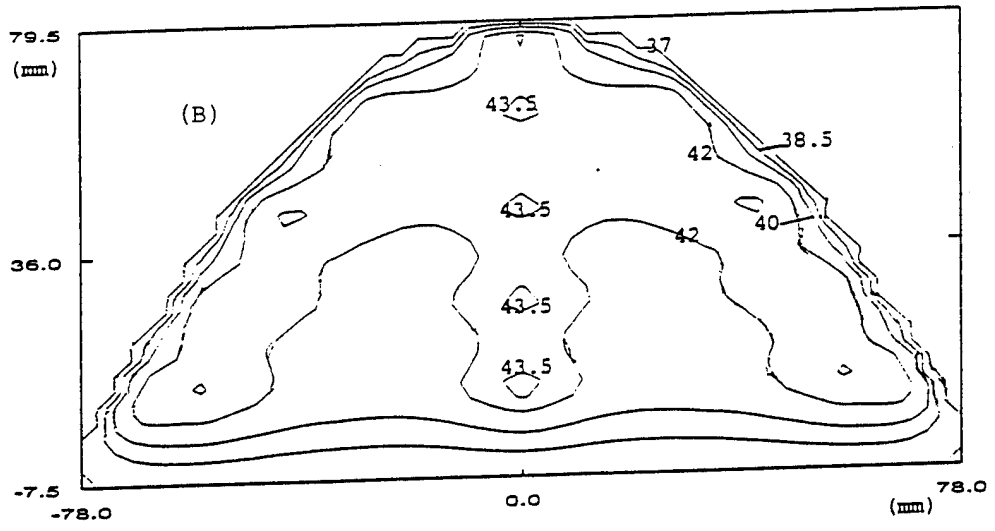
79.5
(mm)
(B)
37
43.5
38.5
42
43.5
40
42
36.0
43.5
43.5
-7.5
-78.0
0.0
78.0
(mm)

FIGURE 7

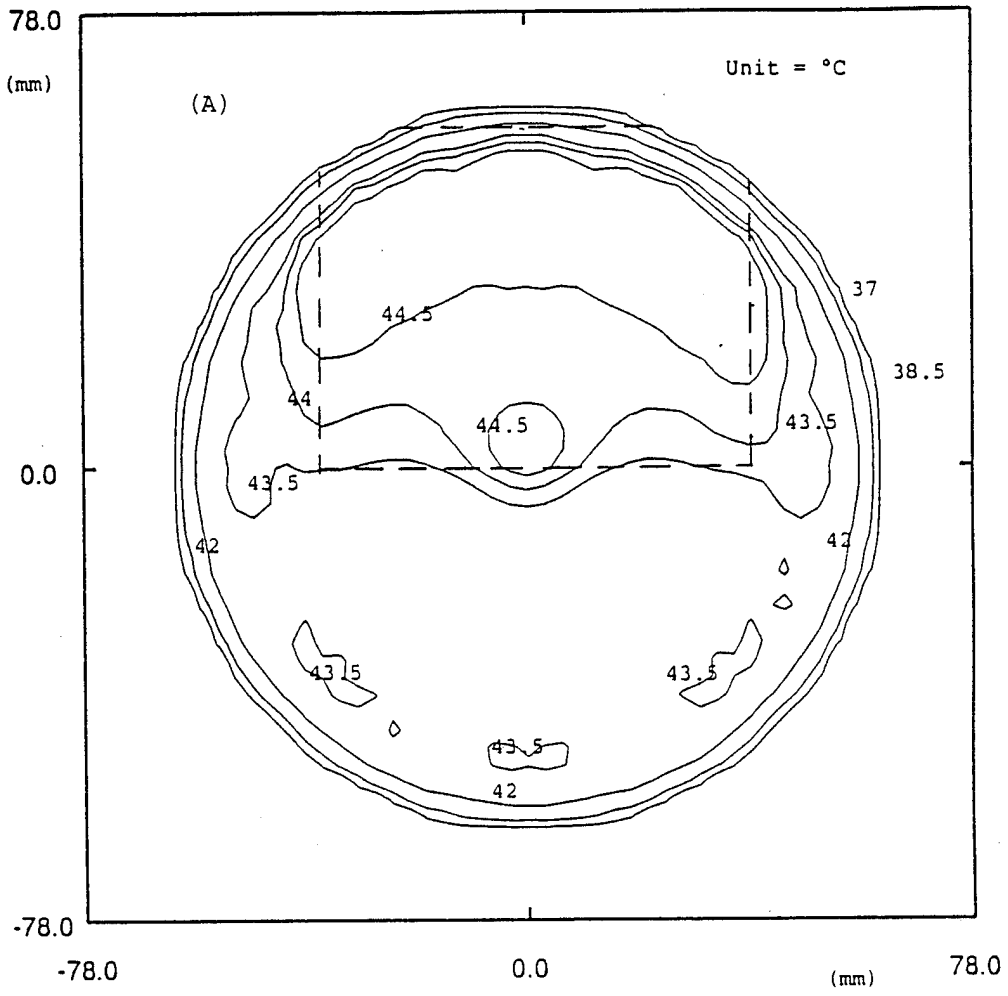
78.0
(mm)
Unit = °C
(A)
37
38.5
44.5
44
44.5
43.5
0.0
43.5
42
42
43.5
43.5
43.5
42
-78.0
-78.0
0.0
(mm)
78.0

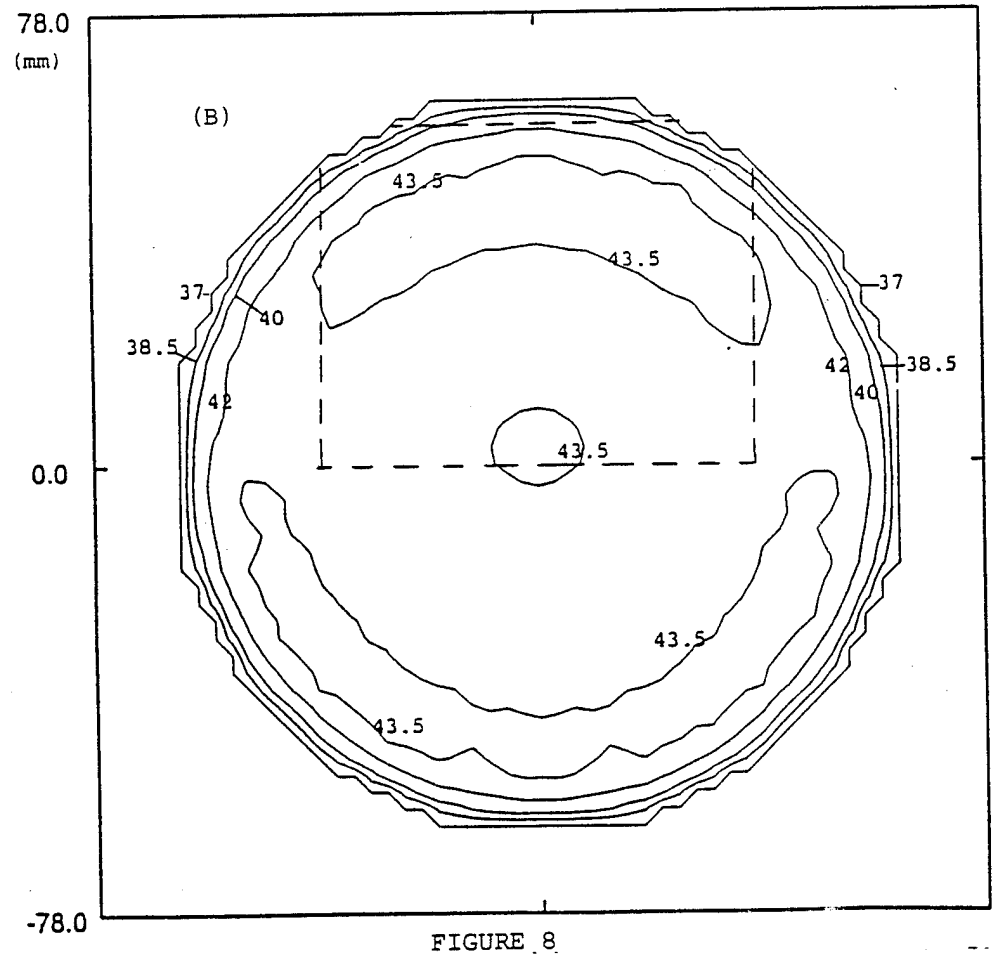
78.0
(mm)
(B)
43.5
43.5
37
37
40
38.5
42
38.5
42
40
0.0
43.5
43.5
43.5
-78.0

FIGURE 8

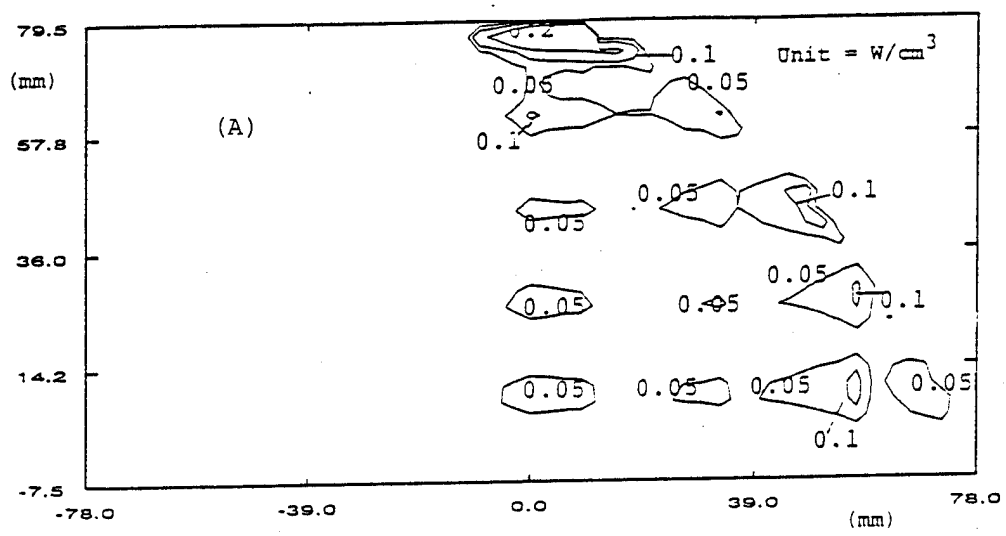
79.5
(mm)
57.8
36.0
14.2
-7.5
-78.0
-39.0
0.0
39.0
78.0
(mm)
(A)
Unit = W/cm3
0.2
0.1
0.05
0.1

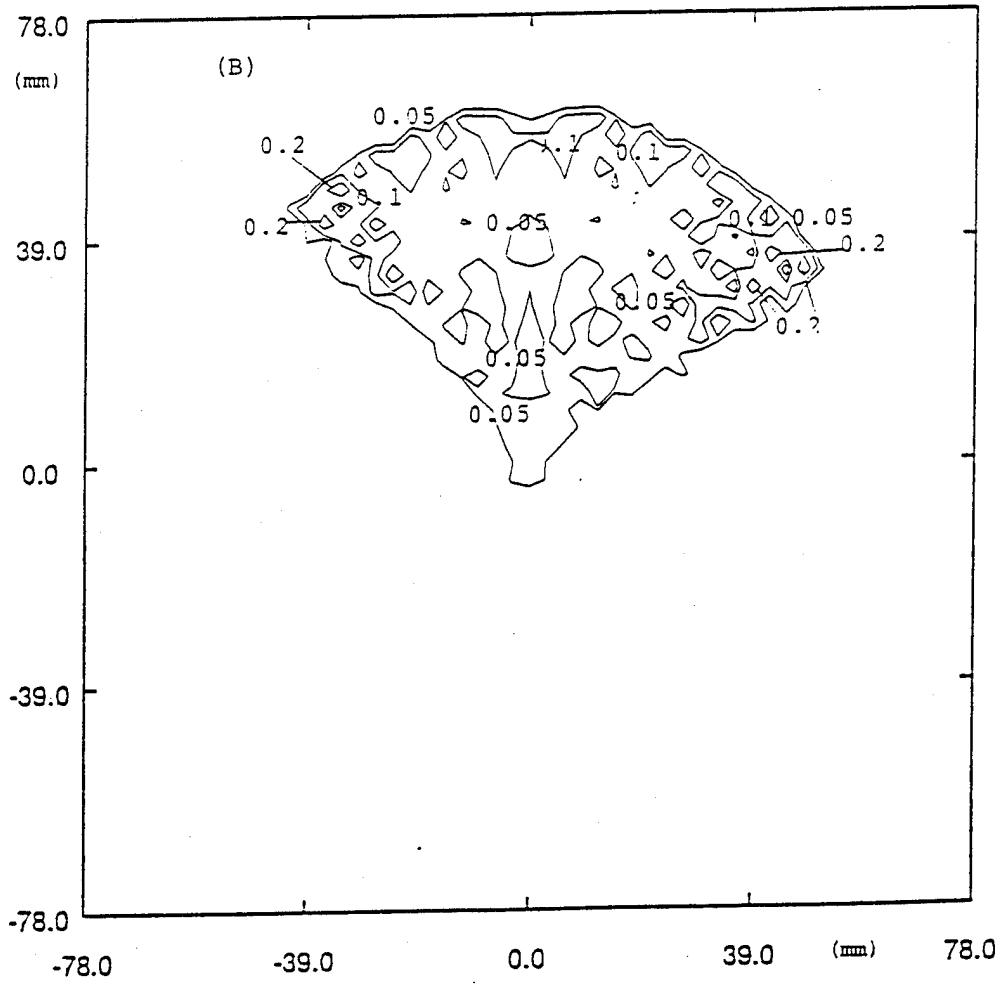
78.0
(mm)
39.0
0.0
-39.0
-78.0
-78.0
-39.0
0.0
39.0
(mm)
78.0
(B)
0.05
0.2
0.1

FIGURE 9

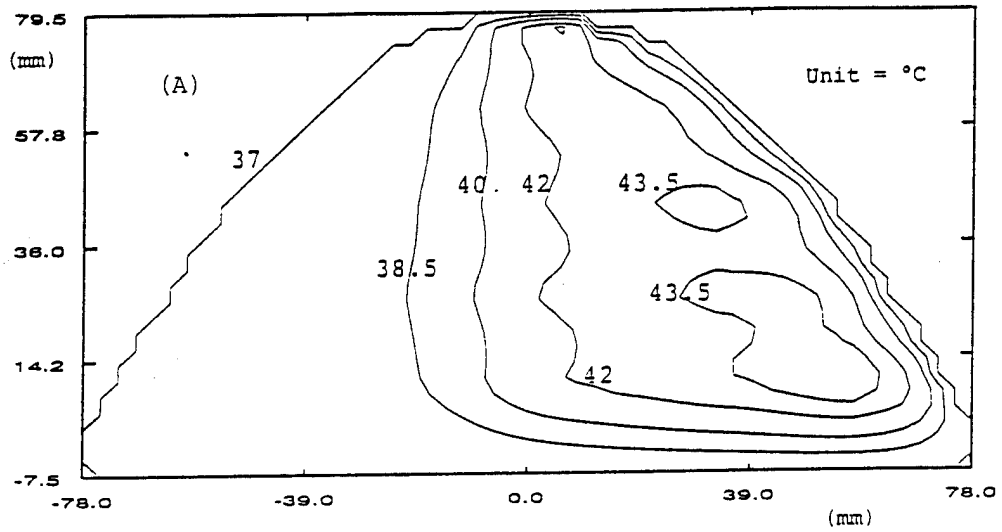
79.5
(mm)
(A)
Unit = °C
57.8
36.0
14.2
-7.5
37
40
42
43.5
38.5
43.5
42
-78.0
-39.0
0.0
39.0
78.0
(mm)

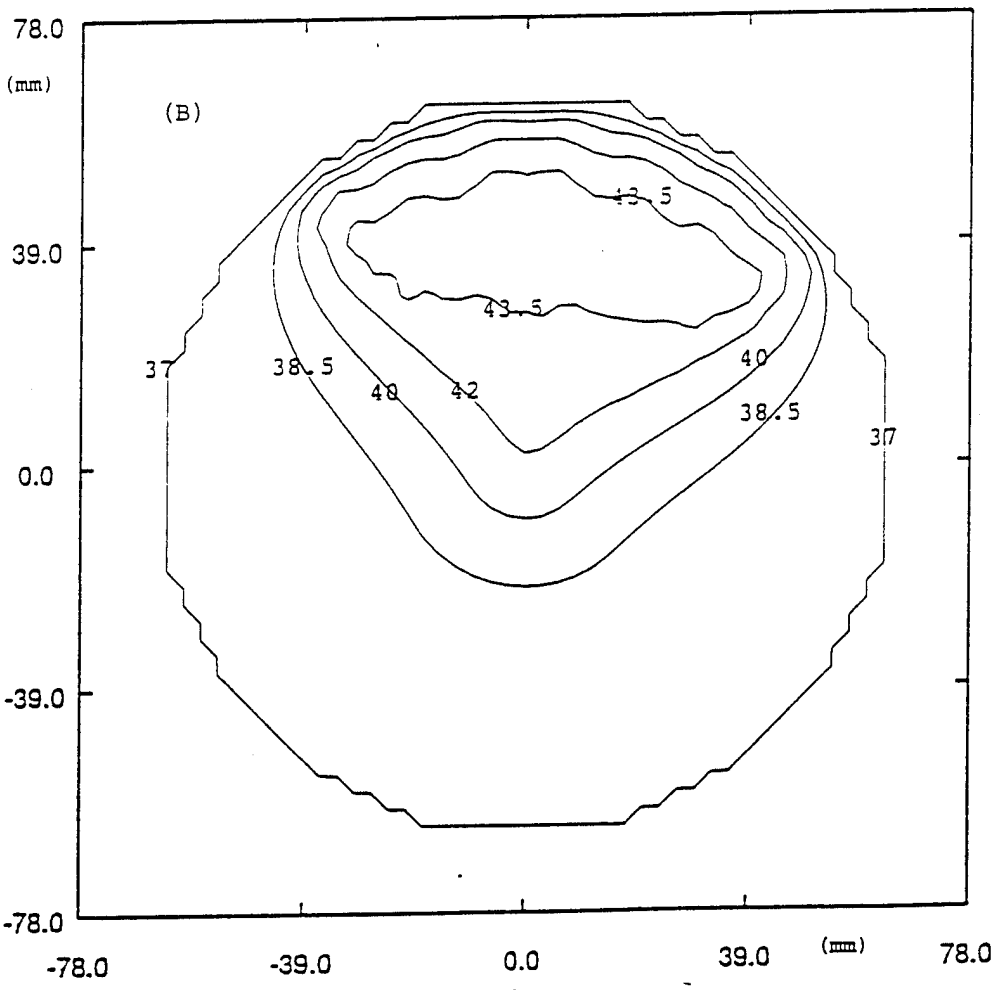
78.0
(mm)
(B)
39.0
0.0
-39.0
-78.0
43.5
43.5
37
38.5
40
42
40
38.5
37
-78.0
-39.0
0.0
39.0
(mm)
78.0

FIGURE 10

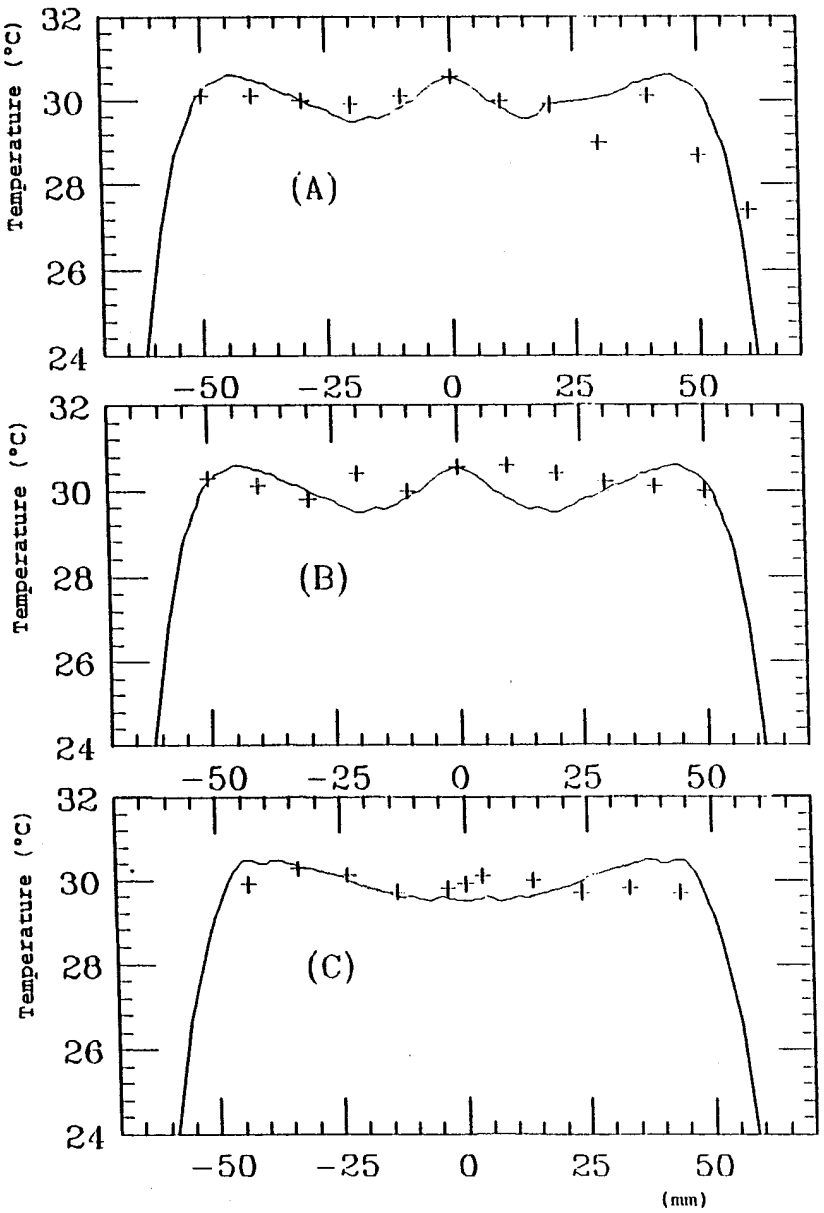

FIGURE 11

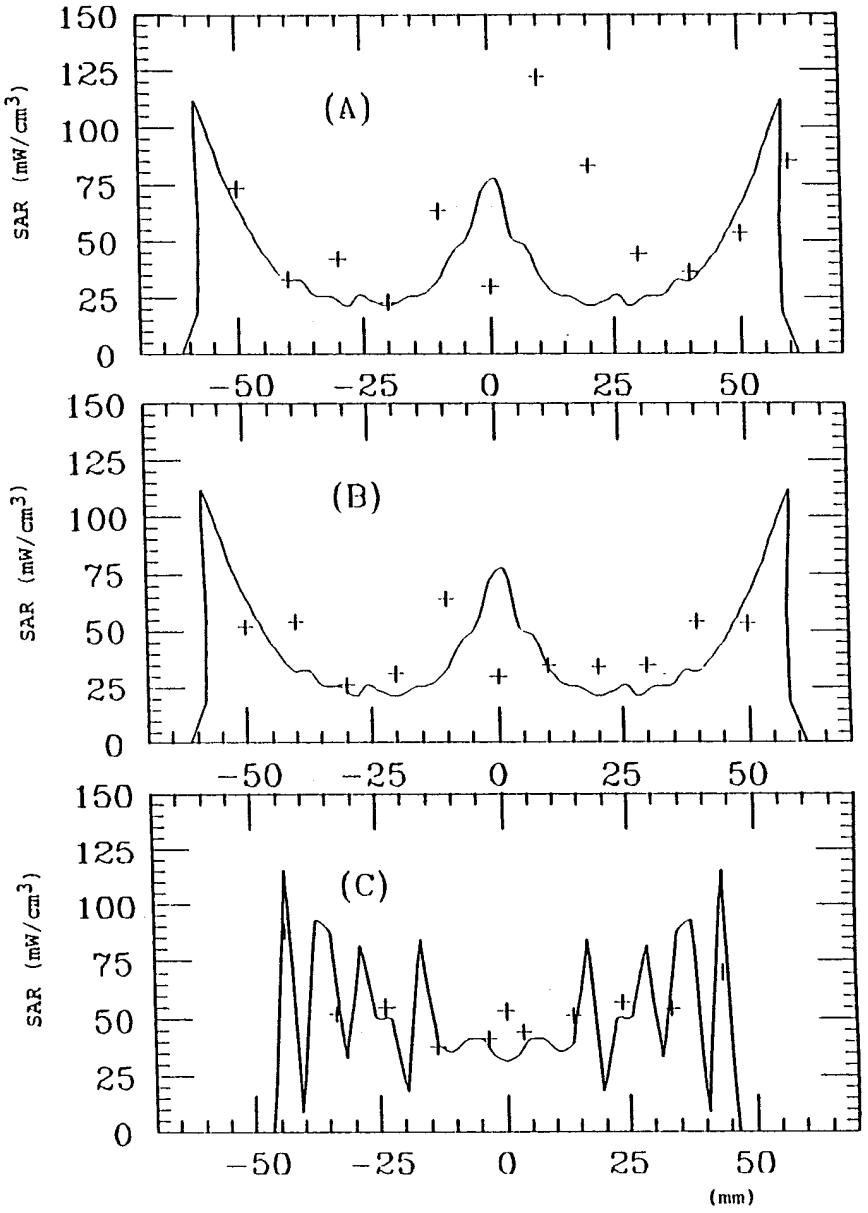

FIGURE !2

Appendix B

Ultrasound Power Deposition In A Water - Soft Tissue Medium

X-Q. Lu[1], E.C. Burdette [2], G. K. Svensson [1]

Joint Center for Radiation Therapy
Department of Radiation Oncology
Harvard Medical School
Boston, MA 02115

[2]Dornier Medical Systems Inc.
Champaign, IL 61820

April 1995

Ultrasound Power Deposition In A Water - Soft Tissue Medium

X-Q. Lu [1], E.C. Burdette [2], G. K. Svensson [1]

[1] Joint Center for Radiation Therapy
Department of Radiation Oncology
Harvard Medical School
Boston, MA 02115

[2] Dornier Medical Systems Inc.
Champaign, IL 61820

April 20, 1995

Abstract

A numerical method is presented for ultrasound field calculation in a two-layer medium for a continuous wave baffled plane source. It is shown that when the attenuation coefficient is very different but the density and speed of sound are similar in the two layers, such as water and most soft tissues, approximation can be made for this calculation. It is not necessary for the interface of the two layers to be perpendicular to the central axis and it can be a curved surface. Conditions for the approximation are discussed and examples relevant to the medical applications are presented.

Key Words: Ultrasound field, power deposition, hyperthermia, safety of diagnostic ultrasound.

1 Introduction

Calculation of the ultrasound power deposition is often of interest in medicine. For hyperthermia treatment of cancer, the power deposition is essential for the estimation of temperature elevation. In diagnostic ultrasound applications, the knowledge of the power deposition is also important because of safety concerns.

Many authors have worked on the sound field calculation (Zemanck 1971, Lockwood and Willete, 1973. Marini and Rivenez, 1974). An efficient field calculation method has been developed for continuous waves, generated by a baffled piston vibrating square source (Ocheltree and Frizzell, 1989). This method divides the plane source into small rectangular areas, surrounded by a rigid baffle. It sums the contribution to the pressure at a field point from these areas chosen to be small enough that the farfield approximation is appropriate. Compared with other theoretical calculations, this method required the least time to achieve a given accuracy.

Ocheltree's method is very useful for the calculation of the sound field in a homogeneous medium. In many applications, however, a two-layer medium is more relevant, for instance in the case where a 'water bag' or 'standoff' is used, which is placed between the ultrasound source and the tissue for the purpose of skin sparing and avoiding near-field complications. This two-layer medium problem has been addressed recently (Wu and Nyborg, 1992).

It was pointed out that in a medium with water (or body fluids) and most soft tissues, reflection at the interface is less than 1% and thus may be neglected, and that for a Gaussian beam source the sound field calculation in this two-layer medium can be performed using a modified formula valid for a homogeneous medium. The advantage of use the Gaussian beam is its simple field characteristics, which can be represented by an analytic expression (Du and Breazeale, 1987, Du and Wu 1990). To extend this analytic expression to the two-layer situation, the interface of the two media has to be a plane perpendicular to the central axis of the transducer (Wu and Nyborg, 1992).

It would be desirable if the sound field calculation for a two-layer medium also can be done for 'piston-in-a-baffle' sources, because this kind of source is a good representation for the most commonly used transducers. While the 'piston-in-a-baffle' assumption is probably never strictly true, the theory so developed has proved very successful in accounting for important features of actual fields (Harris, 1981a, 1981b). The purpose of this paper is to extend the numerical method developed by Ocheltree et al. to the two-layer medium situation for the piston transducer. In this approach, for the interface of the two layers it is not necessary to be perpendicular to the central axis. The conditions required for an appropriate approximation are discussed in the paper. Results for the cases particularly relevant and useful to the medical applications are presented.

2 Method

Commonly, an ultrasound beam generated by a piston transducer propagates through a medium with low attenuation coefficient (such as water) before reaching a second medium (such as soft tissue) with higher attenuation but similar density (ρ) and sound speed (C). It will be shown in this section that under certain conditions the numerical method for sound calculation in a homogeneous medium (Ocheltree and Frizzell 1989) can be extended to this two-layer medium situation. We will use the same notations that were used in Ocheltree's paper whenever possible. The assumptions for various approximations are stated only briefly when deriving the formula. They will be summarized and further discussed later.

In Ocheltree's approach, the plane source was divided into N rectangular element areas, each has a size of $\Delta A = \Delta h \cdot \Delta w$. This size is small enough

that certain simplifying assumptions can be applied, but it is too large to be represented as a point source, therefore an integral over the area is required. The center of each element n is denoted by $(x_n,\ y_n)$ in a coordinate system, with the origin in the center of the transducer as shown in Figure 1. A second coordinate system is defined in $x_0,\ y_0$ with its origin centered on a element n. The total pressure p_0 at a point in the field is the sum of the pressure contributed from each element:

$$p_0 = \frac{j\rho c}{\lambda} \cdot \Sigma_{n=1}^{N} u_n \int_{\Delta A} \frac{\epsilon^{-(\alpha+jk)r}}{r} dA$$

$$= \frac{j\rho c}{\lambda} \cdot \Sigma_{n=1}^{N} u_n \int_{-\Delta h/2}^{\Delta h/2} \int_{-\Delta w/2}^{\Delta w/2} \frac{\epsilon^{-(\alpha+jk)r}}{r} dx_0 dy_0, \qquad (1)$$

where λ is the wavelength, k is the wave number, α is attenuation coefficient in the homogeneous medium, r is the distance between the field point and a point inside the element area n. u_n is the complex surface velocity of element n. When a uniformly excited source is considered, all u_n are the same. Equation (1) is based on Huygen's principle (Zemanck 1971). When the Fraunhofer approximation is valid under the condition of small size ΔA, Equation (1) can be simplified and the total pressure p_0 can be calculated accurately by an effective numerical method.

Based on the same principle, the total pressure p_0 at a point in the field can be obtained in a two-layer medium, neglecting the reflection and refraction at the interface:

$$p_0 = \frac{j\rho c}{\lambda} \cdot \Sigma_{n=1}^{N} u_n \int_{-\Delta h/2}^{\Delta h/2} \int_{-\Delta w/2}^{\Delta w/2} \frac{\epsilon^{-(\alpha_1 r_1 + \alpha_2 r_2 + jkr)}}{r} dx_0 dy_0, \qquad (2)$$

where α_1 and α_2 are the attenuation coefficients in medium 1 and 2, r_1 and r_2 are the potions of distance r in medium 1 and 2 , respectively.

To simplify the formula the distance between the center of the element n to the field point is denoted as R. The distance R can be expressed as:

$$R = R_1 + R_2 = \sqrt{z^2 + (x - x_n)^2 + (y - y_n)^2}$$

$$= \sqrt{z^2 + (x_n')^2 + (y_n')^2}, \qquad (3)$$

where R_1 and R_2 are the distances in media 1 and media 2, $x_n' = x - x_n$ and $y_n' = y - y_n$. The distance r can then be expressed as:

$$r = r_1 + r_2 = \sqrt{z^2 + (x - x_n - x_0)^2 + (y - y_n - y_0)^2}$$

$$= \sqrt{z^2 + (x_n' - x_0)^2 + (y_n' - y_0)^2}$$

$$= \sqrt{R^2 - 2x_n'x_0 - 2y_n'y_0 + x_0^2 + y_0^2}, \quad (4)$$

To assure that the Fraunhofer approximation can be applied to Equation (2), Δh and Δw are chosen to be much smaller than the distance R. We may apply approximations $r_1 = r \cdot R_1/R$ and $r_2 = r \cdot R_2/R$ to the exponential term in Equation (2):

$$\epsilon^{-(\alpha_1 r_1 + \alpha_2 r_2 + jkr)} = \epsilon^{-(\alpha_1 R_1/R + \alpha_2 R_2/R + jk)r}$$

$$= \epsilon^{-(\alpha_1 R_1/R + \alpha_2 R_2/R + jk) \cdot \sqrt{R^2 - 2x_n'x_0 - 2y_n'y_0 + x_0^2 + y_0^2}}. \quad (5)$$

Using the first two terms of a binomial expansion of the radical on the right side of (5) yields:

$$\epsilon^{-(\alpha_1 r_1 + \alpha_2 r_2 + jkr)} = \epsilon^{-(\alpha_1 R_1/R + \alpha_2 R_2/R + jk) \cdot (R - \frac{x_n'x_0}{R} - \frac{y_n'y_0}{R} + \frac{x_0^2}{2R} + \frac{y_0^2}{2R})}. \quad (6)$$

When $(\frac{x_0^2}{2R} + \frac{y_0^2}{2R})$ is small compared to π and $\alpha_1, \alpha_2 << k$, omission of these terms produces a negligible phase error and gives the expression:

$$\epsilon^{-(\alpha_1 r_1 + \alpha_2 r_2 + jkr)} = \epsilon^{-(\alpha_1 R_1/R + \alpha_2 R_2/R + jk) \cdot (R - \frac{x_n'x_0}{R} - \frac{y_n'y_0}{R})}. \quad (7)$$

Assuming $1/r \approx 1/R$, and substituting (7) into (2) give

$$p_0 = \frac{j\rho c}{\lambda} \cdot \Sigma_{n=1}^{N} \frac{u_n}{R} \epsilon^{-(\alpha_1 R_1 + \alpha_2 R_2 + jkR)}$$

$$\cdot \int_{-\Delta w/2}^{\Delta w/2} \epsilon^{(\alpha_1 R_1/R + \alpha_2 R_2/R + jk)\frac{x_n'x_0}{R}} dx_0$$

$$\cdot \int_{-\Delta h/2}^{\Delta h/2} \epsilon^{(\alpha_1 R_1/R + \alpha_2 R_2/R + jk)\frac{y_n'y_0}{R}} dy_0. \quad (8)$$

With an assumption that $\epsilon^{(\alpha_1 R_1/R + \alpha_2 R_2/R)\frac{x_n'x_0}{R}} \approx 1$ for $\Delta w/2 > x_0 > -\Delta w/2$ and the equivalent condition for y_0, the two integrals in (8) are reduced to Fourier transform expressions which upon evaluation yield

$$p_0 = \frac{j\rho c}{\lambda} \cdot \Sigma_{n=1}^{N} [\frac{u_n}{R} \cdot \epsilon^{-(\alpha_1 R_1 + \alpha_2 R_2 + jkR)} \cdot sinc\frac{kx_n'\Delta w}{2R} \cdot sinc\frac{ky_n'\Delta h}{2R}]. \quad (9)$$

This formula is a straightforward summation of complex terms, representing the pressure due to a rectangular source. Using Formula (9) the sound field in the two-layer medium can be calculated numerically, provided all the required conditions are satisfied.

The conditions involved in the deduction of Equation (9) can be summarized below:

1. $\alpha_1, \alpha_2 << k$.

2. $\frac{kx_0^2}{2R} + \frac{ky_0^2}{2R}$ is small compared to π. Since the maximum absolute values of x_0 and y_0 are $\Delta w/2$ and $\Delta h/2$, this condition can be expressed as

$$cos(\frac{k\Delta w^2}{8R} + \frac{k\Delta h^2}{8R}) \approx 1. \tag{10}$$

3. $e^{(\alpha_1 R_1/R + \alpha_2 R_2/R)\frac{x_n' x_0}{R}} \approx 1$ for $\Delta w/2 > x_0 > -\Delta w/2$, and the equivalent condition for y_0. Again, since the maximum absolute values of x_0 and y_0 are $\Delta W/2$ and $\Delta h/2$, this condition can be expressed as

$$e^{(\alpha_1 R_1/R + \alpha_2 R_2/R)\frac{x_n' \Delta w + y_n' \Delta h}{2R}} \approx 1 \tag{11}$$

4. $r/R \approx 1$

5. The density (ρ), sound speed (c) and impedance ($Z = \rho c$) in the two media are close, so that the reflection and refraction can be ignored.

6. $r_1 = r \cdot \frac{R_1}{R}$ and $r_2 = r \cdot \frac{R_2}{R}$.

Among these assumptions, condition 1 is in general true for ultrasound in water and soft tissue. In Condition 3, the value of term $(\alpha_1 R_1/R + \alpha_2 R_2/R)$ is between α_1 and α_2, therefore can be replaced by α_2, resulting a more stringent condition. As a result, condition 2-4 are exactly the same requirements for the method in a homogeneous medium (Ocheltree and Frizzell, 1989). As pointed out by the previous authors when Δw (and Δh) satisfies:

$$\Delta w \leq \sqrt{\frac{4\lambda z}{F}}, \tag{12}$$

conditions 2, 3 and 4 are all ensured, where the constant F represents the distance from the source to the field point relative to the distance to the nearfield-farfield transition for a source of size Δw, and $F = 10$ was recommended. This condition in fact guarantees the validity of the Fraunhofer approximation.

Items 5 and 6 are the additional conditions for the two-layer media situation. For water (or body fluids) and most soft tissues, Condition 5 is approximately true. The density and speed of sound for water are 1.0 $g\ cm^{-3}$ and 1519 $m\ sec^{-1}$ (at 35° C, Kaye and Laby, 1973), which are close to those for most soft tissues. For instance, for breast tissue they are $1.02 \pm 0.04\ g\ cm^{-3}$ (F. Duck, 1990) and $1553 \pm 35\ m\ sec^{-1}$ (Scherzinger et al. 1989). Thus, the ratio of the speed in these two media is 1.02 ± 0.02, and the ratio of their acoustic impedances is 1.04 ± 0.06. With this small difference the intensity reflection and the refraction at the surface of the breast are negligible in most cases. As illustrated in figure 2, when the angle of incidence is less than 70°, the intensity reflection is less than a few percent, and for a plane wave the direction of propagation changes less than 4° in the interface.

For condition 6 only the approximation $r_2 = r \cdot \frac{R_2}{R}$ should be considered, because when this approximation holds, $r_1 = r \cdot \frac{R_1}{R}$ will follow. By examining figure 1, a geometric relation can be obtained:

$$r_2 = r \cdot \frac{R_2}{R} + s \cdot \frac{R_2}{R} \cdot \frac{sin(\gamma - \beta)}{sin\gamma}, \tag{13}$$

where s is the distance between (x_n, y_n) and (x_0, y_0). Therefore, the error of the approximation in condition 6 is:

$$\delta r_2 = s \cdot \frac{R_2}{R} \cdot \frac{sin(\gamma - \beta)}{sin\gamma}, \tag{14}$$

which is negligible in most cases. For instance, when the interface is in parallel to the transducer surface, i.e. $\angle\gamma = \angle\beta$, then the error δr_2 vanishes. When $\angle\gamma$ is large then 30°, the absolute value of $\frac{sin(\gamma-\beta)}{sin\gamma}$ is no more than 2 in any case, and δr_2 is in the order of $\Delta w \cdot \frac{R_2}{R}$. If $\Delta w = \Delta h = 0.1\ cm$ is chosen, δr_2 is less than 1 millimeter.

3 Results and discussions

Results for several examples relevant to medical applications are discussed in this section. Breast tissue is assumed, which has an attenuation coefficient of $0.086\ f^{1.5}\ np\ cm^{-1}$ (Foster and Hunt, 1979). For water it is $0.0002\ f^2\ np\ cm^{-1}$ (Kaye and Laby, 1973). The size of the element area ($\Delta w \cdot \Delta h$) was chosen to satisfy the conditions discussed in the last section.

First, we consider a case when the tissue surface is parallel to the transducer surface. In Figure 3 the transducer size is $1.5\ cm \times 1.5\ cm$ operating at a frequency of 2 MHz. The sound field calculated for longitudinal sections in the y-z plane (x=0) is shown in Figure 3(A)-3(C). In 3(A) the normalized pressures along the central axis are shown in three cases. For curve a there is no tissue in the water, for curve b and c the distances between the interface surface and transducer surface along the central axis ($z_{interface}$) are 10 and 5 cm, respectively. In 3(B) contours are plotted for the -3 and -6 db levels, which represent an intensity of 1/2 and 1/4 of its axial value at the same coordinate z. Also shown in 3(B) are the maxima, that occur close to the transducer surface, representing an intensity of 1.5 of the axial value at the same coordinate z. It was noticed that the contour plots are nearly independent from the distance between the transducer surface and the interface. Therefore, only one contour plot is shown for the three cases. In 3(C), the power deposition, i.e. the specific absorption rate (SAR), in the longitudinal section for $z_{interface} = 5\ cm$ is shown, which is calculated by

$$SAR = \alpha P_0^2/\rho c, \tag{15}$$

where P_0 is the sound pressure amplitude, and the attenuation coefficient α is considered identical to the absorption rate. In each field point the value of α for water or breast is chosen depending on its location. For a square field, showing only a longitudinal section is not complete, therefore, a transverse section for the power deposition at $z = 8\ cm$ for $z_{interface} = 5\ cm$ is provided in Figure 3(D).

In Figure 4 the normalize pressure in the central axis and the contour plots for a $1.5\ cm \times 1.5\ cm$ transducer operating at 4 MHz for different tissue positions are shown. Figure 5 shows the same plots for a transducer size of $3\ cm \times 3cm$ operating at 1 MHz.

Next, cases are considered when the tissue surface is not parallel to the transducer surface. We assume the angle between the central axis and the

interface is 45° and $z_{interface} = 5\ cm$. The contour plot in the longitudinal section is show in Figure 6(A), and the power deposition in the same section is shown in Figure 6(B). These plots should be compared with those in Figure 3(B) and 3(C). The field in the y-z plane shown in Figure 6 is clearly tilted.

A comparison of the curves (b) and (c) in Figures 3(A), 4(A) and 5(A) shows that the pressure attenuation in the tissue not only depends on the frequency, but also changes significantly with the distance between the interface and the transducer when the tissue is in the near-field region. This illustrates the importance of a detailed field calculation in the design of an ultrasound applicator.

Extended from the previously published work, this study supplies a useful tool for the sound field calculation in the two-layer medium. When all conditions are satisfied, the accuracy should be comparable with the calculation to the homogeneous case. As pointed out by the previous paper (Ocheltree and Frizzell, 1989), significant cancellation of errors occurs from the contribution to the field from one edge of an element to the other, so that actual errors are less than would be predicted by a first order approximation.

The fact, that the interface need not to be perpendicular to the central axis and it can be a curved surface as long as the required conditions satisfied, makes this method flexible to deal with many practical problems. The method has been successfully used in the design, simulation and experiment verification for a dedicated ultrasonic hyperthermia unit for breast cancer treatment (Svensson et al. 1994, Burdette et al 1995, Lu et al. 1995).

This method may be extended directly to cases where more than two layers exist if the reflection and refraction in each interface can be ignored. One such case could be a bladder irradiated by ultrasound through abdomen, where the sound path is water-tissue-water-tissue. Since there are three interfaces, at each interface conditions more stringent than that discussed in last Section might be needed. Furthermore, although the method studied in the paper is for a rectangular transducer, there is no condition imposed in the deduction that the transducer should be restricted to this particular shape.

4 Conclusions

A flexible, efficient numerical method has been developed for the sound field calculation of a plane source in a water-soft tissue medium. The method divides the transducer into small rectangular elements, surrounded by a rigid baffle. A simplification is then made to sum the contribution to the pressure at a field point from each elements. This study is an extension of a previously published method for the calculation in a homogeneous medium. A main condition for this method is that the reflection and refraction at the interface can be neglected, which is a good approximation in most cases for a water-soft tissue medium.

5 Acknowledgment

This work is supported by the US Army Medical Research and Development Command, under contract #DAMD 17-93-C-3098. The views, opinions and/or findings contained in this paper are those of the authors and should not be construed as an official department of the Army position, policy or decision unless so designated by other documentation. The authors would like to thank Junru Wu, Ph.D for many helpful discussions.

Figure Captions

Figure 1. Geometry and coordinate system used for the two-layer medium problem.

Figure 2. (A). Intensity reflection coefficient vs. the angle of incidence at the water-breast tissue interface. (B). Propagation direction change for a plane wave vs. the angle of incidence at the water-breast tissue interface.

Figure 3. The ultrasound field generated by a single transducer with a size of 1.5 $cm \times 1.5$ cm at 2 MHz. The water-tissue interface is parallel to the transducer plane. (A). Normalized pressure in the central axis. Three cases are shown: no tissue in the water (curve a), tissue is 10 cm away from the transducer (curve b), tissue is 5 cm away from the transducer (curve c). (B). Contours in the longitudinal (y-z) plane normalized at each axial distance. The -3, -6 db levels and the maxima, representing intensities of 1/2, 1/4 and 1.5 normalized to the axis value in the same z, are shown. (C). Normalized power deposition in the longitudinal (y-z) plane. (D). Normalized power deposition in a transverse plane ($z = 8$ cm). In both (C) and (D), the tissue is 5 cm away from the transducer, corresponding to curve c in (A).

Figure 4. The ultrasound field generated by a single transducer with a size of 1.5 $cm \times 1.5$ cm at 4 MHz. The water-tissue interface is parallel to the transducer plane. (A). Normalized pressure in the central axis. Three cases are shown: no tissue in the water (curve a), tissue is 10 cm away from the transducer (curve b), tissue is 5 cm away from the transducer (curve c). (B). Contours in the longitudinal (y-z) plane normalized at each axial distance. The -3, -6 db levels and the maxima, representing intensities of 1/2, 1/4 and 1.5 normalized to the axis value in the same z, are shown.

Figure 5. The ultrasound field generated by a single transducer with a size of 3.0 $cm \times 3.0$ cm at 1 MHz. The water-tissue interface is parallel to the transducer plane. (A). Normalized pressure in the central axis. Three cases are shown: no tissue in the water (curve a), tissue is 10 cm away from the transducer (curve b), tissue is 5 cm away from the transducer (curve c). (B). Contours in the longitudinal (y-z) plane normalized at each axial distance. The -3, -6 db levels and the maxima, representing intensities of 1/2, 1/4 and 1.5 normalized to the axis value in the same z, are shown.

Figure 6. The ultrasound field generated by a single transducer with a size of 1.5 $cm \times 1.5$ cm at 2 MHz. The water-tissue interface is not parallel to

the transducer plane. It has an angle of ($\beta = 45°$) with the central axis. The tissue is 5 cm away from the transducer in the central axis. (A). Contours in the longitudinal (y-z) plane normalized at each axial distance. The -3 and -6 db levels and the maxima, representing intensities of 1/2, 1/4 and 1.5 normalized to the axis value in the same z, are shown. (B). Normalized power deposition in the longitudinal (y-z) plane.

References

- Du, G, Breazeale, M.A., 1987, Theoretical description of a focused Gaussian ultrasonic beam in a nonlinear medium, J. Acoust. Soc. Am. **81**, 51-57.

- Du, G, Wu, J., 1989, A design of ultrasonic transducer with curved back- electrodes. Proceedings of IEEE Ultras. Symp. New York; Institute of Electrical and Electronic Engineers, 709-711.

- Duck, F. A., 1990, Physical Properties of Tissue - A Comprehensive Reference Book, Academic Press Inc., 138.

- Foster, F. S. and Hunt, J. W., 1979, Transmission of ultrasound beams through human tissue - focusing and attenuation studies, Ultrasound in Med & Biol., **5**, 257-268.

- Harris, G. R. (1981a), Review of transient field theory for a baffled planar piston, J. Acoust. Soc. Am. **70**, 10.

- Harris, G. R. (1981b) Transient field of a baffled planar piston having an arbitrary vibration amplitude distribution, J. Acoust. Soc. Am. **70**, 186

- Kaye, G.W.C. and Laby, T. H., 1973, Tables of Physical and Chemical Constants, Longman, London.

- Lockwood, J.C. and Willete, J. G., 1973, High-Speed Method for computing the Exact Solution for the Pressure Variations in the nearfield of a Baffled Piston. J. Acoust. Soc. Am. **53**, 735-741.

- Lu, X-Q., Burdette, E.C., Bornstein, B.A., Hansen, J.L, Svensson, G.K., 1995, The design of an ultrasonic hyperthermia unit for breast cancer treatment. submitted to Int. J. Hyperthermia.

- Marini, J. and Rivenez, J., 1974, Acoustic Field from Rectangular Ultrasonic Transducers for Nondestructive testing and medical diagnosis, Ultrasound, **12**, 251-256.

- Ocheltree, K. B. and Frizzell, L. A., 1989, Sound Field Calculation for Rectangular Sources, IEEE Transactions on Ultrasonic, Ferroelectrics, and Frequency Control. **36(2)**, 242-247.

- Schesinger A.L., Belgam, R.A., Carson, P.L., 1989, Assessment of Ultrasonic Computed Tomography in Symptomatic Breast Patients by Discriminant Analysis, Ultrasound in Med & Biol, **15**, 21-28.

- Svensson, G.K., Lu, X-Q, Hansen, J.L., Bornstein, B.A., Burdette, E.C., 1994, Simulation of A Multi-Transducer, Dual-Frequency Ultrasound Applicator For Hyperthermia Treatment of Breast Cancer, 1994 International Symposium on Electromagnetic Compatibility, 433-436.

- Wu, J. and Nyborg, W.L., 1992, Temperature Rise Generated By A Focused Gaussian Beam In A Two-Layer Medium, Ultrasound in Med. & Biol. **18(3)**, 293-302.

- Zemanck, J. 1971, Beam behavior within the nearfield of a vibrating piston, J. Acoust.. Soc. Am. **49(1)**, 181-191

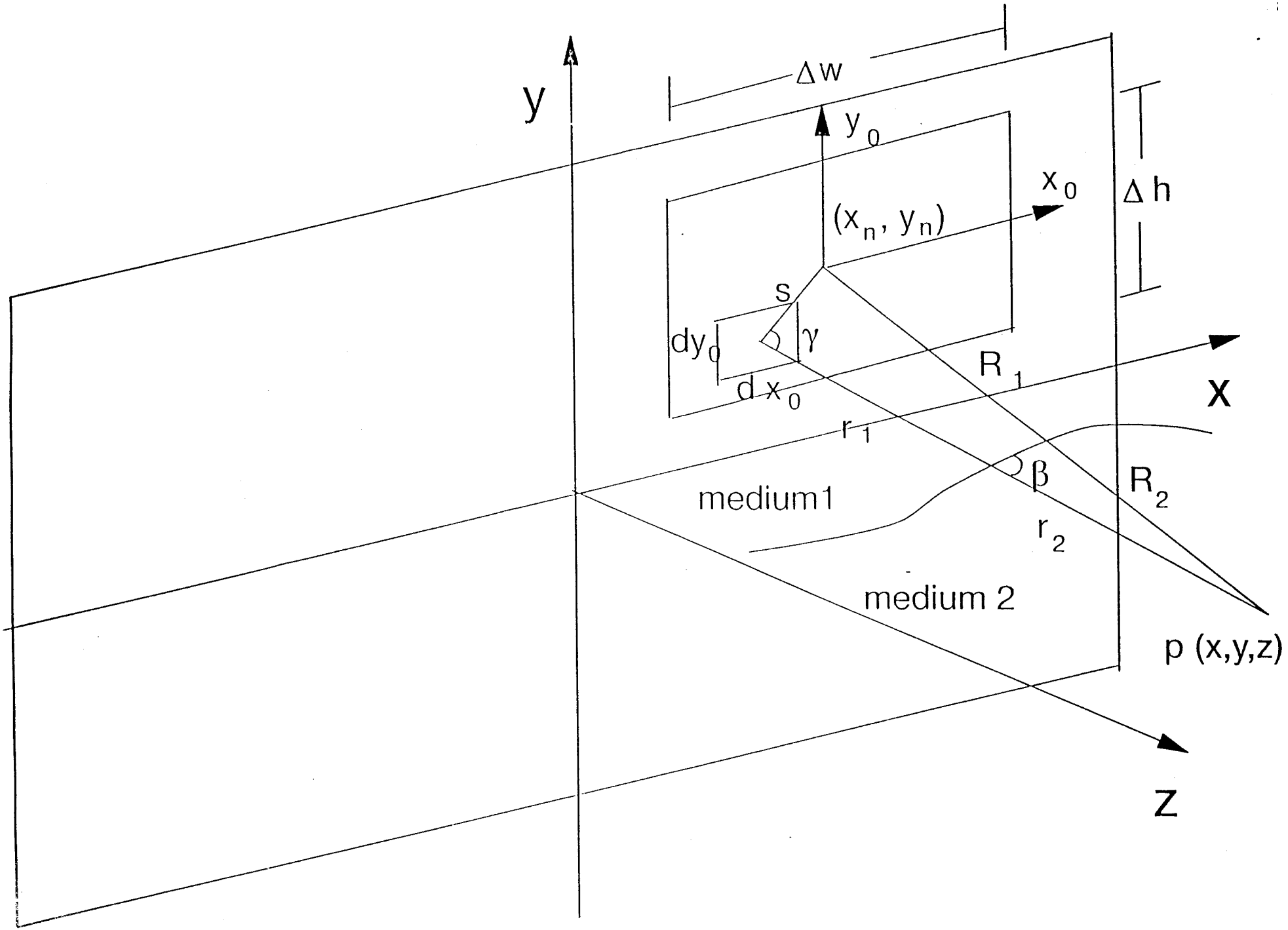
y
Δw
y 0
x 0
Δ h
(x n , y n)
s
dy 0
γ
d x 0
R 1
x
r 1
β
R 2
medium1
r 2
medium 2
p (x,y,z)
z

Figure 1

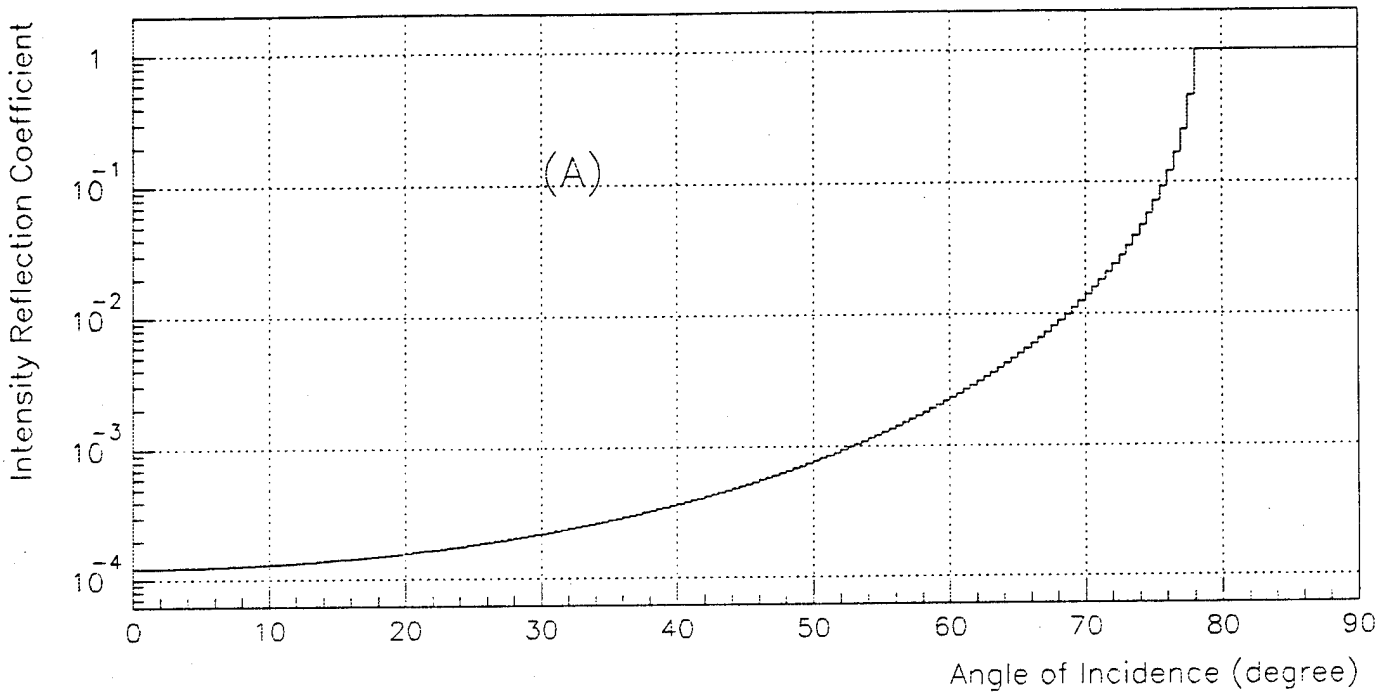
Intensity Reflection Coefficient
1
10^{-1}
10^{-2}
10^{-3}
10^{-4}
(A)
0
10
20
30
40
50
60
70
80
90
Angle of Incidence (degree)

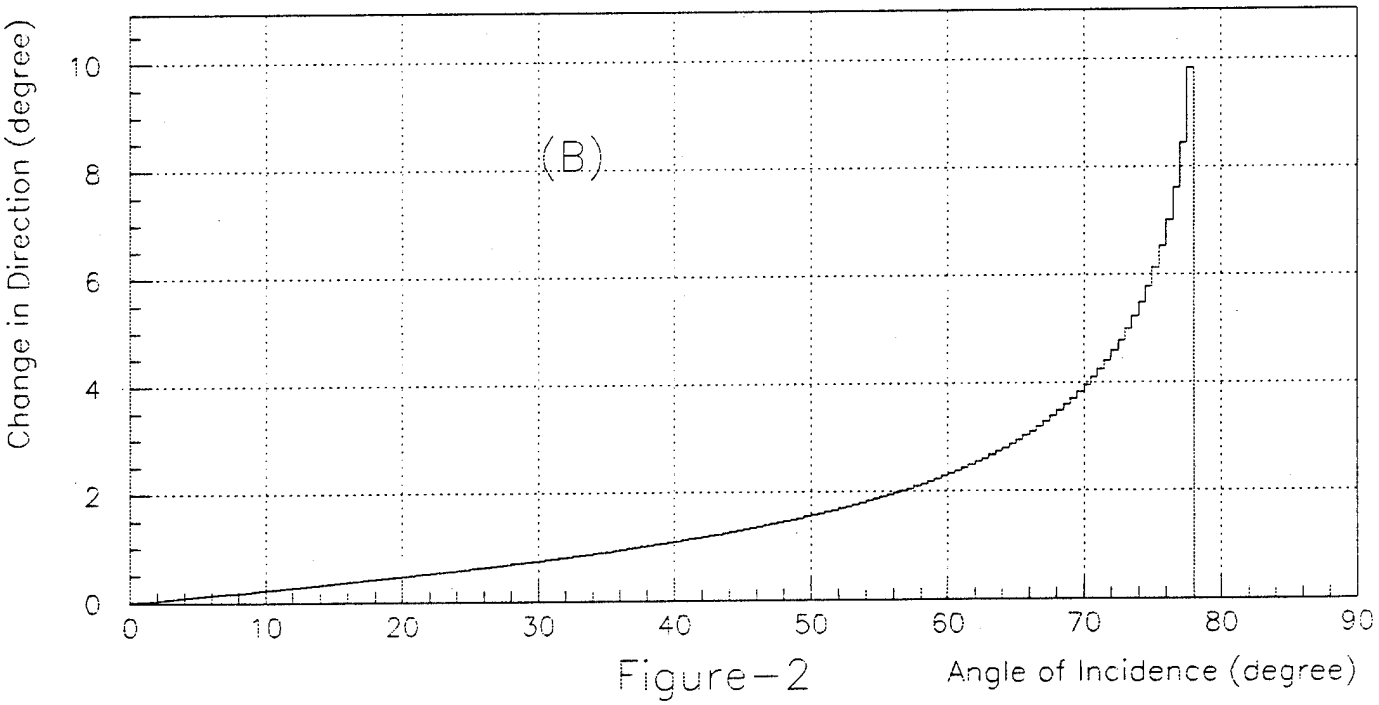
Change in Direction (degree)
10
8
6
4
2
0
(B)
0
10
20
30
40
50
60
70
80
90
Angle of Incidence (degree)

Figure−2

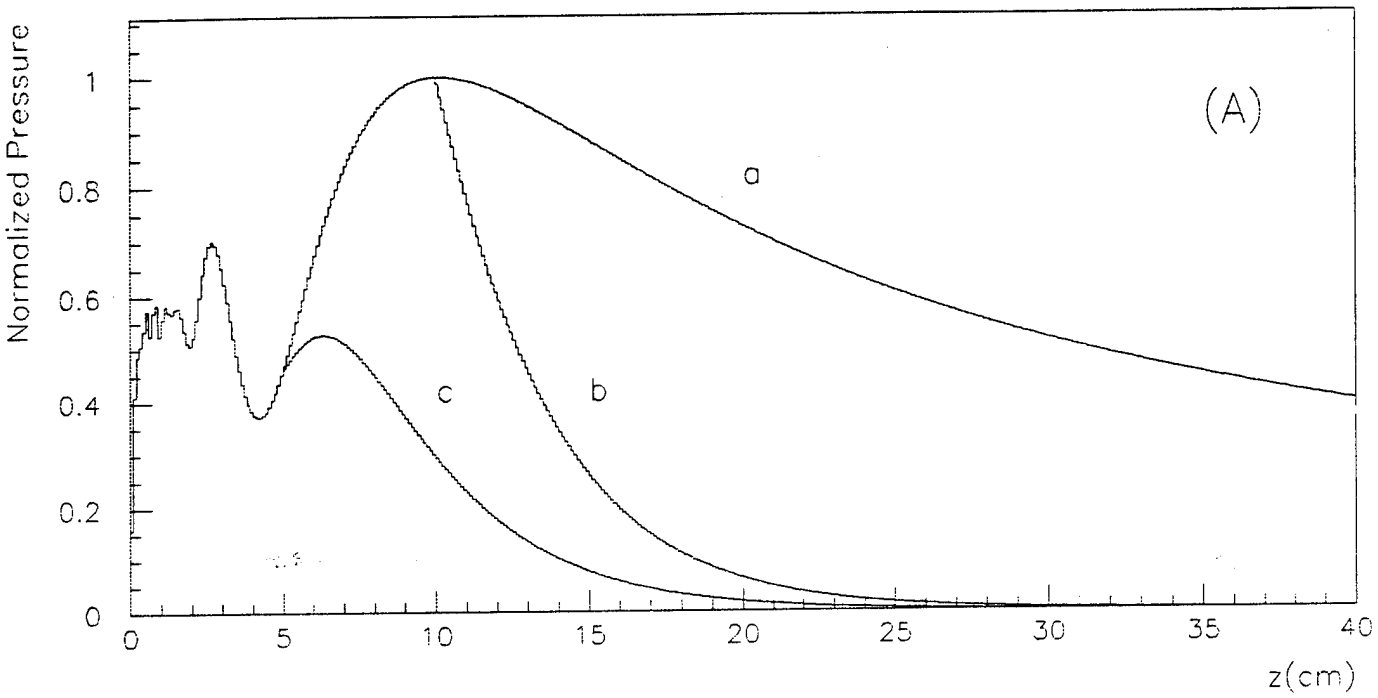
Normalized Pressure
1
0.8
0.6
0.4
0.2
0
0
5
10
15
20
25
30
35
40
z(cm)
(A)
a
b
c

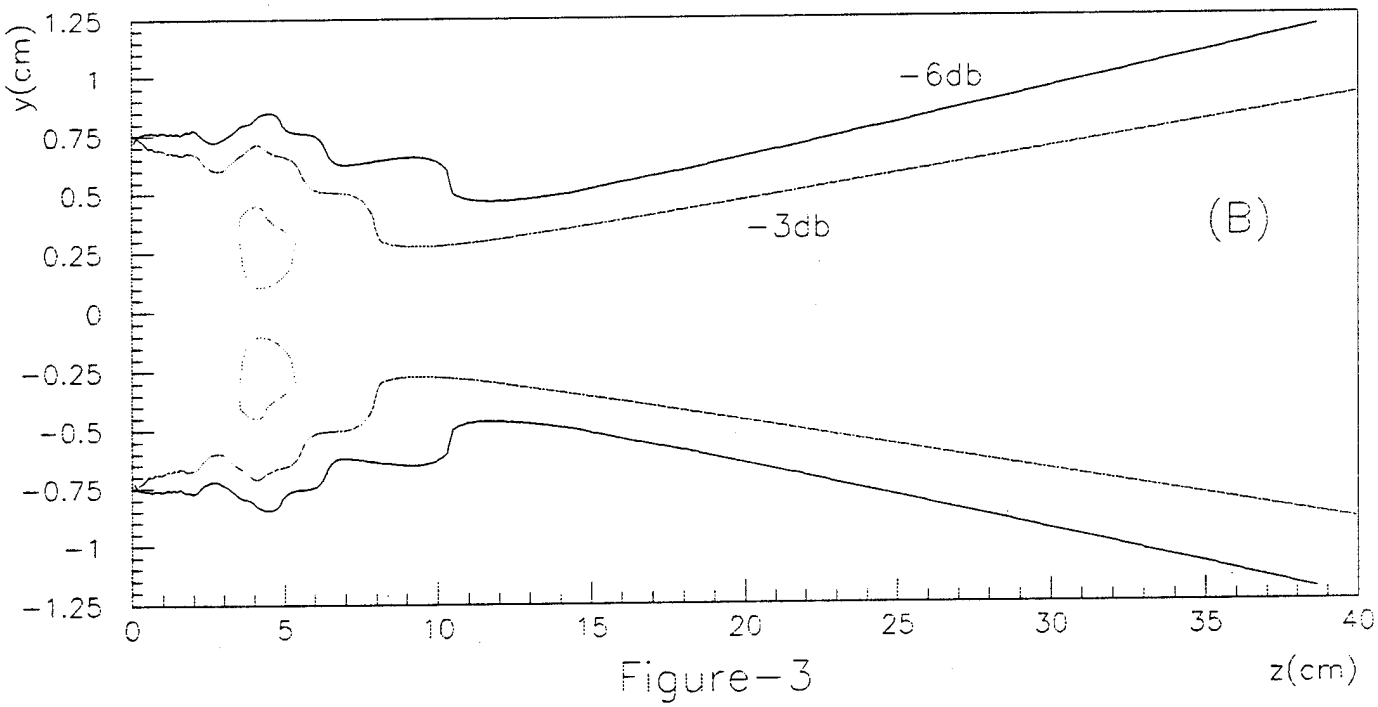
y(cm)
1.25
1
0.75
0.5
0.25
0
−0.25
−0.5
−0.75
−1
−1.25
0
5
10
15
20
25
30
35
40
z(cm)
−6db
−3db
(B)

Figure−3

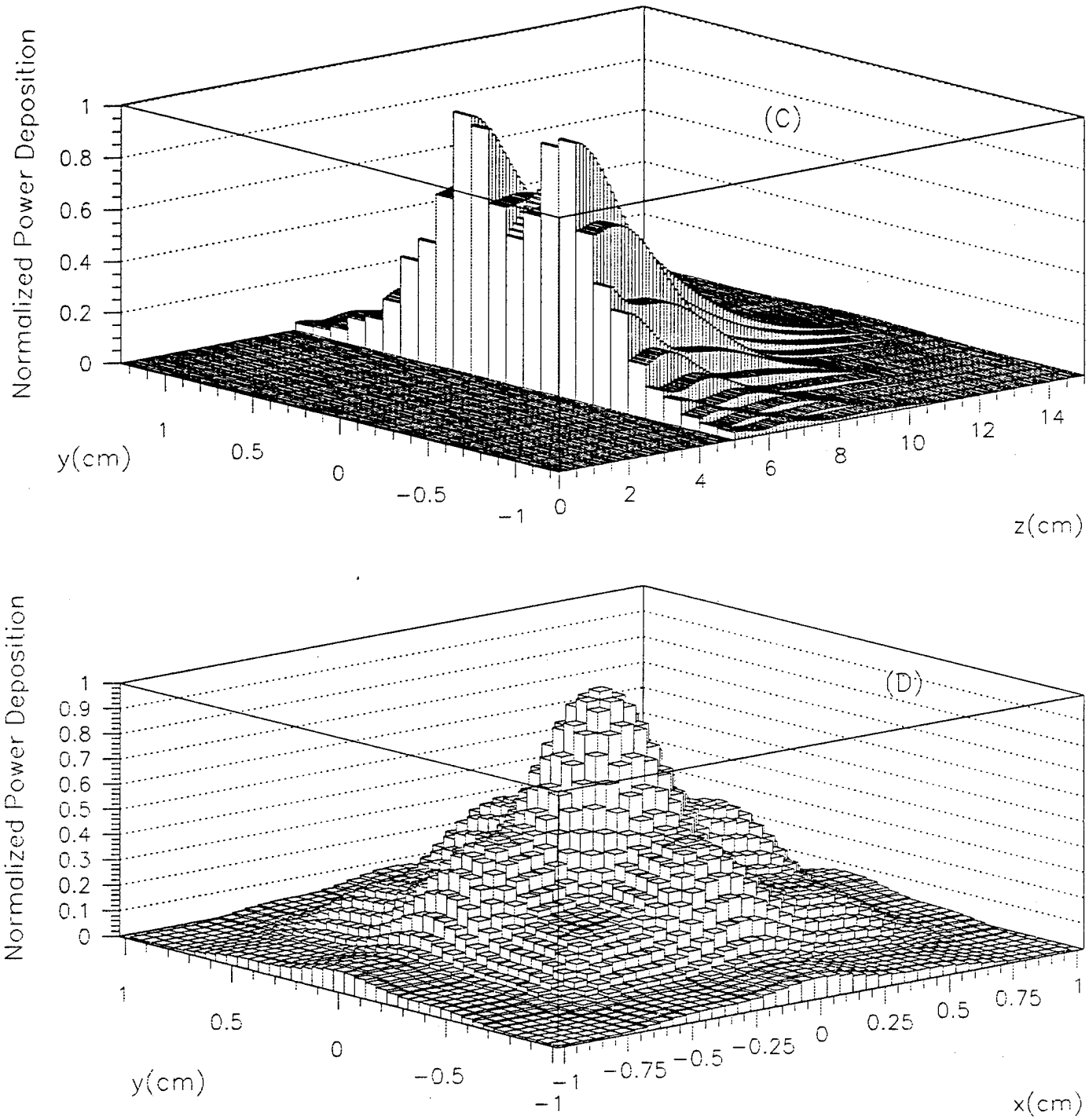
Normalized Power Deposition
(C)
1
0.8
0.6
0.4
0.2
0
y(cm)
1
0.5
0
−0.5
−1
0
2
4
6
8
10
12
14
z(cm)
Normalized Power Deposition
(D)
1
0.9
0.8
0.7
0.6
0.5
0.4
0.3
0.2
0.1
0
y(cm)
1
0.5
0
−0.5
−1
−1
−0.75
−0.5
−0.25
0
0.25
0.5
0.75
1
x(cm)

Figure−3

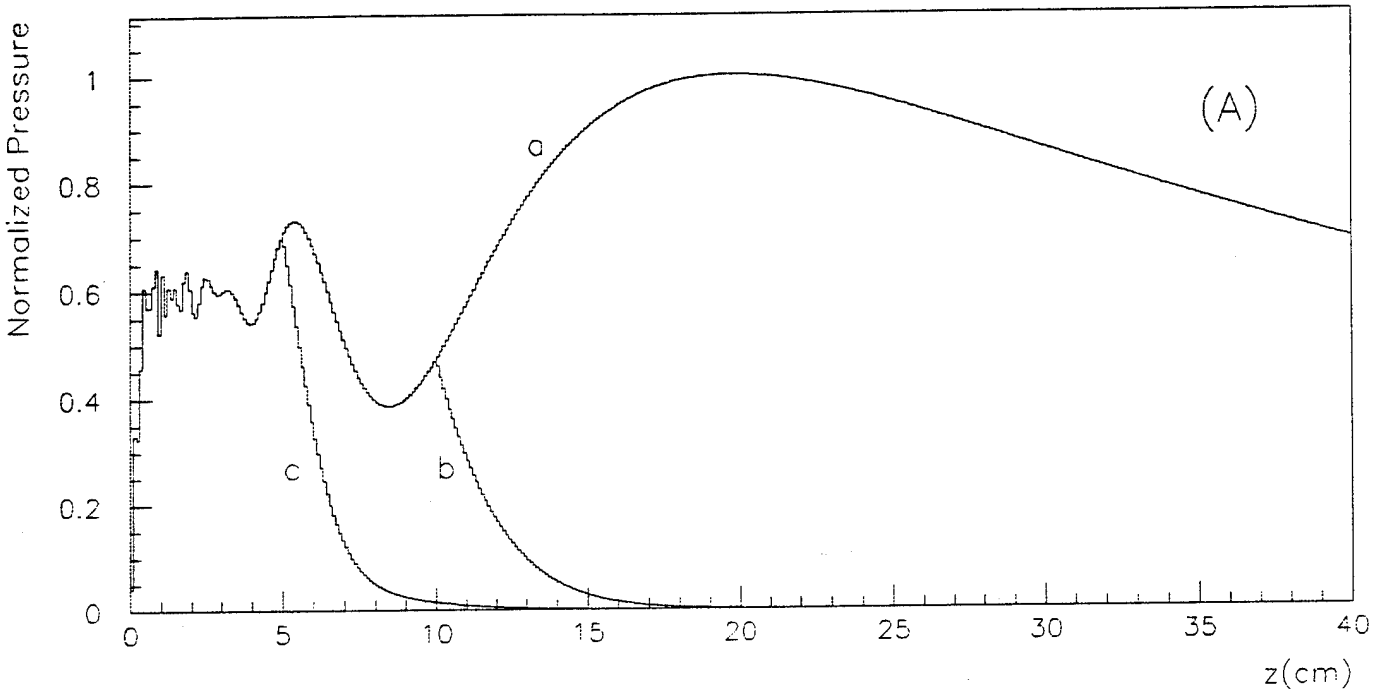
Normalized Pressure
1
0.8
0.6
0.4
0.2
0
0
5
10
15
20
25
30
35
40
z(cm)
(A)
a
b
c

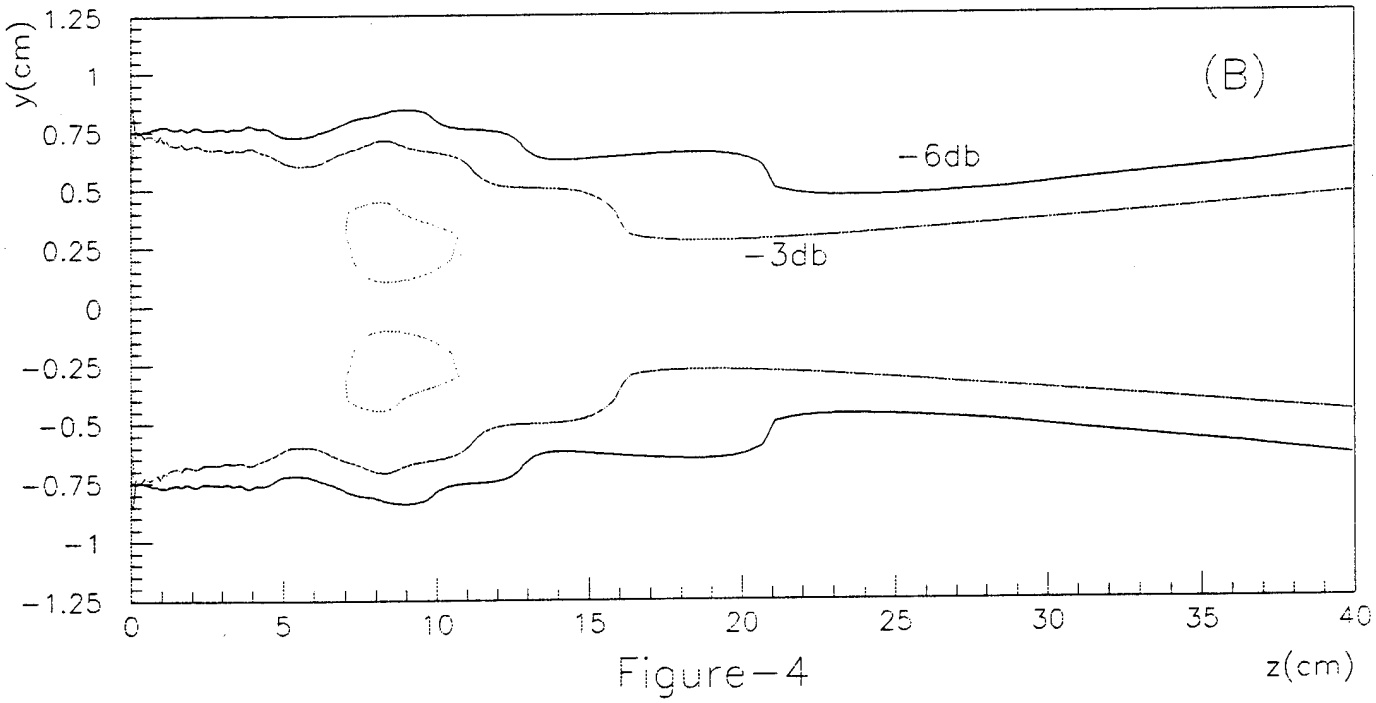
y(cm)
1.25
1
0.75
0.5
0.25
0
-0.25
-0.5
-0.75
-1
-1.25
0
5
10
15
20
25
30
35
40
z(cm)
(B)
-6db
-3db

Figure-4

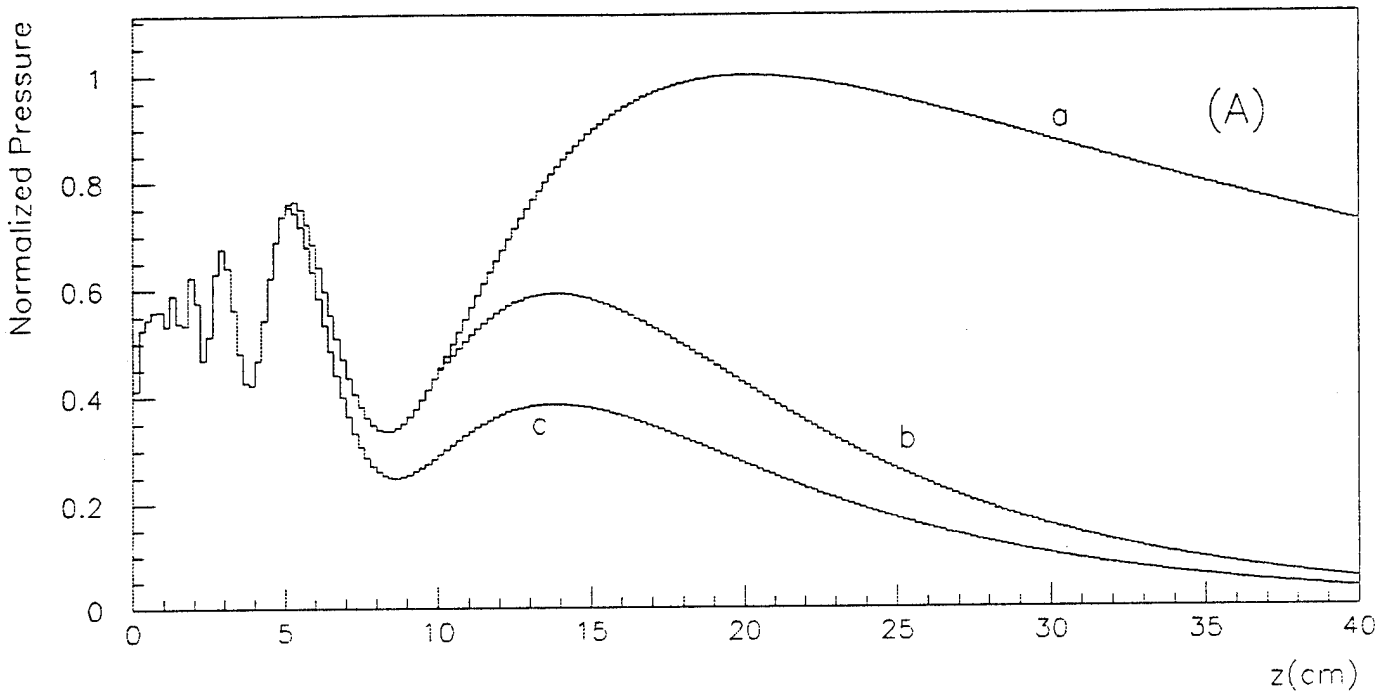
Normalized Pressure
1
0.8
0.6
0.4
0.2
0
0
5
10
15
20
25
30
35
40
z(cm)
a
b
c
(A)

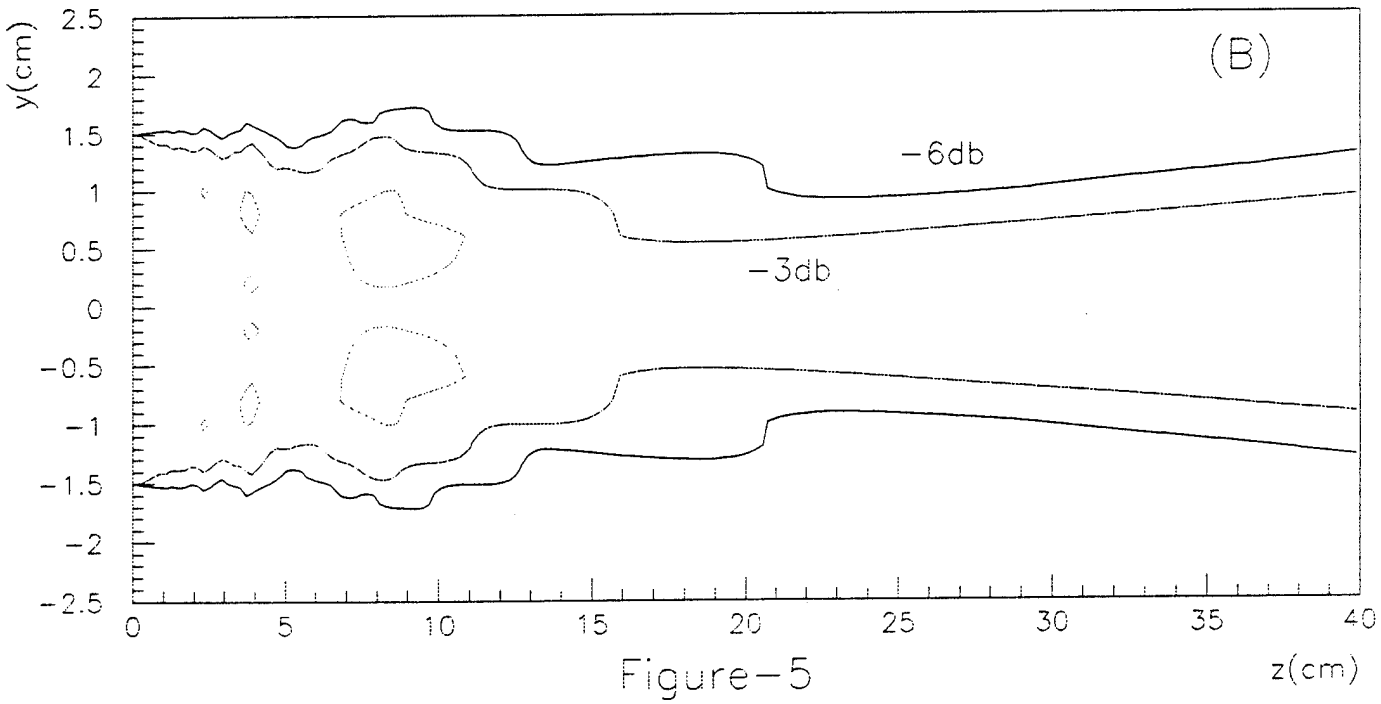
y(cm)
2.5
2
1.5
1
0.5
0
-0.5
-1
-1.5
-2
-2.5
0
5
10
15
20
25
30
35
40
z(cm)
-6db
-3db
(B)

Figure-5

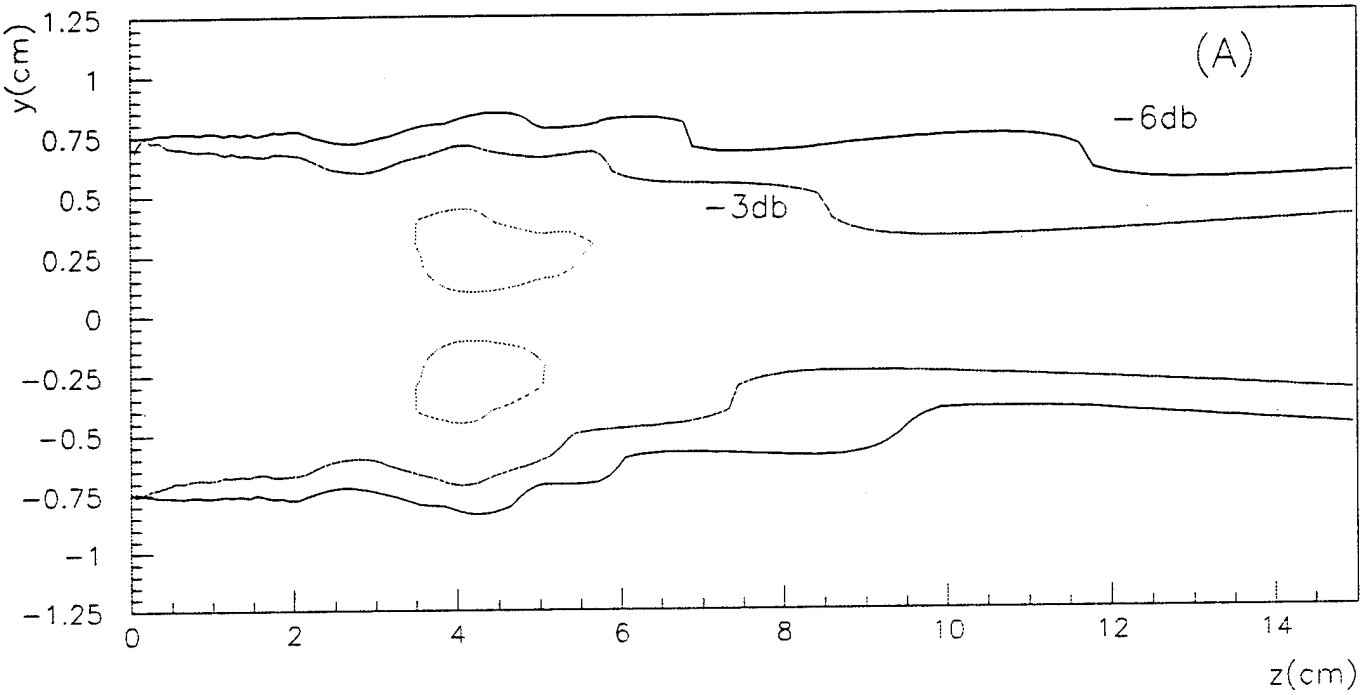
(A)
-6db
-3db
y(cm)
1.25
1
0.75
0.5
0.25
0
-0.25
-0.5
-0.75
-1
-1.25
0
2
4
6
8
10
12
14
z(cm)

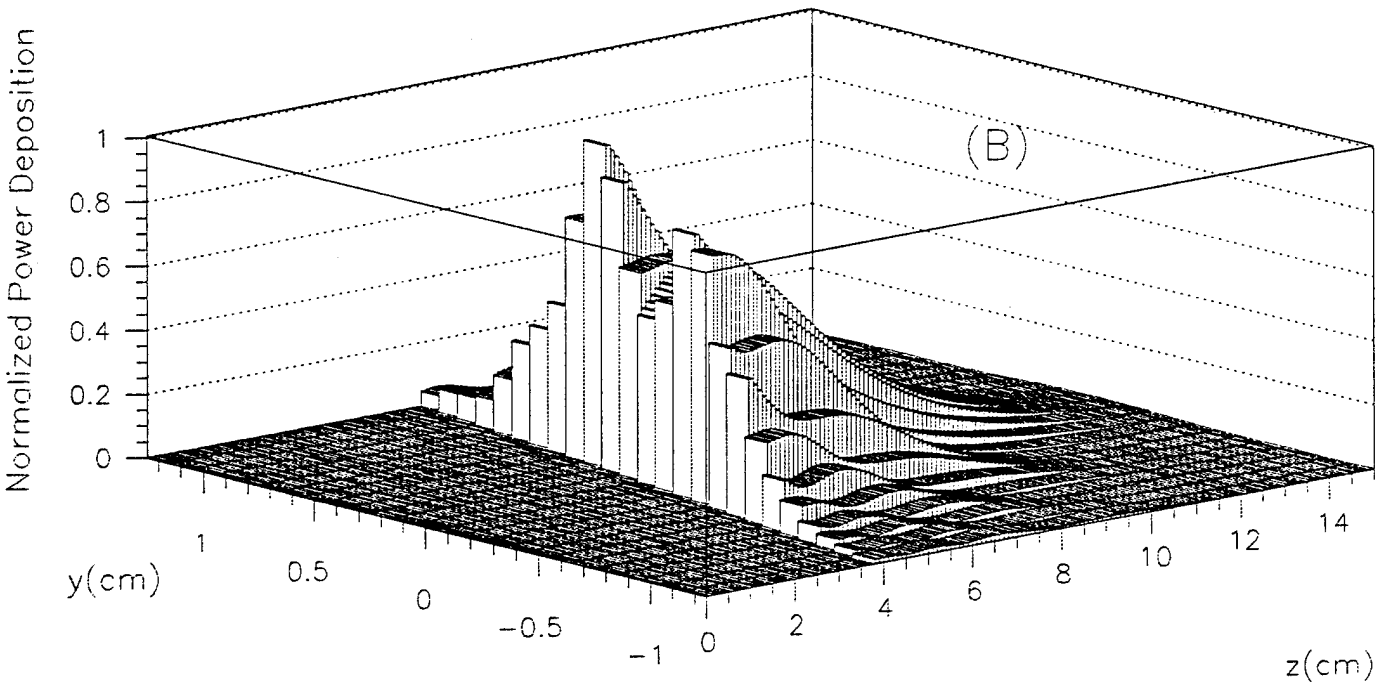
(B)
Normalized Power Deposition
1
0.8
0.6
0.4
0.2
0
y(cm)
1
0.5
0
-0.5
-1
0
2
4
6
8
10
12
14
z(cm)

Figure-6

Appendix C

Efficiency Data for each Transducer in the Cylindrical Array

Transducer#	Col	#	Rng	#	Freq in MHz	Measured Acoustic Watts at D/A V = 2.37	Calculated Acoustic Watts at D/A V = 5.00	Calculated D/A Voltage at 0.5 Watts	Calculated D/A Voltage at 4.5 Watts
4-230A	C	2	R	1	4.80	2.64	11.75	1.03	3.09
4-214	C	2	R	2	4.82	2.84	12.64	0.99	2.98
4-217	C	2	R	3	4.81	2.88	12.82	0.99	2.96
4-237B	C	2	R	4	4.78	1.98	8.81	1.19	3.57
4-188	C	4	R	1	4.49	1.90	8.46	1.22	3.65
4-154	C	4	R	2	4.49	1.52	6.77	1.36	4.08
4-144	C	4	R	3	4.49	1.42	6.32	1.41	4.22
4-163	C	4	R	4	4.50	1.18	5.25	1.54	4.63
4-265	C	6	R	1	4.71	1.58	7.03	1.33	4.00
4-272	C	6	R	2	4.71	1.58	7.03	1.33	4.00
4-277	C	6	R	3	4.68	1.54	6.85	1.35	4.05
4-273	C	6	R	4	4.68	1.48	6.59	1.38	4.13
4-232B	C	8	R	1	4.73	2.02	8.99	1.18	3.54
4-230B	C	8	R	2	4.71	1.92	8.55	1.21	3.63
4-234A	C	8	R	3	4.70	1.94	8.63	1.20	3.61
4-216	C	8	R	4	4.69	1.98	8.81	1.19	3.57
4-210	C	10	R	1	4.67	2.16	9.61	1.14	3.42
4-221	C	10	R	2	4.67	1.76	7.83	1.26	3.79
4-249	C	10	R	3	4.66	2.00	8.90	1.19	3.56
4-242	C	10	R	4	4.67	1.56	6.94	1.34	4.03
4-281	C	12	R	1	4.67	1.80	8.01	1.25	3.75
4-271	C	12	R	2	4.68	1.50	6.68	1.37	4.10
4-262	C	12	R	3	4.67	1.62	7.21	1.32	3.95
4-267	C	12	R	4	4.66	1.58	7.03	1.33	4.00
4-218	C	14	R	1	4.62	2.06	9.17	1.17	3.50
4-240A	C	14	R	2	4.65	1.58	7.03	1.33	4.00
4-241A	C	14	R	3	4.63	1.58	7.03	1.33	4.00
4-229	C	14	R	4	4.61	1.60	7.12	1.32	3.97
4-225	C	16	R	1	4.61	1.62	7.21	1.32	3.95
4-238A	C	16	R	2	4.61	1.54	6.85	1.35	4.05
4-235A	C	16	R	3	4.61	1.54	6.85	1.35	4.05
4-241B	C	16	R	4	4.62	1.40	6.23	1.42	4.25
4-278	C	18	R	1	4.65	1.60	7.12	1.32	3.97
4-280	C	18	R	2	4.61	1.58	7.03	1.33	4.00
4-279	C	18	R	3	4.62	1.38	6.14	1.43	4.28
4-239B	C	18	R	4	4.61	1.60	7.12	1.32	3.97
4-130	C	20	R	1	4.60	1.68	7.48	1.29	3.88
4-234B	C	20	R	2	4.60	1.56	6.94	1.34	4.03
4-246	C	20	R	3	4.60	1.48	6.59	1.38	4.13
4-236A	C	20	R	4	4.60	1.52	6.77	1.36	4.08
4-211	C	22	R	1	4.58	1.64	7.30	1.31	3.93
4-212	C	22	R	2	4.58	1.56	6.94	1.34	4.03
4-137	C	22	R	3	4.59	1.50	6.68	1.37	4.10
4-231B	C	22	R	4	4.59	1.52	6.77	1.36	4.08
4-233B	C	24	R	1	4.58	1.66	7.39	1.30	3.90
4-223	C	24	R	2	4.58	1.54	6.85	1.35	4.05
4-245	C	24	R	3	4.58	1.52	6.77	1.36	4.08
4-233A	C	24	R	4	4.58	1.46	6.50	1.39	4.16

4-232A	C	26	R	1	4.57	1.62	7.21	1.32	3.95
4-140	C	26	R	2	4.57	1.54	6.85	1.35	4.05
4-243	C	26	R	3	4.57	1.54	6.85	1.35	4.05
4-239A	C	26	R	4	4.58	1.42	6.32	1.41	4.22
4-219	C	28	R	1	4.55	1.54	6.85	1.35	4.05
4-224	C	28	R	2	4.55	1.48	6.59	1.38	4.13
4-187	C	28	R	3	4.57	1.54	6.85	1.35	4.05
4-248	C	28	R	4	4.57	1.50	6.68	1.37	4.10
4-264	C	30	R	1	4.57	1.58	7.03	1.33	4.00
4-189	C	30	R	2	4.55	1.66	7.39	1.30	3.90
4-128	C	30	R	3	4.57	1.18	5.25	1.54	4.63
4-101A	C	30	R	4	4.55	1.40	6.23	1.42	4.25
4-208	C	32	R	1	4.53	1.58	7.03	1.33	4.00
4-102A	C	32	R	2	4.55	1.42	6.32	1.41	4.22
4-133	C	32	R	3	4.55	1.42	6.32	1.41	4.22
4-157	C	32	R	4	4.52	1.48	6.59	1.38	4.13
4-237A	C	34	R	1	4.55	1.54	6.85	1.35	4.05
4-153	C	34	R	2	4.55	1.52	6.77	1.36	4.08
4-213	C	34	R	3	4.55	1.46	6.50	1.39	4.16
4-134	C	34	R	4	4.54	1.42	6.32	1.41	4.22
4-186	C	36	R	1	4.54	1.58	7.03	1.33	4.00
4-174	C	36	R	2	4.53	1.44	6.41	1.40	4.19
4-138	C	36	R	3	4.55	1.40	6.23	1.42	4.25
4-177	C	36	R	4	4.55	1.36	6.05	1.44	4.31
4-197	C	38	R	1	4.53	1.54	6.85	1.35	4.05
4-103A	C	38	R	2	4.53	1.42	6.32	1.41	4.22
4-169	C	38	R	3	4.53	1.28	5.70	1.48	4.44
4-159	C	38	R	4	4.52	1.46	6.50	1.39	4.16
4-171	C	40	R	1	4.52	1.66	7.39	1.30	3.90
4-204	C	40	R	2	4.52	1.52	6.77	1.36	4.08
4-205	C	40	R	3	4.52	1.58	7.03	1.33	4.00
4-114A	C	40	R	4	4.52	1.30	5.79	1.47	4.41
4-145	C	42	R	1	4.55	1.44	6.41	1.40	4.19
4-146	C	42	R	2	4.53	1.44	6.41	1.40	4.19
4-129	C	42	R	3	4.52	1.44	6.41	1.40	4.19
4-135	C	42	R	4	4.52	1.34	5.96	1.45	4.34
4-166	C	44	R	1	4.51	1.52	6.77	1.36	4.08
4-165	C	44	R	2	4.52	1.50	6.68	1.37	4.10
4-193	C	44	R	3	4.51	1.44	6.41	1.40	4.19
4-207	C	44	R	4	4.51	1.30	5.79	1.47	4.41
4-143	C	46	R	1	4.50	1.58	7.03	1.33	4.00
4-173	C	46	R	2	4.50	1.52	6.77	1.36	4.08
4-180	C	46	R	3	4.50	1.46	6.50	1.39	4.16
4-160	C	46	R	4	4.49	1.42	6.32	1.41	4.22
4-274	C	48	R	1	4.77	2.26	10.06	1.11	3.34
4-275	C	48	R	2	4.73	2.24	9.97	1.12	3.36
4-263	C	48	R	3	4.74	1.88	8.37	1.22	3.67
4-266	C	48	R	4	4.77	1.88	8.37	1.22	3.67
4-181	C	2	R	5	4.48	1.52	6.77	1.36	4.08
4-183	C	2	R	6	4.48	1.52	6.77	1.36	4.08
	C	2	R	7					
	C	2	R	8					

4-231A	C	4	R	5	4.49	1.24	5.52	1.50	4.51
4-199	C	4	R	6	4.49	1.36	6.05	1.44	4.31
	C	4	R	7					
	C	4	R	8					
4-184	C	6	R	5	4.50	1.38	6.14	1.43	4.28
4-132	C	6	R	6	4.49	1.08	4.81	1.61	4.84
	C	6	R	7					
	C	6	R	8					
4-215	C	8	R	5	4.47	1.38	6.14	1.43	4.28
4-203	C	8	R	6	4.48	1.46	6.50	1.39	4.16
	C	8	R	7					
	C	8	R	8					
4-227	C	10	R	5	4.47	1.40	6.23	1.42	4.25
4-235B	C	10	R	6	4.47	1.28	5.70	1.48	4.44
	C	10	R	7					
	C	10	R	8					
4-116A	C	12	R	5	4.45	1.50	6.68	1.37	4.10
4-141	C	12	R	6	4.46	1.32	5.88	1.46	4.38
	C	12	R	7					
	C	12	R	8					
4-201	C	14	R	5	4.45	1.50	6.68	1.37	4.10
4-162	C	14	R	6	4.49	1.16	5.16	1.56	4.67
	C	14	R	7					
	C	14	R	8					
4-228	C	16	R	5	4.45	1.28	5.70	1.48	4.44
4-182	C	16	R	6	4.44	1.24	5.52	1.50	4.51
	C	16	R	7					
	C	16	R	8					
4-155	C	18	R	5	4.43	1.36	6.05	1.44	4.31
4-131	C	18	R	6	4.43	1.24	5.52	1.50	4.51
	C	18	R	7					
	C	18	R	8					
4-238B	C	20	R	5	4.44	1.40	6.23	1.42	4.25
4-198	C	20	R	6	4.41	1.32	5.88	1.46	4.38
	C	20	R	7					
	C	20	R	8					
4-142	C	22	R	5	4.42	1.36	6.05	1.44	4.31
4-206	C	22	R	6	4.42	1.30	5.79	1.47	4.41
	C	22	R	7					
	C	22	R	8					
4-172	C	24	R	5	4.43	1.32	5.88	1.46	4.38
4-152	C	24	R	6	4.42	1.28	5.70	1.48	4.44
	C	24	R	7					
	C	24	R	8					
4-222	C	26	R	5	4.48	1.34	5.96	1.45	4.34
4-175	C	26	R	6	4.49	1.22	5.43	1.52	4.55
	C	26	R	7					
	C	26	R	8					
4-149	C	28	R	5	4.48	1.48	6.59	1.38	4.13
4-164	C	28	R	6	4.49	1.28	5.70	1.48	4.44
	C	28	R	7					
	C	28	R	8					

4-176	C	30	R	5	4.48	1.34	5.96	1.45	4.34
4-136	C	30	R	6	4.47	1.20	5.34	1.53	4.59
	C	30	R	7					
	C	30	R	8					
4-158	C	32	R	5	4.47	1.18	5.25	1.54	4.63
4-194	C	32	R	6	4.45	1.22	5.43	1.52	4.55
	C	32	R	7					
	C	32	R	8					
4-200	C	34	R	5	4.46	1.30	5.79	1.47	4.41
4-151	C	34	R	6	4.46	1.16	5.16	1.56	4.67
	C	34	R	7					
	C	34	R	8					
4-269	C	36	R	5	4.47	1.26	5.61	1.49	4.48
4-185	C	36	R	6	4.45	1.26	5.61	1.49	4.48
	C	36	R	7					
	C	36	R	8					
4-202	C	38	R	5	4.45	1.22	5.43	1.52	4.55
4-209	C	38	R	6	4.44	1.24	5.52	1.50	4.51
	C	38	R	7					
	C	38	R	8					
4-195	C	40	R	5	4.43	1.24	5.52	1.50	4.51
4-148	C	40	R	6	4.43	1.16	5.16	1.56	4.67
	C	40	R	7					
	C	40	R	8					
4-276	C	42	R	5	4.45	1.30	5.79	1.47	4.41
4-191	C	42	R	6	4.44	1.22	5.43	1.52	4.55
	C	42	R	7					
	C	42	R	8					
4-156	C	44	R	5	4.42	1.26	5.61	1.49	4.48
4-220	C	44	R	6	4.43	1.22	5.43	1.52	4.55
	C	44	R	7					
	C	44	R	8					
4-178	C	46	R	5	4.40	1.28	5.70	1.48	4.44
4-167	C	46	R	6	4.41	1.20	5.34	1.53	4.59
	C	46	R	7					
	C	46	R	8					
4-179	C	48	R	5	4.38	1.30	5.79	1.47	4.41
4-192	C	48	R	6	4.33	1.30	5.79	1.47	4.41
	C	48	R	7					
	C	48	R	8					

Total No. Tested 144		Freq in MHz	Measured Acoustic Watts at D/A V = 2.37	Calculated Acoustic Watts at D/A V = 5.00	Calculated D/A Voltage at 0.5 Watts	Calculated D/A Voltage at 4.75 Watts
	AVE	4.55	1.51	6.72	1.38	4.14
	MIN	4.33	1.08	4.81	0.99	2.96
	MAX	4.82	2.88	12.82	1.61	4.84

Transducer#	Most Efficient Frequency, in MHz	Ultrasound Power, Watts	DC Watts	DC to Ultrasound Efficiency,%	Transducer Efficiency, %
4-011	4.45	1.36	4.65	29.23	49.40
4-101A	4.55	1.40	4.60	30.42	51.41
4-102A	4.55	1.42	4.69	30.28	51.17
4-103A	4.53	1.42	4.69	30.29	51.19
4-114A	4.52	1.30	4.56	28.54	48.23
4-116A	4.45	1.50	4.74	31.62	53.44
4-128	4.57	1.18	4.18	28.22	47.69
4-129	4.52	1.44	4.74	30.36	51.31
4-130	4.60	1.68	5.01	33.51	56.63
4-131	4.43	1.24	4.09	30.32	51.24
4-132	4.53	1.16	4.26	27.22	46.00
4-133	4.55	1.42	4.75	29.92	50.56
4-134	4.54	1.42	4.65	30.54	51.61
4-135	4.52	1.34	4.63	28.97	48.96
4-136	4.47	1.20	4.14	28.96	48.94
4-137	4.59	1.50	4.67	32.11	54.27
4-138	4.55	1.40	4.65	30.12	50.90
4-140	4.57	1.54	4.80	32.06	54.18
4-141	4.46	1.32	4.26	30.99	52.37
4-142	4.42	1.36	4.26	31.91	53.93
4-143	4.50	1.58	4.80	32.89	55.58
4-144	4.49	1.42	4.65	30.53	51.60
4-145	4.55	1.44	4.75	30.31	51.22
4-146	4.53	1.44	4.77	30.21	51.05
4-147	4.49	1.26	4.22	29.84	50.43
4-148	4.43	1.16	4.08	28.41	48.01
4-149	4.48	1.48	4.64	31.89	53.89
4-151	4.46	1.16	4.00	29.03	49.06
4-152	4.42	1.28	4.17	30.66	51.82
4-153	4.55	1.52	4.91	30.93	52.27
4-154	4.49	1.52	5.05	30.10	50.87
4-155	4.43	1.36	4.40	30.89	52.20
4-156	4.42	1.26	4.28	29.45	49.77
4-157	4.52	1.48	5.06	29.26	49.45
4-158	4.47	1.18	4.06	29.03	49.06
4-159	4.52	1.46	4.85	30.09	50.85
4-160	4.49	1.42	4.71	30.18	51.00
4-162	4.49	1.16	4.01	28.96	48.94
4-163	4.50	1.18	4.22	27.96	47.25
4-164	4.49	1.28	4.69	27.32	46.17
4-165	4.52	1.50	4.96	30.24	51.11
4-166	4.51	1.52	4.84	31.41	53.08
4-167	4.41	1.20	3.98	30.14	50.94

4-169	4.49	1.20	4.20	28.58	48.30
4-171	4.52	1.66	4.89	33.98	57.43
4-172	4.43	1.32	4.31	30.60	51.71
4-173	4.50	1.52	5.32	28.56	48.27
4-174	4.53	1.44	4.62	31.15	52.64
4-175	4.49	1.22	4.43	27.56	46.58
4-176	4.48	1.34	4.44	30.21	51.05
4-177	4.55	1.36	4.70	28.96	48.94
4-178	4.40	1.28	4.17	30.71	51.90
4-179	4.38	1.30	4.31	30.18	51.00
4-180	4.50	1.46	4.86	30.06	50.80
4-181	4.48	1.52	4.86	31.28	52.86
4-182	4.44	1.24	4.17	29.75	50.28
4-183	4.48	1.52	4.69	32.38	54.72
4-184	4.50	1.38	4.47	30.84	52.12
4-185	4.45	1.26	4.18	30.15	50.95
4-186	4.54	1.58	5.02	31.47	53.18
4-187	4.57	1.54	4.99	30.84	52.12
4-188	4.49	1.90	5.23	36.34	61.41
4-189	4.55	1.66	5.06	32.80	55.43
4-191	4.44	1.22	4.15	29.37	49.64
4-192	4.33	1.30	4.74	27.42	46.34
4-193	4.51	1.44	4.78	30.14	50.94
4-194	4.45	1.22	4.14	29.45	49.77
4-195	4.43	1.24	4.01	30.94	52.29
4-197	4.53	1.54	5.26	29.29	49.50
4-198	4.41	1.32	4.35	30.35	51.29
4-199	4.49	1.36	4.98	27.30	46.14
4-200	4.46	1.30	4.37	29.78	50.33
4-201	4.45	1.50	4.87	30.82	52.09
4-202	4.45	1.22	4.13	29.55	49.94
4-203	4.48	1.46	4.74	30.77	52.00
4-204	4.52	1.52	4.84	31.41	53.08
4-205	4.52	1.58	4.83	32.74	55.33
4-206	4.42	1.30	4.30	30.23	51.09
4-207	4.51	1.30	4.42	29.42	49.72
4-208	4.53	1.58	4.92	32.13	54.30
4-209	4.44	1.24	4.62	26.83	45.34
4-210	4.67	2.16	5.66	38.19	64.54
4-211	4.58	1.64	4.86	33.76	57.05
4-212	4.58	1.56	4.92	31.69	53.56
4-213	4.55	1.46	4.81	30.38	51.34
4-214	4.82	2.84	6.65	42.71	72.18
4-215	4.47	1.38	4.39	31.43	53.12
4-216	4.69	1.98	6.51	30.43	51.43

4-217	4.81	2.88	6.78	42.48	71.79
4-218	4.62	2.06	4.73	43.56	73.62
4-219	4.55	1.54	4.78	32.20	54.42
4-220	4.43	1.22	4.35	28.06	47.42
4-221	4.67	1.76	4.95	35.53	60.05
4-222	4.48	1.34	4.20	31.89	53.89
4-223	4.58	1.54	4.75	32.43	54.81
4-224	4.55	1.48	4.66	31.78	53.71
4-225	4.61	1.62	4.99	32.44	54.82
4-227	4.47	1.40	4.63	30.23	51.09
4-228	4.45	1.28	4.28	29.89	50.51
4-229	4.61	1.60	4.89	32.69	55.25
4-230A	4.80	2.64	6.01	43.95	74.28
4-230B	4.71	1.92	5.81	33.06	55.87
4-231A	4.49	1.24	4.30	28.84	48.74
4-231B	4.59	1.52	4.93	30.86	52.15
4-232A	4.57	1.62	5.01	32.35	54.67
4-232B	4.73	2.02	5.89	34.28	57.93
4-233A	4.58	1.46	4.82	30.31	51.22
4-233B	4.58	1.66	4.99	33.25	56.19
4-234A	4.70	1.94	5.90	32.90	55.60
4-234B	4.60	1.56	4.91	31.79	53.73
4-235A	4.61	1.54	4.79	32.15	54.33
4-235B	4.47	1.28	4.30	29.75	50.28
4-236A	4.60	1.52	4.98	30.50	51.55
4-237A	4.55	1.54	4.97	30.98	52.36
4-237B	4.78	1.98	5.81	34.10	57.63
4-238A	4.61	1.54	4.86	31.67	53.52
4-238B	4.44	1.40	4.61	30.37	51.33
4-239A	4.58	1.42	5.00	28.38	47.96
4-239B	4.61	1.60	5.17	30.97	52.34
4-240A	4.65	1.58	5.00	31.62	53.44
4-241A	4.63	1.58	4.83	32.74	55.33
4-241B	4.62	1.40	4.89	28.63	48.38
4-242	4.67	1.56	4.98	31.31	52.91
4-243	4.57	1.54	4.85	31.73	53.62
4-245	4.58	1.52	4.68	32.49	54.91
4-246	4.60	1.48	4.73	31.32	52.93
4-248	4.57	1.50	4.92	30.46	51.48
4-249	4.66	2.00	5.62	35.57	60.11
4-262	4.67	1.62	5.43	29.81	50.38
4-263	4.74	1.88	5.47	34.38	58.10
4-264	4.57	1.58	4.99	31.68	53.54
4-265	4.71	1.58	4.99	31.64	53.47
4-266	4.77	1.88	5.77	32.59	55.08

4-267	4.66	1.58	5.10	30.96	52.32
4-269	4.47	1.26	4.43	28.42	48.03
4-271	4.68	1.50	4.89	30.65	51.80
4-272	4.71	1.58	5.05	31.28	52.86
4-273	4.68	1.48	4.70	31.50	53.24
4-274	4.77	2.26	5.57	40.59	68.60
4-275	4.73	2.24	5.82	38.50	65.07
4-276	4.45	1.30	4.80	27.10	45.80
4-277	4.68	1.54	4.68	32.94	55.67
4-278	4.65	1.60	4.94	32.42	54.79
4-279	4.62	1.38	4.46	30.94	52.29
4-280	4.61	1.58	4.94	31.98	54.05
4-281	4.67	1.80	5.41	33.30	56.28

Transducer#	Frequency,in MH Most Efficient	Power, Watts Ultrasound	DC Watts	Efficiency,% DC to Ultrasound	Transducer Efficiency,%
Average	4.5469	1.51	4.79	31.29	52.88
SD	0.10	0.29	0.51	2.90	4.90
# Of Samples	146.00				
Max Value	4.82	2.88	6.78	43.95	74.28
Min Value	4.33	1.16	3.98	26.83	45.34

Bad Xducr Serial #	Most Efficient Frequency, in MHz	Ultrasound Power, Watts	DC Watts	DC to Ultrasound Efficiency, %	Transducer Efficiency, %
4-003	missing wire		#DIV/0!		0.00
4-010	no polarity 4.45	1.22	4.31	28.31	47.84
4-012	missing wire		#DIV/0!		0.00
4-150	4.34	1.24	5.11	24.27	41.02
4-161	4.53	1.42	5.35	26.55	44.87
4-168	4.60	3.08	5.43	56.71	95.84
4-170	4.56	34.70	4.92	705.89	1192.95
4-190	no polarity 4.52	1.54	4.92	31.30	52.90
4-196	4.35	1.20	4.80	24.99	42.23
4-226	4.41	1.26	4.84	26.02	43.97
4-236B	4.50	1.28	4.82	26.53	44.84
4-240B	4.34	1.36	5.26	25.84	43.67
4-244	4.48	1.32	5.02	26.32	44.48
4-247	4.36	1.28	4.93	25.96	43.87
4-268	4.57	1.28	5.05	25.33	42.81
4-270	4.50	1.14	4.77	23.92	40.42

12 pairs of transducers with identical serial numbers.

*2 - defective (wedge) surface: note #4-170 & #4-168 transducer.

4 - with one serial number written on top of a different serial number: Ex:

Transducer #	Col	#	Rng	#	Freq in MHz	Measured Acoustic Watts at D/A V = 2.37	Calculated Acoustic Watts at D/A V = 5.00	Calculated D/A Voltage at 0.5 Watts	Calculated D/A Voltage at 8 Watts
2.5-176	C	1	R	5	2.51	2.38	10.59	1.09	4.35
2.5-140	C	1	R	6	2.56	2.02	8.99	1.18	4.72
2.5-115	C	1	R	7	2.53	2.22	9.88	1.12	4.50
2.5-109	C	1	R	8	2.47	2.62	11.66	1.04	4.14
2.5-120	C	3	R	5	2.55	2.06	9.17	1.17	4.67
2.5-168	C	3	R	6	2.52	2.12	9.44	1.15	4.60
2.5-133	C	3	R	7	2.56	2.14	9.52	1.15	4.58
2.5-177	C	3	R	8	2.50	2.18	9.70	1.14	4.54
2.5-157	C	5	R	5	2.56	2.12	9.44	1.15	4.60
2.5-107	C	5	R	6	2.54	2.14	9.52	1.15	4.58
2.5-161	C	5	R	7	2.51	2.08	9.26	1.16	4.65
2.5-164	C	5	R	8	2.44	2.52	11.22	1.06	4.22
2.5-155	C	7	R	5	2.55	2.04	9.08	1.17	4.69
2.5-153	C	7	R	6	2.53	2.08	9.26	1.16	4.65
2.5-121	C	7	R	7	2.50	2.22	9.88	1.12	4.50
2.5-169	C	7	R	8	2.50	2.10	9.35	1.16	4.63
2.5-106	C	9	R	5	2.53	2.12	9.44	1.15	4.60
2.5-167	C	9	R	6	2.52	2.26	10.06	1.11	4.46
2.5-149	C	9	R	7	2.52	2.06	9.17	1.17	4.67
2.5-147	C	9	R	8	2.51	2.08	9.26	1.16	4.65
2.5-143	C	11	R	5	2.57	1.96	8.72	1.20	4.79
2.5-139	C	11	R	6	2.54	2.06	9.17	1.17	4.67
2.5-125	C	11	R	7	2.54	2.06	9.17	1.17	4.67
2.5-162	C	11	R	8	2.49	2.26	10.06	1.11	4.46
2.5-142	C	13	R	5	2.58	2.02	8.99	1.18	4.72
2.5-111	C	13	R	6	2.54	2.14	9.52	1.15	4.58
2.5-148	C	13	R	7	2.51	2.08	9.26	1.16	4.65
2.5-178	C	13	R	8	2.48	2.18	9.70	1.14	4.54
2.5-112	C	15	R	5	2.55	2.00	8.90	1.19	4.74
2.5-175	C	15	R	6	2.46	2.16	9.61	1.14	4.56
2.5-104	C	15	R	7	2.57	1.94	8.63	1.20	4.81
2.5-136	C	15	R	8	2.51	2.18	9.70	1.14	4.54
2.5-117	C	17	R	5	2.57	1.90	8.46	1.22	4.86
2.5-150	C	17	R	6	2.56	2.06	9.17	1.17	4.67
2.5-123	C	17	R	7	2.54	2.06	9.17	1.17	4.67
2.5-101	C	17	R	8	2.50	2.02	8.99	1.18	4.72
2.5-152	C	19	R	5	2.57	1.90	8.46	1.22	4.86
2.5-132	C	19	R	6	2.53	2.06	9.17	1.17	4.67
2.5-124	C	19	R	7	2.52	2.08	9.26	1.16	4.65
2.5-141	C	19	R	8	2.47	2.16	9.61	1.14	4.56
2.5-131	C	21	R	5	2.53	2.08	9.26	1.16	4.65
2.5-171	C	21	R	6	2.52	2.28	10.15	1.11	4.44
2.5-151	C	21	R	7	2.51	2.24	9.97	1.12	4.48
2.5-166	C	21	R	8	2.42	2.78	12.37	1.01	4.02
2.5-116	C	23	R	5	2.57	1.82	8.10	1.24	4.97
2.5-135	C	23	R	6	2.55	2.08	9.26	1.16	4.65
2.5-108	C	23	R	7	2.54	1.96	8.72	1.20	4.79
2.5-102	C	23	R	8	2.52	2.02	8.99	1.18	4.72
2.5-160	C	25	R	5	2.57	1.84	8.19	1.24	4.94
2.5-113	C	25	R	6	2.57	1.98	8.81	1.19	4.76
	C	25	R	7					
	C	25	R	8					

2.5-154	C	27	R	5	2.56	2.06	9.17	1.17	4.67
2.5-138	C	27	R	6	2.55	2.06	9.17	1.17	4.67
	C	27	R	7					
	C	27	R	8					
2.5-144	C	29	R	5	2.53	1.94	8.63	1.20	4.81
2.5-129	C	29	R	6	2.53	1.98	8.81	1.19	4.76
	C	29	R	7					
	C	29	R	8					
2.5-110	C	31	R	5	2.54	2.14	9.52	1.15	4.58
2.5-134	C	31	R	6	2.54	2.02	8.99	1.18	4.72
	C	31	R	7					
	C	31	R	8					
2.5-103	C	33	R	5	2.51	2.00	8.90	1.19	4.74
2.5-146	C	33	R	6	2.51	2.26	10.06	1.11	4.46
	C	33	R	7					
	C	33	R	8					
2.5-122	C	35	R	5	2.48	2.26	10.06	1.11	4.46
2.5-158	C	35	R	6	2.48	2.50	11.13	1.06	4.24
	C	35	R	7					
	C	35	R	8					
2.5-174	C	37	R	5	2.51	2.02	8.99	1.18	4.72
2.5-163	C	37	R	6	2.50	2.30	10.24	1.11	4.42
	C	37	R	7					
	C	37	R	8					
2.5-145	C	39	R	5	2.51	2.06	9.17	1.17	4.67
2.5-173	C	39	R	6	2.50	1.98	8.81	1.19	4.76
	C	39	R	7					
	C	39	R	8					
2.5-118	C	41	R	5	2.50	2.22	9.88	1.12	4.50
2.5-159	C	41	R	6	2.49	2.38	10.59	1.09	4.35
	C	41	R	7					
	C	41	R	8					
2.5-170	C	43	R	5	2.47	2.60	11.57	1.04	4.16
2.5-172	C	43	R	6	2.48	2.42	10.77	1.08	4.31
	C	43	R	7					
	C	43	R	8					
2.5-105	C	45	R	5	2.48	2.42	10.77	1.08	4.31
2.5-156	C	45	R	6	2.48	2.42	10.77	1.08	4.31
	C	45	R	7					
	C	45	R	8					
2.5-130	C	47	R	5	2.48	2.18	9.70	1.14	4.54
2.5-119	C	47	R	6	2.48	2.34	10.41	1.10	4.38
	C	47	R	7					
	C	47	R	8					

Total No. Tested	72	Freq in MHz	Measured Acoustic Watts at D/A V = 2.37	Calculated Acoustic Watts at D/A V = 5.00	Calculated D/A Voltage at 0.5 Watts	Calculated D/A Voltage at 8 Watts
	AVE	2.52	2.15	9.55	1.15	4.59
	MIN	2.42	1.82	8.10	1.01	4.02
	MAX	2.58	2.78	12.37	1.24	4.97

Transducer #	Min. Refl. Pwr. Frequency, in MHz	Ultrasound Power, Watts	DC Watts	DC to Ultrasound Efficiency, %	Transducer Efficiency, %
2.5-101	2.50	2.02	4.38	46.11	70.65
2.5-102	2.52	2.02	4.41	45.76	70.11
2.5-103	2.51	2.00	4.42	45.24	69.32
2.5-104	2.57	1.94	4.19	46.27	70.89
2.5-105	2.48	2.42	5.73	42.23	64.70
2.5-106	2.53	2.12	4.47	47.45	72.70
2.5-107	2.54	2.14	4.47	47.88	73.36
2.5-108	2.54	1.96	4.29	45.67	69.97
2.5-109	2.47	2.62	5.40	48.52	74.34
2.5-110	2.54	2.14	4.72	45.32	69.44
2.5-111	2.54	2.14	4.57	46.81	71.72
2.5-112	2.55	2.00	4.29	46.67	71.51
2.5-113	2.57	1.98	4.44	44.63	68.38
2.5-115	2.53	2.22	4.56	48.66	74.56
2.5-116	2.57	1.82	4.00	45.46	69.65
2.5-117	2.57	1.90	4.12	46.17	70.74
2.5-118	2.50	2.22	4.97	44.71	68.50
2.5-119	2.48	2.34	5.67	41.27	63.23
2.5-120	2.55	2.06	4.27	48.26	73.94
2.5-121	2.50	2.22	4.66	47.62	72.96
2.5-122	2.48	2.26	5.07	44.57	68.29
2.5-123	2.54	2.06	4.45	46.25	70.86
2.5-124	2.52	2.08	4.52	46.06	70.57
2.5-125	2.54	2.06	4.39	46.91	71.87
2.5-129	2.53	1.98	4.46	44.44	68.09
2.5-130	2.48	2.18	5.16	42.26	64.75
2.5-131	2.53	2.08	4.52	45.98	70.45
2.5-132	2.53	2.06	4.48	46.03	70.53
2.5-133	2.56	2.14	4.45	48.12	73.73
2.5-134	2.54	2.02	4.63	43.65	66.88
2.5-135	2.55	2.08	4.56	45.65	69.94
2.5-136	2.51	2.18	4.70	46.37	71.05
2.5-138	2.55	2.06	4.57	45.08	69.07
2.5-139	2.54	2.06	4.39	46.97	71.97
2.5-140	2.56	2.02	4.18	48.32	74.03
2.5-141	2.47	2.16	4.69	46.06	70.57
2.5-142	2.58	2.02	4.33	46.70	71.55
2.5-143	2.57	1.96	4.18	46.87	71.81
2.5-144	2.53	1.94	4.31	45.06	69.04
2.5-145	2.51	2.06	4.56	45.18	69.22
2.5-146	2.51	2.26	5.43	41.62	63.77
2.5-147	2.51	2.08	4.39	47.41	72.64
2.5-148	2.51	2.08	4.44	46.80	71.71
2.5-149	2.52	2.06	4.36	47.27	72.43
2.5-150	2.56	2.06	4.46	46.16	70.72
2.5-151	2.51	2.24	4.87	46.00	70.48

2.5-152	2.57	1.90	4.13	46.06	70.57
2.5-153	2.53	2.08	4.35	47.78	73.21
2.5-154	2.56	2.06	4.55	45.25	69.33
2.5-155	2.55	2.04	4.28	47.64	72.99
2.5-156	2.48	2.42	5.93	40.83	62.56
2.5-157	2.56	2.12	4.42	47.91	73.41
2.5-158	2.48	2.50	5.98	41.79	64.03
2.5-159	2.49	2.38	5.77	41.26	63.22
2.5-160	2.57	1.84	4.06	45.28	69.38
2.5-161	2.51	2.08	4.35	47.87	73.34
2.5-162	2.49	2.26	4.80	47.10	72.17
2.5-163	2.50	2.30	5.16	44.61	68.35
2.5-164	2.44	2.52	5.26	47.95	73.47
2.5-166	2.42	2.78	6.07	45.83	70.22
2.5-167	2.52	2.26	4.76	47.45	72.70
2.5-168	2.52	2.12	4.40	48.14	73.76
2.5-169	2.50	2.10	4.40	47.72	73.12
2.5-170	2.47	2.60	5.99	43.39	66.48
2.5-171	2.52	2.28	4.97	45.87	70.28
2.5-172	2.48	2.42	5.83	41.50	63.58
2.5-173	2.50	1.98	4.42	44.76	68.58
2.5-174	2.51	2.02	4.44	45.45	69.64
2.5-175	2.46	2.16	4.64	46.54	71.31
2.5-176	2.51	2.38	4.70	50.67	77.63
2.5-177	2.50	2.18	4.55	47.95	73.47
2.5-178	2.48	2.18	4.66	46.82	71.74

Transducer #	Frequency, in MHz Most Efficient	Power, Watts Ultrasound	DC Watts	Efficiency, % DC to Ultrasound	Efficiency, % Transducer
Average	2.5197	2.15	4.6865	45.92	70.35
SD	0.03	0.18	0.51	2.00	3.07
# of samples	73.00				
Max Value	2.58	2.78	6.07	50.67	77.63
Min Value	2.42	1.82	4.00	40.83	62.56

Bad Xducr Serial #	Most Efficient Frequency, in MHz	Ultrasound Power, Watts	DC Watts	DC to Ultrasound Efficiency, %	Transducer Efficiency, %
2.5-114	2.52	1.78	4.49	39.67	60.78
2.5-126	2.48	2.24	5.62	39.86	61.07
2.5-127	2.49	2.20	5.79	37.97	58.18
2.5-128	2.48	2.40	6.08	39.46	60.46
2.5-137	2.47	2.58	6.44	40.09	61.42
2.5-165	no polarity 2.5	2.22	4.60	48.25	73.93

	Trans #	Most Efficient Frequency, in MHz	Ultrasound Watts	DC Watts	DC to Ultrasound Efficiency, %	Transducer Efficiency, %
1	*2-001*	2.09	2.46	4.83	50.98	84.97
2	*2-002*	2.10	2.58	5.08	50.74	84.57
3	*2-008*	2.08	2.40	4.67	51.41	85.68
4	*2-015*	2.08	2.50	4.91	50.89	84.82
5	*2-116*	2.12	2.62	5.44	48.20	80.33
6	*2-120*	2.10	2.68	5.28	50.73	84.55
7	*2-121*	2.13	2.18	4.38	49.72	82.87
8	*2-122*	2.09	2.34	4.63	50.53	84.22
9	*2-123*	2.08	2.86	5.64	50.69	84.48
10	*2-124*	2.09	2.62	5.32	49.23	82.05
11	*2-125*	2.07	2.70	5.91	45.71	76.18
12	*2-126*	2.15	2.56	5.53	46.27	77.12
13	*2-127*	2.09	2.68	5.22	51.33	85.55
14	*2-128*	2.08	2.82	5.51	51.14	85.23
15	*2-129*	2.09	2.58	5.19	49.74	82.90
16	*2-130*	2.12	2.44	4.78	51.03	85.05
17	*2-131*	2.16	2.34	4.85	48.21	80.35
18	*2-133*	2.11	2.54	4.93	51.49	85.82
19	*2-134*	2.09	2.66	5.18	51.34	85.57
20	*2-135*	2.07	2.98	6.05	49.28	82.13
21	*2-136*	2.10	2.52	5.18	48.61	81.02
22	*2-137*	2.08	2.72	5.34	50.93	84.88
23	*2-138*	2.10	2.46	4.73	52.04	86.73
24	*2-139*	2.09	2.50	5.30	47.14	78.57
25	*2-140*	2.09	2.34	4.84	48.32	80.53
26	*2-141*	2.09	2.68	5.33	50.30	83.83
27	*2-142*	2.12	3.00	5.63	53.27	88.78
28	*2-143*	2.10	2.54	5.01	50.68	84.47
29	*2-144*	2.08	2.86	5.67	50.45	84.08
30	*2-145*	2.08	2.74	5.50	49.80	83.00
31	*2-147*	2.11	2.36	4.89	48.25	80.42
32	*2-151*	2.09	3.14	6.60	47.57	79.28
33	*2-157*	2.09	2.48	5.34	46.41	77.35
34	*2-159*	2.07	2.76	6.13	44.99	74.98
35	*2-162*	2.09	2.40	5.00	48.03	80.05
36	*2-164*	2.11	2.54	4.98	51.04	85.07
37	*2-166*	2.08	3.10	6.20	49.97	83.28
38	*2-167*	2.11	3.02	6.14	49.17	81.95
39	*2-168*	2.15	2.48	4.81	51.53	85.88
40	*2-169*	2.09	2.82	5.56	50.75	84.58
41	*2-170*	2.10	2.72	5.22	52.11	86.85
42	*2-171*	2.12	2.32	4.63	50.14	83.57
43	*2-172*	2.07	3.66	7.93	46.17	76.95
44	*2-173*	2.07	3.26	7.08	46.02	76.70
45	*2-174*	2.10	2.84	5.71	49.78	82.97
46	*2-175*	2.11	2.52	4.98	50.62	84.37
47	*2-176*	2.10	2.80	5.59	50.11	83.52

48	*2-177*	2.09	2.76	5.44	50.76	84.60
49	*2-178*	2.09	3.24	6.90	46.97	78.28
50	*2-179*	2.11	2.64	5.28	49.96	83.27
51	*2-180*	2.10	2.40	4.76	50.40	84.00
52	*2-181*	2.09	2.86	5.71	50.13	83.55
53	*2-183*	2.08	2.92	5.72	51.02	85.03
54	*2-184*	2.10	2.66	5.19	51.29	85.48
55	*2-185*	2.09	2.88	5.89	48.87	81.45
56	*2-186*	2.17	2.20	4.44	49.54	82.57
57	*2-187*	2.09	2.98	6.21	47.97	79.95
58	*2-188*	2.09	2.42	5.02	48.25	80.42
59	*2-189*	2.12	2.56	5.21	49.17	81.95
60	*2-190*	2.10	2.54	5.33	47.68	79.47
61	*2-191*	2.10	2.60	5.25	49.50	82.50
62	*2-192*	2.10	2.50	5.02	49.83	83.05
63	*2-193*	2.08	2.72	5.80	46.88	78.13
64	*2-194*	2.08	3.62	7.77	46.57	77.62
65	*2-195*	2.09	2.42	4.94	48.97	81.62
66	*2-196*	2.09	3.00	5.81	51.60	86.00
67	*2-197*	2.10	2.48	4.94	50.21	83.68
68	*2-198*	2.11	2.54	5.42	46.88	78.13
69	*2-200*	2.09	2.74	5.42	50.58	84.30
70	*2-201*	2.17	2.34	4.68	49.95	83.25
71	*2-203*	2.08	3.12	6.48	48.16	80.27
72	*2-204*	2.09	2.88	6.13	46.97	78.28
73	*2-205*	2.18	2.22	4.61	48.16	80.27
74	*2-206*	2.15	3.22	6.33	50.87	84.78
75	*2-207*	2.10	2.98	5.82	51.21	85.35
76	*2-208*	2.08	2.90	5.81	49.92	83.20
77	*2-209*	2.15	2.06	4.23	48.67	81.12
78	*2-210*	2.17	2.28	4.61	49.46	82.43
79	*2-211*	2.20	2.48	4.94	50.21	83.68
80	*2-212*	2.13	2.40	4.64	51.70	86.17
81	*2-213*	2.12	2.52	5.12	49.18	81.97
82	*2-214*	2.16	2.78	5.26	52.85	88.08
83	*2-215*	2.17	2.14	4.32	49.53	82.55
84	*2-216*	2.11	2.30	4.53	50.77	84.62
85	*2-217*	2.11	2.48	4.89	50.76	84.60
86	*2-218*	2.10	2.26	4.87	46.45	77.42
87	*2-300*	2.12	2.24	4.51	49.67	82.78
88	*2-301*	2.08	2.60	5.30	49.10	81.83
89	*2-302*	2.10	2.48	4.89	50.70	84.50

Trans #	Frequency, MHz	DC Watts	US Watts	DC to US Eff. %	Trans Eff. %
Average	2.1046	2.65	5.35	49.55	82.59
SD	0.03	0.30	0.69	1.74	2.90
Max	2.20	3.66	7.93	53.27	88.78
Min	2.07	2.06	4.23	44.99	74.98

	Bad Xducr Serial #	Most Efficient Frequency, in MHz	Ultrasound Power, Watts	DC Watts	DC to Ultrasound Efficiency, %	Transducer Efficiency, %
1	*2-003*	no polarity 2.14	2.30	4.76	48.35	80.58
2	*2-132*	2.09	1.28	3.78	33.87	56.45
3	*2-146*	2.10	1.72	4.46	38.55	64.25
4	*2-148*	2.10	0.90	2.94	30.63	51.05
5	*2-149*	2.07	0.70	2.85	24.58	40.97
6	*2-150*	2.08	0.32	2.33	13.74	22.90
7	*2-152*	2.07	0.14	2.27	6.16	10.26
8	*2-153*	2.02	2.68	8.65	30.98	51.63
9	*2-154*	2.05	0.18	2.16	8.32	13.87
10	*2-155*	2.12	0.32	2.42	13.21	22.02
11	*2-156*	2.07	0.38	2.38	15.99	26.65
12	*2-158*	2.08	0.32	2.78	11.50	19.17
13	*2-160*	2.10	0.74	2.80	26.43	44.05
14	*2-161*	2.06	0.06	2.03	2.95	4.92
15	*2-163*	2.11	0.08	1.99	4.02	6.70
16	*2-165*	2.08	0.34	2.28	14.93	24.88
17	*2-199*	2.08	2.92	6.63	44.02	73.37
18	*2-202*	no polarity 2.09	2.48	5.03	49.33	82.22

Trans #	Col	#	Rng	#	Freq in MHz	Measured Acoustic Watts at D/A V = 2.37	Calculated Acoustic Watts at D/A V = 5.00	Calculated D/A Voltage at 0.5 Watts	Calculated D/A Voltage at 9 Watts
2-186	C	1	R	1	2.16	2.78	12.37	1.01	4.26
2-206	C	1	R	2	2.15	3.22	14.33	0.93	3.96
2-168	C	1	R	3	2.15	2.48	11.04	1.06	4.51
2-211	C	1	R	4	2.20	2.48	11.04	1.06	4.51
2-147	C	3	R	1	2.10	2.72	12.11	1.02	4.31
2-212	C	3	R	2	2.13	2.40	10.68	1.08	4.59
2-130	C	3	R	3	2.12	2.44	10.86	1.07	4.55
2-116	C	3	R	4	2.11	2.54	11.31	1.05	4.46
2-133	C	5	R	1	2.11	2.54	11.31	1.05	4.46
2-164	C	5	R	2	2.11	2.52	11.22	1.06	4.48
2-217	C	5	R	3	2.11	2.48	11.04	1.06	4.51
2-216	C	5	R	4	2.11	2.30	10.24	1.11	4.69
2-207	C	7	R	1	2.10	2.98	13.26	0.97	4.12
2-120	C	7	R	2	2.10	2.68	11.93	1.02	4.34
2-184	C	7	R	3	2.10	2.66	11.84	1.03	4.36
2-002	C	7	R	4	2.10	2.58	11.48	1.04	4.43
2-198	C	9	R	1	2.10	2.46	10.95	1.07	4.53
S-5C009	C	9	R	2	2.17	2.36	10.50	1.09	4.63
2-302	C	9	R	3	2.10	2.48	11.04	1.06	4.51
2-180	C	9	R	4	2.10	2.40	10.68	1.08	4.59
2-169	C	11	R	1	2.09	2.82	12.55	1.00	4.23
2-177	C	11	R	2	2.09	2.76	12.28	1.01	4.28
2-200	C	11	R	3	2.09	2.74	12.20	1.01	4.30
2-127	C	11	R	4	2.09	2.68	11.93	1.02	4.34
2-141	C	13	R	1	2.09	2.68	11.93	1.02	4.34
2-134	C	13	R	2	2.09	2.66	11.84	1.03	4.36
2-001	C	13	R	3	2.09	2.46	10.95	1.07	4.53
2-122	C	13	R	4	2.09	2.34	10.41	1.10	4.65
2-183	C	15	R	1	2.08	2.92	13.00	0.98	4.16
2-123	C	15	R	2	2.08	2.86	12.73	0.99	4.20
2-144	C	15	R	3	2.08	2.86	12.73	0.99	4.20
2-128	C	15	R	4	2.08	2.82	12.55	1.00	4.23
2-190	C	17	R	1	2.09	3.00	13.35	0.97	4.10
2-137	C	17	R	2	2.08	2.72	12.11	1.02	4.31
2-015	C	17	R	3	2.08	2.50	11.13	1.06	4.50
S-5C008	C	17	R	4	2.14	2.70	12.02	1.02	4.33
2-205	C	19	R	1	2.18	2.34	10.41	1.10	4.65
2-201	C	19	R	2	2.17	2.28	10.15	1.11	4.71
2-215	C	19	R	3	2.17	2.20	9.79	1.13	4.79
2-214	C	19	R	4	2.17	2.14	9.52	1.15	4.86
2-121	C	21	R	1	2.13	2.18	9.70	1.14	4.82
2-189	C	21	R	2	2.12	2.56	11.39	1.05	4.44
2-213	C	21	R	3	2.12	2.52	11.22	1.06	4.48
2-171	C	21	R	4	2.12	2.32	10.33	1.10	4.67
2-167	C	23	R	1	2.11	3.02	13.44	0.96	4.09
2-179	C	23	R	2	2.11	2.64	11.75	1.03	4.38
2-174	C	23	R	3	2.10	2.84	12.64	0.99	4.22
2-176	C	23	R	4	2.10	2.80	12.46	1.00	4.25
2-191	C	25	R	1	2.10	2.60	11.57	1.04	4.41
2-192	C	25	R	2	2.10	2.50	11.13	1.06	4.50
2-197	C	25	R	3	2.10	2.48	11.04	1.06	4.51
2-185	C	25	R	4	2.09	2.88	12.82	0.99	4.19

2-181	C	27	R	1	2.09	2.86	12.73	0.99	4.20
2-124	C	27	R	2	2.09	2.62	11.66	1.04	4.39
2-129	C	27	R	3	2.09	2.58	11.48	1.04	4.43
S-5C010	C	27	R	4	2.16	2.66	11.84	1.03	4.36
2-195	C	29	R	1	2.09	2.42	10.77	1.08	4.57
2-166	C	29	R	2	2.08	3.10	13.80	0.95	4.04
2-208	C	29	R	3	2.08	2.90	12.91	0.98	4.18
2-145	C	29	R	4	2.08	2.74	12.20	1.01	4.30
2-301	C	31	R	1	2.08	2.60	11.57	1.04	4.41
2-194	C	31	R	2	2.07	2.98	13.26	0.97	4.12
2-210	C	31	R	3	2.17	2.22	9.88	1.12	4.77
2-131	C	31	R	4	2.16	2.34	10.41	1.10	4.65
2-175	C	33	R	1	2.12	2.62	11.66	1.04	4.39
2-170	C	33	R	2	2.11	2.36	10.50	1.09	4.63
2-136	C	33	R	3	2.10	2.54	11.31	1.05	4.46
2-138	C	33	R	4	2.11	2.54	11.31	1.05	4.46
2-218	C	35	R	1	2.10	2.52	11.22	1.06	4.48
2-151	C	35	R	2	2.09	3.14	13.98	0.95	4.01
2-196	C	35	R	3	2.10	2.26	10.06	1.11	4.73
2-182	C	35	R	4	2.10	3.18	14.15	0.94	3.99
2-188	C	37	R	1	2.09	2.42	10.77	1.08	4.57
2-178	C	37	R	2	2.09	3.24	14.42	0.93	3.95
2-125	C	37	R	3	2.07	2.70	12.02	1.02	4.33
S-5C002	C	37	R	4	2.17	2.62	11.66	1.04	4.39
2-162	C	39	R	1	2.09	2.40	10.68	1.08	4.59
2-204	C	39	R	2	2.09	2.88	12.82	0.99	4.19
2-139	C	39	R	3	2.09	2.50	11.13	1.06	4.50
S-5C003	C	39	R	4	2.18	2.60	11.57	1.04	4.41
2-187	C	41	R	1	2.09	2.98	13.26	0.97	4.12
2-157	C	41	R	2	2.09	2.48	11.04	1.06	4.51
2-193	C	41	R	3	2.08	3.62	16.11	0.88	3.74
S-5C004	C	41	R	4	2.16	2.60	11.57	1.04	4.41
2-140	C	43	R	1	2.09	2.34	10.41	1.10	4.65
2-135	C	43	R	2	2.08	2.72	12.11	1.02	4.31
2-172	C	43	R	3	2.07	3.66	16.29	0.88	3.72
2-117	C	43	R	4	2.14	2.54	11.31	1.05	4.46
2-203	C	45	R	1	2.08	3.12	13.89	0.95	4.03
2-173	C	45	R	2	2.07	3.26	14.51	0.93	3.94
2-159	C	45	R	3	2.07	2.76	12.28	1.01	4.28
S-5C006	C	45	R	4	2.17	2.52	11.22	1.06	4.48
2-209	C	47	R	1	2.15	2.06	9.17	1.17	4.95
2-142	C	47	R	2	2.14	2.30	10.24	1.11	4.69
2-126	C	47	R	3	2.15	2.56	11.39	1.05	4.44
2-300	C	47	R	4	2.12	2.24	9.97	1.12	4.75

Total No. Tested	96	Freq in MHz	Measured Acoustic Watts at D/A V = 2.37	Calculated Acoustic Watts at D/A V = 5.00	Calculated D/A Voltage at 0.5 Watts	Calculated D/A Voltage at 9 Watts
	AVE	2.11	2.64	11.76	1.04	4.39
	MIN	2.07	2.06	9.17	0.88	3.72
	MAX	2.20	3.66	16.29	1.17	4.95

Trans #	Col	#	Rng	#	Most Efficient Frequency, in MHz	Ultrasound Watts	DC to Ultrasound Efficiency, %	Transducer Efficiency, %
2-186	C	1	R	1	2.16	2.78	52.85	87.50
2-206	C	1	R	2	2.15	3.22	50.87	85.00
2-168	C	1	R	3	2.15	2.48	51.53	85.00
2-211	C	1	R	4	2.20	2.48	50.21	82.50
2-147	C	3	R	1	2.10	2.72	52.11	87.50
2-212	C	3	R	2	2.13	2.40	51.70	85.00
2-130	C	3	R	3	2.12	2.44	51.03	85.00
2-116	C	3	R	4	2.11	2.54	51.49	85.00
2-133	C	5	R	1	2.11	2.54	51.04	85.00
2-164	C	5	R	2	2.11	2.52	50.62	85.00
2-217	C	5	R	3	2.11	2.48	50.76	85.00
2-216	C	5	R	4	2.11	2.30	50.77	85.00
2-207	C	7	R	1	2.10	2.98	51.21	85.00
2-120	C	7	R	2	2.10	2.68	50.73	85.00
2-184	C	7	R	3	2.10	2.66	51.29	85.00
2-002	C	7	R	4	2.10	2.58	50.74	85.00
2-198	C	9	R	1	2.10	2.46	52.04	87.50
S-5C009	C	9	R	2	2.17	2.36	49.85	75.00
2-302	C	9	R	3	2.10	2.48	50.70	85.00
2-180	C	9	R	4	2.10	2.40	50.40	85.00
2-169	C	11	R	1	2.09	2.82	50.75	85.00
2-177	C	11	R	2	2.09	2.76	50.76	85.00
2-200	C	11	R	3	2.09	2.74	50.58	85.00
2-127	C	11	R	4	2.09	2.68	51.33	85.00
2-141	C	13	R	1	2.09	2.68	50.30	85.00
2-134	C	13	R	2	2.09	2.66	51.34	85.00
2-001	C	13	R	3	2.09	2.46	50.98	85.00
2-122	C	13	R	4	2.09	2.34	50.53	85.00
2-183	C	15	R	1	2.08	2.92	51.02	85.00
2-123	C	15	R	2	2.08	2.86	50.69	85.00
2-144	C	15	R	3	2.08	2.86	50.45	85.00
2-128	C	15	R	4	2.08	2.82	51.14	85.00
2-190	C	17	R	1	2.09	3.00	51.60	85.00
2-137	C	17	R	2	2.08	2.72	50.93	85.00
2-015	C	17	R	3	2.08	2.50	50.89	85.00
S-5C008	C	17	R	4	2.14	2.70	51.36	77.50
2-205	C	19	R	1	2.18	2.34	49.95	82.50
2-201	C	19	R	2	2.17	2.28	49.46	82.50
2-215	C	19	R	3	2.17	2.20	49.54	82.50
2-214	C	19	R	4	2.17	2.14	49.53	82.50
2-121	C	21	R	1	2.13	2.18	49.72	82.50
2-189	C	21	R	2	2.12	2.56	49.17	82.50
2-213	C	21	R	3	2.12	2.52	49.18	82.50
2-171	C	21	R	4	2.12	2.32	50.14	82.50
2-167	C	23	R	1	2.11	3.02	49.17	82.50
2-179	C	23	R	2	2.11	2.64	49.96	82.50
2-174	C	23	R	3	2.10	2.84	49.78	82.50
2-176	C	23	R	4	2.10	2.80	50.11	82.50
2-191	C	25	R	1	2.10	2.60	49.50	82.50
2-192	C	25	R	2	2.10	2.50	49.83	82.50
2-197	C	25	R	3	2.10	2.48	50.21	82.50
2-185	C	25	R	4	2.09	2.88	48.87	82.50

2-181	C	27	R	1	2.09	2.86	50.13	82.50
2-124	C	27	R	2	2.09	2.62	49.23	82.50
2-129	C	27	R	3	2.09	2.58	49.74	82.50
S-5C010	C	27	R	4	2.16	2.66	51.35	77.50
2-195	C	29	R	1	2.09	2.42	48.97	82.50
2-166	C	29	R	2	2.08	3.10	49.97	82.50
2-208	C	29	R	3	2.08	2.90	49.92	82.50
2-145	C	29	R	4	2.08	2.74	49.80	82.50
2-301	C	31	R	1	2.08	2.60	49.10	82.50
2-194	C	31	R	2	2.07	2.98	49.28	82.50
2-210	C	31	R	3	2.17	2.22	48.16	80.00
2-131	C	31	R	4	2.16	2.34	48.21	80.00
2-175	C	33	R	1	2.12	2.62	48.20	80.00
2-170	C	33	R	2	2.11	2.36	48.25	80.00
2-136	C	33	R	3	2.10	2.54	47.68	80.00
2-138	C	33	R	4	2.11	2.54	46.88	77.50
2-218	C	35	R	1	2.10	2.52	48.61	80.00
2-151	C	35	R	2	2.09	3.14	47.57	80.00
2-196	C	35	R	3	2.10	2.26	46.45	77.50
2-182	C	35	R	4	2.10	3.18	47.94	80.00
2-188	C	37	R	1	2.09	2.42	48.25	80.00
2-178	C	37	R	2	2.09	3.24	46.97	77.50
2-125	C	37	R	3	2.07	2.70	45.71	75.00
S-5C002	C	37	R	4	2.17	2.62	50.27	77.50
2-162	C	39	R	1	2.09	2.40	48.03	80.00
2-204	C	39	R	2	2.09	2.88	46.97	77.50
2-139	C	39	R	3	2.09	2.50	47.14	77.50
S-5C003	C	39	R	4	2.18	2.60	50.99	77.50
2-187	C	41	R	1	2.09	2.98	47.97	80.00
2-157	C	41	R	2	2.09	2.48	46.41	77.50
2-193	C	41	R	3	2.08	3.62	46.57	77.50
S-5C004	C	41	R	4	2.16	2.60	50.84	77.50
2-140	C	43	R	1	2.09	2.34	48.32	80.00
2-135	C	43	R	2	2.08	2.72	46.88	77.50
2-172	C	43	R	3	2.07	3.66	46.17	77.50
2-117	C	43	R	4	2.14	2.54	46.26	77.50
2-203	C	45	R	1	2.08	3.12	48.16	80.00
2-173	C	45	R	2	2.07	3.26	46.02	77.50
2-159	C	45	R	3	2.07	2.76	44.99	75.00
S-5C006	C	45	R	4	2.17	2.52	49.97	75.00
2-209	C	47	R	1	2.15	2.06	48.67	80.00
2-142	C	47	R	2	2.14	2.30	48.35	80.00
2-126	C	47	R	3	2.15	2.56	46.27	77.50
2-300	C	47	R	4	2.12	2.24	49.67	82.50

Transducer Number		2-139				% Efficiency	
Freq. MHz	DC mA	DC Volts	US Watts	DC Watts	RF Watts	DC to US	RF to US
2.04	220.10	25.87	2.58	5.69	3.43	45.31%	75.22%
2.05	214.30	25.89	2.52	5.55	3.34	45.47%	75.49%
2.06	211.60	25.89	2.50	5.48	3.30	45.63%	75.75%
2.07	214.20	25.89	2.56	5.55	3.34	46.16%	76.63%
2.08	212.40	25.89	2.56	5.50	3.31	46.55%	77.28%
2.09	204.70	25.91	2.50	5.30	3.20	47.14%	78.25%
2.10	197.30	25.94	2.40	5.12	3.08	46.89%	77.84%
2.11	193.00	25.95	2.36	5.01	3.02	47.12%	78.22%
2.12	189.30	25.96	2.30	4.91	2.96	46.80%	77.69%
2.13	183.80	25.97	2.22	4.77	2.88	46.51%	77.20%
2.14	178.20	25.99	2.12	4.63	2.79	45.77%	75.99%
2.15	178.30	25.99	2.10	4.63	2.79	45.32%	75.23%
2.16	183.30	25.97	2.14	4.76	2.87	44.96%	74.63%
2.17	186.90	25.97	2.18	4.85	2.92	44.91%	74.56%
2.18	186.90	25.96	2.18	4.85	2.92	44.93%	74.58%

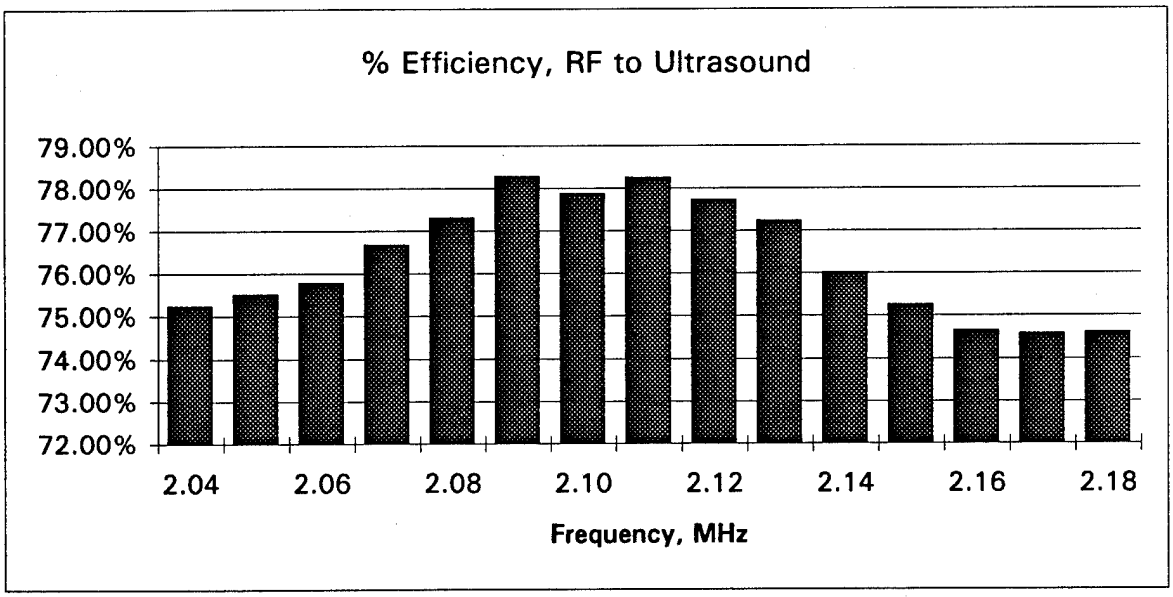

Efficiency from DC to RF is 60% as measured with Bird meter at 2 to 3 watts ultrasound.
DC to RF efficiency increases to around 75% at 10 watts ultrasound power
DC to RF efficiency increases to around 90% at 20 watts ultrasound power

Appendix D

T/R MUX Applicator Transducer Interconnections Map

OCTANT 1

10 Apr, 1995

COL 0	COL 1	COL 2	COL 3	COL 4	COL 5
2.0M C1 CH1	4.5M C2 CH1	2.0M C3 CH1	4.5M C4 CH1	2.0M C5 CH1	4.5M C6 CH1
2.0M C1 CH5	4.5M C2 CH5	2.0M C3 CH5	4.5M C4 CH5	2.0M C5 CH5	4.5M C6 CH5
2.0M C1 CH9	4.5M C2 CH9	2.0M C3 CH9	4.5M C4 CH9	2.0M C5 CH9	4.5M C6 CH9
2.0M C1 CH13	4.5M C2 CH13	2.0M C3 CH13	4.5M C4 CH13	2.0M C5 CH13	4.5M C6 CH13
2.5M C13 CH1	4.5M C14 CH1	2.5M C15 CH1	4.5M C16 CH1	2.5M C17 CH1	4.5M C18 CH1
2.5M C13 CH5	4.5M C14 CH5	2.5M C15 CH5	4.5M C16 CH5	2.5M C17 CH5	4.5M C18 CH5
2.5M C13 CH9	4.5M C14 CH9	2.5M C15 CH9	4.5M C16 CH9	2.5M C17 CH9	4.5M C18 CH9
2.5M C13 CH13	4.5M C14 CH13	2.5M C15 CH13	4.5M C16 CH13	2.5M C17 CH13	4.5M C18 CH13

OCTANT 2

10 Apr, 1995

COL 6	COL 7	COL 8	COL 9	COL 10	COL 11
2.0M C7 CH1	4.5M C8 CH1	2.0M C9 CH1	4.5M C10 CH1	2.0M C11 CH1	4.5M C12 CH1
2.0M C7 CH5	4.5M C8 CH5	2.0M C9 CH5	4.5M C10 CH5	2.0M C11 CH5	4.5M C12 CH5
2.0M C7 CH9	4.5M C8 CH9	2.0M C9 CH9	4.5M C10 CH9	2.0M C11 CH9	4.5M C12 CH9
2.0M C7 CH13	4.5M C8 CH13	2.0M C9 CH13	4.5M C10 CH13	2.0M C11 CH13	4.5M C12 CH13
2.5M C19 CH1	4.5M C20 CH1	2.5M C21 CH1	4.5M C22 CH1	2.5M C23 CH1	4.5M C24 CH1
2.5M C19 CH5	4.5M C20 CH5	2.5M C21 CH5	4.5M C22 CH5	2.5M C23 CH5	4.5M C24 CH5
2.5M C19 CH9	4.5M C20 CH9	2.5M C21 CH9	4.5M C22 CH9	2.5M C23 CH9	4.5M C24 CH9
2.5M C19 CH13	4.5M C20 CH13	2.5M C21 CH13	4.5M C22 CH13	2.5M C23 CH13	4.5M C24 CH13

OCTANT 3

10 Apr, 1995

COL 12	COL 13	COL 14	COL 15	COL 16	COL 17
2.0M C13 CH2	4.5M C14 CH2	2.0M C15 CH2	4.5M C16 CH2	2.0M C17 CH2	4.5M C18 CH2
2.0M C13 CH6	4.5M C14 CH6	2.0M C15 CH6	4.5M C16 CH6	2.0M C17 CH6	4.5M C18 CH6
2.0M C13 CH10	4.5M C14 CH10	2.0M C15 CH10	4.5M C16 CH10	2.0M C17 CH10	4.5M C18 CH10
2.0M C13 CH14	4.5M C14 CH14	2.0M C15 CH14	4.5M C16 CH14	2.0M C17 CH14	4.5M C18 CH14
2.5M C1 CH2	4.5M C2 CH2	2.5M C3 CH2	4.5M C4 CH2	2.5M C5 CH2	4.5M C6 CH2
2.5M C1 CH6	4.5M C2 CH6	2.5M C3 CH6	4.5M C4 CH6	2.5M C5 CH6	4.5M C6 CH6
2.5M C1 CH10	4.5M C2 CH10	2.5M C3 CH10	4.5M C4 CH10	2.5M C5 CH10	4.5M C6 CH10
2.5M C1 CH14	4.5M C2 CH14	2.5M C3 CH14	4.5M C4 CH14	2.5M C5 CH14	4.5M C6 CH14

OCTANT 4

10 Apr, 1995

COL 18	COL 19	COL 20	COL 21	COL 22	COL 23
2.0M C19 CH2	4.5M C20 CH2	2.0M C21 CH2	4.5M C22 CH2	2.0M C23 CH2	4.5M C24 CH2
2.0M C19 CH6	4.5M C20 CH6	2.0M C21 CH6	4.5M C22 CH6	2.0M C23 CH6	4.5M C24 CH6
2.0M C19 CH10	4.5M C20 CH10	2.0M C21 CH10	4.5M C22 CH10	2.0M C23 CH10	4.5M C24 CH10
2.0M C19 CH14	4.5M C20 CH14	2.0M C21 CH14	4.5M C22 CH14	2.0M C23 CH14	4.5M C24 CH14
2.5M C7 CH2	4.5M C8 CH2	2.5M C9 CH2	4.5M C10 CH2	2.5M C11 CH2	4.5M C12 CH2
2.5M C7 CH6	4.5M C8 CH6	2.5M C9 CH6	4.5M C10 CH6	2.5M C11 CH6	4.5M C12 CH6
2.5M C7 CH10	4.5M C8 CH10	2.5M C9 CH10	4.5M C10 CH10	2.5M C11 CH10	4.5M C12 CH10
2.5M C7 CH14	4.5M C8 CH14	2.5M C9 CH14	4.5M C10 CH14	2.5M C11 CH14	4.5M C12 CH14

OCTANT 5

10 Apr, 1995

COL 24	COL 25	COL 26	COL 27	COL 28	COL 29
2.0M C13 CH3	4.5M C14 CH3	2.0M C15 CH3	4.5M C16 CH3	2.0M C17 CH3	4.5M C18 CH3
2.0M C13 CH7	4.5M C14 CH7	2.0M C15 CH7	4.5M C16 CH7	2.0M C17 CH7	4.5M C18 CH7
2.0M C13 CH11	4.5M C14 CH11	2.0M C15 CH11	4.5M C16 CH11	2.0M C17 CH11	4.5M C18 CH11
2.0M C13 CH15	4.5M C14 CH15	2.0M C15 CH15	4.5M C16 CH15	2.0M C17 CH15	4.5M C18 CH15
2.5M C1 CH3	4.5M C2 CH3	2.5M C3 CH3	4.5M C4 CH3	2.5M C5 CH3	4.5M C6 CH3
2.5M C1 CH7	4.5M C2 CH7	2.5M C3 CH7	4.5M C4 CH7	2.5M C5 CH7	4.5M C6 CH7
2.5M C1 CH11	4.5M C2 CH11	2.5M C3 CH11	4.5M C4 CH11	2.5M C5 CH11	4.5M C6 CH11
2.5M C1 CH15	4.5M C2 CH15	2.5M C3 CH15	4.5M C4 CH15	2.5M C5 CH15	4.5M C6 CH15

OCTANT 6

10 Apr, 1995

COL 30	COL 31	COL 32	COL 33	COL 34	COL 35
2.0M C19 CH3	4.5M C20 CH3	2.0M C21 CH3	4.5M C22 CH3	2.0M C23 CH3	4.5M C24 CH3
2.0M C19 CH7	4.5M C20 CH7	2.0M C21 CH7	4.5M C22 CH7	2.0M C23 CH7	4.5M C24 CH7
2.0M C19 CH11	4.5M C20 CH11	2.0M C21 CH11	4.5M C22 CH11	2.0M C23 CH11	4.5M C24 CH11
2.0M C19 CH15	4.5M C20 CH15	2.0M C21 CH15	4.5M C22 CH15	2.0M C23 CH15	4.5M C24 CH15
2.5M C7 CH3	4.5M C8 CH3	2.5M C9 CH3	4.5M C10 CH3	2.5M C11 CH3	4.5M C12 CH3
2.5M C7 CH7	4.5M C8 CH7	2.5M C9 CH7	4.5M C10 CH7	2.5M C11 CH7	4.5M C12 CH7
2.5M C7 CH11	4.5M C8 CH11	2.5M C9 CH11	4.5M C10 CH11	2.5M C11 CH11	4.5M C12 CH11
2.5M C7 CH15	4.5M C8 CH15	2.5M C9 CH15	4.5M C10 CH15	2.5M C11 CH15	4.5M C12 CH15

OCTANT 7

10 Apr, 1995

COL 36	COL 37	COL 38	COL 39	COL 40	COL 41
2.0M C1 CH4	4.5M C2 CH4	2.0M C3 CH4	4.5M C4 CH4	2.0M C5 CH4	4.5M C6 CH4
2.0M C1 CH8	4.5M C2 CH8	2.0M C3 CH8	4.5M C4 CH8	2.0M C5 CH8	4.5M C6 CH8
2.0M C1 CH12	4.5M C2 CH12	2.0M C3 CH12	4.5M C4 CH12	2.0M C5 CH12	4.5M C6 CH12
2.0M C1 CH16	4.5M C2 CH16	2.0M C3 CH16	4.5M C4 CH16	2.0M C5 CH16	4.5M C6 CH16
2.5M C13 CH4	4.5M C14 CH4	2.5M C15 CH4	4.5M C16 CH4	2.5M C17 CH4	4.5M C18 CH4
2.5M C13 CH8	4.5M C14 CH8	2.5M C15 CH8	4.5M C16 CH8	2.5M C17 CH8	4.5M C18 CH8
2.5M C13 CH12	4.5M C14 CH12	2.5M C15 CH12	4.5M C16 CH12	2.5M C17 CH12	4.5M C18 CH12
2.5M C13 CH16	4.5M C14 CH16	2.5M C15 CH16	4.5M C16 CH16	2.5M C17 CH16	4.5M C18 CH16

OCTANT 8

10 Apr, 1995

COL 42	COL 43	COL 44	COL 45	COL 46	COL 47
2.0M C7 CH4	4.5M C8 CH4	2.0M C9 CH4	4.5M C10 CH4	2.0M C11 CH4	4.5M C12 CH4
2.0M C7 CH8	4.5M C8 CH8	2.0M C9 CH8	4.5M C10 CH8	2.0M C11 CH8	4.5M C12 CH8
2.0M C7 CH12	4.5M C8 CH12	2.0M C9 CH12	4.5M C10 CH12	2.0M C11 CH12	4.5M C12 CH12
2.0M C7 CH16	4.5M C8 CH16	2.0M C9 CH16	4.5M C10 CH16	2.0M C11 CH16	4.5M C12 CH16
2.5M C19 CH4	4.5M C20 CH4	2.5M C21 CH4	4.5M C22 CH4	2.5M C23 CH4	4.5M C24 CH4
2.5M C19 CH8	4.5M C20 CH8	2.5M C21 CH8	4.5M C22 CH8	2.5M C23 CH8	4.5M C24 CH8
2.5M C19 CH12	4.5M C20 CH12	2.5M C21 CH12	4.5M C22 CH12	2.5M C23 CH12	4.5M C24 CH12
2.5M C19 CH16	4.5M C20 CH16	2.5M C21 CH16	4.5M C22 CH16	2.5M C23 CH16	4.5M C24 CH16

Appendix E

Measured Angular Beam Profile Data for 2.0 Mhz and 4.5 Mhz Transducers

4.5 MHz Beam Pattern for Square Transducer, Case 1

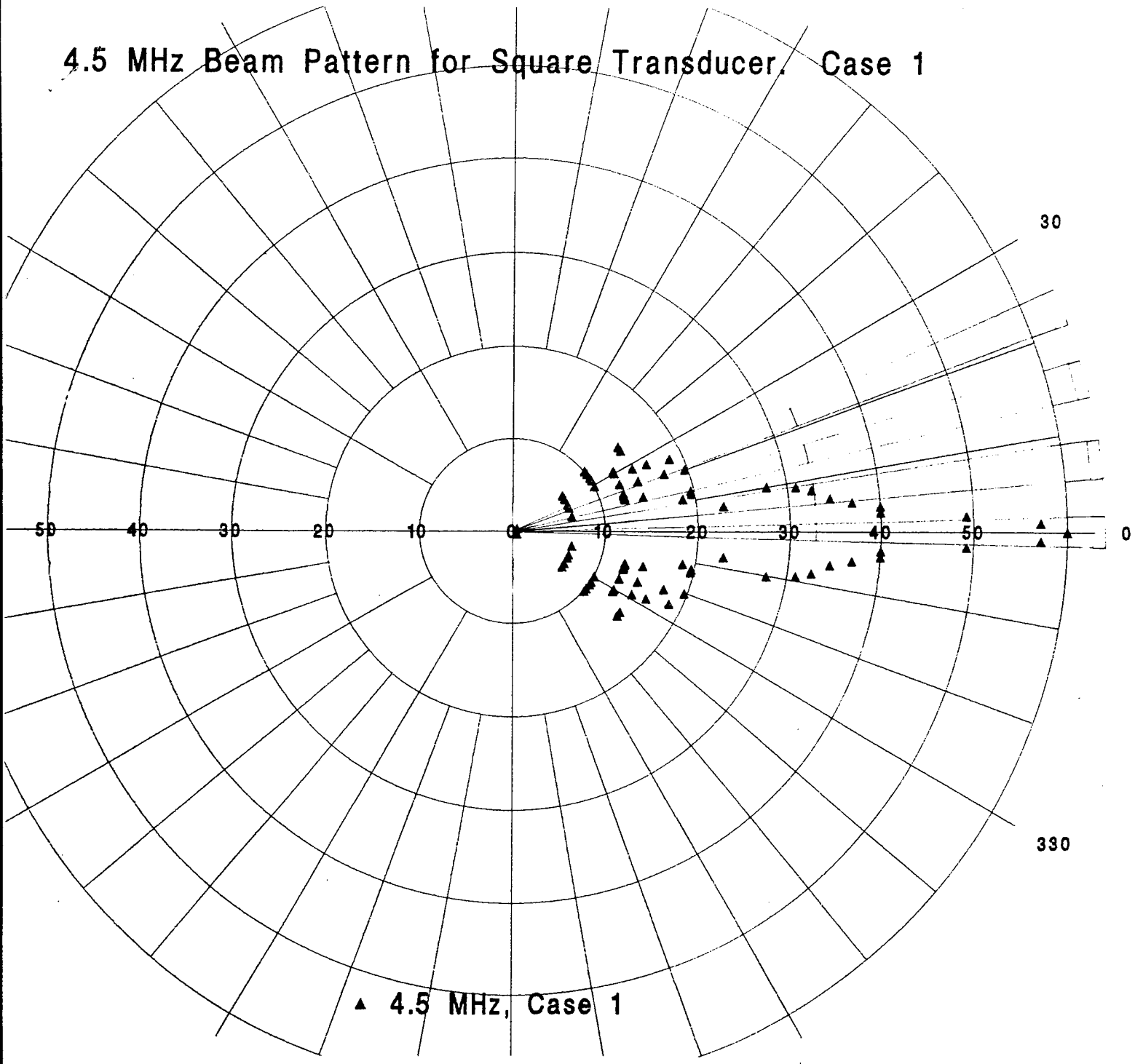

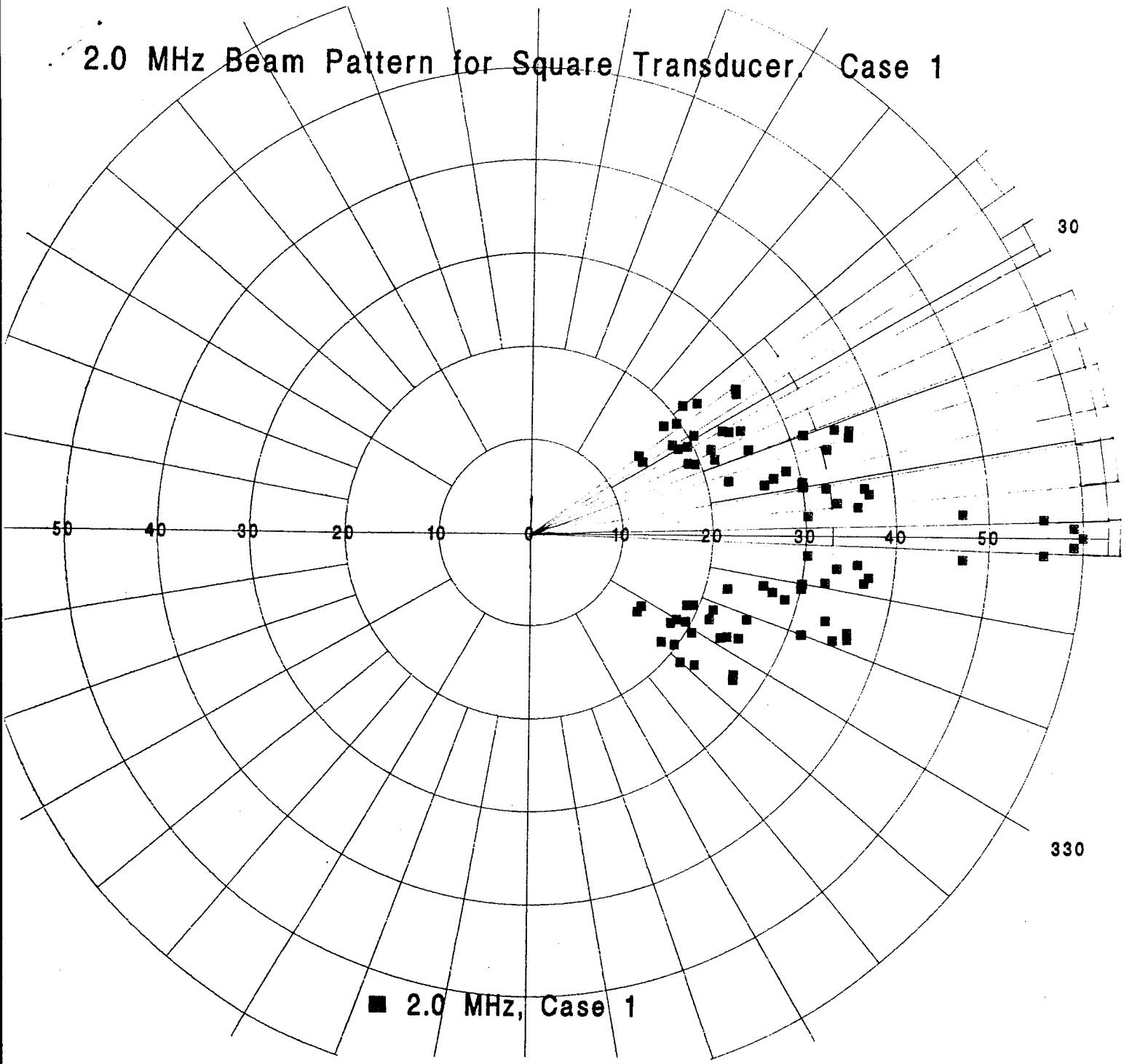
2.0 MHz Beam Pattern for Square Transducer. Case 1
30
330
50
40
30
20
10
0
10
20
30
40
50
2.0 MHz, Case 1

Appendix F

Breast Phantom Pulse-Echo and Through-Transmission Noninvasive Receiver Measurements Data Used for Tomographic Reconstructions

Appendix F contains the measured data used to determine the receiver performance and in the initial tomographic reconstruction study. These measurements provided the basis for verification of the required dynamic range and sensitivity for the receivers. It also permitted us to identify sources of noise in the T.R Mux circuits and take appropriate steps to improve their performance.

Measurements of both pulse-echo and through-transmission data were taken. The VCO-RF Amps were pulsed with various waveforms. A 10 ms pulse train was selected for the measurements based upon our observations of the hybrid response and overall signal to noise when detecting weak signals. Complete sets of pulse-echo and through-transmission data were taken for pulsing of each transducer separately, examining its echo response and while receiving the transmitted signal on transducers located on the opposite side of the ring. For each "transmit" transducer configuration, receive measurements were made from 15 opposing transducers, creating a "fan beam" of measured data which encompassed the area of a "slice" through the breast phantom. Thus, a total of 48x16 (=768) measurements of amplitude and time-of-flight (=1536) were recorded for one ring of the cylindrical array. Further, in order to permit tomographic reconstruction of the breast phantom target slice, the beam pattern effects of individual transducers had to be normalized out of the received through-transmission data. This was accomplished by first performing a full set of measurements with no breast target present and then inserting the target and recording all of the measurements again. By subtracting out the baseline data with no target present, it was possible to use the algebraic reconstruction algorithm to construct a tomographic profile of the through transmission within a slice of the breast.

Enclosed is an example the fan beam data with the attenuation information recorded. Also included are transmission attenuation measurements for receive transducers opposite the transmitting transducer for several individual cases. Measurements were taken at both the fundamental and harmonic frequencies.

Another group of data include information at both the transducer resonant frequency and varied frequencies around resonance for transducers 1,5,18 and 22. Histograms and data sheets are included for those examples. These data were recorded to examine the sensitivity of frequency variations upon the detection and time-of-flight measurement determination. Through these measurements, it was determined that a DSP would likely to be required for accurate time measurement processing.

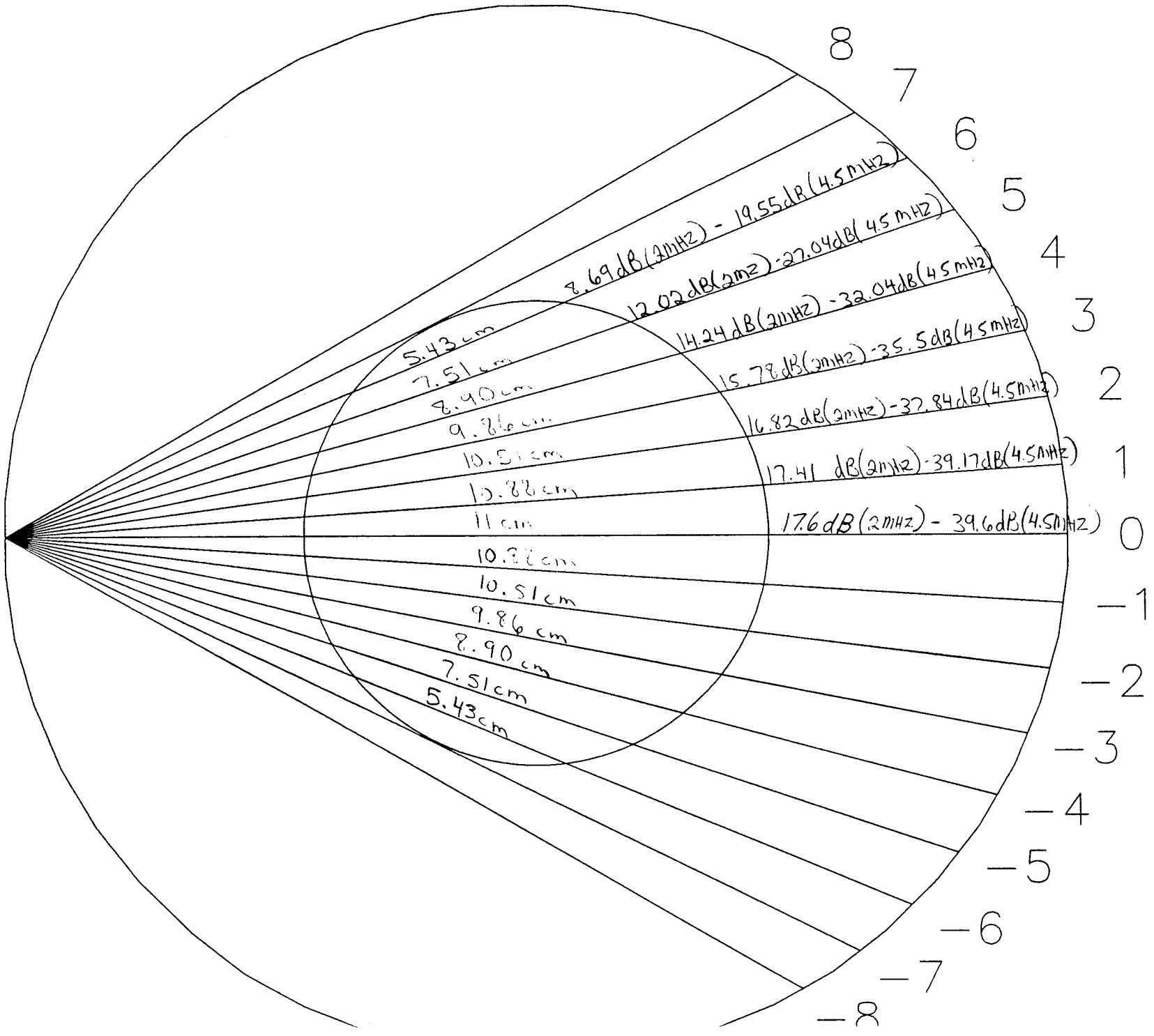
8
7
6
5
4
3
2
1
0
−1
−2
−3
−4
−5
−6
−7
−8
8.69dB(2mHz) - 19.55dB(4.5mHz)
12.02dB(2mz)-27.04dB(4.5mHz)
14.24dB(2mHz) -32.04dB(4.5mHz)
15.78dB(2mHz)-35.5dB(4.5mHz)
16.82dB(2mHz)-37.84dB(4.5mHz)
17.41 dB(2mHz)-39.17dB(4.5mHz)
17.6dB(2mHz) - 39.6dB(4.5mHz)
5.43cm
7.51cm
8.90cm
9.86cm
10.51cm
10.88cm
11cm
10.88cm
10.51cm
9.86cm
8.90cm
7.51cm
5.43cm

Fundamental

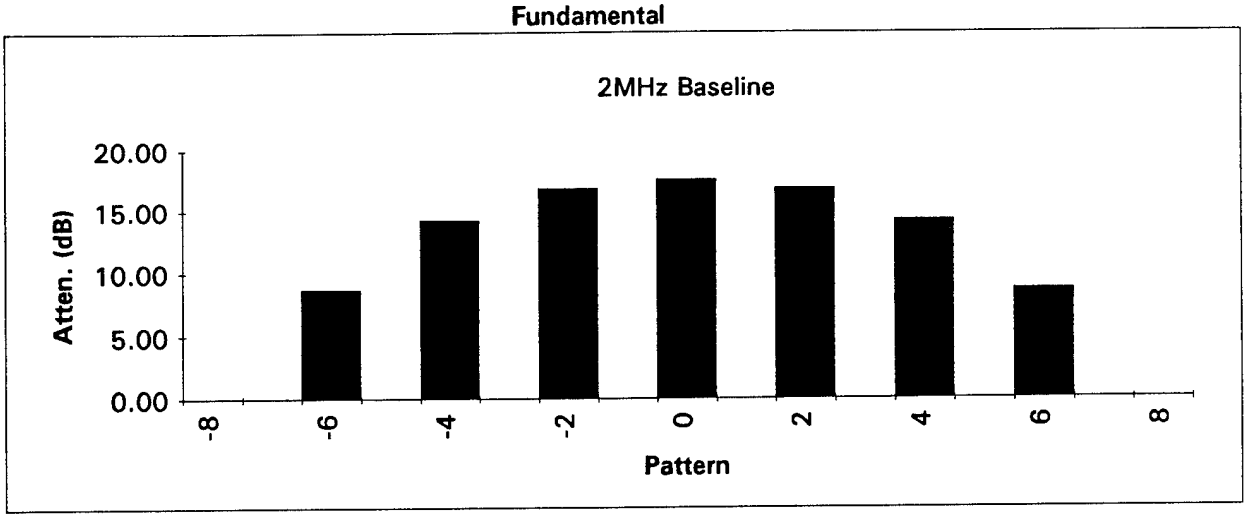

Harmonic

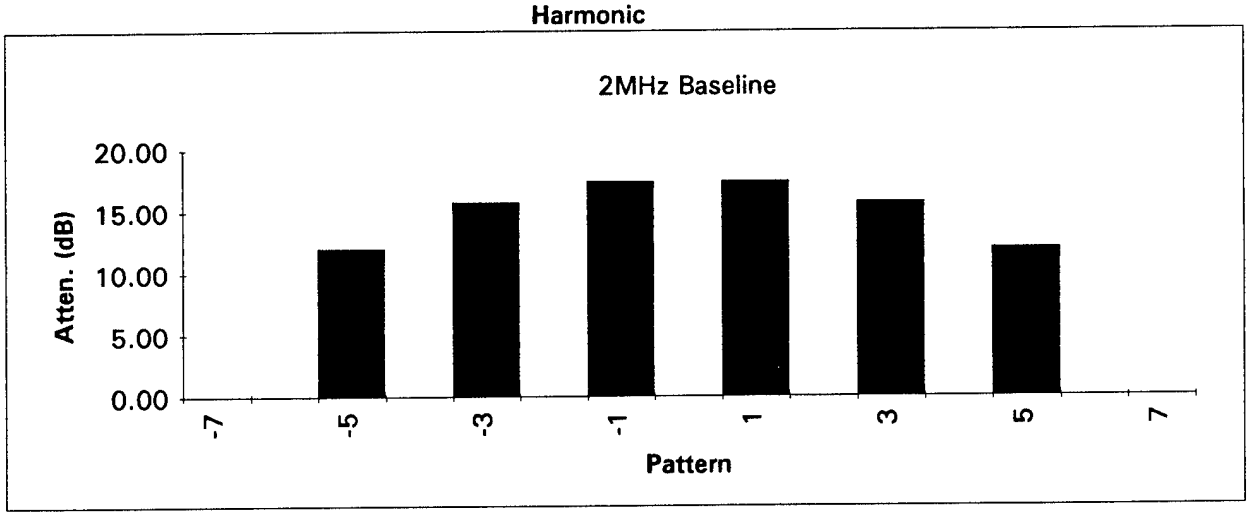

Fundamental

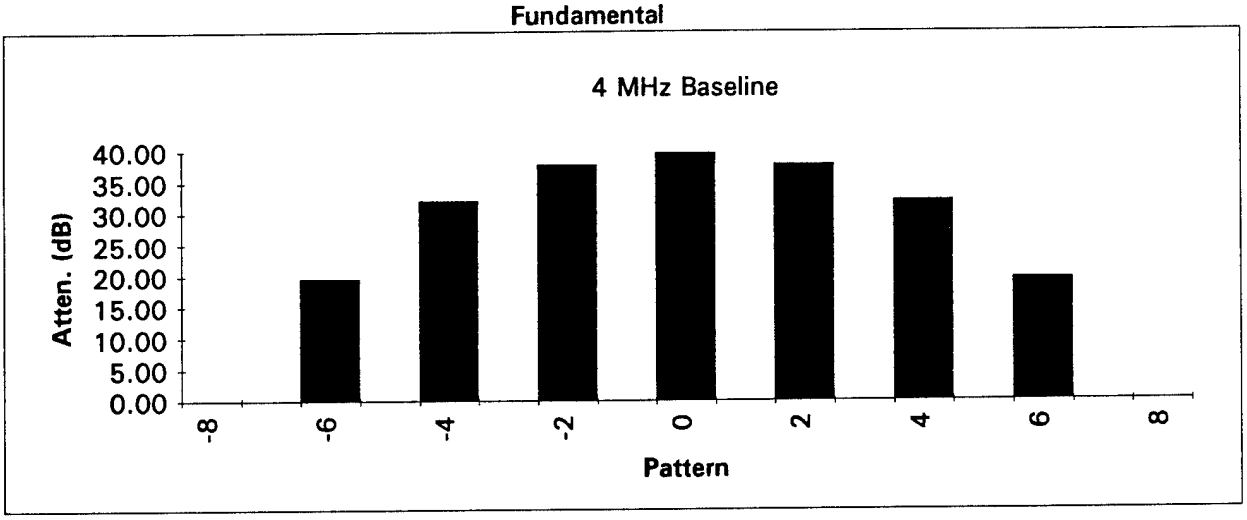

Harmonic

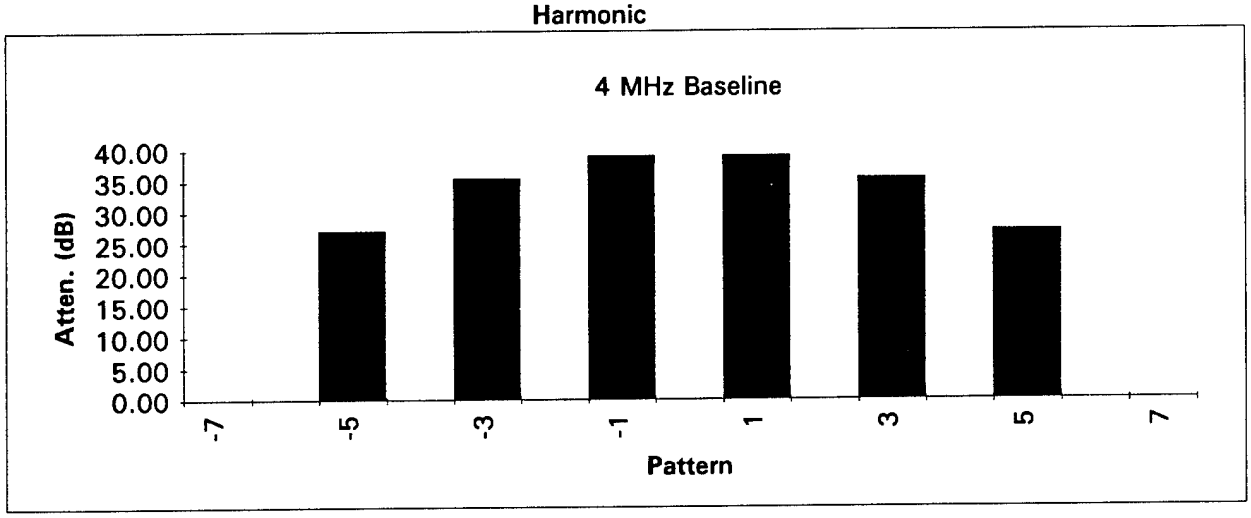

RESONA
FQ

Fundamental

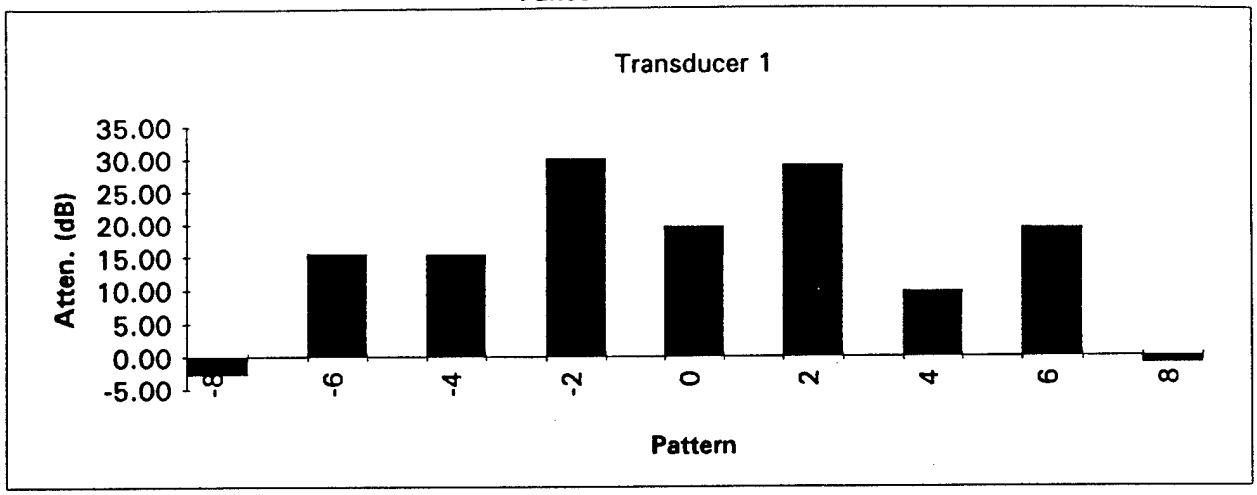

Harmonic

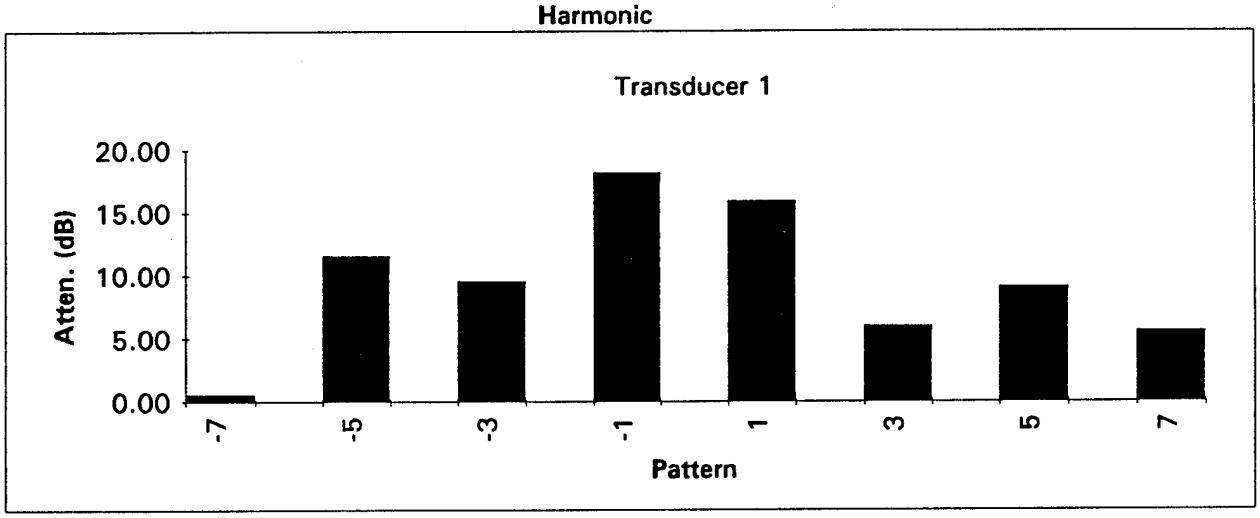

RESOI
FQ

Transducer 1 without Breast Target

	Actual Input Voltage	Actual Fundamental Voltage	Actual Harmonic Voltage	Normalized Fundamental Voltage	Normalized Harmonic Voltage	Transmission Time microsec.
8	71.000	0.80		9.58E-04		144
7	71.000		2.40		2.87E-03	152
6	71.000	4.20		5.03E-03		154
5	71.000		1.60		1.92E-03	158
4	15.000	2.00		1.13E-02		162
3	71.000		2.90		3.47E-03	164
2	2.400	3.70		1.31E-01		167
1	2.400		1.90		6.73E-02	168
Center	0.103	7.80		6.44E+00		168
-1	2.400		1.48		5.24E-02	168
-2	2.400	3.20		1.13E-01		167
-3	71.000		3.00		3.59E-03	164
-4	15.000	1.14		6.46E-03		162
-5	71.000		1.24		1.48E-03	158
-6	71.000	2.80		3.35E-03		154
-7	71.000		2.40		2.87E-03	152
-8	71.000	0.70		8.38E-04		144

Transducer 1 with Breast Target

	Actual Input Voltage	Actual Fundamental Voltage	Actual Harmonic Voltage	Normalized Fundamental Voltage	Normalized Harmonic Voltage	Transmission Time microsec.
8	71.000	1.100		1.32E-03		144
7	71.000		2.250		2.69E-03	152
6	71.000	0.700		8.38E-04		154
5	71.000		0.350		5.08E-04	162
4	71.000	1.600		1.92E-03		162
3	71.000		0.800		1.16E-03	168
2	71.000	3.400		4.07E-03		168
1	71.000		5.700		8.27E-03	168
Center	0.500	3.900		6.63E-01		168
-1	71.000		5.800		8.41E-03	168
-2	71.000	3.300		3.95E-03		167
-3	71.000		1.240		1.80E-03	166
-4	71.000	1.750		2.10E-03		162
-5	71.000		0.360		5.22E-04	160
-6	71.000	0.300		3.59E-04		156
-7	71.000		1.040		1.51E-03	152
-8	71.000	0.800		9.58E-04		144

Odd Numbers denote adjacent crystals at the DIFFERENT resonance frequencies than the Center. Even numbers denote crystals at the SAME frequency as the Center.
The reference used for data normalization was the smallest input voltage of 0.085 V.
The input voltage range spans from 0.085V to 71V or 58db for all measurements.

RESONA
FQ

Fundamental

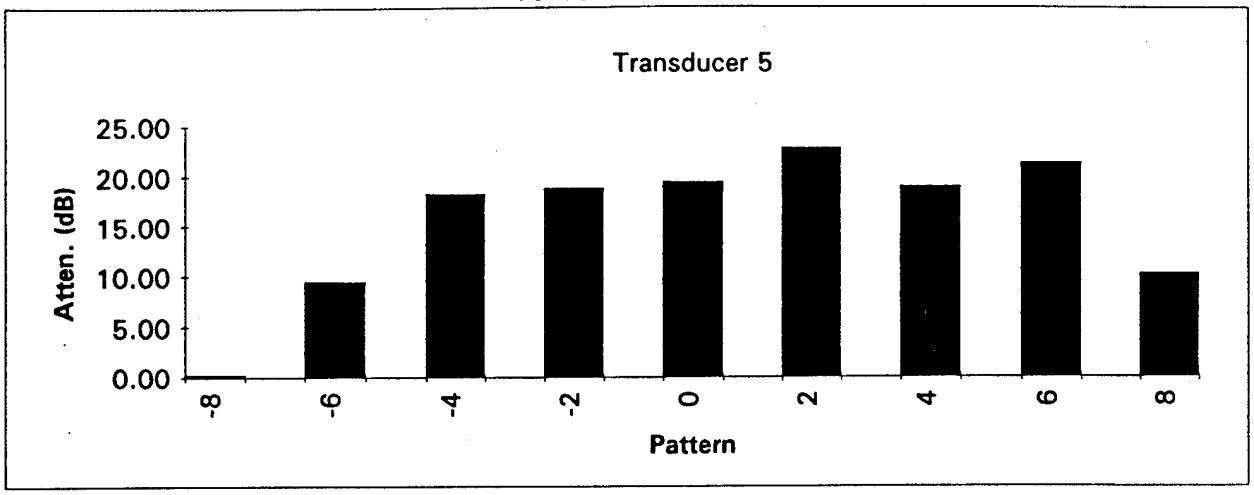

Harmonic

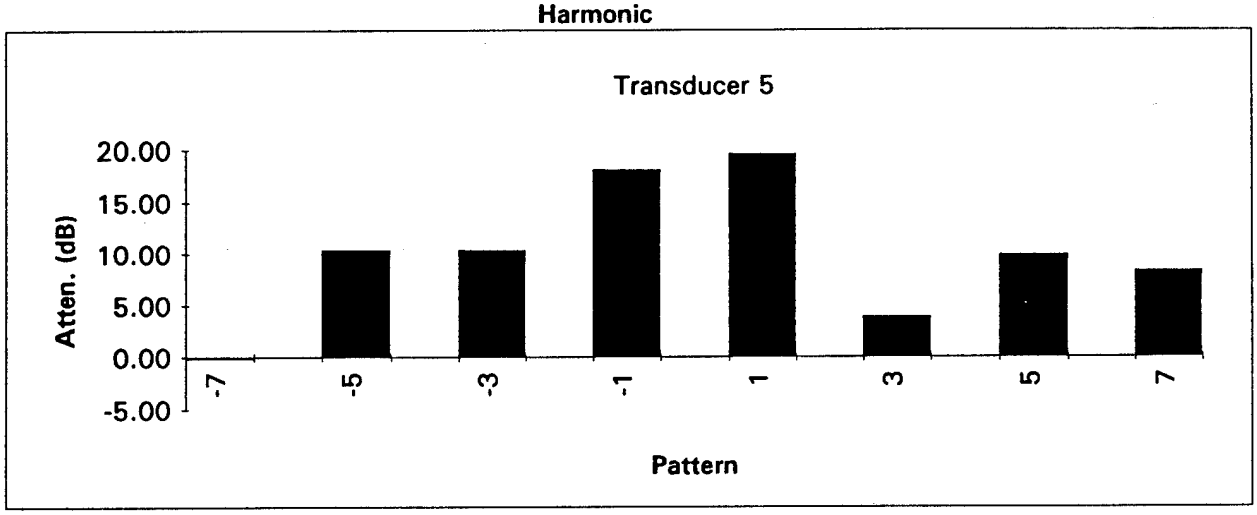

RESONA
FQ

Transducer 5 without Breast Target

	Actual Input Voltage	Actual Fundamental Voltage	Actual Harmonic Voltage	Normalized Fundamental Voltage	Normalized Harmonic Voltage	Transmission Time microsec.
8	71.000	1.70		2.04E-03		144
7	71.000		2.30		2.75E-03	152
6	71.000	1.60		1.92E-03		154
5	71.000		1.24		1.48E-03	158
4	71.000	6.40		7.66E-03		162
3	71.000		2.00		2.39E-03	164
2	2.400	2.00		7.08E-02		168
1	2.400		1.80		6.38E-02	168
Center	0.103	6.80		5.61E+00		168
-1	2.400		1.60		5.67E-02	168
-2	2.400	2.40		8.50E-02		168
-3	71.000		1.25		1.50E-03	166
-4	15.000	3.40		1.93E-02		162
-5	71.000		1.36		1.63E-03	158
-6	15.000	2.10		1.19E-02		156
-7	71.000		4.30		5.15E-03	152
-8	71.000	4.00		4.79E-03		150

Transducer 5 with Breast Target

	Actual Input Voltage	Actual Fundamental Voltage	Actual Harmonic Voltage	Normalized Fundamental Voltage	Normalized Harmonic Voltage	Transmission Time microsec.
8	71.000	1.650		1.98E-03		144
7	71.000		2.350		2.81E-03	152
6	71.000	0.540		6.46E-04		154
5	71.000		0.310		4.50E-04	160
4	71.000	0.780		9.34E-04		162
3	71.000		0.500		7.25E-04	164
2	71.000	6.700		8.02E-03		166
1	71.000		5.500		7.98E-03	168
Center	0.500	3.500		5.95E-01		166
-1	71.000		4.100		5.95E-03	168
-2	71.000	5.100		6.11E-03		166
-3	71.000		0.660		9.57E-04	164
-4	71.000	1.800		2.15E-03		162
-5	71.000		0.360		5.22E-04	160
-6	71.000	0.860		1.03E-03		154
-7	71.000		1.360		1.97E-03	150
-8	71.000	1.240		1.48E-03		144

Odd Numbers denote adjacent crystals at the DIFFERENT resonance frequencies than the Center. Even numbers denote crystals at the SAME frequency as the Center.
The reference used for data normalization was the smallest input voltage of 0.085 V.
The input voltage range spans from 0.085V to 71V or 58db for all measurements.

RESONANT
FQ.

Fundamental

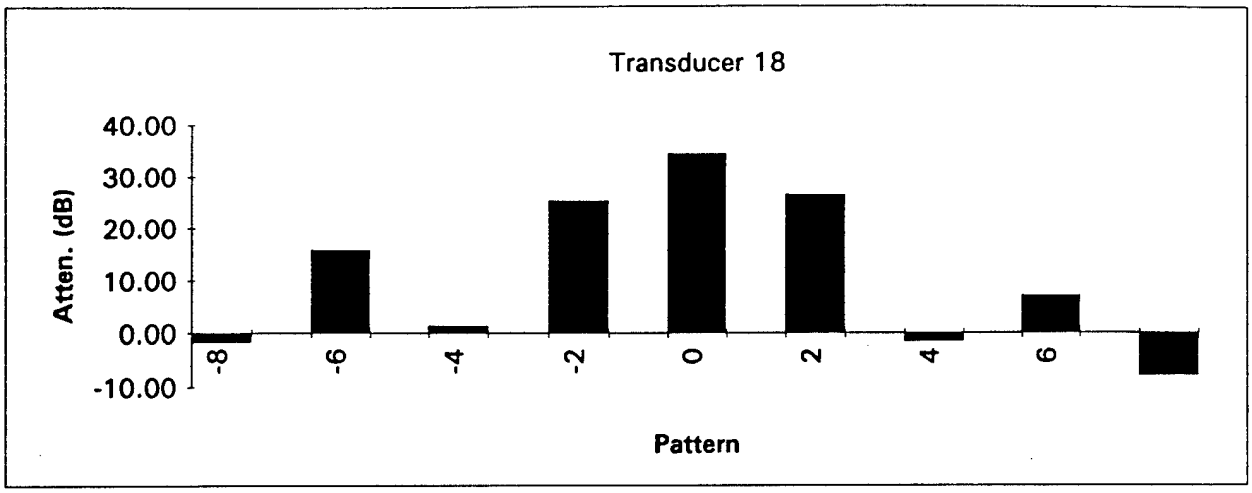

Harmonic

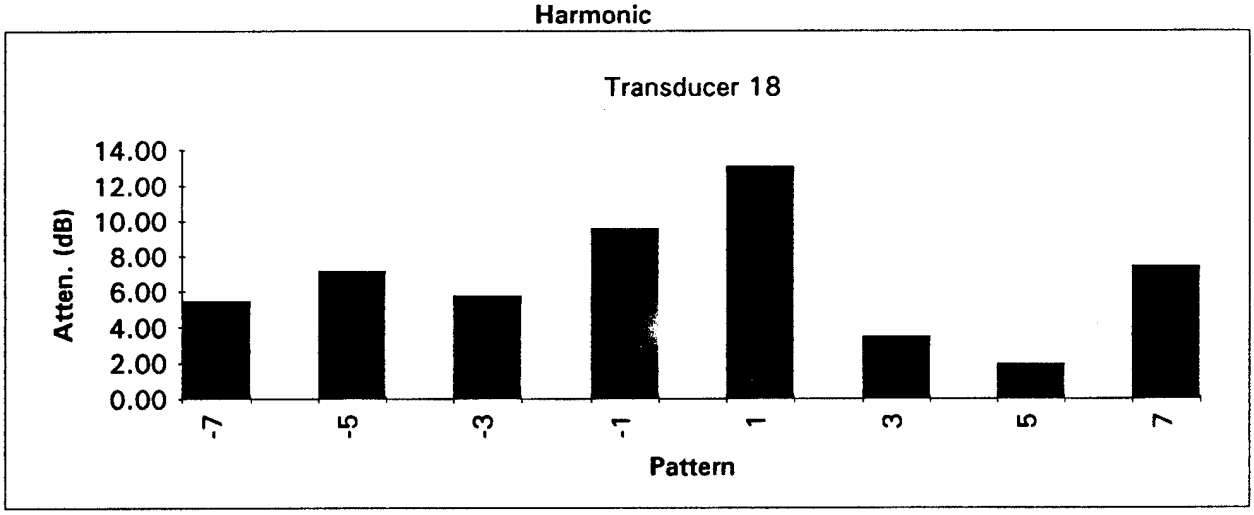

RESONANT FQ

Transducer 18 without Breast Target

	Actual Input Voltage	Actual Fundamental Voltage	Actual Harmonic Voltage	Normalized Fundamental Voltage	Normalized Harmonic Voltage	Transmission Time microsec.
8	63.000	0.56		7.56E-04		144
7	63.000		1.20		1.62E-03	152
6	63.000	1.80		2.43E-03		154
5	63.000		1.30		1.75E-03	160
4	63.000	0.80		1.08E-03		162
3	63.000		1.55		2.09E-03	166
2	12.000	5.50		3.90E-02		168
1	12.000		1.60		1.13E-02	167
Center	0.085	5.80		5.80E+00		167
-1	12.000		2.40		1.70E-02	168
-2	12.000	6.00		4.25E-02		168
-3	63.000		1.30		1.75E-03	164
-4	63.000	0.72		9.71E-04		161
-5	63.000		0.76		1.03E-03	160
-6	63.000	0.52		7.02E-04		154
-7	63.000		2.50		3.37E-03	154
-8	63.000	0.76		1.03E-03		150

Transducer 18 with Breast Target

	Actual Input Voltage	Actual Fundamental Voltage	Actual Harmonic Voltage	Normalized Fundamental Voltage	Normalized Harmonic Voltage	Transmission Time microsec.
8	63.000	0.68		9.17E-04		144
7	63.000		0.64		8.63E-04	150
6	63.000	0.29		3.91E-04		158
5	63.000		0.47		7.68E-04	164
4	63.000	0.68		9.17E-04		166
3	63.000		0.66		1.08E-03	166
2	63.000	1.56		2.10E-03		166
1	63.000		2.30		3.76E-03	166
Center	2.000	2.60		1.11E-01		168
-1	63.000		2.30		3.76E-03	167
-2	63.000	1.50		2.02E-03		167
-3	63.000		0.72		1.18E-03	167
-4	63.000	0.86		1.16E-03		164
-5	63.000		0.50		8.17E-04	164
-6	63.000	0.23		3.10E-04		153
-7	63.000		0.88		1.44E-03	152
-8	63.000	1.90		2.56E-03		150

Odd Numbers denote adjacent crystals at the DIFFERENT resonance frequencies than the Center. Even numbers denote crystals at the SAME frequency as the Center.
The reference used for data normalization was the smallest input voltage of 0.085 V.
The input voltage range spans from 0.085V to 71V or 58db for all measurements.

RESONANT FQ.

Fundamental

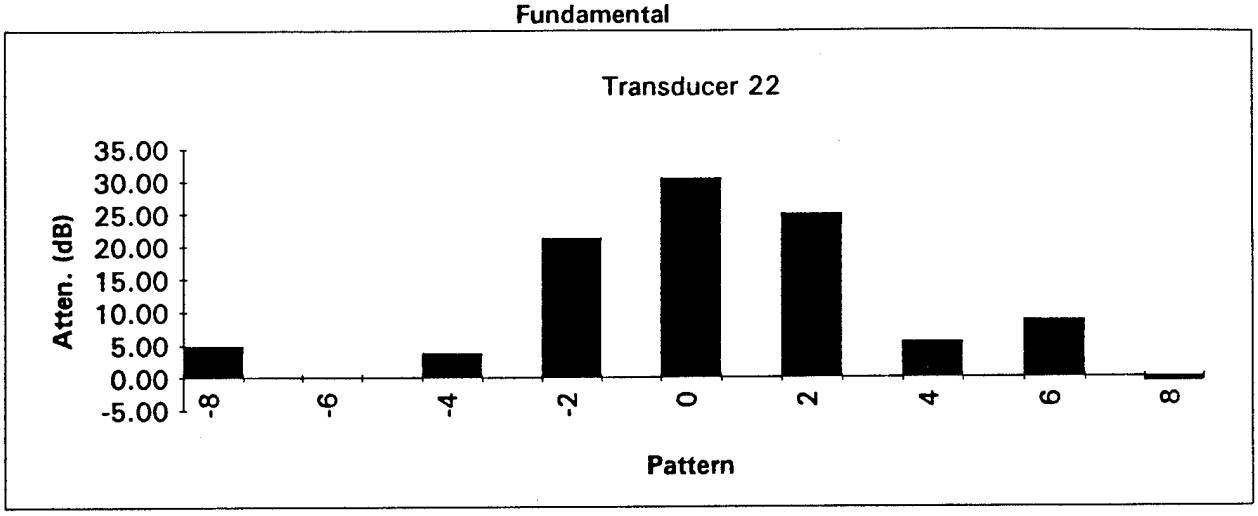

Harmonic

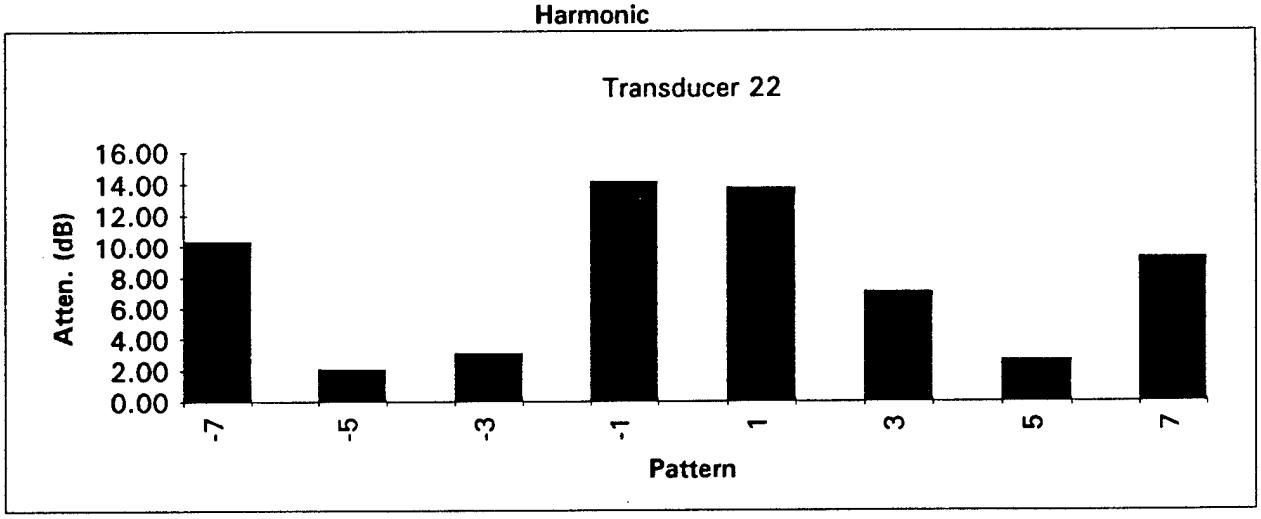

RESONANT FQ.

Transducer 22 without Breast Target

	Actual Input Voltage	Actual Fundamental Voltage	Actual Harmonic Voltage	Normalized Fundamental Voltage	Normalized Harmonic Voltage	Transmission Time microsec.
8	63.000	1.55		2.09E-03		148
7	63.000		2.50		3.37E-03	150
6	63.000	0.48		6.48E-04		156
5	63.000		0.80		1.08E-03	160
4	63.000	1.40		1.89E-03		161
3	63.000		1.04		1.40E-03	164
2	12.000	2.50		1.77E-02		166
1	12.000		3.00		2.13E-02	167
Center	0.085	3.00		3.00E+00		167
-1	12.000		1.80		1.28E-02	167
-2	12.000	3.80		2.69E-02		166
-3	63.000		1.80		2.43E-03	167
-4	63.000	1.80		2.43E-03		162
-5	63.000		1.05		1.42E-03	160
-6	63.000	0.88		1.19E-03		154
-7	63.000		3.70		4.99E-03	154
-8	63.000	0.68		9.17E-04		146

Transducer 22 with Breast Target

	Actual Input Voltage	Actual Fundamental Voltage	Actual Harmonic Voltage	Normalized Fundamental Voltage	Normalized Harmonic Voltage	Transmission Time microsec.
8	63.000	0.88		1.19E-03		148
7	63.000		0.76		1.03E-03	154
6	63.000	0.48		6.48E-04		164
5	63.000		0.52		8.50E-04	164
4	63.000	0.90		1.21E-03		166
3	63.000		0.60		9.81E-04	167
2	63.000	1.12		1.51E-03		166
1	63.000		2.55		4.17E-03	166
Center	2.000	2.10		8.93E-02		166
-1	63.000		1.60		2.62E-03	167
-2	63.000	1.12		1.51E-03		167
-3	63.000		0.66		1.08E-03	166
-4	63.000	0.96		1.30E-03		166
-5	63.000		0.64		1.05E-03	164
-6	63.000	0.32		4.32E-04		154
-7	63.000		1.05		1.72E-03	152
-8	63.000	0.74		9.98E-04		144

Odd Numbers denote adjacent crystals at the DIFFERENT resonance frequencies than the Center. Even numbers denote crystals at the SAME frequency as the Center.
The reference used for data normalization was the smallest input voltage of 0.085 V.
The input voltage range spans from 0.085V to 71V or 58db for all measurements.

FQ
VARIED

Fundamental

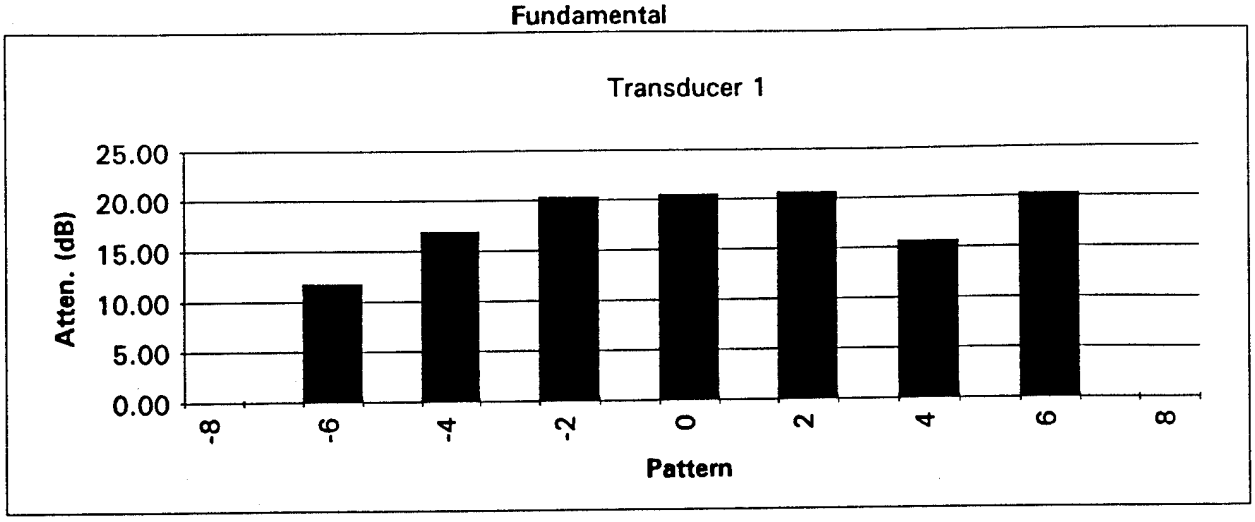

Harmonic

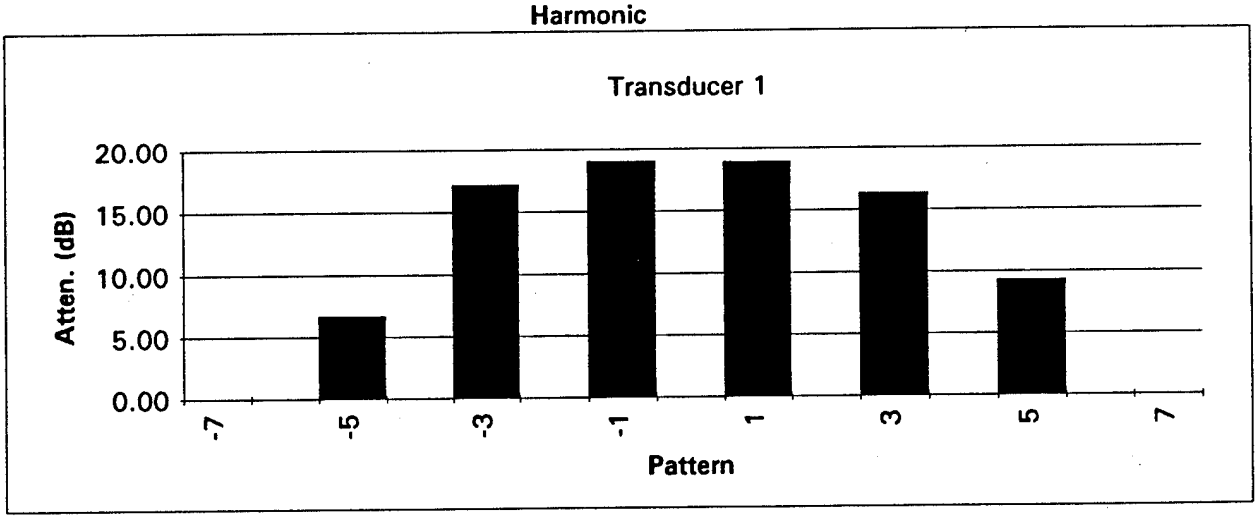

Fundamental and Harmonic

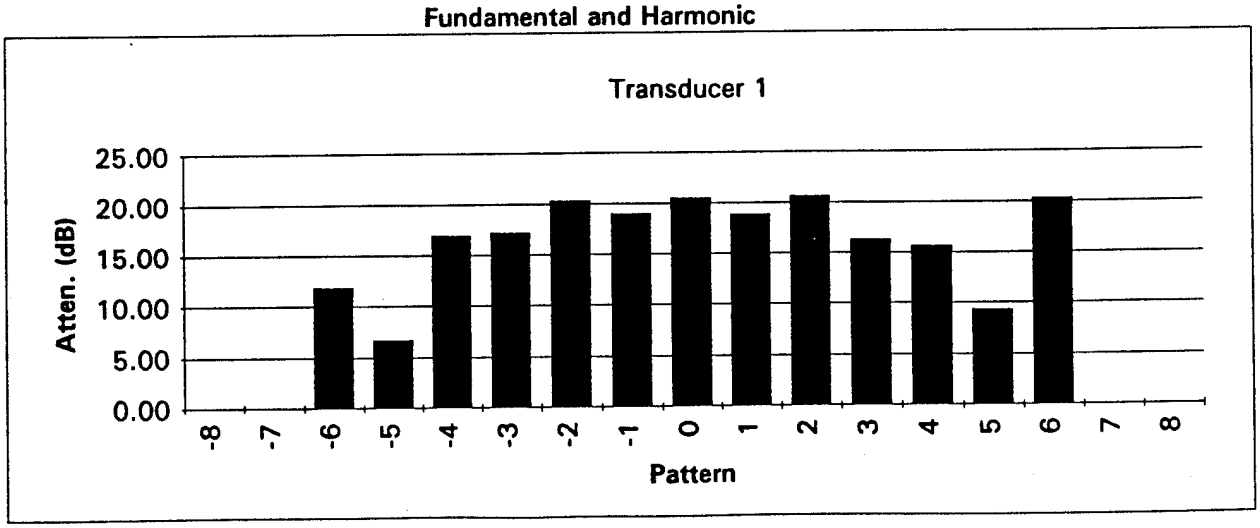

FQ
VARIED

Transducer 1 without Breast Target

	Actual Input Voltage	Actual Fundamental Voltage	Actual Harmonic Voltage	Normalized Fundamental Voltage	Normalized Harmonic Voltage	Transmission Time microsec.
8				#DIV/0!		
7					#DIV/0!	
6	13.500	1.85		1.16E-02		
5	68.000		1.70		2.13E-03	
4	13.500	1.80		1.13E-02		
3	68.000		1.90		2.38E-03	
2	1.400	3.80		2.31E-01		
1	13.500		5.40		3.40E-02	
Center	0.103	7.00		5.78E+00		
-1	13.500		4.70		2.96E-02	000
-2	1.400	4.20		2.55E-01		000
-3	68.000		2.10		2.63E-03	000
-4	68.000	5.20		6.50E-03		000
-5	68.000		1.10		1.38E-03	000
-6	13.500	1.70		1.07E-02		000
-7	0.000				#DIV/0!	000
-8	0.000			#DIV/0!		000

Transducer 1 with Breast Target

	Actual Input Voltage	Actual Fundamental Voltage	Actual Harmonic Voltage	Normalized Fundamental Voltage	Normalized Harmonic Voltage	Transmission Time microsec.
8				#DIV/0!		
7					#DIV/0!	
6	68.000	0.90		1.13E-03		
5	68.000		0.48		7.27E-04	
4	68.000	1.50		1.88E-03		
3	68.000		0.24		3.64E-04	
2	13.500	3.40		2.14E-02		
1	68.000		2.55		3.86E-03	
Center	0.500	3.20		5.44E-01		
-1	68.000		2.20		3.33E-03	000
-2	13.500	3.90		2.46E-02		000
-3	68.000		0.24		3.64E-04	000
-4	68.000	0.74		9.25E-04		000
-5	68.000		0.42		6.36E-04	000
-6	68.000	2.20		2.75E-03		000
-7	0.000				#DIV/0!	000
-8	0.000			#DIV/0!		000

Odd Numbers denote adjacent crystals at the DIFFERENT resonance frequencies than the Center. Even numbers denote crystals at the SAME frequency as the Center.
The reference used for data normalization was the smallest input voltage of 0.085 V.
The input voltage range spans from 0.085V to 71V or 58db for all measurements.

FQ
VARIED

Fundamental

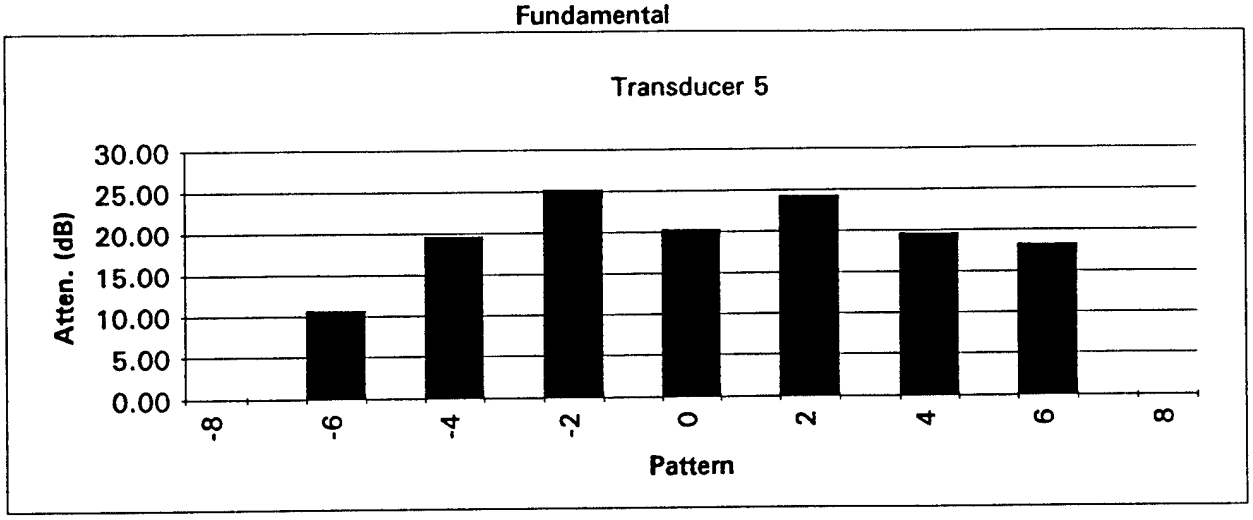

Harmonic

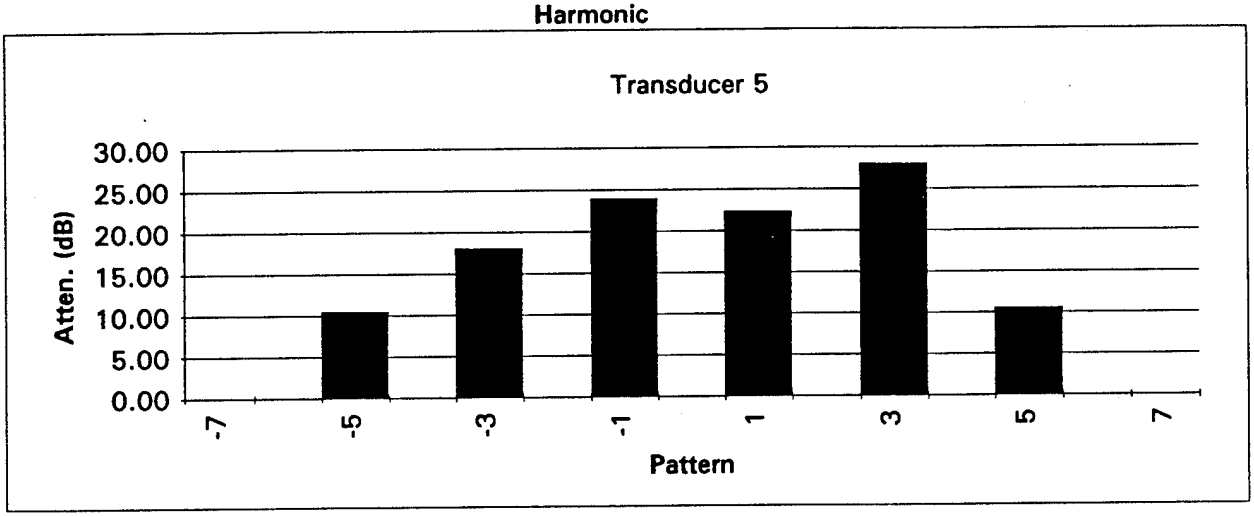

Fundamental and Harmonic

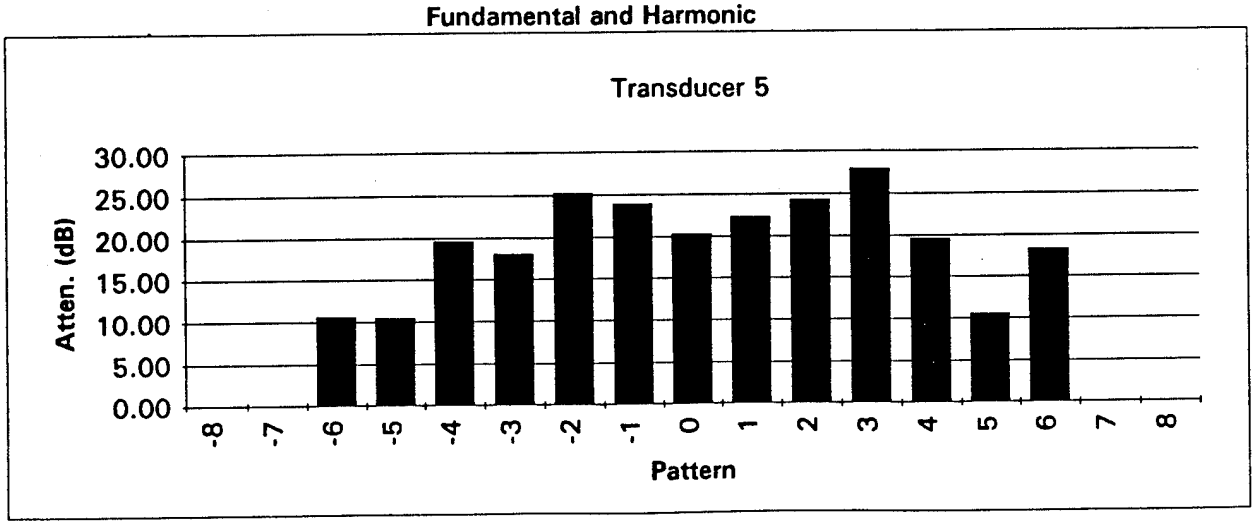

Fc
VAR

Transducer 5 without Breast Target

	Actual Input Voltage	Actual Fundamental Voltage	Actual Harmonic Voltage	Normalized Fundamental Voltage	Normalized Harmonic Voltage	Transmission Time microsec.
8				#DIV/0!		
7					#DIV/0!	
6	13.500	1.30		8.19E-03		154
5	68.000		2.45		3.06E-03	158
4	13.500	1.60		1.01E-02		162
3	13.500		1.80		1.13E-02	165
2	1.400	3.40		2.06E-01		168
1	1.400		1.70		1.03E-01	168
Center	0.103	6.80		5.61E+00		168
-1	1.400		1.65		1.00E-01	168
-2	1.400	3.60		2.19E-01		168
-3	68.000		2.70		3.38E-03	164
-4	13.500	3.60		2.27E-02		162
-5	68.000		2.35		2.94E-03	158
-6	13.500	1.90		1.20E-02		154
-7	0.000				#DIV/0!	000
-8	0.000			#DIV/0!		000

Transducer 5 with Breast Target

	Actual Input Voltage	Actual Fundamental Voltage	Actual Harmonic Voltage	Normalized Fundamental Voltage	Normalized Harmonic Voltage	Transmission Time microsec.
8				#DIV/0!		
7					#DIV/0!	
6	68.000	0.80		1.00E-03		154
5	68.000		0.60		9.09E-04	160
4	68.000	0.84		1.05E-03		161
3	68.000		0.30		4.54E-04	165
2	13.500	2.00		1.26E-02		167
1	68.000		5.20		7.88E-03	168
Center	0.500	3.20		5.44E-01		168
-1	68.000		4.20		6.36E-03	168
-2	13.500	1.90		1.20E-02		167
-3	68.000		0.28		4.24E-04	166
-4	68.000	1.90		2.38E-03		161
-5	68.000		0.58		8.79E-04	160
-6	68.000	2.80		3.50E-03		158
-7	0.000				#DIV/0!	000
-8	0.000			#DIV/0!		000

Odd Numbers denote adjacent crystals at the DIFFERENT resonance frequencies than the Center. Even numbers denote crystals at the SAME frequency as the Center.
The reference used for data normalization was the smallest input voltage of 0.085 V.
The input voltage range spans from 0.085V to 71V or 58db for all measurements.

F
VARIE

Fundamental

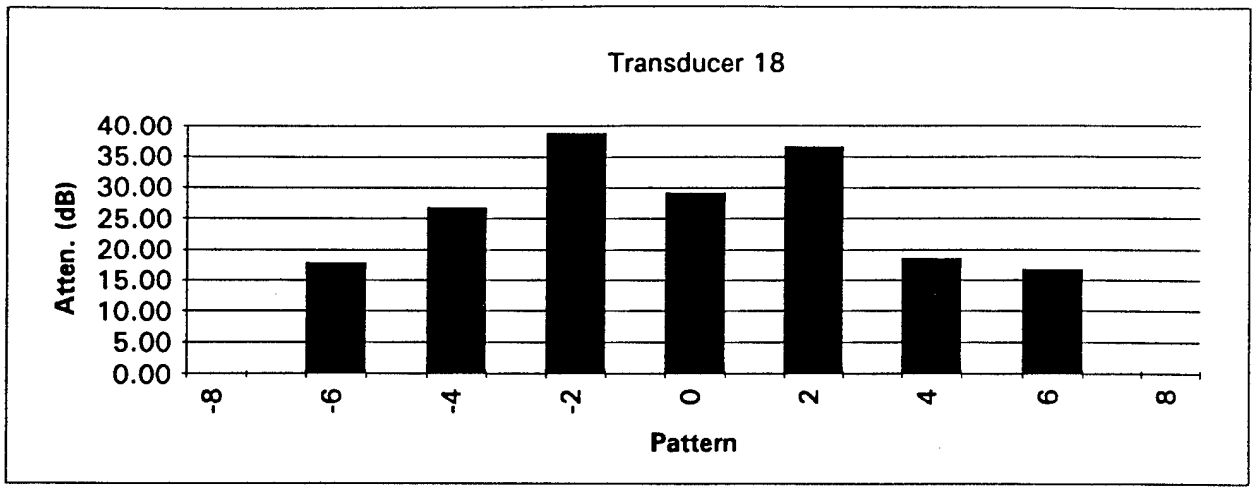

Harmonic

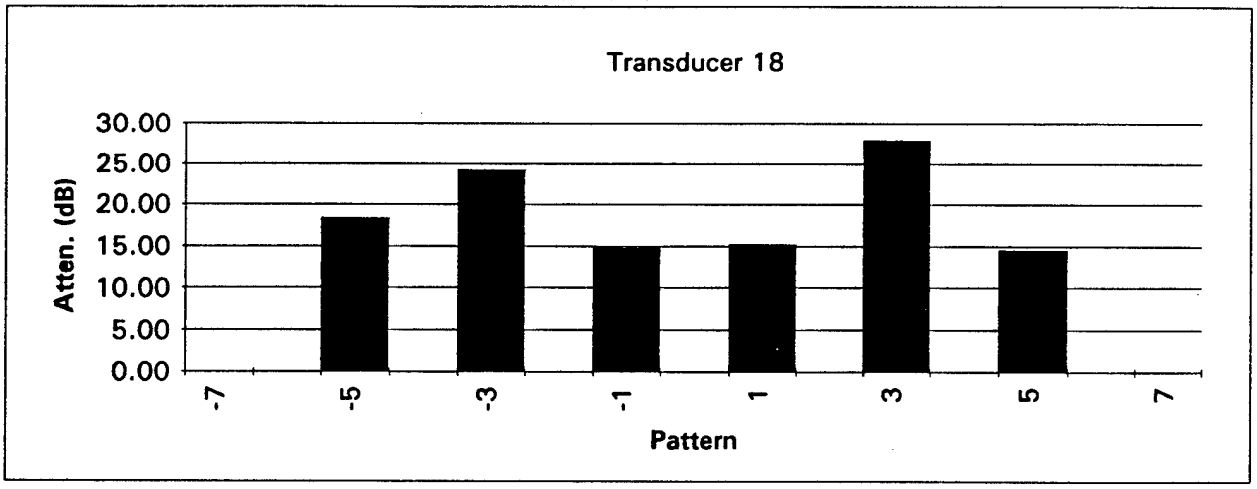

Fundamental and Harmonic

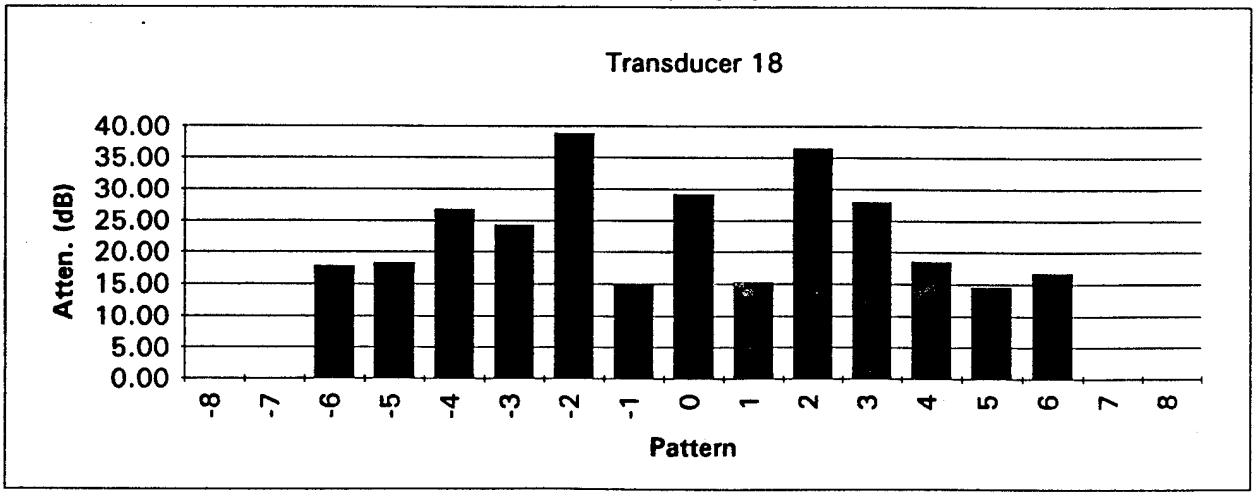

Fq
VARIED

Transducer 18 without Breast Target

	Actual Input Voltage	Actual Fundamental Voltage	Actual Harmonic Voltage	Normalized Fundamental Voltage	Normalized Harmonic Voltage	Transmission Time microsec.
8				#DIV/0!		
7					#DIV/0!	
6	63.000	1.10		1.48E-03		158
5	63.000		3.60		4.86E-03	158
4	63.000	1.10		1.48E-03		162
3	63.000		6.00		8.10E-03	164
2	12.000	4.10		2.90E-02		167
1	2.000		2.10		8.93E-02	168
Center	0.085	3.00		3.00E+00		168
-1	2.000		1.20		5.10E-02	168
-2	12.000	4.00		2.83E-02		168
-3	63.000		6.30		8.50E-03	165
-4	63.000	2.60		3.51E-03		162
-5	63.000		1.60		2.16E-03	158
-6	63.000	1.40		1.89E-03		158
-7	0.000				#DIV/0!	000
-8	0.000			#DIV/0!		000

Transducer 18 with Breast Target

	Actual Input Voltage	Actual Fundamental Voltage	Actual Harmonic Voltage	Normalized Fundamental Voltage	Normalized Harmonic Voltage	Transmission Time microsec.
8				#DIV/0!		
7					#DIV/0!	
6	63.000	0.16		2.16E-04		158
5	63.000		0.56		9.16E-04	158
4	63.000	0.13		1.75E-04		164
3	63.000		0.20		3.27E-04	166
2	63.000	0.32		4.32E-04		167
1	12.000		1.80		1.55E-02	168
Center	2.000	2.45		1.04E-01		168
-1	63.000		5.70		9.32E-03	168
-2	63.000	0.24		3.24E-04		167
-3	63.000		0.32		5.23E-04	166
-4	63.000	0.12		1.62E-04		165
-5	63.000		0.16		2.62E-04	162
-6	63.000	0.18		2.43E-04		156
-7	0.000				#DIV/0!	000
-8	0.000			#DIV/0!		000

Odd Numbers denote adjacent crystals at the DIFFERENT resonance frequencies than the Center. Even numbers denote crystals at the SAME frequency as the Center.
The reference used for data normalization was the smallest input voltage of 0.085 V.
The input voltage range spans from 0.085V to 71V or 58db for all measurements.

Fundamental

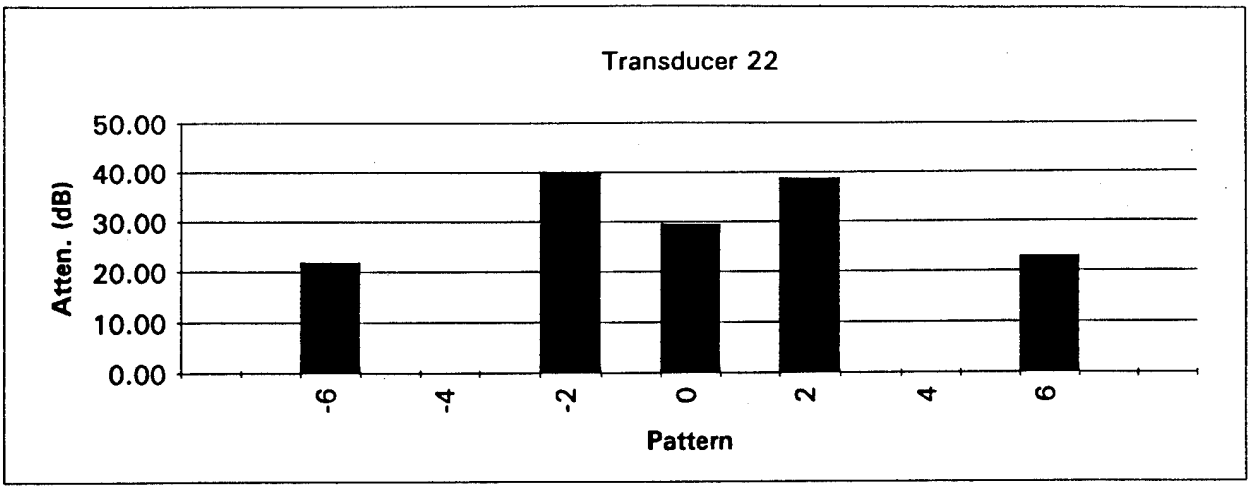

Harmonic

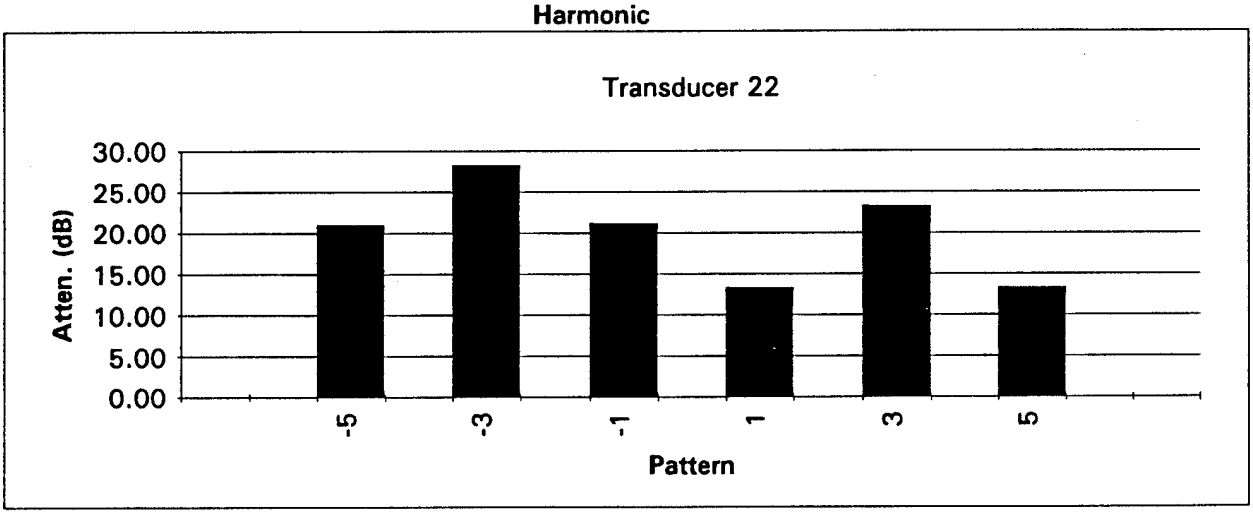

Fundamental and Harmonic

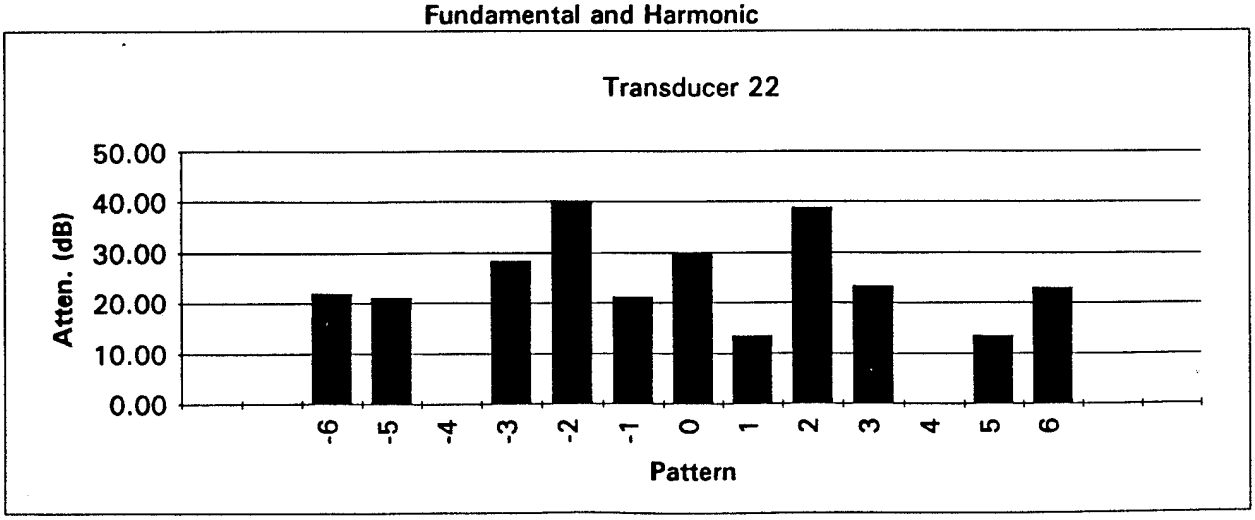

PQ
VARIED

Transducer 22 without Breast Target

	Actual Input Voltage	Actual Fundamental Voltage	Actual Harmonic Voltage	Normalized Fundamental Voltage	Normalized Harmonic Voltage	Transmission Time microsec.
6	63.000	1.40		1.89E-03		160
5	63.000		3.60		4.86E-03	162
4	63.000	1.10		1.48E-03		164
3	63.000		5.30		7.15E-03	166
2	12.000	6.00		4.25E-02		168
1	2.000		3.00		1.28E-01	168
Center	0.085	1.30		1.30E+00		168
-1	2.000		0.90		3.83E-02	168
-2	12.000	5.80		4.11E-02		167
-3	12.000		3.00		2.13E-02	166
-4	63.000	1.70		2.29E-03		164
-5	63.000		4.60		6.21E-03	162
-6	63.000	2.50		3.37E-03		154

Transducer 22 with Breast Target

	Actual Input Voltage	Actual Fundamental Voltage	Actual Harmonic Voltage	Normalized Fundamental Voltage	Normalized Harmonic Voltage	Transmission Time microsec.
6	63.000	0.10		1.35E-04		160
5	63.000		0.64		1.05E-03	162
4	63.000			0.00E+00		164
3	63.000		0.30		4.90E-04	166
2	63.000	0.36		4.86E-04		168
1	12.000		3.20		2.75E-02	168
Center	12.000	6.10		4.32E-02		168
-1	63.000		2.05		3.35E-03	168
-2	63.000	0.30		4.05E-04		167
-3	63.000		0.50		8.17E-04	166
-4	63.000			0.00E+00		166
-5	63.000		0.34		5.56E-04	162
-6	63.000	0.20		2.70E-04		154

Odd Numbers denote adjacent crystals at the DIFFERENT resonance frequencies than the Center. Even numbers denote crystals at the SAME frequency as the Center.
The reference used for data normalization was the smallest input voltage of 0.085 V.
The input voltage range spans from 0.085V to 71V or 58db for all measurements.

Appendix G

Protocol and Consent Form
for a Phase I - Device Evaluation Study
for Breast Ultrasound Therapy System

Title: Radiation and Thermal Therapy for Extensive Intraductal Carcinoma

DANA-FARBER
CANCER INSTITUTE

44 Binney Street, Boston, MA 02115

PROTOCOL ADMINISTRATION OFFICE
Tel: 617-632-3029
Fax: 617-632-2655

THE JIMMY FUND

CURRENT ISSUE: _____

GROUP #: None
SPONSOR: U.S. Army R&D
IND/IDE #: _____

PROTOCOL NUMBER*: 95-006

PROTOCOL NICKNAME: RT and HT for Breast Cancer

PROTOCOL NAME: Radiation and Thermal Therapy for Extensive Intraductal Carcinoma

PHASE OF STUDY: I

DRUGS: None

DFCI STUDY CHAIRPERSON(S):
Bruce A. Bornstein, MD
Jay R. Harris, MD

OTHER INVESTIGATORS:
Everette C. Burdette, PhD
Jorgen L. Hansen, MSc
Daniel F. Hayes, MD
Xing-Qi Lu, PhD
Kathleen J. Propert, ScD
Abram Recht, MD
Kitt Shaffer, MD, PhD
Charles L. Shapiro, MD
Goran K. Svensson, PhD
Deborah L. Toppmeyer. MD

INSTITUTIONAL PARTICIPANTS:

DFCI INPATIENT	____
DFCI ADULT CLINIC	X
DFCI PEDIATRIC CLINIC	____
CHILDREN'S HOSPITAL	____
BRIGHAM & WOMEN'S	____
BETH ISRAEL	____
DEACONESS HOSPITAL	X
HARVARD COMM. HEALTH	____

OTHER INSTITUTIONS:
Joint Center for Radiation Therapy

APPROVED FOR CCOP USE? ____
RANDOMIZED? ____

TARGET POPULATIONS:

ADULT PATIENTS	X
PEDIATRIC PATIENTS	____
VOLUNTEERS:	
Pediatric	____
Adult	____

MODALITIES:

RADIATION THERAPY	X
CHEMOTHERAPY	____
SURGERY	____
BONE MARROW TRANSPLANTATION	____
QUALITY OF LIFE	____
HYPERTHERMIA	X

SCHEMA

PHASE I

DEVICE EVALUATION STUDY

Radiation and Thermal Therapy for Extensive Intraductal Carcinoma

(in patients undergoing definitive radiation therapy for breast cancer)

Patients with: Infiltrating ductal carcinoma of the breast with an extensive intraductal component (EIC ⊕) **or** Ductal carcinoma in situ (DCIS) of the breast **&** • re-excision with residual tumor • positive or close (<2 mm) margins	REGISTER	**Radiation Therapy** 6100 cGy / 6 weeks + **Hyperthermia** T =40-43 °C X 45 min. x 2 Tx (no target volume temperature ≥ 43 °C)

TABLE OF CONTENTS

1.0 INTRODUCTION

The use of radiation therapy in combination with breast-conserving surgery has been established as a standard option for patients with early-stage breast cancer (1). The goal of this approach is to eradicate the cancer locally and to preserve the cosmetic appearance of the breast. This is achieved by resecting the tumor in the breast and using moderate doses of irradiation to destroy any remaining cancer cells in the breast. Randomized studies have demonstrated equivalent survival for patients treated with mastectomy and with breast conserving surgery and irradiation (2, 3).

1.1 Invasive Breast Cancer

Local recurrence of the cancer following breast-conserving treatment is seen in about 10 -15% of cases and, most commonly, these recurrences are treated by mastectomy (4). Studies from our institution, and elsewhere, have demonstrated that the likelihood of local recurrence is related to the presence and extent of the intraductal component of the cancer (5-9). Those cancers with an extensive intraductal component (EIC) have a much higher risk of local recurrence compared with those without an EIC. Boyages and colleagues at the Joint Center for Radiation Therapy (JCRT) found a recurrence rate of 26% (43/166) for patients with EIC-positive tumors compared to 7% (29/418) for EIC-negative tumors (p=0.0001) (9). Schnitt reviewed 181 patients treated at the JCRT with conservative surgery and radiation therapy and whose final microscopic margins of resection were evaluable (10). No recurrences were observed in 18 patients with EIC-positive cancers with negative, close, or focally positive margins. However, among 12 EIC-positive patients with more than focally positive margins (cancer present at the margins in more than three low-power fields) 50% had a true recurrence or marginal miss. On the basis of these findings, the use of breast conserving treatment in patients with cancer containing an EIC and more than focally positive margins is not recommended. Most commonly, these patients are treated by mastectomy.

1.2 Non-Invasive Breast Cancer

Ductal carcinoma in situ, (intraductal carcinoma, DCIS) is a heterogeneous group of lesions whose common histologic feature is the proliferation of presumably malignant epithelial cells confined to the mammary ducts and lobules <u>without demonstrable evidence of invasion</u> through the basement membrane into the surrounding stroma. The treatment options for woman with DCIS include mastectomy, conservative surgery (CS) and radiation therapy (RT), or conservative surgery alone. Mastectomy for DCIS is associated with excellent disease-free and overall survival but, as with invasive cancers many women desire breast conservation. However, little information is available on the long-term results of breast-conserving treatment with either conservative surgery alone or conservative surgery combined with radiotherapy.

The NSABP B-17 trial is the only randomized study comparing CS with CS & RT that has reported results (59). With relatively short follow-up (mean, 43 months), the 5-year actuarial risk of local failure was 20.9% in 391 patients treated with CS alone, compared to 10.4% in 399 patients treated with CS & RT.

Figure 1 shows the results of treatment. The length of follow-up and the number of patients treated is limited, however these results suggest that there is a high risk of local recurrence over time. Overall, 50% of the recurrences were invasive. The results also suggest that RT reduces the rate of local recurrence. Possible prognostic factors (e.g., histology) have not been analyzed in this series yet. Similar findings have been found in single institution retrospective studies of either conservative surgery alone or conservative surgery and radiation therapy (11-14).

Figure 1.

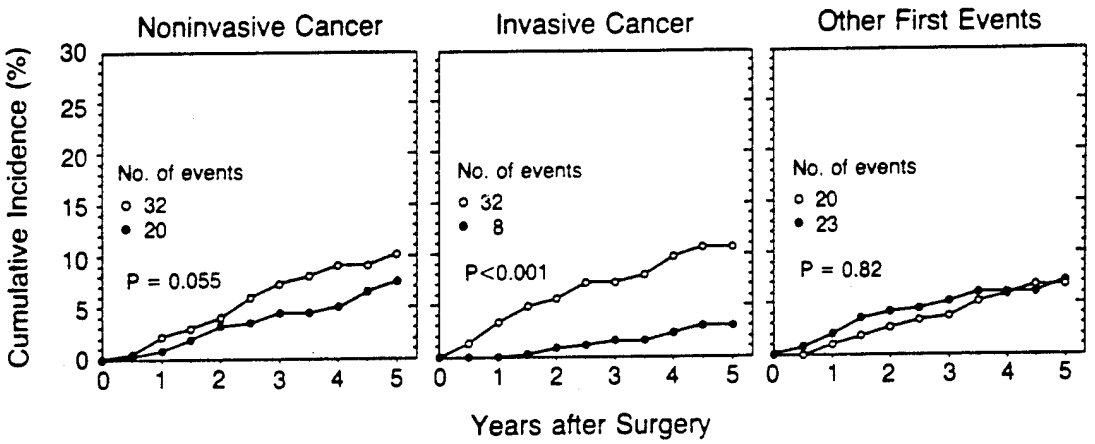

Cumulative Incidence of Noninvasive and Invasive Ipsilateral Breast Cancers and of All Other First Events in Women Treated by Lumpectomy (C) or Lumpectomy and Radiation Therapy (●).
P values are for the comparisons of average annual incidence rates between treatment groups.

from Fisher et al. (59)

1.3 Why are breast cancers containing intraductal carcinoma less effectively managed by radiation therapy?

Breast conserving treatment is an important option for many women with breast cancer. Invasive breast cancers with an EIC or pure non-invasive intraductal breast cancers have a much higher risk of local recurrence as compared to breast cancers without these histologies. Prior experience has shown that breast cancers with an intraductal component are less effectively managed by radiation therapy (4-14).

The reason for the association between pure DCIS or an EIC-postive invasive breast cancer and recurrence are not well established. There is some evidence to suggest that these cancers may be more extensive in the breast than other cancers and that the doses of irradiation consistent with maintaining the cosmetic appearance is

often insufficient to destroy the numerous remaining cancer cells in these patients (5). It has also been noted that intraductal carcinoma is characterized by proliferation of cancer cells within breast ducts typically showing central necrosis. Lindley, et al., examined the histologic features predictive for an increased risk of early local recurrence in 272 patients after treatment with conservative surgery and radiation therapy with pathologic data available (8). In 213 EIC-negative patients 21 (10%) had local recurrence compared to 13 of 59 patients (22%) with EIC-positive cancers. Furthermore, when the EIC-positive group was examined for the presence of extensive necrosis (comedonecrosis), they found that the recurrence rate was 50% (9/18) in this subgroup compared to 10% (4/41) for the group without extensive necrosis. This necrosis is related to the absence of blood supply within the ducts and has been shown to correspond to hypoxemic regions based on the calculation of oxygen diffusion (15). This is in agreement with evidence that even in microscopic tumors there can be hypoxic areas ($pO_2 < 12$ mmHg) (16). Since hypoxia is known to increase radioresistance by as much as a factor of 3, it is possible that this may account, in part, for the poor results seen with irradiation in these patients (17, 18). Okunieff et al., recently reported that tumor oxygenation alone was sufficient to account for the slope of the observed dose response curve for human breast carcinoma (60). Moreover, the oxygen tension distribution is a critical modifier of radiation treatment response.

It is also known that heat is effective at killing cells in an hypoxic environment (18-21). In fact, the synergistic effect of heat and radiation on hypoxic tumor cells both *in vivo* and *in vitro* has been well demonstrated (19, 22, 23). Most studies find a greater interaction between these modalities when x-rays and heat are delivered as close together as possible, but potentiation is seen even for treatments given greater than an hour apart (23-25). Thus, patients with extensive amounts intraductal carcinoma may significantly benefit from a combined approach using thermal therapy and irradiation.

It is reasonable to anticipate that combined use of thermal therapy and radiation therapy may be more effective than radiation therapy alone (19, 22). Thus, it is of great clinical significance that this combined treatment approach extends breast conserving therapy to high risk breast cancer patients, offering the prospect of avoiding mastectomy for many patients.

1.4 Hyperthermia

Hyperthermia is a potent radiosensitizing agent. It is the use of temperatures above 37 °C (98.6 °F) to treat tumors. Temperatures are typically prescribed in the range of 40 °C to 43 °C (104-109 °F) when hyperthermia is combined with radiation or drugs. The investigation of hyperthermia in the laboratory is extensive. Hyperthermia has been shown in vitro to kill tumor cells (26) and markedly sensitize cells to the cytotoxicity of radiation (27) and chemotherapy (28). Cells are particularly sensitive to hyperthermia when they are at low pH or when they have insufficient nutrition. These are environmental conditions that reduce cell killing by radiation (19-21).

This provides the rationale for the potential therapeutic gain when hyperthermia is used alone or with radiation therapy (29). In the clinic, the results using hyperthermia alone have been disappointing. This has been the basis of a shift away from the use of hyperthermia as a sole modality of cancer therapy to hyperthermia being used in conjunction with radiation therapy or chemotherapy (30-33). The majority of early clinical studies of hyperthermia were not concerned with the feasibility of a particular technical approach, but rather efficacy and toxicity. Therefore, the capability of many devices to deliver heat uniformly to a specific target volume is unknown. In addition, most clinical studies of hyperthermia were done before the development of hyperthermia quality assurance guidelines (34-36). Not only were many of the techniques of heating inadequate, but also the sparse and artifact prone thermometry to measure temperature was inadequate. Few devices were designed and manufactured to optimize therapy to a specific tumor site, but rather were designed as machines that could treat everything. These devices were claimed to treat most tumor sites, but unfortunately they treated no tumor site well. In the field of radiation oncology, linear accelerators can treat most sites remarkably well, however, there are some sites that demand modification of the accelerator to afford therapy tailored to that site; e.g., the brain leading to the development of stereotactic radiotherapy and radiosurgery. The same is even more true of hyperthermia given the limited depths of heat penetration and the effect of biologic parameters, such as blood flow, on heating ability. Despite the technical limitations of hyperthermia some conclusions can be drawn.

1.41 Hyperthermia for Breast Cancer

A major clinical use of hyperthermia in patients with breast cancer is the treatment of chest wall recurrence following mastectomy. The long-term local control rate of recurrent chest wall lesions using radiation therapy alone is less than 50%. The combination of hyperthermia with radiation therapy, for infiltrating carcinomas, has resulted in complete response rates of 57-93% (37-46), which are superior to those seen in many series using radiotherapy alone (47-53). For example, in a study by the Radiation Therapy Oncology Group (RTOG) of twice-weekly hyperthermia and radiotherapy (given in conventional fractionation to 60-66 Gy), complete regression was seen in 85% of patients (n=54) with locally recurrent breast cancer (39). Among the small number of patients followed for 2 years, complete response was maintained in nearly all evaluable patients. Lindholm and associates (40) reported on 11 patients with multiple superficial recurrent breast cancers. The complete response rate for 17 lesions treated with radiation therapy and hyperthermia was 65% compared to only 35% for 17 matched lesions given radiation alone ($p=0.0253$). Other investigators have reported similar results (41-46).

In summary, for gross tumor nodules (infiltrating carcinomas) response rates of 70% to over 90% have been reported in patients treated with low-dose radiotherapy and hyperthermia, with many or most patients achieving maintained complete response and acceptable complication rates (37, 38, 40-46, 54-56).

More recently Kapp and colleagues (57) reported on the use of thermoradiotherapy for residual microscopic infiltrating breast cancer after local regional recurrence. They treated 262 fields in 89 patients and had a 68% three-year actuarial local-control rate. The number of acute and long term complications was small. For example, blisters developed after only 22 of 445 treatments (5%) and were usually self-limited. This is the first clinical report to suggest that hyperthermia may be given in the adjuvant setting of recurrent breast cancer.

1.5 Clinical Study

Our specific goal is to develop the thermal therapy technologies required to optimize the synergistic efficacy between heat and radiation for patients with infiltrating breast cancer containing an extensive intraductal component or for patients with extensive pure intraductal carcinoma. The data suggests that intraductal carcinoma is frequently necrotic or associated with necrosis and that this may be secondary to hypoxia (8, 15, 16, 60). The hypoxic environment of intraductal carcinoma may explain the relative radioresistance of tumors with extensive amounts of intraductal tumor (17, 18). Since heat is effective at killing cells in an hypoxic environment it is reasonable to anticipate that combined use of hyperthermia and radiation therapy may be more effective than radiation therapy alone (18-24).

Thermal therapy of the breast will be accomplished by a site specific multi-transducer ultrasound array applicator, developed under contract with the U.S. Army, USAMRDC Contract # DAMD 17-93-C-3098. A description of the applicator is given in the next section. The specific clinical study we propose is a Phase I - Device Evaluation Study to establish our ability to safely deliver heat to the breast using this new device (58). The purpose is to determine if we can control heat delivery and deliver heat uniformly.

Once we have established our ability to uniformly heat the breast can we then begin a Phase I/II clinical study to establish a safe and effective treatment protocol for combining thermal therapy and irradiation. We will test the hypothesis that patients with breast cancer containing an extensive intraductal component or with extensive pure intraductal carcinoma will have a reduced risk for local recurrence from a combined and non-disfiguring treatment approach using irradiation and thermal therapy. It will be of great clinical significance if this combined treatment approach extends breast conserving therapy to high risk breast cancer patients, offering the prospect of avoiding mastectomy for many patients.

1.6 Hardware: Treatment System

The device consists of the hardware components illustrated in Figure 2. A breast site-specific cylindrical array applicator of ultrasound transducers is used for thermal therapy induction and for multiple monitoring functions. The "heart" of the

hardware consists of the cylindrical array of transducers that deposits power into the breast tissue for therapy and monitors the dynamic course of the treatment.

The ultrasound transducers are geometrically arranged and operated to provide several monitoring functions. One important monitoring function is to determine the breast contour and the location of the breast within the treatment cylinder.

The system consists of an Instrument Computer (Figure 2) which provides all direct control and data interaction with the RF power subsystem, receiver subsystem, transmit/receive/multiplexing modules, thermistor thermometry subsystem, and cooling subsystem. The system electronics, instrument computer, and cylindrical transducer array/treatment cavity are integrated into a patient table assembly/subsystem, which provides a comfortable treatment support for the patient, accurate positioning of the breast within the treatment cavity, and convenient means for consolidating system components and functions.

Figure 3 is a schematic of the patient support system. The RF power subsystem generates the drive power for the transducers during therapy and is used for pulse-echo imaging of the breast contour and for ultrasound velocity measurements during a brief period every 4 seconds when the therapy is gated "off." The transmit/receive/multiplexing modules select which transducers are active for receiving or transmitting at any given moment during therapy.

The thermometry subsystem is used to provide high density (14 sensors per needle) invasive thermistor thermometry information within the breast regions of interest. This is a stand-alone module, which will be integrated into the overall system in the future.

The cooling subsystem consists of thermoelectric coolers attached to the cylindrical array shell and a temperature controller interfaced to the instrument computer. The control computer, including all operator interfaces, display and treatment recording functions, is located separately in the operator console.

1.7 Food and Drug Administration Investigational Device Exemption

Pending Institutional Review Board approval, this protocol will be included as a part of the FDA Investigational Device Exemption application for this new device. This study can not begin until after FDA approval is granted.

1.8 Future Studies

If the treatment device achieves tolerable hyperthermia in the breast target volume we plan to do a Phase I/II Study examining the long-term toxicity and efficacy of treatment. The findings of the current study may make necessary a change in the number of hyperthermia treatments or the duration of treatment required to achieve the clinicly recommended therapeutic goal of T_{90} at 10 minutes equivalent to 43 ^{o}C.

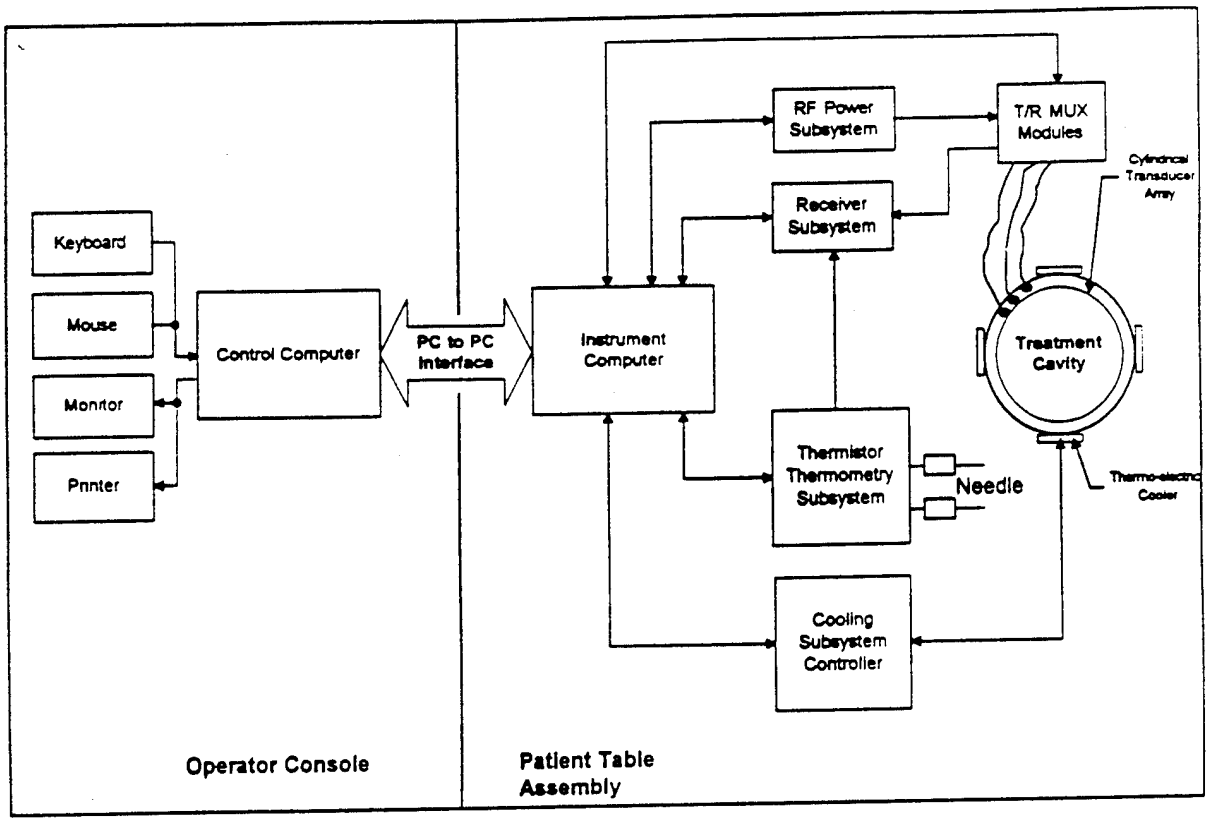

Figure 2. System hardware block diagram.

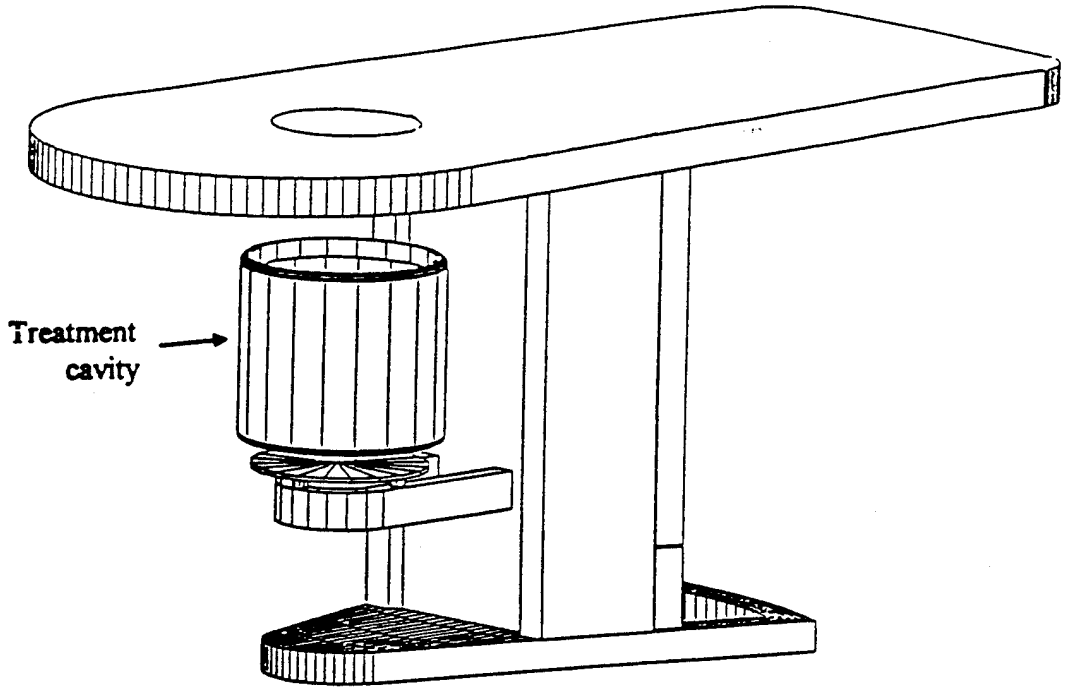

Figure 3. Schematic drawing of treatment table and cavity

2.0 OBJECTIVES

2.1 Evaluate the capabilities and limitations of the breast treatment device to deliver homogeneous heat therapy in a specified quadrant, half, or whole breast.

2.2 Evaluate the acute and long-term toxicity and cosmetic outcome of thermal therapy combined with radiation therapy to treat early breast cancer.

3.0 PATIENT SELECTION

3.1 Histologic confirmation of breast cancer with all 3 criteria below:

3.11 Patients must have either:

A). Infiltrating ductal carcinoma with an extensive intraductal component (EIC+)

or

B). Ductal carcinoma in situ (DCIS) without invasion.

3.12 A re-excision of the biopsy cavity must show residual non-invasive tumor.

3.13 Margins of the re-excision must be positive or close (< 2 mm).

3.2 Breast imaging:

3.21 Preoperative film-screen mammography.

3.22 Postoperative mammograms may be valuable in assessing the extent of residual disease (if in question) for patients presenting with microcalcifications.

3.23 Postoperative MRI of the breast as a baseline, prior to treatment is suggested, but not mandatory.

3.3 Staging studies:

3.31 Chest x-ray.

3.32 Bone scan, only for patients with infiltrating ductal carcinoma.

3.4 EKG.

3.5 CBC with differential and platelet count. PTT and PT. (Bleeding time in patients with platelet counts <100,000.)

3.6 Age ≥18 years.

3.7 Karnofsky Performance Status ≥70 (capable of self care) [Appendix A].

3.8 Expected survival of at least 3 months.

3.9 Informed consent obtained.

3.10 Criteria for ineligibility:

3.10.1 Abnormal bleeding propensity that would make thermal probe placement excessively hazardous.

3.10.2 Previous treatment:

3.10.2.1 Previous radiotherapy to ipsilateral breast.

3.10.2.2 Chemotherapy in the previous 2 weeks.

3.10.3 Patients with severe insulin-dependent diabetes mellitus, and evidence of neuropathy or vasculopathy.

3.10.4 Patients with unstable cardiac status including:

3.10.4.1 Unstable angina pectoris on medication.

3.10.4.2 Patients with documented myocardial infarction within six months of protocol entry.

3.10.4.3 Congestive heart failure requiring medication.

3.10.4.4 Patients on anti-arrhythmic drugs.

3.10.4.5 Severe hypertension (diastolic BP > 100 on medication).

3.10.5 Severe cerebrovascular disease (multiple CVA or CVA within 6 months).

3.10.6 Pregnancy.

3.10.7 Inability to give informed consent.

4.0 PATIENT ENTRY

4.1 Confirm eligibility (Pathology checklist).

4.2 Contact Study Chair to enter a patient on study.

4.3 The Study Chair will contact the Quality Control Center(QCC), J810, (617) 632-3761, FAX (617) 632-2295 before the patient begins treatment with the following information:

-Your name and telephone number
-Protocol name and number
-Date treatment begins
-Patient name
-Date of birth
-Patient ID number
-Primary physician
-Primary treatment institution

5.0 TREATMENT PROGRAMS

This is a pilot study. Specifically it is a device evaluation study of a new ultrasound thermal therapy machine for the treatment of the breast. This is one of the few devices designed and built to specifically treat a single site with hyperthermia and possibly the only device made to treat the breast. The treatment programs objective is to integrate thermal therapy into a course of "standard" breast irradiation.

5.1 Timing and sequencing of treatment.

5.11 Radiation therapy will begin within 8 weeks of the patients' last breast surgery. If systemic chemotherapy is given prior to definitive radiation therapy then radiation therapy can begin more than 8 weeks after the patients' last breast surgery.

5.12 Thermal therapy will be given twice during the course of whole breast irradiation. Hyperthermia will be delivered one time per week during any two of the five weeks of external beam whole breast irradiation. Thermal therapy can not be given on the first or second day of radiation therapy, but can commence anytime after the second radiation treatment. The two treatments must be separated by a minimum of 72 hours.

5.13 On the day of thermal therapy radiation will follow hyperthermia by 30-60 minutes.

5.2 Radiation therapy:

5.21 Megavoltage linear accelerators with dose rates of between 200-400 cGy/min will be used.

5.22 The dose to the breast: 4500 cGy in 25 fractions (180 cGy/day), 5x/week.

5.23 Boost dose: 1600 cGy in 8 fractions, 5x/week; if electron beam therapy is used it is prescribed to the 80% isodose line.

5.24 Regional nodes (when treated): Supraclavicular +/- axillary nodes, dose: 4500 cGy in 25 fractions (180 cGy/day), 5x/week. An additional axillary boost if indicated is permitted. Internal mammary nodes when treated are included in the tangential fields.

5.3 Thermal therapy:

5.31 Equipment: Hyperthermia will be delivered by the ultrasonic breast treatment system developed under contract from the U.S. Army Medical Research and Development Command. Treatment is delivered with the patient in the prone position and her treated breast submersed into water. The treatment cylinder contains of degassed water has a disposable liner that is discarded or sterilized after each treatment session.

5.32 The target volume is the quadrant of the breast that contains the biopsy cavity. If the biopsy cavity occupies two quadrants e.g., biopsy cavities located at 3, 6, 9, or 12 o'clock then the target volume is both quadrants (half the breast).

5.33 The treatment volume prescription temperature is 40 ^{o}C to 43 ^{o}C for 45 minutes.

5.34 Hyperthermia treatment duration is defined as <u>starting</u> 10 minutes after onset of power application or attainment of 40 ^{o}C in any part of the target volume, if the latter occurs in fewer than 10 minutes. After the starting time, treatment will <u>continue</u> for 45 minutes.

5.35 Ultrasound applicator transducer power will be increased until any <u>one</u> of the following occurs:

5.35.1 The recording of a target volume temperature > 43 ^{o}C for more than 1 continuous minute.

5.35.2 The maximum tolerated power level is reached.

5.36 Conditions dictating reduction of applied power and/or cessation of treatment:

5.36.1 Patient request.

5.36.2 Intractable pain or chest pain.

5.36.3 Monitored normal tissue temperature > 43 °C.

5.36.4 Pulse > 160.

5.36.5 Blood Pressure:

5.36.5.1 Systolic > 180 mmHg, diastolic > 100 mmHg.

5.36.5.2 Systolic < 90 mmHg, diastolic < 50 mmHg.

5.36.6 Altered mental status.

5.36.7 Systemic Temperature ≥ 40 °C.

5.4 Thermometry:

Target volume temperatures will be monitored continuously by interstitial and external temperature probes. Probes are placed interstitially using local anesthesia.

5.41 We will attempt to place two invasive thermometry probes, each containing 1 to 14 sensors, orthogonally with the target volume. Thermometry sensors will also be placed superficially on the surface of the breast.

5.42 Thermometry probe location:

5.42.1 The location of the regions for thermometry and the paths of insertion of the probes will be selected during therapy planning. RTOG guidelines (34-36) and methodology for estimating probe paths and location will be used compatible with patient safety.

5.42.2 Suggested specific locations to sample temperature include:

5.42.2.1 The biopsy cavity region, especially at the edges and center of the cavity. This is measured with the invasive probe.

5.42.2.2 At surgical scars, especially the biopsy cavity scar. This is typically measured with the non-invasive superficial skin sensors.

5.42.2.3 Measurements at the surface of the nipple.

5.42.2.4 Predicted "hot spots" within the breast, determined by treatment planning.

5.43 Thermometry probe insertion:

5.43.1 Diagnostic ultrasound will be attempted for probe placement in all patients (unless probes can be placed safely by clinical or by radiographic means and also be compatible with the requirements of treatment planning).

5.43.2 The thermometric probes will be inserted along the pre-selected tracks and inserted to the desired depth under diagnostic ultrasound guidance with patients in the prone treatment position.

5.43.3 After insertion, the location of the probes relative to the breast and target volume will be visualized with the ultrasound treatment unit.

5.43.4 A photograph will be taken to document the thermometry probe position prior to each treatment session.

5.44 A minimum of 28 invasive temperature points per treatment will be attempted.

5.45 Temperature sensors:

5.45.1 All temperatures will be measured by NIST traceable sensors.

5.45.2 Thermocouples or thermistors in 18-22 gauge needle probes with 1-14 sensors per needle will be used for static points [see Appendix B].

5.45.3 At the completion of the hyperthermia treatment session, the temperature sensing probes will be removed.

5.5 Other invasive sensors:

5.51 In selected cases, thermocouple/thermistor probes will be replaced by the Enhanced Thermal Diffusion Probe that, in addition to temperature, measures thermal conductivity, thermal diffusivity, and tissue blood flow [see Appendix B].

5.52 In selected cases, oxygen tension will be measured in the target volume, scar/biopsy cavity region both pre- and post-treatment.

5.6 Additional monitoring:

5.61 The P.I. or a physician designated by the P.I. will be in attendance during every treatment.

5.62 The treatment nurse will monitor vital signs continuously.

5.63 During treatment, the patient's pulse rate and EKG will be continually monitored. An automatic blood pressure device will obtain blood pressure every 5 minutes.

5.64 General anesthesia cannot be used, but light sedation (e.g. Ativan, Percocet, etc.) can be employed as well as previously prescribed analgesics. All patients, however, must be able to discern mild to moderate treatment-associated pain in order to avoid potentially severe thermal injury.

5.7 Adverse reactions and their management

5.71 Anticipated toxicities:

5.71.1 RADIATION THERAPY; related morbidity is discussed with the patient using a separate radiation therapy consent form. However, common immediate side effects include fatigue and skin redness and irritation in the treated breast. In patients that receive chemotherapy prior to treatment on this protocol, they may experience myelosupression.

5.71.2 THERMAL THERAPY; related morbidity includes acute pain in the treatment region secondary to treatment. Also associated with treatment are possible, burns, blisters, itching, or fever during the treatment session. If any of these are observed, it may be possible to change the heating pattern to eliminate the effect. Patients may feel warm or sweat. After the hyperthermia session it is possible to develop pain, burns, or blisters that might persist. Patients may become uncomfortable from lying in the prone treatment position

Late tissue changes, such as fibrosis, necrosis, ulceration, and vascular changes, in the treated breast could be seen. Some of these effect such as fibrosis could make follow-up examinations of the breast more difficult.

5.71.3 THERMOMETRY, related morbidity include pain during probe insertion, despite local anesthesia. As with any invasive procedure, there is a risk of bleeding or infection.

5.72 Toxicity management:

We expect most side effects associated with the use of thermal therapy and radiation therapy to be controllable. Thermal therapy related pain, warmth, and other acute effects are commonly eliminated by adjustment of the heating pattern or energy. Some burns and skin ulcers can be observed after superficial hyperthermia (heat) treatments to persist for more than 6 months in about 15% of patients who receive burns. These are usually treated with complete resolution of symptoms in the majority of cases by routine skin care management.

Unfortunately, possible late tissue changes are not reversible and if they develop may make follow-up examinations of the treated breast more difficult.

5.73 Criteria for Removal from Study:

5.73.1 Patient decision to withdraw from study.

5.73.2 Patient noncompliance with the requirements of the protocol.

5.73.3 A patient may be removed from this study if it is believed that the constraints of this protocol are detrimental to the patient's health or the ability to deliver planned radiation therapy to the breast.

5.73.4 Patients who are unable to tolerate therapy because of the side effects of hyperthermia delivery (pain, tachycardia, anxiety, etc.) will have treatment terminated.

5.73.5 Cessation of radiation therapy for any cause will result in the termination of hyperthermia treatments.

6.0 FEDERAL REPORTING REQUIREMENTS FOR ADVERSE REACTIONS

6.1 Unanticipated adverse device effects

6.11 The Protocol Chairman shall submit to the sponsor (U. S. Army Medical Research & Development Command) and to the reviewing IRB's a report of any unanticipated adverse device

effect occurring during an investigation as soon as possible, but in no event later than 10 working days after the investigator first learns of the effect.

6.12 The sponsor who conducts an evaluation of an unanticipated adverse device effect shall report the results of such evaluation to FDA and to all reviewing IRB's and participating investigators within 10 working days after the sponsor first receives notice of the effect. Thereafter the sponsor shall submit such additional reports concerning the effect as FDA requests.

7.0 REQUIRED DATA

7.1 Data to be collected:

Data Set	At Study Entry	Day of Thermal Therapy	At Follow-up*
Age	X		X
Histologic confirmation	X		
Mammograms	X		X†
Chest X-ray	X		
Bone Scan	X		
MRI of Breast	X**		X**
EKG	X		
CBC	X		
Platelets	X		
LFT's	X		
PT and PTT	X		
Quadrant of breast initially containing the tumor	X		
Capability of device to heat breast target volume		X	
Side effects of therapy		X	X
Tumor control (Measurements within the breast)	X	X	X
Survival			X

† An ipsilateral mammogram of the treated breast will be done approximately 6 months after the patients pre-treatment mammogram. Then bilateral mammograms will be done 6 months later and repeated yearly after that.

* The first follow-up appointment will be one month after treatment. The patient will then return for follow-up every 3 months for 2 years and then every 6 months after that.

** MRI of the breast will be encouraged, but is not mandatory, prior to treatment, at the end of radiation therapy, at the first month follow-up, and then every 6 months.

7.2 Data Collection:

Form	Submission Time
On Study	Within 1 month of patient entry
Thermal Therapy Evaluation	Within 2 weeks of treatment
Summary and Evaluation	Within 1 month of completion of therapy
Status Update	At each follow-up visit (see above)

8.0 MODALITY REVIEW

8.1 Evaluation During Treatment Course:

While treatment is in progress, the following will be done at weekly intervals:

8.11 Patients will be examined at least once weekly and a treatment note will be done weekly with particular attention to acute reactions.

8.12 Patient discomfort [see Appendix C].

8.13 Acute systemic stress effects will be detailed and quantified as either non-treatment limiting or treatment limiting by the clinician.

8.14 An end of treatment evaluation and summary must be completed no later than 1 month after treatment.

8.2 Evaluation Post Treatment Course:

8.21 The time intervals to the development of late complications, first relapse, site(s) of relapse, disease-free survival and overall survival will be recorded.

8.22 The first follow-up appointment will be one month after treatment. The patient will then return for follow-up every 3 months for 2 years and then every 6 months after that.

8.23 History and physical examination will be performed at each follow-up. The investigator shall routinely observe and document the impact of the treatment on the patient's condition and provide an assessment in the following areas:

8.23.1 Late tissue changes, such as fibrosis, necrosis, ulceration, and vascular changes, in the treated breast.

8.23.2 Toxicity parameters will be recorded and evaluated according to the RTOG Late Morbidity Scoring Criteria [Appendix D] and the NCI Common Toxicity Criteria [Appendix E].

8.23.3 Breast cosmesis will be determined by physical examination. An attempt shall be made to quantify normal tissue changes/damage and tumor necrosis within the treated volume [Appendix F].

8.3 Thermal Dose Assessment:

In order to evaluate the capabilities and limitations of the breast treatment device to deliver homogeneous heat therapy in a breast we will assess a number of treatment parameters after each treatment. Several thermal parameters will be calculated and recorded [Appendix G]. These parameters include:

T_{min} = minimum temperature in the tumor area
T_{max} = maximum temperature in the tumor area
T_{ave} = average temperature in the tumor area
T_{90} = the temperature index for which 90% of all measured temperature points are above
% < 40.0 = percentage of measured temperature points below 40.0 °C
% > 43.0 = percentage of measured temperature points above 43.0 °C
% > 43.5 = percentage of measured temperature points above 43.5 °C
% > 44.0 = percentage of measured temperature points above 44.0 °C

9.0 STATISTICAL CONSIDERATIONS

The primary objective of this pilot study is to evaluate the ability of the treatment device to deliver homogeneous heat therapy to the breast in patients with extensive intraductal breast cancer. A total of 15 patients, of whom 14 are expected to be fully evaluable, will be entered on study. Accrual is expected to require 18 months.

The primary endpoint for the device evaluation is the proportion of patients for whom the treatment goal was achieved (as defined in Section 8.3 and Appendix G) without intolerable side effects such as persistent pain, or poor cosmetic results secondary to hyperthermia. With 14 evaluable patients, the probability of failing to observe an adverse side effect that occurs in the population at a rate of 20% is 0.044. For rare toxicities occurring in the population at a rate of 10%, this probability is 0.23.

Assuming 14 evaluable patients, the 95% confidence intervals for the proportion of patients who experience intolerable side effects are as follows:

No. with Side Effect	Proportion with Side Effect	95% Confidence Interval
0	0.00	0.00-0.23
1	0.071	0.0021-0.34
2	0.14	0.018-0.43
3	0.21	0.047-0.51
4	0.29	0.084-0.58
5	0.36	0.13-0.65
6	0.43	0.18-0.71
7	0.50	0.23-0.77

Short- and long-term changes toxicities and cosmetic outcome will be evaluated in each patient.

10.0 REFERENCES

1. National Institutes of Health (NIH) consensus development conference statement: Treatment of early stage breast cancer. JAMA 265(3):391-394, 1991.

2. Fisher B, Redmond C, Poisson R, et al. Eight-year results of a randomized clinical trial comparing total mastectomy and lumpectomy with or without irradiation in the treatment of breast cancer. N Engl J Med 320:822-828, 1989.

3. Veronesi U. Rationale and indications for limited surgery in breast cancer: Current data. World J Surg 11:493-498, 1987.

4. Harris JR, Recht A, Connolly J, Cady B, Come S, Henderson C, Koufman C, Love S, Schnitt S, Osteen R. Conservative surgery and radiotherapy for early breast cancer. Cancer 66:1427-1438, 1990.

5. Holland R, Connolly JL, Gelman R, Mravunac M, Hendriks JHCL, Verbeek ALM, Schnitt SJ, Silver B, Boyages J, Harris JR. The presence of an extensive intraductal component following a limited excision correlates with prominent residual disease in the remainder of the breast. J Clin Oncol 8:113-118, 1990.

6. Harris JR, Connolly JL, Schnitt SJ, et al. The use of pathologic features in selecting the extent of surgical resection necessary for breast cancer patients treated by primary radiation therapy. Ann Surg 201:164-169, 1985.

7. Bartelink H, Borger JH, van Dongen JA, Peterse JL. The impact of tumor size and histology on local control after breast-conserving therapy. Radiother Oncol 11:297-303, 1988.

8. Lindley R, Bulman A, Parsons P, Phillips R, Henry K, Ellis H. Histologic features predictive of an increased risk of early local recurrence after treatment of breast cancer by local tumor excision and radical radiotherapy. Surgery 105:13-20, 1989.

9. Boyages J, Recht A, Connolly J, Schnitt SJ, Gelman R, Kooy H, et al. Early breast cancer: predictors of breast recurrence for patients treated with conservative surgery and radiation therapy. Radiother Oncol 19:29-41, 1990.

10. Schnitt SJ, Abner A, Gelman R, Connolly JL, Recht A, Duda RB, Eberlein TJ, Mayzel K, Silver B, Harris JR. The relationship between microscopic margins of resection and the risk of local recurrence in patients with breast cancer treated with breast-conserving surgery and radiation therapy. Cancer 74:1746-1751, 1994.

11. Bornstein BA, Recht A, Connolly JL, Schnitt SJ, Cady B, Koufman C, Love S, Osteen RT, Harris JR. Results of treating ductal carcinoma in situ of the breast with conservative surgery and radiation therapy. Cancer 67:7-13, 1991.

12. Schnitt SJ, Silen W, Sadowsky NL, Connolly JL, Harris HR. Current concepts: ductal carcinoma in situ (intraductal carcinoma) of the breast. N Engl J Med 318:898-903, 1988.

13. van Dongen JA, Fentiman IS, Harris JR, et al. In situ breast cancer: the EORTC consensus meeting. Lancet 2:25-27, 1989.

14. Solin LJ, Recht A, Fourquet A, Kurtz J, Kuske R, McNeese M, McCormick, B, Cross MA, Schultz DJ, Bornstein BA, Spitalier JM, Vilcoq JR, Fowble BL, Harris JR, Goodman RL. Ten year results of breast-conserving surgery and definitive irradiation for intraductal carcinoma (ductal carcinoma in situ) of the breast. Cancer 68:2337-2344, 1991.

15. Mayr NA, Staples JJ, Robinson RA, Vanmetre JE, Hussey DH. Morphometric studies in intraductal breast carcinoma using computerized image analysis. Cancer 67:2805-2812, 1991.

16. Dewhirst MW, Ong ET, Klitzman B, Secomb TW, Vinuya RZ, Dodge R, Brizel D, Gross JF. Perivascular oxygen tensions in a transplantable mammary tumor growing in a dorsal flap window chamber. Rad Res 130:171-182, 1992.

17. Palcic B, Skarsgard LD. Reduced oxygen enhancement ratio at low doses of ionizing radiation. Radiat Res 100:328-339, 1984.

18. Hall EJ. Radiobiology for the Radiologist, 3rd Ed, p 139. JB Lippincott: Philadelphia, 1988.

19. Hahn GM. Hyperthermia and Cancer, p 7. New York, Plenum Press, 1982.

20. Gerweck LE. Modification of cell lethality at elevated temperatures: The pH effect. Radiat Res 70:224-235, 1977.

21. Freeman ML, Dewey WC, Hopwood LE. Effect of pH on hyperthermic cell survival: Brief communication. JNCI 58:1837-1839, 1977.

22. Dewey WC, Hopwood LE, Sapareto SA, Gerweck LE. Cellular response to combinations of hyperthermia and radiation. Radiology 123:463-474, 1977.

23. Hahn GM. Hyperthermia and Cancer, p154-163. New York, Plenum Press, 1982.

24. Hall EJ. Radiobiology for the Radiologist, 3rd Ed, p311-317. JB Lippincott: Philadelphia, 1988.

25. Sapareto SA, Hopwood LE, Dewey WC. Combined effects of x-irradiation and hyperthermia on CHO cells for various temperatures and orders of application. Radiat Res 43:221-233, 1978.

26. Cavaliere R, Ciocatto EC, Giovanella RC, et al. Selective heat sensitivity of cancer dells. Cancer 20:1351, 1967.

27. Belli JA, Bonte FJ: Influence of temperature on the radiation response of mammalian cells in tissue cultures. Radiat Res 18:272-276, 1963.

28. Hahn GM: Potential for therapy of drugs and hyperthermia. Cancer Res 39:2264-2268, 1979.

29. Hall EJ. Radiobiology for the Radiologist, 3rd Ed, p293-329. JB Lippincott: Philadelphia, 1988.

30. Overgaard J: Rationale and problems in the design of clinical trials. In Overgaard J (ed): Hyperthermic Oncology 1984. pp 325-337. London, Taylor and Francis, 1984.

31. Kapp DS: Areas of need for continued Phase II testing in human patients. In Paliwal BR, Hetzel FW, Dewhirst MW (eds): Biological, Physical and Clinical Aspects of Hyperthermia. Medical Physics Monograph, no 16. p424. New York, American Institute of Physics, 1988.

32. Herman TS, Teicher BA, Jochelson MS, et al. Rational for the use of local hyperthermia with radiation therapy and selected anticancer drugs in locally advanced human malignancies. Int J Hyperthermia 4:143-158, 1988.

33. Dahl, O: Interaction of hyperthermia and chemotherapy. Recent Results in Cancer Research, 107:157-169, 1988.

34. Dewhirst MW, Phillips TL, Samulski TV, Stauffer P, Shrivastava P, Paliwal B, Pajak T, Gillim M, Sapozink M, Myerson R, Waterman FM, Sapareto SA, Corry P, Cetas TC, Leeper DB, Fessenden P, Kapp D, Oleson JR, Emami B. RTOG quality assurance guidelines for clinical trials using hyperthermia. Int J Radiat Oncol Biol Phys 18:1249-1259, 1990.

35. Waterman FW, Dewhirst MW, Samulski TV, Herman T, Emami B, Cetas TC, Corry P, Fessenden P, Gillin M, Kapp D, Leeper DB, Myerson R, Oleson TJ, Paliwal B, Pajak T, Phillips TL, Sapareto SA, Sapozink M, Shrivastava P, Stauffer P. RTOG quality assurance guidelines for clinical hyperthermia administered by ultrasound. Int J Radiat Oncol Biol Phys 20:1099-1107, 1991.

36. Sapozink MD, Corry PM, Kapp DS, Myerson RJ, Dewhirst MW, Emami B, Herman T, Prionas S, Ryan T, Samulski T, Sapareto S, Shrivastava T, Stauffer P, Waterman F. RTOG quality assurance guidelines for clinical trials using hyperthermia for deep-seated malignancy. Int J Radiat Oncol Biol Phys 20:1109-1115, 1991.

37. Bornstein BA, Coleman CN. Innovative approaches to local therapy. In Harris JR, Hellman S, Henderson IC, Kinne DW (eds): Breast Diseases. 2nd ed. Philadelphia, JB Lippincott, 1990:673-677.

38. Overgaard J. The current and potential role of hyperthermia in radiotherapy. Int J Radiat Oncol Biol Phys 1989:16:535.

39. Scott R, Gillespie B, Perez CA, et al. Hyperthermia in combination with definitive radiation therapy: results of a phase I/II RTOG study. Int J Radiat Oncol Biol Phys 1988:15;711.

40. Lindholm CE, Kjellen E, Nilsson P, Hertzman S. Microwave-induced hyperthermia and radiotherapy in human superficial tumours: clinical results with a comparative study of combined treatment versus radiotherapy alone. Int J Hyperthermia 1987:3;393.

41. van der Zee J, Treurniet-Donker AD, The SK, et al. Low dose reirradiation in combination with hyperthermia: a palliative treatment for patients with breast cancer recurring in previously irradiated areas. Int J Radiat Oncol Biol Phys 1988:15;1407.

42. Perez CA, Kuske RR, Emami B, Fineberg B. Irradiation alone or combined with hyperthermia in the treatment of recurrent carcinoma of the breast in the chest wall: a nonrandomized comparison. Int J Hyperthermia 1986:2;179.

43. Dragovic J, Seydel HG, Sandhu T, Kolosvary A, Blough J. Local superficial hyperthermia in combination with low-dose radiation therapy for palliation of locally recurrent breast carcinoma. J Clin Oncol 1989:7;30.

44. Jampolis S, Blumenschein G, Gomez-Yeyille JE, et al. Combination hyperthermia and radiation treatment for locally recurrent breast cancer: an analysis of response and prognostic factors. [Abstract] Proc Am Assoc Can Res 1989:30;253.

45. Gonzalez Gonzalez D, van Dijk JDP, Blank LECM. Chestwall recurrences of breast cancer: results of combined treatment with radiation and hyperthermia. Radiother and Oncol 1988:12;95.

46. Kapp DS, Barnett TA, Cox RS, Lee ER, Lohrbach A, Fessenden P. Hyperthermia and radiation therapy of local-regional recurrent breast cancer: prognostic factors for response and local control of diffuse or nodular tumors. Int J Radiat Oncol Biol Phys 20:1147-1164, 1991.

47. Aberizk WJ, Silver B, Henderson IC, Cady B, Harris JR. The use of radiotherapy for treatment of isolated locoregional recurrence of breast carcinoma after mastectomy. Cancer 58:1214-1218, 1986.

48. Chen KKY, Montague ED, Oswald MJ. Results of irradiation in the treatment of locoregional breast cancer recurrence. Cancer 56:1269-1273, 1985.

49. Chu FCH, Lin FJ, Kim JH, Huh SH, Garmatis CJ. Locally recurrent carcinoma of the breast: Results of radiation therapy. Cancer 37:2677-2681, 1976.

50. Deutsch M, Parsons J, Mittal BB. Radiation therapy for local-regional recurrent breast cancer. Int J Radiat Oncol Biol Phys 12:2061-2065, 1986.

51. Mango L, Bignardi M, Micheletti E, et al. Analysis of prognostic factors in patients with isolated chest wall recurrence of breast cancer. Cancer 60:240-244, 1987.

52. Beck TM, Hart NE, Woodard DA, Smith CE. Local or regionally recurrent carcinoma of the breast: results of therapy in 121 patients. J Clin Oncol 1:400-405, 1983.

53. Danoff BF, Coia LR, Canter RI, et al. Locally recurrent breast carcinoma: The effect of adjuvant chemotherapy on prognosis. Radiology 147:849-852, 1983.

54. Valdagni R, Liu FF, Kapp DS. Important prognostic factors influencing outcome of combined radiation and hyperthermia. Int J Radiat Oncol Biol Phys 1988:15:959.

55. Luk KH, Purser PR, Castro JR, Meyler TS, Phillips TL. Clinical experiences with local microwave hyperthermia. Int J Radiat Oncol Biol Phys 1981:7;615.

56. Kapp DS, Fessenden P, Samulski TV, Bagshaw MA, Cox RS, Lee ER, Lohrbach AW, Meyer JL, Prionas SD. Stanford University Institutional Report. Phase I evaluation of equipment for hyperthermia treatment of cancer. Int J Hyperthermia 4:75-115, 1988.

57. Kapp DS, Cox RS, Barnett TA, Ben-Yosef R. Thermoradiotherapy for residual microscopic cancer: elective or post-excisional hyperthermia and radiation therapy in the management of local-regional recurrent breast cancer. Int J Radiat Oncol Biol Phys 24:261-277, 1992.

58. Dewhirst MW, Griffin TW, Smith AR, Parker RG, Hanks GE, Brady LW. Intersociety council on radiation oncology essay on the introduction of new medical treatments into practice. JNCI 85:951-957, 1993.

59. Fisher B, Costantino J, Redmond C, et al. Lumpectomy compared with lumpectomy and radiation therapy for the treatment of intraductal breast cancer. N Engl J Med 328:1581-1586, 1993.

60. Okunieff P, Hoeckel M, Dunphy EP, Schlenger K, Knoop C, Vaupel P. Oxygen tension distributions are sufficient to explain the local response of human breast tumors treated with radiation alone. Int J Radiat Oncol Biol Phys 26:631-636, 1993.

APPENDIX A

KARNOFSKY PERFORMANCE SCALE

100	Normal; no complaints; no evidence of disease
90	Able to carry on normal activity; minor signs or symptoms of disease
80	Normal activity with effort; some sign or symptoms of disease
70	Cares for self; unable to carry on normal activity or do active work
60	Requires occasional assistance, but is able to care for most personal needs
50	Requires considerable assistance and frequent medical care
40	Disabled; requires special care and assistance
30	Severely disabled; hospitalization is indicated, although death not imminent
20	Very sick; hospitalization necessary; active support treatment is necessary
10	Moribund; fatal processes progressing rapidly
0	Dead

APPENDIX B

Description of Non-Commercial Temperature Probes

1. The Enhanced Thermal Diffusion Probe (ETDP):

The Enhanced Thermal Diffusion Probe (ETDP) system can accurately measure tissue temperature, thermal conductivity, thermal diffusivity and derive tissue blood flow. The ETDP measurement instrumentation permits the routine measurement of microcirculatory and physiologic tissue parameters via a single invasive probe. The probe is physically no different than the large diameter temperature measurement probe we use routinely in the hyperthermia clinic. It simply uses thermistors instead of thermocouples as the measurement elements. As is the case with all our temperature probes, the power supply is an isolated, medically certified unit that surpasses UL-544 regulations for isolation voltage and leakage current for medical and dental devices. In addition, the communication link between the host computer and the ETDP is optically isolated. Thus, there is no electrical connection between the ETDP and any of the other equipment in the hyperthermia center. (Please see the attached diagram at the end of this Appendix.) This probe is already approved for use in DFCI protocol 91-063.

2. The Oxygen Tension Probe:

The group providing us with the ETDP probe have added the additional ability to measure oxygen tension via a polarographic cathode that resides in a probe. This modified probe is available for use when treating patients with hyperthermia and is approved by the DFCI IRB for use in DFCI protocol 91-063. Of note, a similar probe is approved for a group of investigators at Brigham and Women's Hospital (BWH) by the BWH IRB for the measurement of oxygen tension.

General Electrical: The oxygen tension measurement is via a polarographic cathode residing in our 16 gauge or 18 gauge probe in conjunction with a conventional gel coated ECG electrode attached to roughened skin. There are no direct electrical connections between the instrument and host computer. In addition electrical isolation of the instrument from the wall ground is provided via use of an UL544 Medical Grade Power Supply. Further isolation of the oxygen tension measurement circuitry is provided via battery power of that portion of the circuit, and isolation of the resulting signal using an isolated amplifier. Finally, as done with our current probe and by the group using the similar probe at BWH we will have the isolation and safety features confirmed by the Biomedical Engineering Services at BWH.

Polarographic Oxygen Measurements: A -0.6 volt potential is applied to the polarographic cathode with respect to the anode, and the resulting induced current (0-10 nanoAmps) is measured and internally converted to oxygen tension by a pre-determined calibration. The driving voltage used is on the order of magnitude of

galvanic stimulation routinely utilized in neurophysiologic testing and poses no added stress or discomfort to the patient. The American Association of Medical Instruments has set a current limit of 10 microAmps for use in implanted devices, and the techniques described here typically establish currents no greater than 10 nanoAmps (less than 0.1% of the safety limit). Passive safety circuitry limits current in the unlikely event of a complete probe and system failure to less than 6 microAmps.

3. Multi-Channel Temperature Probes:

The group providing us with the probe have now been able to manufacture a new multi-channel temperature instrument that is capable of driving one, two, or three multi-channel temperature probes. Each probe can measure temperature at up to 14 sites.

Accurate temperature measurement in both tumor and normal tissue is paramount to delivery of both safe and hopefully effective hyperthermia treatments. Each new multi-channel sensor probe provides only temperature data, however up to 14 sites could be monitored simultaneously per "invasive" placement. This is a major step up from our current commercially available multi-channel probes that can only measure data at a maximum of three sites. Increasing the number of temperature points monitored during treatment may allow us to deliver higher tumor temperatures and provide improved patient comfort.

The probes are either plastic or stainless steel needles, sized from 15 to 20 gauge and from 10 to 30 cm long, containing 10 to 14 thermistor temperature sensors. Each thermistor is individually tested for voltage isolation at an FDA-approved, GMP-certified fabrication facility. The probe instrumentation allows a temperature resolution down to 10-20 millidegrees Centigrade and temperature can be sampled (across all sites) at up to 10 times per second.

A range of probe configurations are provided and permits selection of a probe appropriate for the particular site being monitored. Since there is little change in the size of the probes from those presently in use, it should not add any additional patient discomfort.

General Electrical: There are no direct electrical connections between the patient and ground via the instrumentation. Within the measurement instrumentation, each probe is connected to an individual, electrically isolated probe driver card. The driver cards are powered by a UL-544 Medical Grade Power Supply and signals to and from the driver cards are passed through optical isolators and isolation amplifiers. This isolation ensures that there is no electrical connection between patient and ground. However, as a further safety precaution, hardware protection circuitry is provided to shut off power (within 65 microseconds) to a probe if an "out-of-range" signal is detected due to probe breakage or other mishap. Although the isolation circuitry described earlier ensures that there is no current path from the instrument to ground through the patient under such circumstances, this latter measure provides added assurance of patient safety.

We have shown that the instrument and probes have surpassed the 10 microAmp patient safety limit for leakage current, set by the American Association of Medical Instruments for implanted devices via experiments with a BioTek 170 Digital Safety Analyzer. Of course, as done with our other hyperthermia equipment and probes we will have the isolation and safety features confirmed by the Biomedical Engineering Services at BWH, before any patient use.

We would like to use the multi-channel instrument and all the accompanying temperature probes in appropriate patients. The additional information provided by these probes will add to our knowledge of the physiological changes in tumor and normal tissue during hyperthermia. The use of this thermometry system should not pose any additional risk or discomfort to our patients. Furthermore, the multi-channel temperature probe is of great value in the treatment of large deep tumors where many temperature points must continuously be monitored in order to provide both safe and effective treatment.

Schematic diagram of the isolated power supply of the ETDP system.

As in the case of all our temperature probes, the power supply is an isolated, medically certified unit that surpasses UL-544 regulations for isolation voltage and leakage current for medical and dental devices. In addition, the communication link between the host computer and the ETDP is optically isolated. Thus, there is no electrical connection between the ETDP and any of the other equipment in the hyperthermia center.

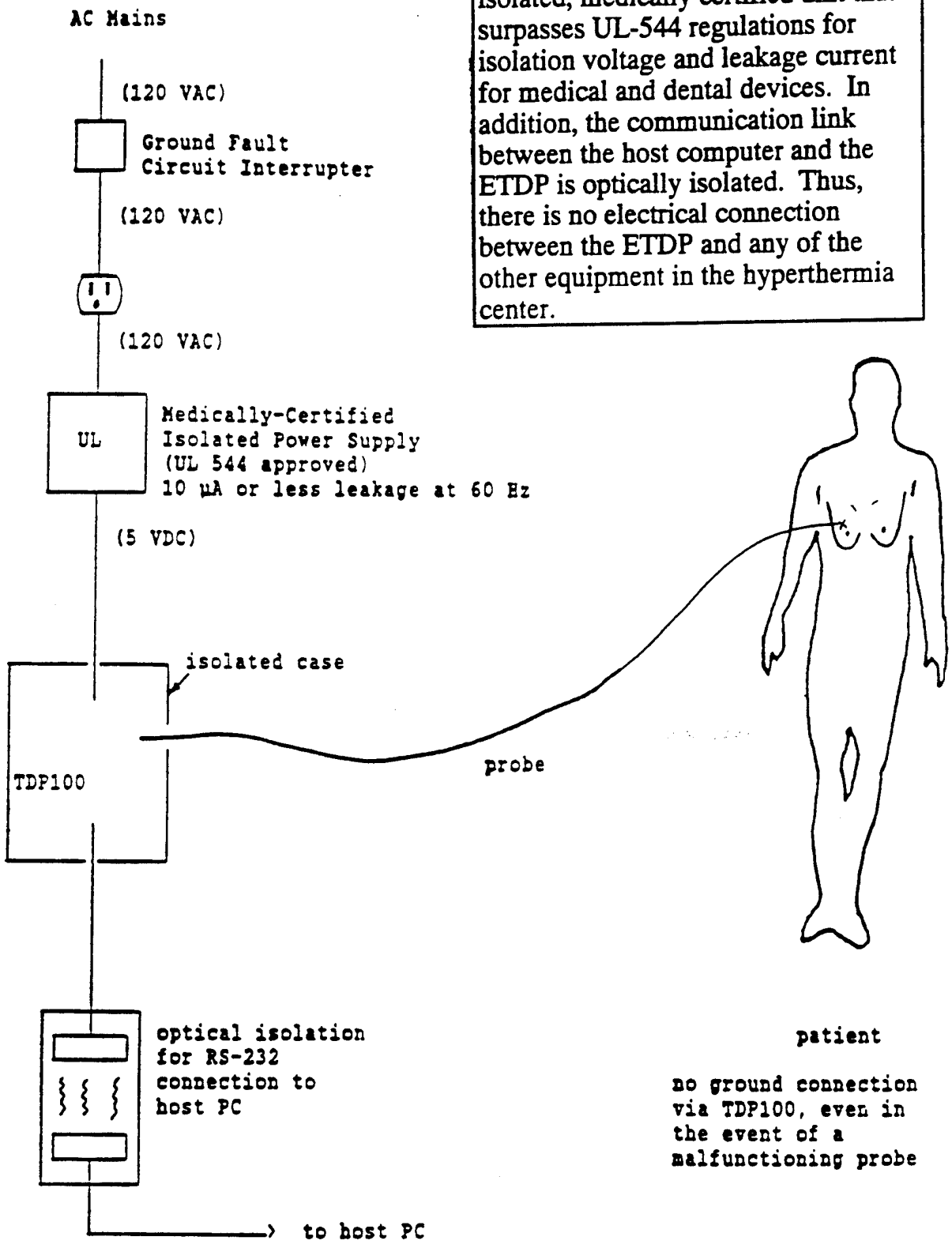

APPENDIX C

GRADING OF PATIENT DISCOMFORT

During Hyperthermia Session*

Grade 1: Patient volunteers complaint of discomfort, which is tolerable, or can be relieved by counseling, medication, or positional changes, without reduction in applied power necessary to elevate tumor temperature.

Grade 2: Reduction in applied power is necessary, however, all scheduled sessions are completed, and minimum temperature elevation evaluability criteria are fulfilled.

Grade 3: One or more scheduled sessions are not completed or are canceled because of intolerable discomfort, however minimum temperature elevation evaluability criteria are fulfilled.

Grade 4: Intolerable discomfort prevents fulfillment of minimum temperature elevation evaluability criteria.

---

* Taken from RTOG Protocol 89-08. A phase I/II study to evaluate radiation therapy and hyperthermia for deep-seated tumors.

APPENDIX D

RTOG Late Morbidity Scoring Criteria

ORGAN/TISSUE	0	GRADE 1	GRADE 2	GRADE 3	GRADE 4	GRADE 5
SKIN	None	Slight atrophy Pigmentation change Some hair loss	Patchy atrophy Moderate telangiectasia Total hair loss	Marked atrophy Gross telangiectasia	Ulceration	
SUBCUTANEOUS TISSUE	None	Slight induration (fibrosis) and loss of subcutaneous fat	Moderate fibrosis but asymptomatic/Slight field contracture/ < 10% linear reduction	Severe induration and loss of subcutaneous tissue Field contracture >10% linear measurement	Necrosis	
MUCOUS MEMBRANE	None	Slight atrophy and dryness	Moderate atrophy and telangiectasia/ Little mucous	Marked atrophy with complete dryness/Severe telangiectasia	Ulceration	
SALIVARY GLANDS	None	Slight dryness of mouth/Good response on stimulation	Moderate dryness of mouth/Poor response on stimulation	Complete dryness of mouth/No response on stimulation	Fibrosis	DEATH
SPINAL CORD	None	Mild L'Hermitte's syndrome	Severe L'Hermitte's syndrome	Objective neurological findings at or below cord level treated	Mono, para quadraplegia	DIRECTLY
BRAIN	None	Mild headache/ Slight lethargy	Moderate headache/ Great lethargy	Severe headache/Severe CNS dysfunction (partial loss of power or dyskinesia)	Seizures or paralysis/coma	
EYE	None	Asymptomatic cataract Minor corneal ulceration or keratitis	Symptomatic cataract Moderate corneal ulceration/Minor retinopathy or glaucoma	Severe keratitis Severe retinopathy or detachment/Severe glaucoma	Panopthalmitis Blindness	
LARYNX	None	Hoarseness/Slight arytenoid edema	Moderate arytenoid edema/Chondritis	Severe edema/Severe chondritis	Necrosis	RELATED
LUNG	None	Asymptomatic or mild symptoms (dry cough) Slight radiographic appearances	Moderate symptomatic fibrosis or pneumonitis (severe cough) Low grade fever/Patchy radiographic appearances	Severe symptomatic fibrosis or pneumonitis/Dense radiographic changes	Severe respiratory insufficiency/Continuous O²/Assisted ventilation	TO
HEART	None	Asymptomatic or mild symptoms/Transient T wave inversion and ST changes/Sinus tachycardia >110 (at rest)	Moderate angina on effort/Mild pericarditis/ Normal heart size/Persistent abnormality T wave and ST changes/ Low QRS	Severe angina/Pericardial effusion/Constrictive pericarditis/Moderate heart failure/Cardiac enlargement/EKG abnormalities	Tamponade/Severe heart failure Severe constrictive pericarditis	RADIATION
ESOPHAGUS	None	Mild fibrosis/Slight difficulty in swallowing solids/No pain on swallowing	Unable to take solid food normally/Swallowing semi-solid food/Dilatation may be indicated	Severe fibrosis/Able to swallow only liquids/May have pain on swallowing Dilatation required	Necrosis/Perforation/Fistula	LATE
SMALL/LARGE INTESTINE	None	Mild diarrhea/Mild cramping/Bowel movement 5 times daily Slight rectal discharge or bleeding	Moderate diarrhea and colic/Bowel movement >5 times daily/Excessive rectal mucus or intermittent bleeding	Obstruction or bleeding requiring surgery	Necrosis/Perforation/Fistula	
LIVER	None	Mild lassitude/Nausea dyspepsia/Slightly abnormal liver function	Moderate symptoms/Some abnormal liver function tests/Serum albumin normal	Disabling hepatitic insufficiency/Liver function tests grossly abnormal/Low albumin/Edema or ascites	Necrosis/Hepatic coma or encephalopathy	EFFECT
KIDNEY	None	Transient albuminuria No hypertension/Mild impairment renal function/Urea 25-35 mg% Creatinine 1.5-2.0 mg% Creat. clearance >75%	Persistent moderate albuminuria (2+)/Mild hypertension/No related anemia/Moderate impairment renal function/Urea >36-60 mg% Creatinine clearance (50-74%)	Severe albuminuria/Severe hypertension/Persistent anemia (< 10Gm%) Severe renal failure/Urea >60 mg% Creatinine >4.0 mg% Creatinine clearance < 50%	Malignant hypertension/Uremic coma Urea > 100%	
BLADDER	None	Slight epithelial atrophy/Minor telangiectasia (microscopic hematuria)	Moderate frequency/Generalized telangiectasia Intermittent macroscopic hematuria	Severe frequency & dysuria Severe generalized telangiectasia (often with petechiae) Frequent hematuria. Reduction in bladder capacity (< 150 cc)	Necrosis/Contracted bladder (capacity < 100 cc) Severe hemorrhagic cystitis	
BONE	None	Asymptomatic/No growth retardation Reduced bone density	Moderate pain or tenderness/Growth retardation Irregular bone sclerosis	Severe pain or tenderness Complete arrest bone growth Dense bone sclerosis	Necrosis/Spontaneous fracture	
JOINT	None	Mild joint stiffness Slight limitation of movement	Moderate stiffness/Intermittent or moderate joint pain/Moderate limitation of movement	Severe joint stiffness/ Pain with severe limitation of movement	Necrosis/Complete fixation	

APPENDIX E

COMMON TOXICITY CRITERIA

TOXICITY	GRADE 0	1	2	3	4
Blood/Bone Marrow					
WBC	≥4.0	3.0 - 3.9	2.0 - 2.9	1.0 - 1.9	<1.0
PLT	WNL	75.0 - normal	50.0 - 74.9	25.0 - 49.9	<25.0
Hgb	WNL	10.0 - normal	8.0 - 10.0	6.5 - 7.9	<6.5
Granulocytes/ Bands	≥2.0	1.5 - 1.9	1.0 - 1.4	0.5 - 0.9	<0.5
Lymphocytes	≥2.0	1.5 - 1.9	1.0 - 1.4	0.5 - 0.9	<0.5
Hemorrhage (clinical)	none	mild, no transfusion	gross, 1-2 units transfusion per episode	gross, 3-4 units transfusion per episode	massive, > 4 units transfusion per episode
Infection	none	mild	moderate	severe	life-threatening
Gastrointestinal					
Nausea	none	able to eat reasonable intake	intake significantly decreased but can eat	no significant intake	—
Vomiting	none	1 episode in 24 hours	2-5 episodes in 24 hours	6-10 episodes in 24 hours	>10 episodes in 24 hrs, or requiring parenteral support
Diarrhea	none	increase of 2-3 stools/day over pre-Rx	increase of 4-6 stools/day, or nocturnal stools, or moderate cramping	increase of 7-9 stools/day, or incontinence, or severe cramping	increase of ≥10 stools/day or grossly bloody diarrhea, or need for parenteral support
Stomatitis	none	painless ulcers, erythema, or mild soreness	painful erythema, edema, or ulcers, but can eat	painful erythema, edema, or ulcers, and cannot eat	requires parenteral or enteral support
Liver					
Bilirubin	WNL	—	<1.5 x N	1.5 - 3.0 x N	>3.0 x N
Transaminase (SGOT, SGPT)	WNL	≤2.5 x N	2.6 - 5.0 x N	5.1 - 20.0 x N	>20.0 x N
Alk Phos or 5'nucleotidase	WNL	≤2.5 x N	2.6 - 5.0 x N	5.1 - 20.0 x N	>20.0 x N
Liver-clinical	no change from baseline	—	—	precoma	hepatic coma
Kidney, Bladder					
Creatinine	WNL	<1.5 x N	1.5 - 3.0 x N	3.1 - 6.0 x N	>6.0 x N
Proteinuria	no change	1+ or <0.3 g% or <3 g/l	2 - 3+ or 0.3 - 1.0 g% or 3 - 10 g/l	4+ or >1.0 g% or >10 g/l	nephrotic syndrome
Hematuria	neg	micro only	gross, no clots	gross + clots	requires transfusion
Alopecia	no loss	mild hair loss	pronounced or total hair loss	—	—
Pulmonary	none or no change	asymptomatic, with abnormality in PFT's	dyspnea on significant exertion	dyspnea at normal level of activity	dyspnea at rest

COMMON TOXICITY CRITERIA

TOXICITY	GRADE 0	1	2	3	4
Heart					
Cardiac dysrhythmias	none	asymptomatic, transient, requiring no therapy	recurrent or persistent, no therapy required	requires treatment	requires monitoring; or hypotension, or ventricular tachycardia, or fibrillation
Cardiac function	none	asymptomatic, decline of resting ejection fraction by less than 20% of baseline value	asymptomatic, decline of resting ejection fraction by more than 20% of baseline value	mild CHF, responsive to therapy	severe or refractory CHF
Cardiac–ischemia	none	non-specific T-wave flattening	asymptomatic, ST and T-wave changes suggesting ischemia	angina without evidence for infarction	acute myocardial infarction
Cardiac–pericardial	none	asymptomatic effusion, no intervention required	pericarditis (rub, chest pain, ECG changes)	symptomatic effusion; drainage required	tamponade; drainage urgently required
Blood Pressure					
Hypertension	none or no change	asymptomatic, transient increase by > 20 mm Hg (D) or to >150/100 if previously WNL. No treatment required	recurrent or persistent increase by >20 mm Hg (D) or to >150/100 if previously WNL. No treatment required	requires therapy	hypertensive crisis
Hypotension	none or no change	changes requiring no therapy (including transient orthostatic hypotension)	requires fluid replacement or other therapy but not hospitalization	requires therapy and hospitalization; resolves within 48 hrs of stopping the agent	requires therapy and hospitalization for >48 hrs after stopping the agent
Neurologic					
Neuro-sensory	none or no change	mild paresthesias, loss of deep tendon reflexes	mild or moderate objective sensory loss; moderate paresthesias	severe objective sensory loss or paresthesias that interfere with function	—
Neuro-motor	none or no change	subjective weakness; no objective findings	mild objective weakness without significant impairment of function	objective weakness with impairment of function	paralysis
Neuro-cortical	none	mild somnolence or agitation	moderate somnolence or agitation	severe somnolence, agitation, confusion, disorientation, or hallucinations	coma, seizures, toxic psychosis
Neuro-cerebellar	none	slight incoordination, dysdiadokinesis	intention tremor, dysmetria, slurred speech, nystagmus	locomotor ataxia	cerebellar necrosis
Neuro-mood	no change	mild anxiety or depression	moderate anxiety or depression	severe anxiety or depression	suicidal ideation
Neuro-headache	none	mild	moderate or severe but transient	unrelenting and severe	—
Neuro-constipation	none or no change	mild	moderate	severe	ileus >96 hrs
Neuro-hearing	none or no change	asymptomatic, hearing loss on audiometry only	tinnitus	hearing loss interfering with function but correctable with hearing aid	deafness not correctable

COMMON TOXICITY CRITERIA

TOXICITY	GRADE 0	1	2	3	4
Neuro-vision	none or no change	—	—	symptomatic subtotal loss of vision	blindness
Skin	none or no change	scattered macular or papular eruption or erythema that is asymptomatic	scattered macular or papular eruption or erythema with pruritus or other associated symptoms	generalized symptomatic macular, papular, or vesicular eruption	exfoliative dermatitis or ulcerating dermatitis
Allergy	none	transient rash, drug fever <38c, 100.4F	urticaria, drug fever =38c, 100.4F mild bronchospasm	serum sickness, bronchospasm, req parenteral meds	anaphylaxis
Fever in absence of infection	none	37.1 - 38.0c 98.7 - 100.4F	38.1 - 40.0c 100.5 - 104.0F	>40.0c >104.0F for < 24 hrs	>40.0c (104.0F) for > 24 hrs or fever accompanied by hypotension
Local	none	pain	pain and swelling, with inflammation or phlebitis	ulceration	plastic surgery indicated
Weight gain/loss	<5.0%	5.0 - 9.9%	10.0 - 19.9%	≥20.0%	—
Metabolic					
Hyperglycemia	<116	116 - 160	161 - 250	251 - 500	>500 or ketoacidosis
Hypoglycemia	>64	55 - 64	40 - 54	30 - 39	<30
Amylase	WNL	<1.5 x N	1.5 - 2.0 x N	2.1 - 5.0 x N	>5.1 x N
Hypercalcemia	<10.6	10.6 - 11.5	11.6 - 12.5	12.6 - 13.5	≥13.5
Hypocalcemia	>8.4	8.4 - 7.8	7.7 - 7.0	6.9 - 6.1	≤6.0
Hypomagnesemia	>1.4	1.4 - 1.2	1.1 - 0.9	0.8 - 0.6	≤0.5
Coagulation					
Fibrinogen	WNL	0.99 - 0.75 x N	0.74 - 0.50 x N	0.49 - 0.25 x N	≤0.24 x N
Prothrombin time	WNL	1.01 - 1.25 x N	1.26 - 1.50 x N	1.51 - 2.00 x N	>2.00 x N
Partial thrombo-plastin time	WNL	1.01 - 1.66 x N	1.67 - 2.33 x N	2.34 - 3.00 x N	>3.00 x N

APPENDIX F

Follow-up Visit Form

FOLLOW-UP VISIT
JOINT CENTER FOR RADIATION THERAPY — DEFINITIVE BREAST CANCER TREATMENT

NAME _____ DATE _____ HOSP. NO. _____ THERAPY NO. _____

Systemic Treatment Since Prior Follow-Up Visit (type) _____

If Recurrence Noted, Indicate Site:

a.) breast, compatible with primary
b.) breast, separate from primary
c.) axilla
d.) supraclavicular area
e.) opposite breast
f.) other (state) _____

NARRATIVE:

NORMAL TISSUE STATUS:	None - 0	Slight - 1	Moderate - 2	Severe - 3
Breast or chest wall tenderness				
Breast retraction				
Breast fibrosis				
Breast edema				
Matchline effect				
Matchline effect at hockey stick				
Telangiectasia (indicate site)				
Hyperpigmentasia				
Arm edema				
Shoulder restriction				
Supraclavicular fibrosis				
Other				

Overall Cosmetic Result:

Physician – Excellent _____ Good _____ Fair _____ Poor _____
Patient – Excellent _____ Good _____ Fair _____ Poor _____

STUDIES ORDERED:

NEXT VISIT:

COPIES SENT:

_____ M.D.
RADIOTHERAPIST

8502-7/81

APPENDIX G

Form HT-Breast-1

Equipment Evaluation Form for Breast Applicator

Last Name: _____
First Name: _____
Therapy #: _____
Tr. Date: _____
Tr. Number: _____

Mark target area, surgical scar, and probe placement:

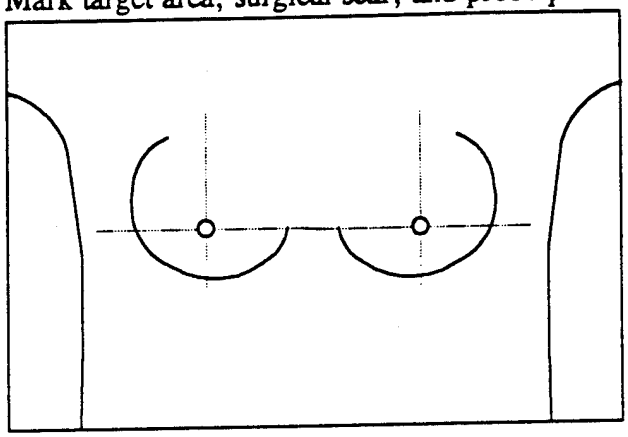

Temperature sensors: Tumor: _____ Normal: _____ Skin: _____

Applicator power:	LF			HF		
	# xducers	Max Pwr	Ave Pwr	# xducers	Max Pwr	Ave Pwr
Ring 1:	_____	_____	_____	_____	_____	_____
Ring 2:	_____	_____	_____	_____	_____	_____
Ring 3:	_____	_____	_____	_____	_____	_____
Ring 4:	_____	_____	_____	_____	_____	_____
Ring 5:	_____	_____	_____	_____	_____	_____
Ring 6:	_____	_____	_____	_____	_____	_____
Ring 7:	_____	_____	_____	_____	_____	_____
Ring 8:	_____	_____	_____	_____	_____	_____

Treatment Descriptors:

T_{min}	_____	$Eq43_{min}$	_____
T_{ave}	_____	T_{90}	_____
T_{max}	_____	% < 40.0°C	_____
T_{peak}	_____	% > 43.0°C	_____
		% > 43.5°C	_____
		% > 44.0°C	_____

Was treatment goal achieved? Yes ☐ No ☐

(Successfull treatment defines as '% < 40.0' ≤ 15% and '% > 43.5' ≤ 10% and '% > 44.0' ≤ 1%)

JLH 1/95

DANA-FARBER CANCER INSTITUTE

INFORMED CONSENT
FOR RESEARCH

Issue Date: _____

PROTOCOL NUMBER & TITLE: 95-006
RT + HT for Breast Cancer

SUBJECT/PATIENT NAME: _____ DFCI I.D. NUMBER: _____

RADIATION AND THERMAL THERAPY FOR EXTENSIVE INTRADUCTAL CARCINOMA OF THE BREAST

INTRODUCTION

Your physician has determined that you either have, invasive breast cancer that contains an extensive amount of intraductal carcinoma (non-invasive cancer), or that your have pure intraductal carcinoma without any associated invasion. Local recurrence of breast cancer following breast conserving treatment with lumpectomy and radiation therapy is seen in 10-15% of cases. However, breast cancers such as yours, with an extensive intraductal component may have a higher risk of local recurrence in the breast than cancers without an extensive intraductal component when treated with breast conservative therapy. For patients with an extensive intraductal component, the option of mastectomy may have a lower risk of breast recurrence, but many patients prefer breast conservation. The overall survival of patients treated with breast conservation is virtually identical to those treated with mastectomy.

Intraductal carcinoma may be more resistant to radiation therapy and this may account for the poor results seen with irradiation in these patients. Thermal therapy or hyperthermia refers to the use of temperatures 42°C (107.6°F) or higher to treat malignant tumors. Laboratory and clinical reports have demonstrated that heat kills

tumors, if tumors are heated to 43°C (109°F) for 30-60 minutes. Many studies suggest that the addition of heat may also improve upon the usual results of radiation therapy for many tumors, including recurrent invasive breast cancer, bladder cancer, and tumors of the head and neck region. Investigators have found an improvement in tumor response rates and a lengthened duration of response. This is the first study to attempt to treat non-invasive breast tumors.

You are being asked to participate in a research project to study the use of thermal therapy (heat treatments produced by sound waves) for the treatment of breast cancer with extensive intraductal carcinoma. We have developed the thermal therapy technologies required to make use of the positive interaction between heat and radiation. The specific clinical study we propose is a study to optimize and establish our ability to safely deliver heat to the breast using a new breast thermal therapy device. The purpose is to determine if we can control heat delivery.

OBJECTIVE

The purpose of this research study is to determine the safety and effectiveness of generating, and delivering, heat to the breast in combination with radiation therapy. We want to evaluate what side effects are associated with this treatment. Fifteen patients will be treated in this research study.

TREATMENT DESCRIPTION

Your radiation oncologist will schedule a radiation therapy treatment planning and an initial thermal therapy planning session. Both of these are conducted at the Dana Farber Cancer Institute even though the radiation therapy is carried out at another hospital. Photographs of the treatment site will be taken during the planning and at each of the thermal therapy sessions.

Thermal Therapy: At the Radiation Therapy Planning Department at the Dana Farber Cancer Institute you will receive two thermal therapy treatments. Each treatment will require at least two hours of preparation time prior to treatment. The heat treatment requires you to lay on your stomach on a soft flat table for approximately two hours. Therefore, on the day of thermal therapy you must plan for a total of approximately 5 hours from the time you arrive for therapy to the time you are ready to leave. The device used to generate heat produces ultrasonic sound waves to heat the breast. This device was developed under contract with the U.S. Army Medical Research & Development Command. This is a new heat treatment device. Your breast will fall through a cut-out (hole) in the table and rest in a tank of water for the heat treatment. The ultrasound energy waves enter the quadrant or half of the breast containing the original lump (tumor) region. The goal will be to reach 40 to 43 °C (104 to 109 °F) in the breast for 45 minutes. During heat treatments you will experience warmth and

occasionally mild discomfort. You will have an intravenous line inserted prior to treatment that may be used to give pain medications if needed. A technologist will be with you during treatment.

During the heat treatment, temperatures will be measured. Prior to each heat treatment at least two metal thermometer needle probes will be inserted into the breast. The thermometer probes help control the temperature in the breast and avoid burns. A Radiation Oncologist and Diagnostic Radiologist will place the small needle probes into the breast through numbed skin under sterile conditions using local anesthesia. The temperature measuring probes will be removed after each thermal therapy treatment. The total time for each treatment session will be at least three hours.

Radiation Therapy: In addition to the heat treatments, you will receive radiation therapy to your breast. Your radiation oncologist will decide what radiation dose you receive. On the basis of experience, we believe that the effectiveness of the radiation may be improved with heat. On days when both radiation and thermal therapy are given, radiation will follow thermal therapy by 30-60 minutes. Radiation will be given daily, five days a week, for 6 to 6 1/2 weeks.

After the treatment course is completed you will be asked to return at regular intervals for follow-up visits to evaluate the results of treatment and the potential long-term side effects. In order to assess your response to treatment certain diagnostic tests will be

done prior to beginning treatment and at intervals following treatment. This may include blood tests, mammography, breast ultrasound, breast magnetic resonance imaging (MRI), and other tests determined to be necessary by your physician. They will be explained to you at the time of your initial evaluation and at follow-up visits.

POTENTIAL BENEFITS

The potential benefits associated with the treatment include a possible reduced risk of tumor recurrence. Heat appears to increase the effectiveness of radiation therapy. However, no guarantee or assurance can be made regarding the results, if any, that may be obtained since research results cannot be foreseen. Your participation will contribute to the development of medical knowledge about the treatment of breast cancer and the use of this thermal therapy device.

If new information develops during the course of your treatment that may be related to the efficacy or risks of your treatment, you will be informed and options will be discussed.

POTENTIAL SIDE EFFECTS

Although hyperthermia has the potential to produce beneficial results, it may be of no benefit and may have injurious effects.

Thermometer probe placement: Despite local anesthesia to diminish pain during thermometer probe insertion, you may experience pain at the time of probe placement. When local anesthesia is given, you will experience a momentary stinging sensation. As with any invasive procedure, there is a risk of bleeding, infection, or perforation of normal structures in or near the region of treatment. There is the small risk of a permanent scar at the point where the thermometry probe enters the skin of the breast, but this risk should be small. There is a minor risk that tumor cells could track along the thermometry probe path in the breast, but this would be rare, and be included in the field receiving radiation therapy treatment.

Radiation Therapy: Your radiation oncologist will describe the possible side effects to you, and you will be asked to sign a separate consent form for the delivery of the radiation therapy. However, common immediate side effects include fatigue and skin redness and irritation in the treated breast. Thermal therapy may also make the normal tissues more sensitive to the toxic effects of radiation. Thus, all of the tissues that receive radiation therapy and heat are potentially more prone to radiation injury. Since this treatment is investigational, it is possible that unforeseen side effects could occur.

Thermal Therapy (heat treatment): Is associated with possible pain, burns, blisters, nausea, itching, or fever during the treatment session. If any of these is observed, it may be possible to change the heating pattern to eliminate them. You may also become

uncomfortable from lying on your stomach, in the treatment position. We will attempt to make you comfortable.

During treatment, your heart may beat faster and you will probably feel warm and begin to sweat. Your heart's electrical pulses and your blood pressure will be monitored during therapy. You may choose to stop receiving the study treatment at any time if any of the related side effects is intolerable. In addition if you experience dizziness, shortness of breath, or chest pain, you must notify your physician immediately, so that the treatment can be modified or stopped. We expect most side effects associated with the use of thermal therapy and radiation therapy to be controllable and reversible. We do, however, emphasize that we cannot rule out any unsuspected side effect. During this study, provisions and precautions will be taken to insure your safety throughout the course of treatment.

Should any of the above side effects appear, your physician(s) will take steps to reduce or eliminate these effects by whatever means are necessary, but there can be no assurance that such effects can be reduced or eliminated.

After the thermal therapy session it is possible to develop pain, burns, or blisters that might persist. In addition, infection or ulceration may occur. If persistent pain should develop, this may represent muscle or nerve injury. You will be evaluated by your

physician and further heat treatment sessions will be stopped until such problems have resolved.

Tissue changes, such as fibrosis (scar tissue), necrosis (dead tissue), and ulceration, in the treated breast could happen at any time following treatment and be permanent. Some of these effects such as fibrosis could make follow-up examinations of your breast by you or your physician more difficult. In addition, thermal therapy may make follow-up mammograms of the breast more difficult to interpret.

This is a new deep-heating device and with all investigational treatments, it is possible that unforeseen complications could occur.

ALTERNATIVE TREATMENTS

The alternative treatment is mastectomy with or without reconstruction of the breast. Reconstruction can be done at the time of the mastectomy or at a later time. Another alternative treatment would be conventional radiation therapy alone. Your physician has explained these procedures and both their advantages and their disadvantages to you.

CONTRAINDICATIONS

Thermal therapy is not to be given to patients whose sensitivity to heat sensation has been significantly decreased in the area to be treated by any means (previous treatment, anesthesia, diabetic nerve damage, etc.), patients with cardiac pacemakers, and patients having a known decrease in circulation in the area to be heated. General or regional anesthetic must not be given with thermal therapy and will not be used in your treatments. Pain-medication, sedatives, or tranquilizers may be used in your treatments as long as they do not significantly decrease your awareness of pain sensation in the treatment area.

FOR WOMEN OF CHILDBEARING POTENTIAL

Radiation therapy may have an adverse effect on an unborn child and should not be performed during pregnancy. You are advised NOT to become pregnant before or during this study. If you become pregnant, you would automatically be excluded from radiation therapy and this protocol study.

PARTICIPATION

Your participation is voluntary and you may refuse to participate and/or withdraw your consent and discontinue participation in the project at any time without penalty,

loss of benefits to which you are otherwise entitled, or penalty of prejudice in your future treatment.

Also, your physician can terminate your participation without your consent at any time in the event of physical injury or other condition that makes further treatment an unnecessary risk in the medical opinion of your physician.

CHARGES

You will not be charged for the hyperthermia treatment. However, you will be charged for the ultrasound examination of the breast that will occur at the time of thermometer probe placement. You will be charged in the usual fashion for radiation therapy, doctors visits, and any other portion of your care that is considered standard care. You are also responsible for payment of all charges for medical procedures to treat conditions resulting from adverse outcomes related to the study treatment.

CONTACT PERSONS

For more information concerning the research and research-related risks or injuries, you can contact Dr. Bruce Bornstein, the investigator in charge, at (617) 632-3591.